Walkey, H.C. (2003). Visual performance in the mesopic range. (Unpublished Doctoral thesis, City University London)

CITY UNIVERSITY LONDON

City Research Online

Original citation: Walkey, H.C. (2003). Visual performance in the mesopic range. (Unpublished Doctoral thesis, City University London)

Permanent City Research Online URL: http://openaccess.city.ac.uk/7609/

Copyright & reuse

City University London has developed City Research Online so that its users may access the research outputs of City University London's staff. Copyright © and Moral Rights for this paper are retained by the individual author(s) and/ or other copyright holders. All material in City Research Online is checked for eligibility for copyright before being made available in the live archive. URLs from City Research Online may be freely distributed and linked to from other web pages.

Versions of research

The version in City Research Online may differ from the final published version. Users are advised to check the Permanent City Research Online URL above for the status of the paper.

Enquiries

If you have any enquiries about any aspect of City Research Online, or if you wish to make contact with the author(s) of this paper, please email the team at publications@city.ac.uk.

VISUAL PERFORMANCE IN THE MESOPIC RANGE

Helen Clare Walkey

Doctor of Philosophy

City University
Department of Optometry and Visual Science

January 2003

ALL MISSING PAGES ARE BLANK

IN

ORIGINAL

Contents

Acknowledgements 17

Declaration.....19

Abstract 21

1 Introduction 23

1.1 Anatomy and physiology of the eye and the visual pathway 23

1.1.1 The eye 23

a. The lens 25

1.1.2 The retina 26

a. The pigment epithelium 29

b. The photoreceptors 29

c. Phototransduction 32

d. Bipolar cells and ganglion cells 33

e. Horizontal and amacrine cells 34

f. Receptive field structure of ganglion cells 35

g. Rod pathways 37

h. Spatial organisation of the retina 37

1.1.3 The optic nerve, optic chiasm and optic tracts 40

a. The optic nerve 40

b. The optic chiasm and optic tracts 41

1.1.4 The lateral geniculate nucleus and other subcortical nuclei that receive retinal projections 42

a. The lateral geniculate nucleus 42

b. Receptive fields, and the magnocellular and parvocellular pathways 44

c. Other nuclei that receive ganglion cell input 45

1.1.5 The visual cortex 46

a. Receptive fields of cortical neurons 47

b. Orientation and ocular dominance columns 49

c. Further functional segregation in the cortex 49

1.2 Colour vision 51

1.2.1 Trichromacy and cone spectral sensitivities 52

1.2.2 The coding of colour in the visual system 56

1.2.3 Colorimetry and the CIE standard colorimetric observers 59

1.2.4 Chromaticity diagrams 62

1.2.5 Photometry and the CIE standard photometric observers 64

1.2.6 Chromatic discrimination 69

1.2.7 Uniform chromaticity diagrams and uniform colour spaces 73

1.2.8 Colour spaces based on retinal physiology 75

1.2.9 Colour order systems 79

1.2.10 Congenital colour vision deficiencies 80

1.2.11 Tests for colour vision deficiencies 85

1.3 The dual nature of the retina and aspects of visual function under mesopic conditions 87

1.3.1 Differences between rod and cone mediated vision 87

a. Absolute threshold 87

b. Dark adaptation and increment thresholds 89

c. Saturation of the rod and cone systems 94

d. Spatial and temporal characteristics of rod and cone pathways 95

1.3.2 Mesopic spectral luminous efficiency 97

1.3.3 Rod-cone interactions 990

1.4 A summary of the investigations 100

2 Equipment and methods 105

2.1 CRT display-based systems 106

2.1.1 Neutral density filters 107

2.1.2 Pupil measurements 108

2.1.3 CRT monitor calibration 109

2.1.4 Colorimetric transformations 111

2.2 Maxwellian view optical system 113

2.3 Colour vision test employing luminance·contrast noise 114

2.3.1 Colour vision testing under photopic conditions. 115

2.3.2 Colour vision testing under mesopic conditions 117

2.4 Dark adaptation experiments 119

2.4.1 Calculation of appropriate dark adaptation times 120

2.5 Visual matching procedure 121

2.5.1 Design of the matching procedure for the pilot study 122

2.5.2 Re-design of the conspicuity matching procedure 124

2.6 Visual search task 128

3 Effect of stimulus parameters on chromatic sensitivity 133

3.1 Introduction 133

3.2 Subjects and Methods 136

3.2.1 Subjects 136

3.2.2 Methods 138

3.3 Results 140

3.3.1 Normal trichromats 140

3.3.2 Dichromats 144

3.3.3 Patients with acquired colour vision deficiency 146

3.4 Discussion 148

3.4.1 Detection of chromatic bars over different spatial scales 148

3.4.2 Comparison of chromatic sensitivity inherently associated with and independent of stimulus structure 149

4 Chromatic sensitivity in the mesopic range 155

4.1 Introduction 155

4.2 Subjects and Methods 157

4.2.1 Subjects 157

4.2.2 Assessment of the masking technique under mesopic conditions 158

4.2.3 Investigation of chromatic sensitivity in the mesopic range 158

4.2.4 Investigation of possible rod involvement in chromatic processing 160

4.3 Results 162

4.3.1 Effectiveness of the masking technique 162

4.3.2 Foveal measurements 163
4.3.3 Thresholds obtained in the near periphery 166
4.3.4 Change of background chromaticity 169
4.3.5 Ellipses plotted in DKL space 171
4.3.6 Dark adapted vs. cone plateau measurements 174

4.4 Discussion 176

4.4.1 Ellipse orientation: inter-observer differences and changes with eccentricity and field size. 178
4.4.2 The influence of rods on chromatic sensitivity in the mesopic range ... 179
4.4.3 Changes in chromatic sensitivity with reduction of light level, with particular regard to the S-cone system 181

5 A model of conspicuity in the mesopic range 185

5.1 Introduction 185

5.2 Subjects and methods 188

5.2.1 Subjects 189
5.2.2 Methods for the pilot study 190
5.2.3 Methods for collection of a conspicuity matching data set 191
5.2.4 Analysis of the conspicuity matching data set 195

5.3 Results 197

5.3.1 Results of the pilot study 197
5.3.2 The conspicuity matching data set 201
5.3.3 Comparison of the two experimental systems 204
5.3.4 Achromatic matches 204
5.3.5 Measurement variability 205
5.3.6 Dependence of match contrast on test target parameters in the conspicuity matching data set (results of ANOVA) 207
5.3.7 Pupil measurements 211
5.3.8 Development of an empirical model from the conspicuity matching data set 212
5.3.9 Model prediction errors as a function of light level 215

5.3.10 Comparison of conspicuity with photopic contrast, scotopic contrast and mesopic brightness contrast.....216

5.4 Discussion 221

5.4.1 Luminance contrast and conspicuity 221

5.4.2 Colour and conspicuity.....222

5.4.3 The conspicuity model.....225

5.4.4 Photopic contrast, scotopic contrast and mesopic brightness contrast as predictors of conspicuity.....226

6 Conspicuity and visual search performance in the mesopic range 231

6.1 Introduction 231

6.2 Subjects and Methods..... 234

6.2.1 Subjects 234

6.2.2 Methods 235

6.3 Results..... 238

6.3.1 Achromatic visual search.....238

6.3.2 Visual search performance for targets with colour and luminance contrast, and the conspicuity model.....240

6.3.3 Photopic contrast, scotopic contrast and chromatic difference as predictors of visual search performance.....246

6.4 Discussion 252

6.4.1 Changes in visual search performance with light level.....253

6.4.2 Conspicuity as a predictor of visual search performance 254

7 General discussion and concluding remarks 261

7.1 Conclusions..... 268

Appendices 271

Appendix A. Statistical tables 271

Appendix B: Versions of the conspicuity model.....281

Appendix C. 10° systems of mesopic photometry 286

References and bibliography 295

List of Tables

Table 2-1. Stimulus dimensions for mesopic chromatic sensitivity measurements.119

Table 3-1. Stimulus dimensions for the three sizes of pattern test stimuli. 138

Table 3-2. Stimulus dimensions for the three sizes of colour test stimuli.....138

Table 3-3. Major and minor semi-axis lengths for ellipses obtained using the three sizes of pattern test and colour test. 141

Table 3-4. Statistical analysis of the change in major and minor semi-axis length with stimulus size, for the pattern test and the colour test. 141

Table 4-1. Filter densities, background luminances and dark adaptation times for photopic and mesopic measurements of chromatic sensitivity. 159

Table 4-2. Orientations of the fitted, foveal chromatic discrimination ellipses for subjects HA and HW. 165

Table 4-3. Ellipticities of the fitted, foveal chromatic discrimination ellipses of subjects HA and HW. 165

Table 4-4. Major and minor axis asymmetries for the fitted, foveal chromatic discrimination ellipses of subjects HA and HW. 165

Table 4-5. Orientations of the fitted chromatic discrimination ellipses for subjects HA and HW. 166

Table 4-6. Ellipticities of the fitted chromatic discrimination ellipses of subjects HA and HW, obtained at 3.5° eccentricity. 168

Table 4-7. Major and minor axis asymmetries for the fitted chromatic discrimination ellipses of subjects HA and HW, obtained at 3.5° eccentricity. 168

Table 4-8. L-M and S-Lum mechanism asymmetries for the fitted chromatic discrimination ellipses of subjects HA and HW, obtained at the fovea. 174

Table 4-9. L-M and S-Lum mechanism asymmetries for the fitted chromatic discrimination ellipses of subjects HA and HW, obtained at 3.5°.....174

Table 5-1. Stimulus parameters for the pilot conspicuity matching experiments. ..190

Table 5-2. The values of photopic and scotopic contrast incorporated into the experimental design used to collect a data set of conspicuity matches. 193

Table 5-3. Filter densities, background luminances and dark adaptation times for system-1 and system-2. 194

Table 5-4. Results of ANOVA for the system comparison. 204
Table 5-5. Match precision for each observer for two light levels. 206
Table 5-6. The correlation matrix for the explanatory variables. 207
Table 5-7. Results of ANOVA performed on the complete conspicuity matching data set 208
Table 5-8. Results of the ANOVA to investigate the effect of both the magnitude and sign of the luminance contrast. 209
Table 5-9. Results of the ANOVAs performed for each individual light level. 210
Table 5-10. The background luminance (L_{10}) for the three additional light levels at which pupil measurements were made (a1-a3). 211
Table 6-1. Filter densities, background luminances and dark adaptation times for system-1 used in the visual search experiments. 235
Table 6-2. Values of positive achromatic contrast for six of the 12 targets in the visual search experiments. 236
Table 6-3. Values of C_p, C_s and CD for the six colour/luminance combination targets investigated in the visual search experiments. 237
Table 6-4. Values of positive achromatic contrast predicted by the conspicuity model for the colour/luminance targets. 237
Table 6-5. Parameters for the fitted curves shown in Figure 1-1. 239
Table 6-6. The correlation between measured and predicted search times. 241
Table 6-7. Differences between measured and predicted search times. 242
Table 6-8. Assessment of the conspicuity model to accurately predict conspicuity. 244
Table 6-9. Differences between measured search times and search times calculated from the measured match contrasts. 245
Table 6-10. Differences between measured search times for the colour/luminance targets and search times calculated from target photopic contrast. 247
Table 6-11. Differences between measured search times for the colour/luminance targets and search times calculated from target scotopic contrast. 247

List of Figures

Figure 1-1. Horizontal cross section through the human eye..... 24
Figure 1-2. The optical density spectrum of the human lens..... 25
Figure 1-3. The layered structure of the human retina..... 27
Figure 1-4 (A)-(B). Rod and cone photoreceptors. 29
Figure 1-5. The absorption spectrum of rhodopsin. 31
Figure 1-6. The receptive field structure of Wiesel and Hubel's Type I and Type II cells. 36
Figure 1-7. Thinning of the retina at the fovea. 38
Figure 1-8. The optical density of the macular pigment. 39
Figure 1-9. The primary visual pathway. 41
Figure 1-10 (a)-(c). Patterns of ganglion cell axons. 42
Figure 1-11. The layered structure of the lateral geniculate nucleus. 43
Figure 1-12. The visual cortex. 46
Figure 1-13. Location of the primary visual cortex, V1. 47
Figure 1-14. Diagram of the receptive field structure of simple cells. 48
Figure 1-15. Structural organisation of V1 50
Figure 1-16. Estimates of the cone fundamentals. 55
Figure 1-17. The receptive field structure of Wiesel and Hubel's type II cell. 56
Figure 1-18. The receptive field structure for colour coded cells according to the mixed-surround model. 58
Figure 1-19 (A)-(B). Colour matching functions of the CIE 1931 standard colorimetric observer. 60
Figure 1-20. Colour matching functions of the CIE 1964 standard colorimetric observer. 61
Figure 1-21 (A)-(B). Chromaticity diagrams associated with the XYZ systems of the CIE. 63
Figure 1-22. The CIE standard luminous efficiency functions. 66
Figure 1-23. The Judd-Vos modified $V_M(\lambda)$ function. 68
Figure 1-24. Wavelength discrimination curve. 70
Figure 1-25. Wright's measurements of just noticeable differences in chromaticity. 71

Figure 1-26. MacAdam's measurements of chromatic discrimination. 72
Figure 1-27. The CIE 1976 uniform colour space..... 73
Figure 1-28. MacLeod-Boynton chromaticity diagram. 76
Figure 1-29 (A)-(B). Diagrammatic representation of DKL space. 78
Figure 1-30. Arrangement of the Munsell colour order system.. 80
Figure 1-31 (A)-(C). The isochromatic lines and the copunctual point for each class of dichromat:..... 83
Figure 1-32. Spectral luminous efficiency functions for the three classes of dichromat..... 84
Figure 1-33. A typical dark adaptation curve..... 88
Figure 1-34. The effect of cone and rod spectral sensitivity on the dark adaption curve. 89
Figure 1-35. Threshold vs. intensity curve..... 90
Figure 1-36. Stiles π-mechanisms..... 91
Figure 1-37. Dark adaptation and increments threshold curves for a rod monochromat..... 92
Figure 1-38. Equivalent background luminance. 93
Figure 1-39. Rod increment threshold curve showing rod saturation. 94
Figure 1-40. Mesopic luminous efficiency curves..... 97
Figure 2-1. CRT monitor-based system. 106
Figure 2-2. Spectral profile of the neutral density filters. 107
Figure 2-3. Phosphor radiance data. 110
Figure 2-4. Luminance versus gun voltage calibration..... 111
Figure 2-5. Phosphor chromaticities for System-1 and System-2. 111
Figure 2-6. The region of (x, y)-chromaticity space that can be reproduced on a typical CRT monitor. 112
Figure 2-7. Diagram of the single channel Maxwellian view optical system..... 113
Figure 2-8. An example of dynamic random luminance contrast modulation..... 115
Figure 2-9. Example of the stimulus for the pattern test..... 116
Figure 2-10. Example of the stimulus for the colour test..... 116
Figure 2-11. A graphical representation of the combination of random luminance contrast and light flux modulation used in the mesopic colour vision test. ... 117

Figure 2-12 (A)-(B). Example of the stimulus used to measure chromatic thresholds under mesopic conditions. 118
Figure 2-13. The stimulus used in the dark adaptation experiments. 120
Figure 2-14 (A)-(B). The stimulus used in the pilot matching experiments..... 122
Figure 2-15 (A)-(B). The stimulus used in the conspicuity matching experiments. 125
Figure 2-16 (A)-(C). The stimulus used in the visual search experiments..... 129
Figure 3-1. The three pattern test stimuli P1, P2 and P3..... 137
Figure 3-2. The three colour test stimuli C1, C2 and C3..... 138
Figure 3-3. Average thresholds for the six normal trichromats for the three pattern test stimuli P1-P3..... 141
Figure 3-4. Average thresholds for the six normal trichromats for the three colour test stimuli C1-C3..... 142
Figure 3-5. Average chromatic thresholds for three normal trichromats for the pattern test stimulus P2 and the colour test stimulus C2. 143
Figure 3-6. Chromatic thresholds for the deuteranope d-1 for the three pattern test stimuli P1-P3. 143
Figure 3-7. Chromatic thresholds for the deuteranope d-2 for the pattern test stimulus P2 and the colour test stimulus C2. 144
Figure 3-8 (A)-(B). Chromatic thresholds in subjects with acquired colour vision deficiency for the three pattern test stimuli P1-P3. 145
Figure 3-9 (A)-(B). Chromatic thresholds for subjects with acquired colour vision deficiency for pattern test stimulus P2 and colour test stimulus C2..... 147
Figure 4-1 (A)-(B). Dark adaptation curves measured for subject HW..... 161
Figure 4-2 (A)-(B). Comparison of the effect of masking to no masking on achromatic and chromatic thresholds..... 162
Figure 4-3. Chromatic thresholds measured at 0.056 cd m^{-2} for increasing levels of luminance contrast (LC) and light flux (LF) masking. 163
Figure 4-4 (A)-(B). Foveal chromatic thresholds (mesopic)..... 164
Figure 4-5 (A)-(B). Chromatic thresholds measured at 3.5° eccentricity (mesopic). 167
Figure 4-6 (A)-(B). Comparison of chromatic thresholds obtained at the fovea, 3.5° and 7° eccentricity..... 168
Figure 4-7. Peripheral chromatic thresholds for subject HW. 169

Figure 4-8. Chromatic thresholds measured for a change in background chromaticity. 170
Figure 4-9 (A)-(B). Chromatic discrimination ellipses obtained at the fovea, transformed into DKL space 172
Figure 4-10 (A)-(B). Chromatic discrimination ellipses obtained at 3.5° eccentricity, transformed into DKL space 173
Figure 4-11 (A)-(C). Comparison of chromatic thresholds measured after dark adaptation and during the cone plateau of the dark adaptation curve (1) 175
Figure 4-12 (A)-(C). Comparison of chromatic thresholds measured after dark adaptation and during the cone plateau of the dark adaptation curve (2) 176
Figure 5-1. S by P line in CIE 1976 (u′, v′)-chromaticity space 191
Figure 5-2. S by P lines in CIE 1976 (u′, v′)-chromaticity space denoting the range of available chromaticities. 192
Figure 5-3 (A)-(E). Conspicuity matches for targets with zero photopic and scotopic contrast (1) 198
Figure 5-4 (A)-(E). Conspicuity matches for targets with zero photopic and scotopic contrast (2) 199
Figure 5-5 (A)-(B). Chromatic thresholds and the colour directions of the red and green stimuli used in the pilot study. 201
Figure 5-6 (A)-(C). Average conspicuity matches for the five observers at a low photopic and a low mesopic light level. 202
Figure 5-7 (A)-(B). Conspicuity matches for targets with zero photopic contrast and approximately zero scotopic contrast. 203
Figure 5-8 (A)-(B). Comparison of conspicuity matches for test targets of positive or negative achromatic contrast. 205
Figure 5-9. Within-subject variability and measurement precision. 206
Figure 5-10. Between-subject variability as a function of light level 207
Figure 5-11. Mean pupil diameter as a function of log luminance (1). 210
Figure 5-12. Mean pupil diameter as a function of log luminance (2). 211
Figure 5-13. Predictions of match contrast (C_m) for version-a of the conspicuity matching model. 214
Figure 5-14. Predictions of match contrast (C_m) for version-a_r (reduced version) of the conspicuity matching model 215

Figure 5-15. Errors in predicting measured match contrast.....216
Figure 5-16. A comparison of the ability of nine different models to predict matches in conspicuity, throughout the mesopic range. 219
Figure 6-1 (A)-(D). Visual search times for achromatic contrast targets.....238
Figure 6-2 (A)-(D). Visual search times for targets defined by colour and luminance contrast.....241
Figure 6-3. Measured and predictd search times for the targets with a combination of colour and luminance contrast.....243
Figure 6-4 (A)-(D). Search times plotted against target photopic contrast.....248
Figure 6-5 (A)-(D). Search times plotted against target scotopic contrast.....249
Figure 6-6 (A)-(D). Search times plotted against target chromatic difference.....251

Acknowledgements

Firstly I must thank John Barbur; with his help and guidance I have achieved a great deal. I am very grateful for all the encouragement, advice and illuminating discussions.

I would also like to thank the following people for their contribution in helping me realise this goal: Julie Taylor for her support and for sharing her mesopic vision expertise. Walt Makous for informative discussions relating to the work presented in chapter 4. Alister Harlow for generating the control programs. Janet Wolf for donating additional data to complement the investigation reported in chapter 3. Russell Gerrard for useful advice on statistics. Ken Sagawa for performing a lot of number crunching on my behalf, in relation to chapter 5. Theresa-Jane Squire, Yik Tsang and Sarah Walkey for their assistance in collecting a proportion of the data presented in chapter 5. All my subjects for giving up their time to sit in a dark room, stare at a display, and press buttons.

Last, but not least, I would like to thank my family for their support, and especially Tony for his continual encouragement and endless patience.

Declaration

I grant powers of discretion to the University Librarian to allow this thesis to be copied in whole or in part without further reference to me. This permission covers only single copies made for study purposes, subject to normal conditions of acknowledgement.

Abstract

The aims of this work were to assess the effects of different stimulus parameters on chromatic sensitivity, with particular emphasis on the effect of retinal illumination, and to investigate aspects of suprathreshold visual performance under mesopic conditions.

All investigations were performed using visual psychophysical techniques. Chromatic thresholds were obtained using dynamic luminance contrast noise to isolate responses to colour signals. The effects of stimulus size and spatial distribution were examined in normal trichromats, dichromats and subjects with acquired colour vision deficiency. The chromatic sensitivity of normal trichromats was investigated with reduction in light level. Measurements were also performed to assess the possible involvement of rods in chromatic processing at threshold. Suprathreshold performance in the mesopic range was assessed in terms of the relative contributions of colour and luminance contrast to a measure of stimulus conspicuity and to visual search time. The conspicuity of a stimulus defined by colour and luminance contrast was defined as the value of achromatic contrast of a similar stimulus with an equal perceived conspicuity. An empirical model was developed from an extensive data set of conspicuity matches, to enable prediction of conspicuity for a wide range of coloured stimuli. Visual search performance for both achromatic and coloured stimuli was investigated under mesopic conditions, and results for the coloured stimuli were compared to the measure of stimulus conspicuity combined with an achromatic search time calibration.

The results revealed that chromatic sensitivity is dependent on stimulus size, spatial distribution, eccentricity of presentation and level of illumination. These factors are suggested to reflect changes in cone performance and the relative cone contributions to the postreceptoral chromatic channels. Chromatic sensitivity was found to be independent of rod activity in the mesopic range, suggesting separate processing of rod signals and threshold colour signals under mesopic conditions. Measurements of stimulus conspicuity under mesopic conditions revealed individual variations in response to both luminance contrast and chromatic signals indicative of individual differences in gain control of postreceptoral mechanisms. Conspicuity was successfully modelled as a function of photopic contrast, scotopic contrast, chromatic difference to the background and the level of illumination. The nonlinear relationship between search time and luminance contrast was found to change with reduction in light level, reflecting increased contrast thresholds and diminishing effectiveness of unit physical contrast. Mesopic visual search was also found to depend on the photopic contrast, scotopic contrast and chromatic content of the stimulus, but with an apparent greater emphasis on scotopic contrast and reduced emphasis on colour compared to the measure of stimulus conspicuity. Conspicuity was successfully used to predict visual search times, and was found to be an improved indicator of search performance than either photopic or scotopic contrast.

1 Introduction

This body of work consists of an investigation of the characteristics of human colour vision both under daylight conditions and at low light levels, and explores aspects of visual performance under conditions of low ambient illumination. The next sections introduce topics that are relevant to the investigations described in the subsequent chapters. These are followed by a summary of the experimental work described in each chapter.

1.1 Anatomy and physiology of the eye and the visual pathway

Vision is arguably the most important special sense of humans. A vast amount of information about our surroundings is provided through sight. The process of vision begins with the detection of light in the eye, from which signals are produced that are modified and coded in the retina and transported through the optic nerve to reach the brain. In the brain these signals are interpreted to create the sensation of sight.

1.1.1 The eye

The eye is an irregular spheroid, which is housed in the bony orbit of the skull and surrounded by cushioning fatty tissue. The wall of the eye is made up of three layers, shown in Figure 1-1. The outer layer consists of the transparent cornea, the white opaque sclera, and the transition region between the cornea and sclera - the limbus. The cornea and sclera are composed of densely woven collagen fibres and provide a rigid protective layer, and a site of attachment for the six extraocular muscles that control movement of the eye within the orbit. The cornea has a greater curvature than the main body of the eye and forms its primary refractive element. Structures within the limbus are involved in the drainage of fluid inside the eye. The middle layer of the eye-wall comprises the iris, the ciliary body, and the choroid,

known collectively as the uvea. The iris has a central opening, forming the pupil. The iris contains pigment that makes it opaque, so light can only enter the eye through the pupil. The iris consists of two layers of smooth muscle fibres, the pupillary constrictor muscles and the pupillary dilator muscles; these muscles alter the size of the pupil and are controlled by the autonomic nervous system. The ciliary body forms a ring of tissue just inside the sclera, the anterior of which is continuous with the iris and extends to the ora serrata, the anterior edge of the retina. The majority of the ciliary body consists of the ciliary muscle. On the inside of this muscular annulus the epithelium (a basic human tissue type that forms a covering or lining) is arranged in folds forming the ciliary processes, which attach to the suspensory ligaments (zonule fibres) of the lens.

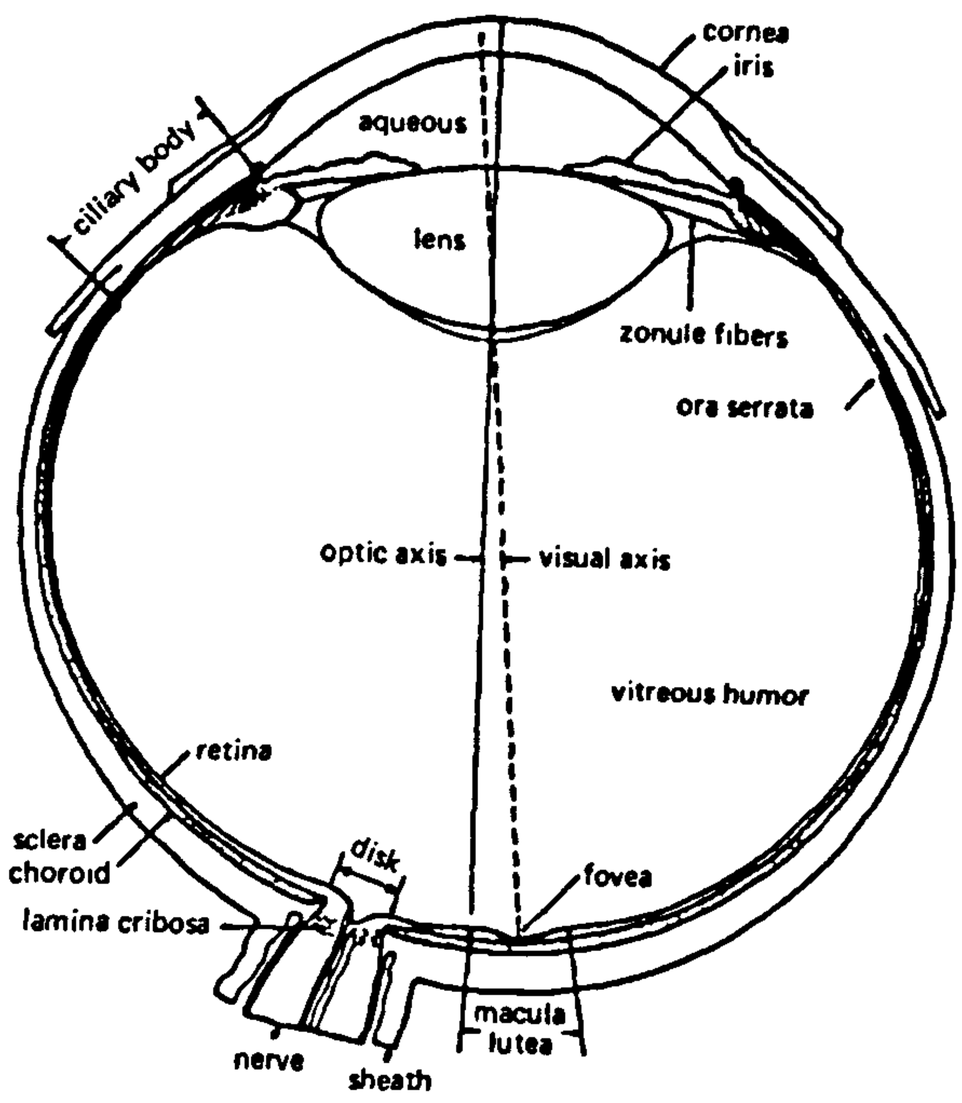

Figure 1-1. Horizontal cross section through the human eye, reproduced from (Boynton 1979) after (Rodieck 1973).

The remainder of the uvea comprises the choroid. The choroid is a vascular coat between the sclera and the retina via which oxygen and nutrients are supplied to the outermost portion of the retina. The innermost layer of the eyeball is the retina. The retina is a multilayered structure comprising the pigment epithelium, the light responsive photoreceptors, and other nerve cells with which the photoreceptors form connections. The process of vision begins with the absorption of photons by the visual pigments, which are contained in the photoreceptors and the nerve cells in the retina are responsible for the preliminary processing of light signals. The

retina also contains blood vessels supplying the inner portion of the retina. These vessels are derived from the main retinal artery and vein, which arrive and depart at the optic nerve head.

The inner body of the eye is divided into three chambers. The anterior chamber extends from the cornea to the iris, the posterior chamber lies between the iris and the ciliary body and lens, and the large vitreous chamber is the cavity posterior to the ciliary body and lens. The anterior and posterior chambers are filled with a transparent fluid known as aqueous humor, which is secreted by the epithelial cells of the ciliary body. Aqueous humor circulates through the anterior and posterior chambers, providing a route for nutrient and waste transport; it is then drained via structures in the limbus, and recycled. The vitreous chamber is filled with the transparent gel-like vitreous humor, which acts as a structural support for the retina.

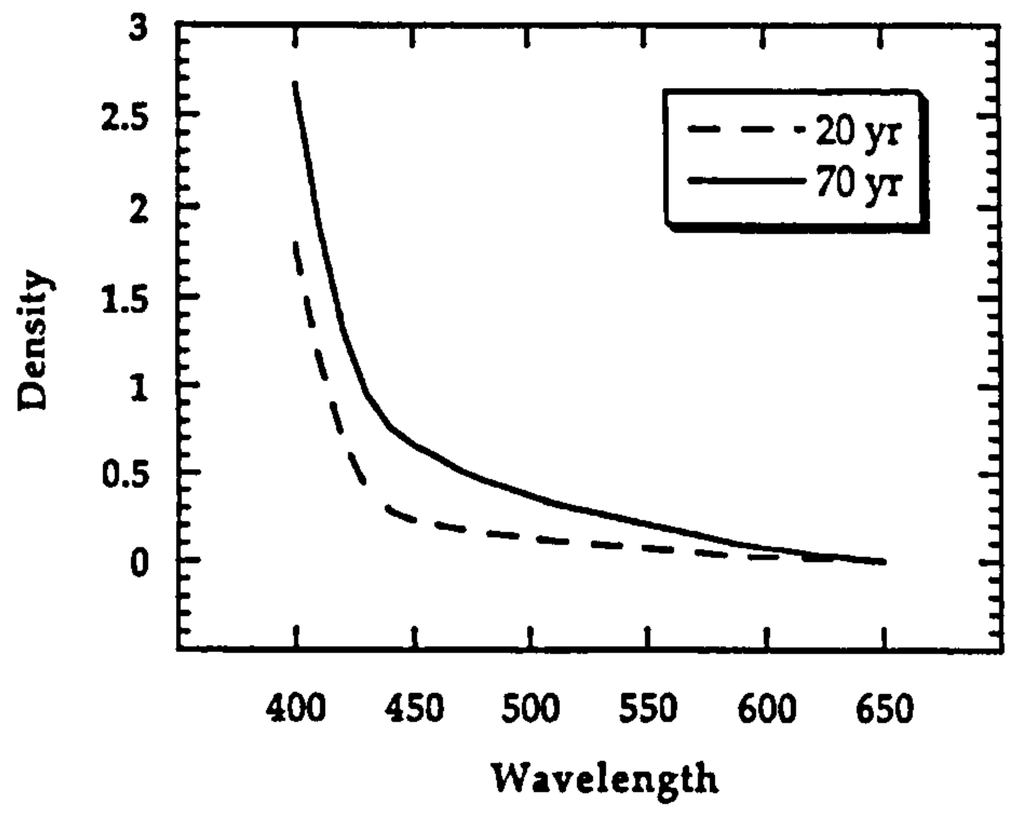

Figure 1-2. The optical density spectrum of the human lens, reproduced from (Pokorny and Smith 1997). The dashed curve represents the lens absorption spectrum of a 20 year old (van Norren and Vos 1974), and the solid curve that of a 70 year old according to the two-component function of Pokorny et al. (1987).

a. The lens

The lens is a multilayered structure of cells enclosed in a fibrous capsule. It is positioned posterior to the iris, and held in place by connections between the ciliary processes of the ciliary body and the zonule fibres attached to the capsule. All light that enters the eye through the pupil also passes through the lens. Changes in the shape of the lens cause corresponding changes in refractive power, which is used to

maintain the image of an object in sharp focus, a process known as accommodation. While the eye is focussed for an object at infinity, the ciliary muscle is relaxed and the zonule fibres exert a pull on the lens flattening its shape. During accommodation, the ciliary muscle contracts, releasing tension in the zonule fibres, and the elasticity of the lens capsule causes the lens to become rounded in shape (Helmholtz 1924/1896).

The visible spectrum is the region of the electromagnetic spectrum extending roughly from 380 nm to 780 nm. The lens absorbs light in the short wavelength region of the visible spectrum and is primarily responsible for light losses in the optic media (van Norren and Vos 1974). Estimates of lens density spectra have been obtained from measurements in excised human lenses and comparison of normal spectral sensitivity curves with those of observers who have had the crystalline lens removed (Wyszecki and Stiles 1967; 1982), and deduced from rod spectral sensitivity curves (van Norren and Vos 1974) using the template of photopigment spectral absorbance curves defined by Dartnall (1953).The optical density profile of the lens is shown in Figure 1-2. Lens density increases with age and can be modelled as a combination of an age invariant and age varying component (Pokorny et al. 1987), which implies that the lens changes in spectral profile as well as density.

1.1.2 The retina

The retina consists largely of transparent structures, including somewhere in the order of 200 million nerve cells. Light enters the inner retina and passes through this arrangement of nerve cells before reaching the light sensitive portion of the photoreceptors. Nerve cells (neurons) consist of a cell body, dendrites (branches of the cell through which inputs are made), and an axon (a long process ending in terminal branches through which outputs are transmitted). Neurons usually conduct electrical activity in the form of action potentials, which are generated at a frequency (firing rate) that relates to the strength of the input signal. Many nerve cells within the retina, however, do not respond in this way. The response characteristics of specific cells are detailed below. Communication between neurons occurs at

chemical synapses, where neurotransmitters are released from the transmitting cell and interact with receptors on the receiving cell.

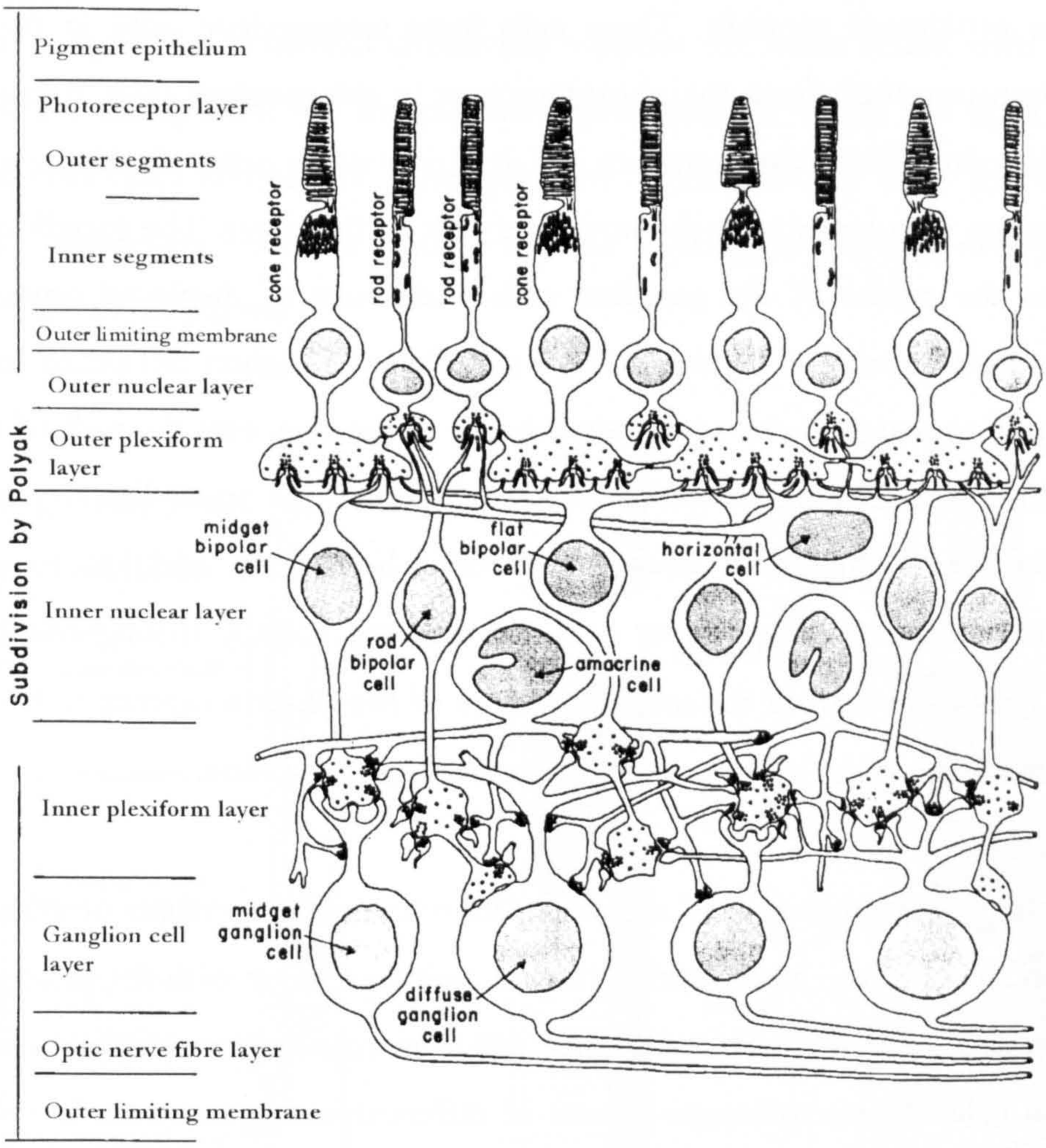

Figure 1-3. The layered structure of the human retina. Modified from (Wyszecki and Stiles 1982) after (Dowling and Boycott 1966).

The retina is organised anatomically and functionally in layers. The traditional labelling of these layers, which are given below and illustrated in Figure 1-3, is based on the classification of Polyak (1941). The outermost layer is the pigment epithelium, the next four layers: the photoreceptor layer, the outer limiting membrane, the outer nuclear layer (ONL), and the outer plexiform layer (OPL), relate to the photoreceptors themselves. The outer and inner segments of the photoreceptors lie in the photoreceptor layer, which is the site for light absorption. The outer limiting membrane separates the inner segments and the ONL. Photoreceptor nuclei form the ONL, and their axons and terminals constitute the OPL, the location where photoreceptors transfer signals to other neurons. The next

layer is the inner nuclear layer (INL), which contains the nuclei of the bipolar, horizontal and amacrine cells. Cell bodies of the horizontal cells are situated outermost in this layer, with the amacrine cells positioned innermost and the bipolars positioned centrally. These cells form intermediate links in the chain of signal transportation from the photoreceptors to the ganglion cells. Axon terminals of the bipolar cells contact ganglion cell dendrites in the inner plexiform layer (IPL); contacts are also made with the amacrine cells in this layer. The ganglion cell layer contains the nuclei of the ganglion cells and those of displaced amacrine cells. Ganglion cell axons constitute the optic fibre layer. Ganglion cell axons traverse the retina and converge at the optic nerve head, where they exit the wall of the eye as the optic nerve. The innermost layer of the retina is the inner limiting membrane, which separates the retina from the vitreous humor. In addition to the neural structure, cells known as Muller cells are oriented radially throughout the retina. Muller cells extend from the inner segments of the photoreceptors to the vitreous, where the ends of the cells form the inner limiting membrane.

The primary transportation of signals in the retina is via a system of vertical wiring from the outer to the inner retina. Vertical pathways begin with the photoreceptors, which pass signals to the bipolar cells, which in turn transport information to the ganglion cells. These pathways consist of different wiring patterns. In a 1:1 wiring pattern, a single bipolar cell contacts a single ganglion cell; this pattern of wiring facilitates signalling of fine spatial detail. Vertical pathways may also be convergent, where single ganglion cells receive information from more than one bipolar cell, which in turn have connections with several photoreceptors. This pattern of wiring produces high sensitivity. These wiring patterns occur in parallel, i.e. photoreceptor signals are transmitted along multiple vertical pathways. There are also systems of lateral pathways in the retina via the horizontal and amacrine cells, by which signals from neighbouring or distant locations may be compared. Lateral wiring patterns are thought to facilitate or inhibit communication between the photoreceptors and the ganglion cells. The initial stages of visual processing take place by virtue of this vertical and horizontal wiring.

a. The pigment epithelium

The pigment epithelium contains the pigment melanin. Melanin absorbs light after it has passed through the neural retina, reducing scatter that would otherwise degrade the retinal image. The choroidal circulation supplies the outer retina with oxygen and nutrients, transported via the pigment epithelium in which the apex of the photoreceptors are embedded. The pigment epithelium is also involved in biochemical reactions with the photoreceptors relating to the regeneration and renewal of the photopigments.

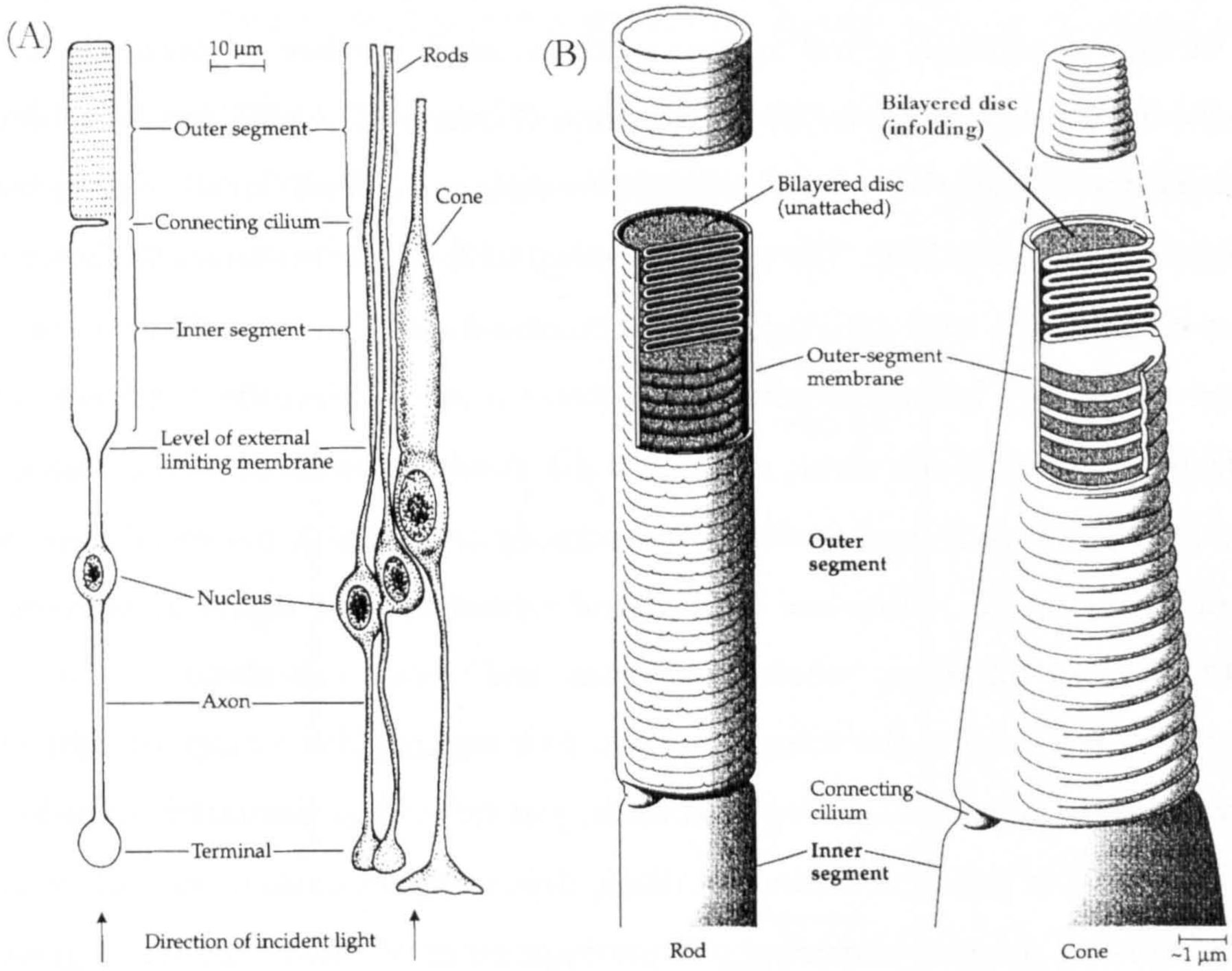

Figure 1-4 (A)-(B). Rod and cone photoreceptors, reproduced from (Oyster 1999). Schematic of photoreceptor anatomy (A), and organisation of photopigment discs in cone and rod outer segments (B).

b. The photoreceptors

There are two classes of photoreceptor in the human retina, the rods and the cones. Both classes consist of an outer segment containing numerous membrane discs in which the visual pigments are stored. The generation of discs is a continual one with new discs formed and shed in less than 2-weeks. The names rod and cone refer to the shape of the outer segment in the two classes of receptor, which are illustrated

in Figure 1-4. A narrow connecting tissue joins the outer segment to the inner segment. The inner segment is continuous with the cell nucleus and axon, and is the location of the cell's metabolic processes. In humans, rod receptors have axon terminals that are termed spherules, and cone receptors have axon terminals that are termed pedicles. Both rod and cone photoreceptors release the neurotransmitter glutamate. Neurotransmitter release occurs maximally in the dark. The photoreceptors do not generate action potentials, but respond in a sustained manner to photon absorption, with response amplitude relating approximately to the logarithm of intensity (Baylor 1987). The time-course of the rod response is longer than that of cones. Absorption of a single photon by a rod receptor is sufficient to produce a rod response and a small number of these events are sufficient to yield conscious signal detection (Hecht et al. 1942), but rods become saturated and unable to signal changes in intensity at moderate levels of illumination (Aguilar and Stiles 1954). The operating range of intensity for cones is higher than that of rods, they have a higher absolute threshold, and they are unlikely to saturate even at very high intensities. The term scotopic is used to describe conditions under which the rods operate alone, i.e., below the absolute threshold of the cones, and the term photopic is used to describe conditions under which the visual response is cone mediated, i.e., above the level of rod saturation. The region in between the scotopic and photopic, where both rods and cones contribute to the visual response, is known as the mesopic region. This region spans a range of light levels, that extends from 5000 scotopic trolands, just below rod saturation (Aguilar and Stiles 1954), to almost absolute threshold, depending on background and stimulus conditions. A stimulus luminance of 3 photopic cd m^{-2} is often quoted as a guide for the upper limit of the mesopic range for centrally viewed fields of the order of a few degrees in size (CIE 1978), and a corresponding guideline for the lower limit is 0.01 photopic cd m^{-2}. The mesopic range therefore encompasses lighting conditions from for example, twilight, night driving and emergency lighting levels to about the luminance of blue sky (Makous 1998).

Rods contain the photopigment rhodopsin, whereas cones contain one of three different photopigments. All four photopigments consist of the pigment known as retinal, but the pigment may be bound to four different proteins; these are called

opsins. The opsin determines the relative probabilities that different wavelengths of light are absorbed by retinal. Photoreceptors respond only to the number of photons absorbed and transmit no wavelength specific information. The three classes of cone are labelled L-, M- and S-cones due to their photopigments absorbing maximally in the long, middle and short wavelength regions of the visual spectrum, respectively. The spectral absorption characteristics of the photopigments found in the three classes of cone are discussed below in section 1.2.1. The absorption spectrum of rhodopsin (shown in Figure 1-5) was first measured by König in the late 19th century using the method of spectrophotometry (described in section 1.2.1). König realised that the spectral absorption curve of rhodopsin was proportional to the spectral sensitivity of human vision at night (under scotopic conditions, see section 1.2.5), when corrections were made for the absorption characteristics of the ocular media (see section 1.1.1 a.).

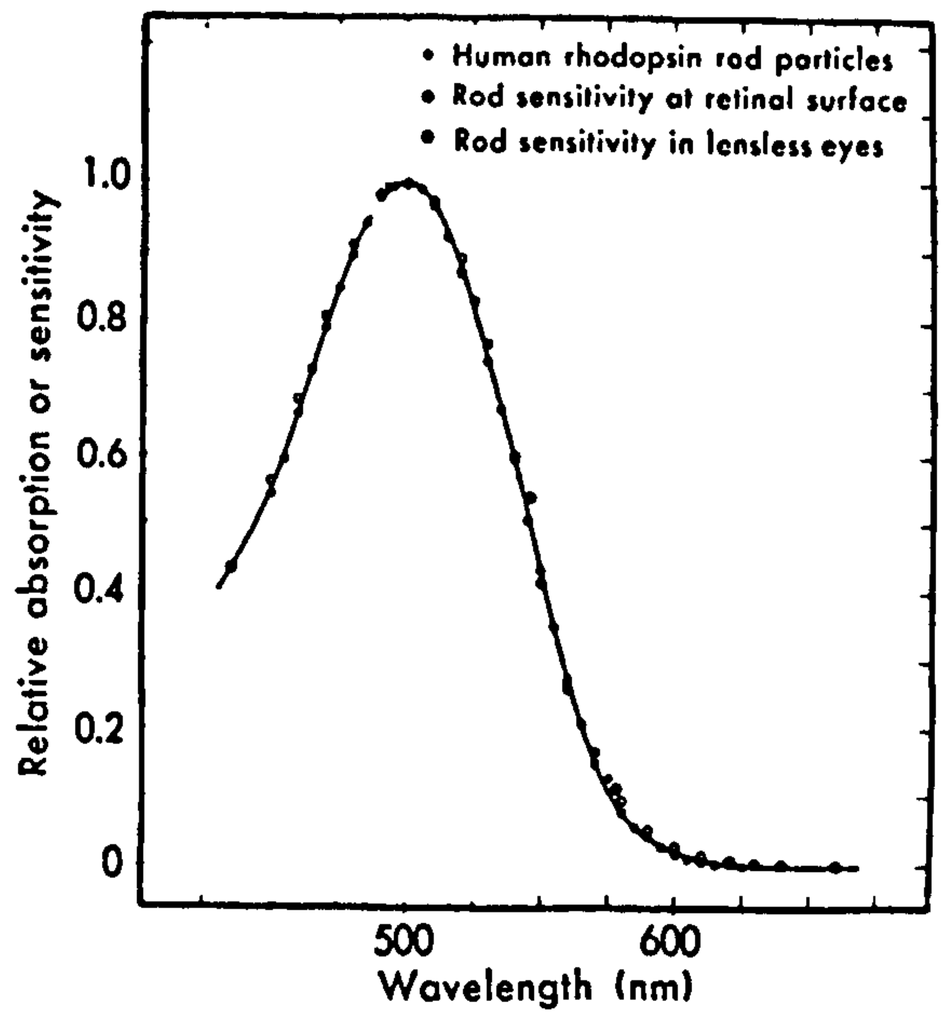

Figure 1-5. The absorption spectrum of rhodopsin, reproduced from (Wald and Brown 1965). The three sets of points represent the absorption spectrum of rhodopsin obtained from rod outer segments in vitro; the spectral sensitivity of rod vision measured at the cornea, corrected for transmission of the ocular media; and scotopic spectral sensitivity measured in a lensless eye.

Stiles and Crawford (1933) discovered another important functional difference between rods and cones relating to their directional sensitivity. They found that cone photoreceptors exhibit a marked improvement in sensitivity to light passing through the centre of the pupil than to light passing through the margins of the

pupil; this is known as the Stiles-Crawford effect. This difference is thought to be due to the greater likelihood that a quantum of light will be absorbed if it enters along the axis of a cone outer segment rather than obliquely. Rod photoreceptors show some directional sensitivity, but the Stiles-Crawford effect in rods is much reduced compared to that of cones (Van Loo and Enoch 1975).

c. Phototransduction

The process of transforming light into an electrical signal is known as phototransduction. This chain of events begins with the absorption of photons by the photopigment in a photoreceptor, and results in a reduction of neurotransmitter release by the photoreceptor. In the dark retinal assumes the configuration termed 11-cis retinal. When a photon is absorbed by a photopigment, for example, rhodopsin, retinal is converted from 11-cis retinal to the form all-trans retinal. This in turn activates the opsin portion of the molecule, which while activated can interact with other molecules in the disc membrane.

Following conversion of retinal into its all-trans form, the rhodopsin molecule begins to break down into retinal and opsin. The photopigment is then said to be bleached and cannot be affected by light. Regeneration of the photopigment involves the conversion of retinal back to its 11-cis configuration by the action of enzymes, before it can recombine with opsin. This conversion takes place in the pigment epithelium and requires time and energy. The regeneration of cone photopigment is faster than that of rhodopsin, and is in part responsible for the difference in temporal response of the two types of receptor. Under steady illumination, equilibrium is reached between the rates of photopigment bleaching and regeneration.

The photoreceptor outer segment membrane contains ion channels that are open in the dark. The inner segment contains metabolically driven ion pumps, which continually pump sodium ions out of the cell. The movement of sodium ions into the outer segment then to the inner segment and out of the cell is known as the dark current. Events occurring in the phototransduction cascade related to the

activation of opsin, act to close the outer segment ion channels, causing the transmembrane potential to become more negative (hyperpolarise) and the rate of neurotransmitter release to decrease.

d. Bipolar cells and ganglion cells

Bipolars relay signals from the photoreceptors to the amacrines and the ganglion cells. There are at least nine types of bipolar cells with which the cones synapse (Wassle and Boycott 1991). These types are divided broadly into two categories; midget bipolars and diffuse bipolars (Polyak 1941). Midget bipolars have small dendritic fields and often contact single cones, whereas diffuse bipolars receive input from a number of cones and have relatively large dendritic fields. The other main classification of bipolar cells is based on their sensitivity to light. Bipolars that depolarise (transmembrane potential becomes less negative) when light intensity increases are labelled ON cells, whereas those that depolarise when light intensity is reduced are labelled OFF cells. ON and OFF bipolars terminate at different levels in the IPL, referred to as sublaminar b and sublaminar a, respectively. In the central retina the majority of midget bipolars of both types (ON, OFF) receive signals from a single M- or L-cone, whereas in the far periphery there is an increased incidence of midget bipolars contacting more than one cone (Wassle et al. 1994). There are six types of diffuse bipolar, which connect to a number of cones (5-10 in the central to mid-peripheral retina), including both M- and L-cones (Wassle 1999). Each L- and M-cone contacts at least one ON and one OFF midget bipolar and it is likely that they also contact at least one of each of the six types of diffuse bipolar cell (Wassle 1999). The ninth type of cone bipolar is the S-cone ON bipolar, which receives input from several S-cones (Kouyama and Marshak 1992), and is thought to be the only route for transport of S-cone ON signals. There does not appear to be an OFF bipolar for the S-cones, but there are indications that S-cones contact both midget and diffuse OFF bipolars (Calkins 1999). Only a single ON bipolar type has been identified for the rod system, which, in the primate, receives input from 15-40 rods, depending on retinal eccentricity (Wassle and Boycott 1991). The pathways of rod signals beyond the rod ON bipolar are discussed below in section 1.1.2 g.

The final neurons in the vertical pathways of the retina are the ganglion cells. The human retina contains a large variety of ganglion cells - over 20 types have been described, but the majority fall into two types, midget cells and parasol cells. Midget and parasol cells are found throughout the retina (Polyak 1941). Midget ganglion cells contact midget bipolar cells, retaining the ON/OFF convention. In and around the fovea there is 1:1 wiring between these neurons (Polyak 1941). In the peripheral retina, midget bipolars connected to single L- and M-cones converge onto midget ganglion cells, providing combined M- and L-cone input to these cells (Dacey and Lee 1999). Diffuse bipolars synapse with parasol ganglion cells, which are also of the ON or OFF type. The recently identified small bistratified ganglion cell receives input from S-cone ON bipolars and from a diffuse bipolar that is connected to M- and L-cones, producing a blue-ON/yellow-OFF response (Dacey and Lee 1994b).

Bipolar cell responses consist of sustained graded potentials. Ganglion cells on the other hand generate axon potentials, which are "all-or-none" responses. Ganglion cells either fire in a sustained manner during the duration of a stimulus or respond transiently to stimulus onset and/or offset.

e. Horizontal and amacrine cells

Lateral connections in the retina begin with the horizontal cells, which make connections with photoreceptors. There are at least two types of horizontal cell; the two types that have been identified are labelled H1 and H2 cells. Both H1 and H2 cells hyperpolarise in response to light. H1 cells preferentially contact L-and M-cones, and make no contacts or infrequent contacts with S-cones (Dacey et al. 1996). H1 cell axon terminals also contact rods (Kolb et al. 1980). It is thought, however, that there is no communication between the two ends of the cell, i.e. between rod and cone input (Wassle and Boycott 1991). H2 cells preferentially contact S-cones, and also receive summed input from L- and M-cones (Dacey et al. 1996), but do not contact rods (Kolb et al. 1980). Horizontal cells are thought to provide a feedback mechanism to the photoreceptors, and to possibly play a role in

generating receptive field surrounds of bipolars and ganglion cells (see sections 1.1.2 f. and 1.2.2).

The second stage of lateral connections in the retina involves the amacrine cells. Amacrine cells are numerous in type, which may be an indication of the number of different lateral pathways in the retina. Amacrine cells receive input from and make synaptic contacts with bipolars, other amacrines, and ganglion cells. The responses of only two distinct types of amacrine cell have been investigated. The first type of amacrine that has been characterised is the AI amacrine, which responds in an additive manner to signals from L- and M-cones (Dacey and Lee 1999). The second type of amacrine that has been characterised, the AII amacrine, plays an important role in the transport of rod signals in the retina (Wassle and Boycott 1991), see section 1.1.2 g. below. Little is understood about the specific functions of amacrines.

The responses of horizontal cells are in the form of sustained graded potentials. Different types of amacrine cell either produce sustained potentials or, like the AI amacrine, respond in a transient manner to the onset and offset of a stimulus (Dacey and Lee 1999).

f. Receptive field structure of ganglion cells

The receptive field of a neuron is the region of space, which when stimulated produces a change in the cell's response. Receptive fields are often described by maps that indicate whether an increase or decrease in the cell's activity occurs in response to the presence or absence of light in different regions of the field. Receptive field maps do not indicate how a cell responds to other stimulus characteristics such as movement. Early receptive field maps were obtained from recordings in the lateral geniculate nuclei (see section 1.1.4) of primates (Wiesel and Hubel 1966). The types of receptive field map found in the lateral geniculate nuclei (LGN) are also observed in ganglion cells.

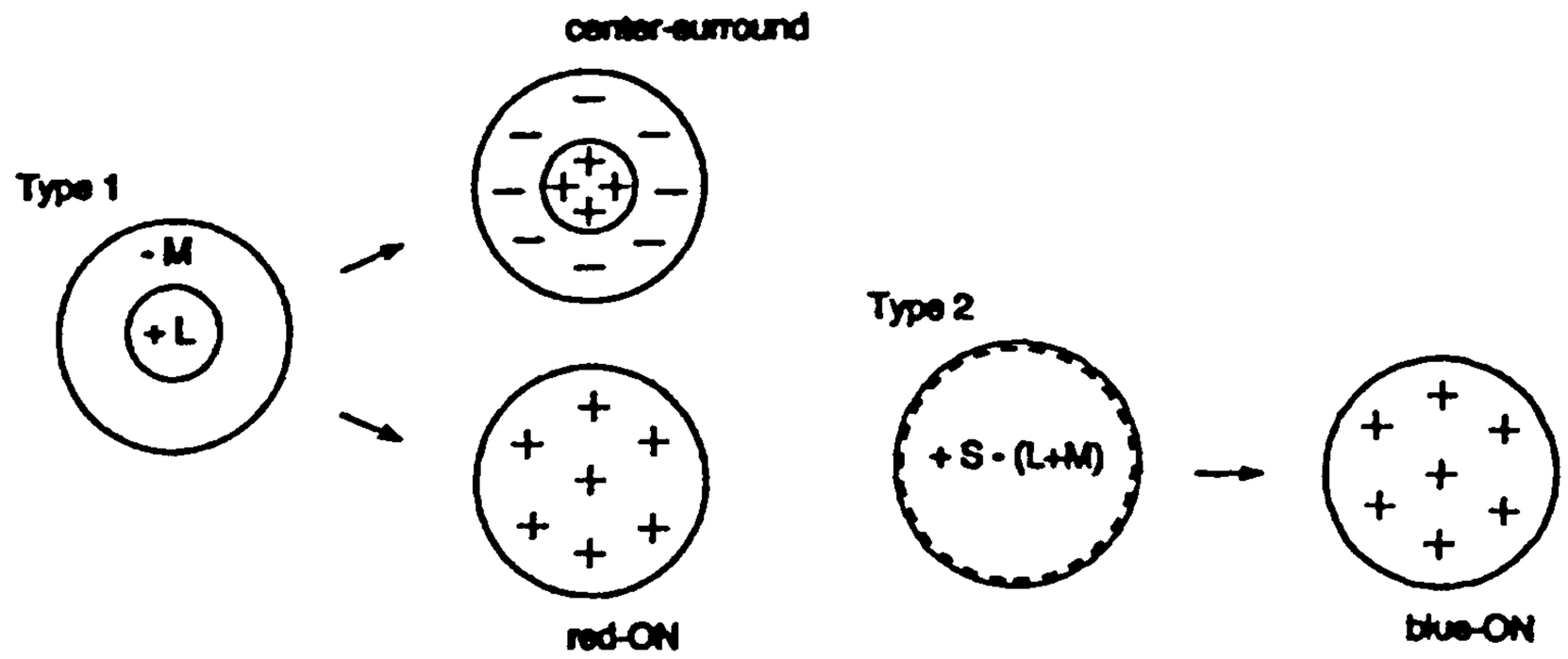

Figure 1-6. Representations of the receptive field structure of Wiesel and Hubel's Type I and Type II cells, reproduced from (Dacey 1996). See text for a description of each cell type.

Ganglion and LGN cell receptive fields have been shown to typically consist of either a concentric centre-surround organisation, meaning that the cells respond maximally to differential illumination of a central region and its surrounding area, or consist of opponent input from cones in a coextensive field. Wiesel and Hubel found three different groups of cells with the first type of receptive field organisation, which they termed Type I, Type III and Type IV cells. They found one class of cell with the latter receptive field organisation, which they termed Type II cells. Diagrammatic representations of Type I and Type II cells are shown in Figure 1-6. For a centre-surround cell with what is termed an ON centre receptive field, the cell is optimally stimulated by light covering the centre of the receptive field and not the surround, whereas light falling on the surround causes inhibition of the cells response. Similarly a cell with an OFF centre receptive field is excited maximally when light covers the surround and not the centre, and light falling on the centre results in response inhibition. Light falling on the whole receptive field of cells with an antagonistic centre-surround organisation, produces a weak response. Thus, these antagonistic centre-surround receptive fields signal contrast, with ON centre cells excited by positive contrast and OFF centre cells excited by negative contrast. Cells with coextensive receptive field inputs are ideal for signalling wavelength information, but no spatial information. It has been suggested that Type I and Type II cells do not form two distinct groups, rather that there is a continuum between these types of cell in the retina and LGN (Derrington et al. 1984; Reid and

Shapley 1992). The retinal circuitry underlying ganglion cell receptive field structure is discussed further in section 1.2.2 below.

g. Rod pathways

The primary pathway for signals originating in the rod receptors is via the rod ON bipolar; however, rod bipolar cells do not synapse with ganglion cells. The output of the rod bipolar is transferred to the AII amacrine cell, which in turn, feeds into the cone circuitry (Wassle and Boycott 1991). The output of AII amacrine cells either excites diffuse ON cone bipolar cells or inhibits diffuse OFF cone bipolars, which synapse with ON and OFF ganglion cells, respectively. There is also anatomical and human psychophysical and electrophysiological evidence for a second rod pathway (Daw et al. 1990; Sharpe and Stockman 1999; Bloomfield and Dacheux 2001). The physiological and psychophysical evidence suggests the presence of a slow sensitive rod signal, which is likely to be conducted through the primary rod pathway, and a fast, less sensitive signal that predominates at higher mesopic light levels. The anatomical origin of the pathway for this fast rod signal is via rod-cone gap junctions, whereby rod signals may be fed into cone bipolar-ganglion cell circuits at an earlier stage in the pathway. Rod input to ganglion cells varies with ganglion cells type. A strong input of rod signals to parasol ganglions can be detected at low levels of illumination (Lee et al. 1997). Small bistratified ganglions appear to receive no rod input; but a weak rod response can be recorded from midget ganglion cells (Lee et al. 1997).

h. Spatial organisation of the retina

There is substantial spatial variation across the retina, with the density, size and arrangement of each type of retinal cell changing with eccentricity. The region of the retina responsible for signalling the finest spatial detail is the fovea. When one looks directly at an object (fixates an object) the image of that object falls on the fovea. There is a small depression in the retina at this location caused by lateral displacement of cells in the inner retinal layers, leading to a thinning of the retinal structure, and creating a more direct path for light to reach the photoreceptors (see Figure 1-7). The absence of blood vessels in the centre of the fovea, however, is the

primary factor responsible for the reduction in light scatter and absorption at this location.

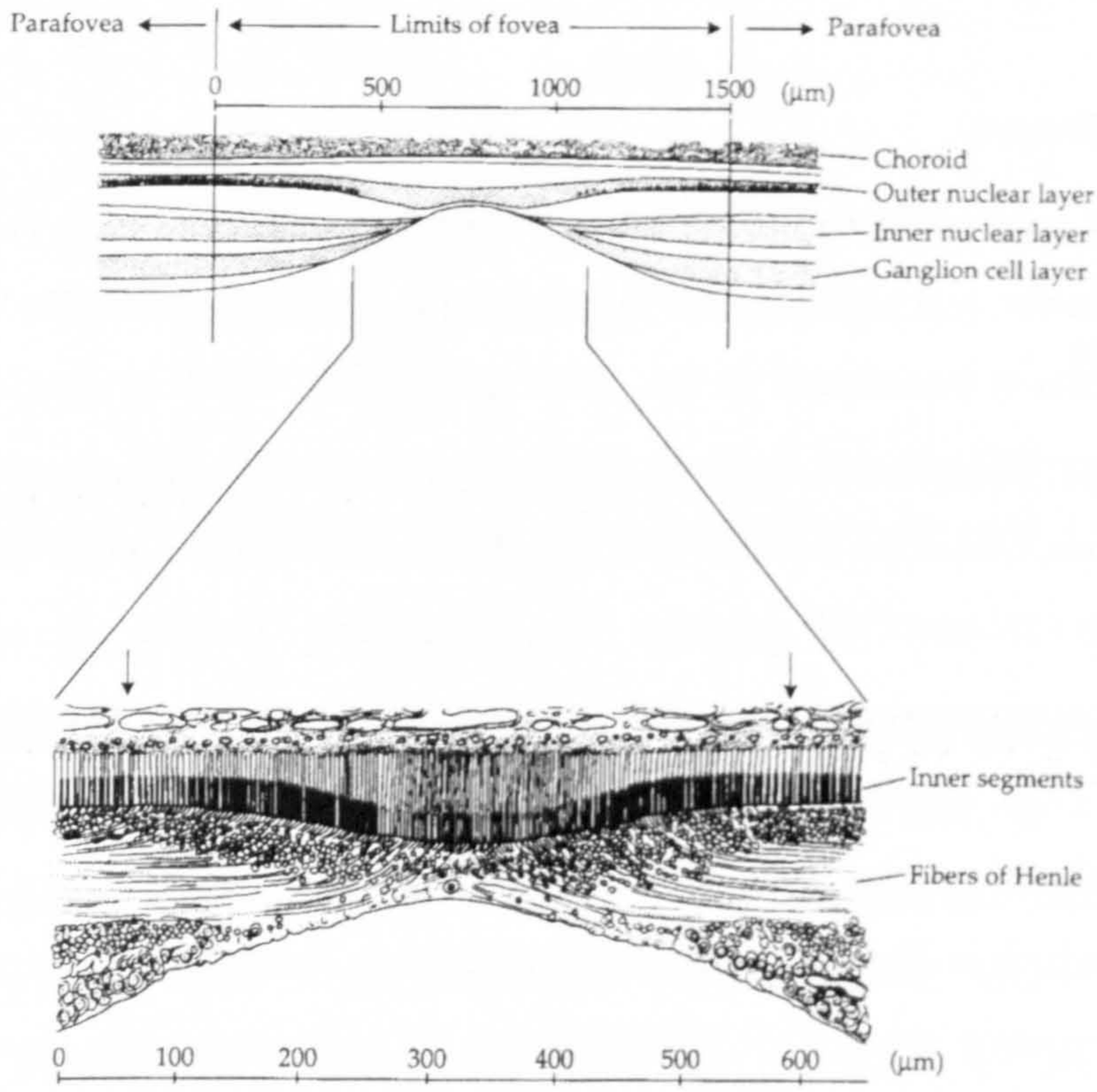

Figure 1-7. Thinning of the retina at the fovea due to the lateral displacement of cells in the inner retinal layers. Reproduced from (Oyster 1999).

The outer segments of cones in the fovea are long and thin, allowing the highest density of these cells found over any area in the retina: 120,000 to 324,000 cones/mm^2 (Curcio et al. 1990). There are also a greater number of 1:1 vertical pathways to the optic nerve from foveal cones. The almost flat central area of the fovea is known as the foveola. There are no rod receptors in the centre of the foveola, over a region corresponding to about 1° visual angle (Osterberg 1935). S-cones are also absent from the central foveola over a small area that falls within the rod free region. The area surrounding the fovea is known as the parafovea, which extends up to about 8° visual angle, and the region beyond this up to about 20° is called the perifovea. These regions are classified by the thickness of different retinal layers within them.

There are approximately 4.5 million cones in the retina and 91 million rods (Curcio et al. 1990). The distribution of cones falls abruptly outside the fovea to 4-5000

cones/mm^2, and thereafter declines slowly to a minimum of 3000 cones/mm^2 in the periphery (Osterberg 1935; Curcio et al. 1990). The maximum density of S-cones occurs between 0.1 - 0.3 mm eccentricity, and is greater than 2000 S-cones/mm^2 (Curcio et al. 1991). The S-cones account for 4-8% of the total number of cones. In-vivo estimates of the percentage of L- and M-cones in two colour normal subjects, obtained using a combination of adaptive optics and retinal densitometry, produced values of 50.6-75.8% and 20.0-44.2% for the L- and M-cones, respectively (Roorda and Williams 1999). Psychophysical estimates of the relative numbers of L- and M-cones suggest that, on average, L-cones outnumber M-cones by a ratio of 2:1 (Kremers et al. 2000). Rod density grows from 0 rods/mm^2 at the centre of the foveola to a peak density of roughly 190,000 rods/mm^2 at an eccentricity of about 20°, dropping to a value of 60,000-70,000 at the extreme periphery (Osterberg 1935; Curcio et al. 1990). Photoreceptors are absent over the area of the optic disc, which causes a physiological "blind spot" in the visual field corresponding to an area of 5-6° horizontally and 7-8° vertically, positioned at about 16° temporally. The number of ganglion cells in the human retina is estimated to be between 0.7 to 1.5 million. The density of ganglion cells peaks just outside the fovea at roughly 35,000 cells/mm^2 and gradually drops to a level of about 100 cells/mm^2 in the extreme periphery (Curcio and Allen 1990).

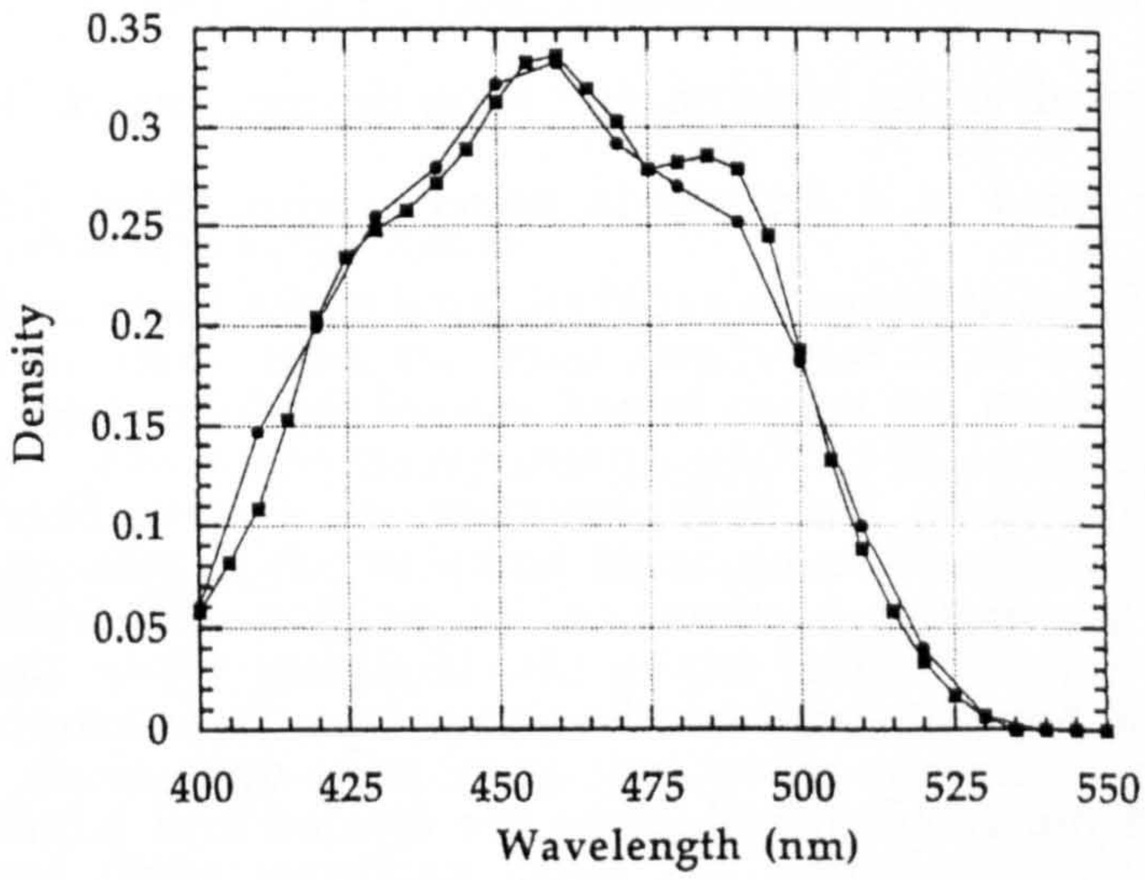

Figure 1-8. The optical density of the macular pigment, reproduced from (Pokorny and Smith 1997). The circles indicate the function proposed by Vos (1972), and the squares show the data of Wyszecki and Stiles (1967; 1982). The two functions have been normalised to produce curves of equal area.

Another topographical feature of the retina is the macula lutea; a region of yellow pigment (known as the macular pigment) that permeates the inner layers of the retina and covers the fovea and much of the parafovea (Wyszecki and Stiles 1982; Vos 1972). Macular pigment density has been estimated from the differences between measurements of absolute threshold obtained at the fovea and in the periphery where there is little or no density of pigment (Wald 1945a; Wyszecki and Stiles 1967), or from the differences between foveal and peripheral colour matches (Ruddock 1963). The macular pigment absorbs light in the short to middle wavelength region of the spectrum, with peak absorption occurring at 460 nm. The optical density spectrum of the macular pigment is shown in Figure 1-8.

1.1.3 The optic nerve, optic chiasm and optic tracts

a. The optic nerve

Coded signals emerge from the ganglion cells and travel along the optic nerve and optic tracts to reach the lateral geniculate nucleus and finally the cortex; constituting the primary visual pathway (see Figure 1-9). The 1 million or so ganglion cell axons traverse the retina to converge at the optic nerve head. The optic nerve head is positioned nasally in the retina just below the horizontal meridian, giving rise to the physiological "blind spot", described in section 1.1.2 h. The bundles of ganglion cell axons exit the eyeball at this location, and form the optic nerve. The axons travel to the optic nerve head in a systematic pattern, with fibres from ganglion cells temporal to the fovea arranged to avoid crossing of the fovea itself, see Figure 1-10. Axons emanating from the region in and around the fovea form what is known as the pupilomacular bundle. The initial arrangement of nerve fibres within the optic nerve relates to the relative positions of the ganglion cells from which the fibres originate, with the pupilomacular bundle occupying a large temporal section. At the optic nerve head the ganglion cell axons are divided into bundles before passing through the collagenous structure, the laminar cribrosa, after which the axons gain a myelin sheath (wrapping that increases the speed of action potential propagation). The optic nerves from each eye run though their respective optic canals and merge to form the optic chiasm, from which the optic tracts emerge. The arrangement of axon bundles within the optic nerve at this point is shifted relative to the

arrangement at the optic nerve head, with the pupilomacular bundle occupying the central region surrounded by axons from gradually more peripheral regions of the retina, as shown in Figure 1-10.

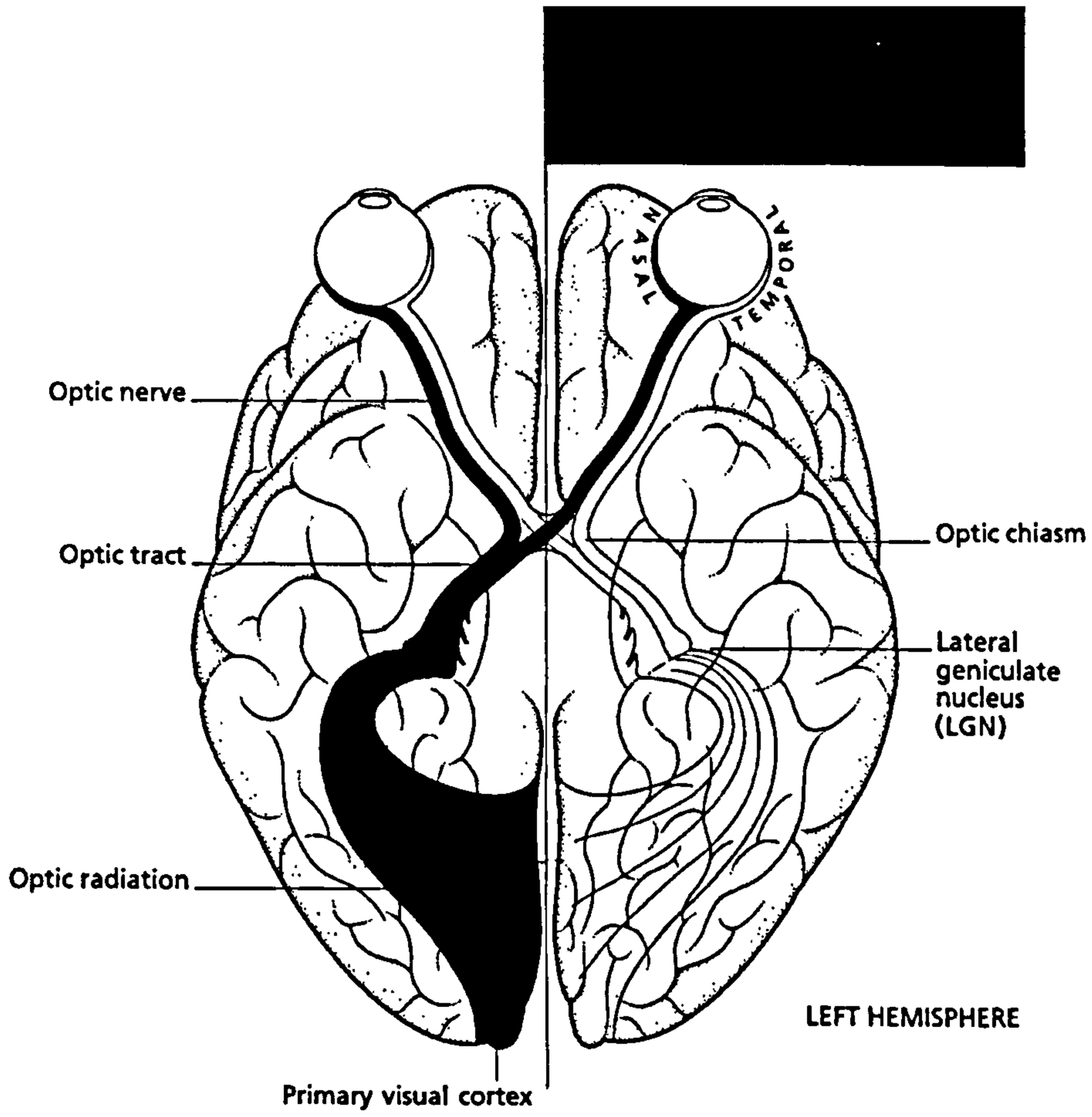

Figure 1-9. The primary visual pathway, reproduced from (Zeki 1993).

b. The optic chiasm and optic tracts

At the optic chiasm, fibres from the nasal hemiretinas cross from their respective optic nerves to the optic tracts transporting signals to the contralateral side of the brain. Fibres originating in the temporal hemiretinas travel along the optic tracts transporting signals to the ipsilateral side of the brain. This process is known as decussation. The decussation of axons in the chiasm appears to be imperfect, with some nasal retinal fibres travelling along the ipsilateral optic tract and some temporal retinal fibres crossing over to the contralateral tract, leading to a double representation of the fovea in each hemisphere of the visual cortex (Bunt and Minkler 1977; Fukuda et al. 1989). There is further reorganisation of the

arrangement of neuronal fibres within the optic tracts before reaching their target destinations.

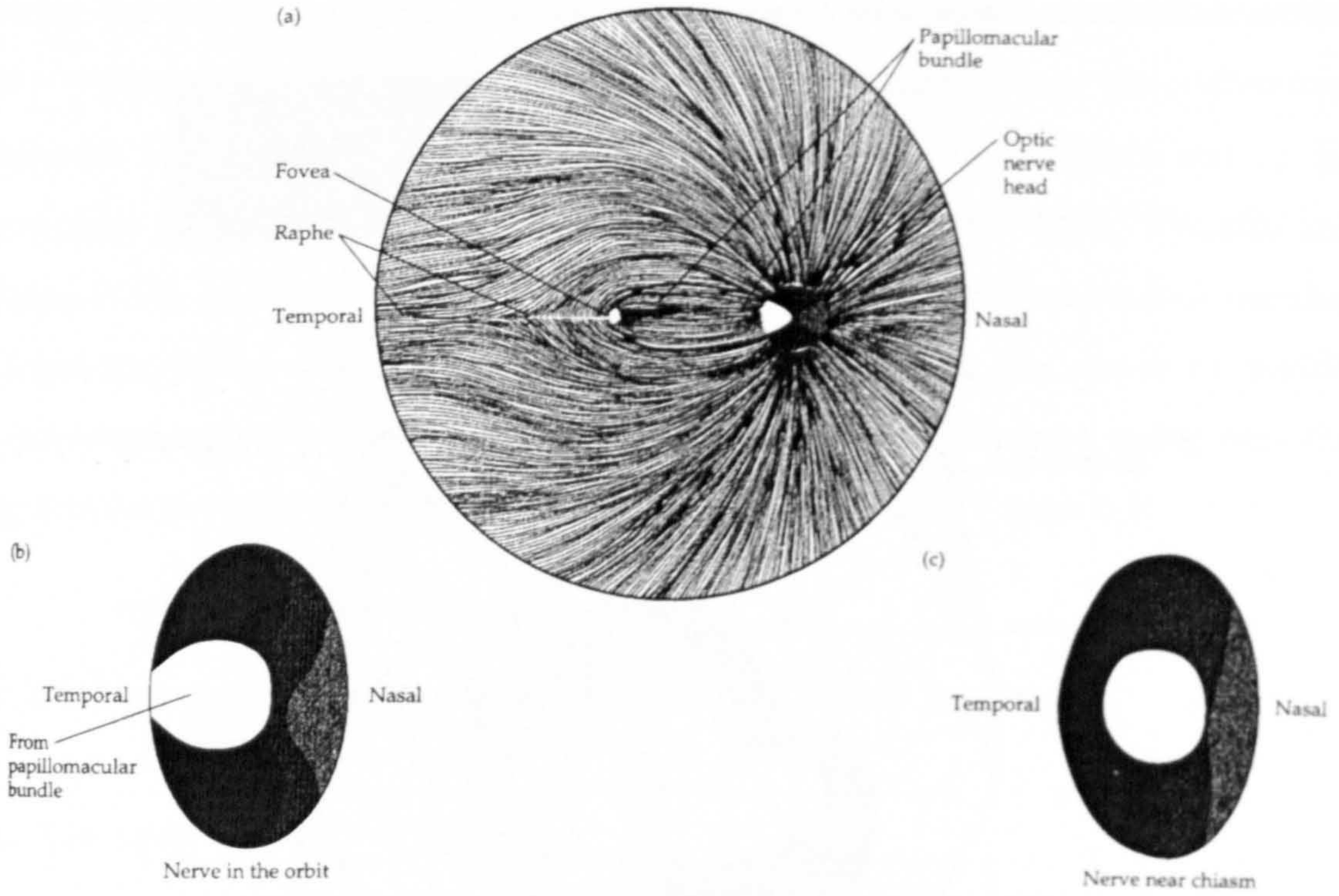

Figure 1-10 (a)-(c). The pattern of ganglion cell axons as they traverse the retina to form the optic nerve (a). The distribution of axons in the optic nerve, originating from different areas of the retina, before leaving the orbit (b), and near the optic chiasm (c). Reproduced from (Oyster 1999).

1.1.4 The lateral geniculate nuclei and other subcortical nuclei that receive retinal projections

a. The lateral geniculate nuclei

The vast majority of ganglion cell axons terminate in the lateral geniculate nuclei (LGN), through which information is relayed to the primary visual cortex. The lateral geniculate nuclei in primates (shown in Figure 1-11) are traditionally described as comprising six distinct layers, but interlaminar regions have also been identified (Kaas et al. 1978; Jones and Hendry 1989). The ventral layers, numbered 1-2, are made up of neurons with large cell bodies and termed the magnocellular layers. The dorsal layers, numbered 3-6, consist of small-bodied nerve cells and are termed the parvocellular layers. The interlaminar regions are also termed koniocellular layers because the neurons in these regions have the smallest cell

bodies and the regions can be quite distinct in some species. In general, the axons of parasol ganglion cells project to the magnocellular layers of the LGN, forming what is termed the magnocellular pathway; and the axons of midget ganglion cells project to the parvocellular layers, forming what is known as the parvocellular pathway (Perry et al. 1984). Cells of the parvocellular and magnocellular pathways are often referred to as P-cells, and M-cells, respectively. There is evidence that neurons in the koniocellular layers constitute a third pathway from the retina to the visual cortex (Casagrande 1994); the koniocellular layer cells projecting to cortical regions known as blobs (Hendry and Yoshioka 1994), which are believed to be colour selective (see section 1.1.5 c). It has been reported that the small-bistratified ganglion cells project to the parvocellular layers of the LGN (Rodieck 1991), but blue-ON cells have also been identified in the interlaminar regions of the primate LGN, suggesting that the blue-yellow colour channel may be part of this third visual pathway (Martin et al. 1997). The two lateral geniculate nuclei provide differentiation of information pertaining to each half of the visual field. The left LGN receives input from the right hemifield and the right LGN input from the left hemifield. There is also separation of information from each eye within each LGN. Layers 1, 4 and 6 receive input from the contralateral eye, and layers 2, 3 and 5 from the ipsilateral eye.

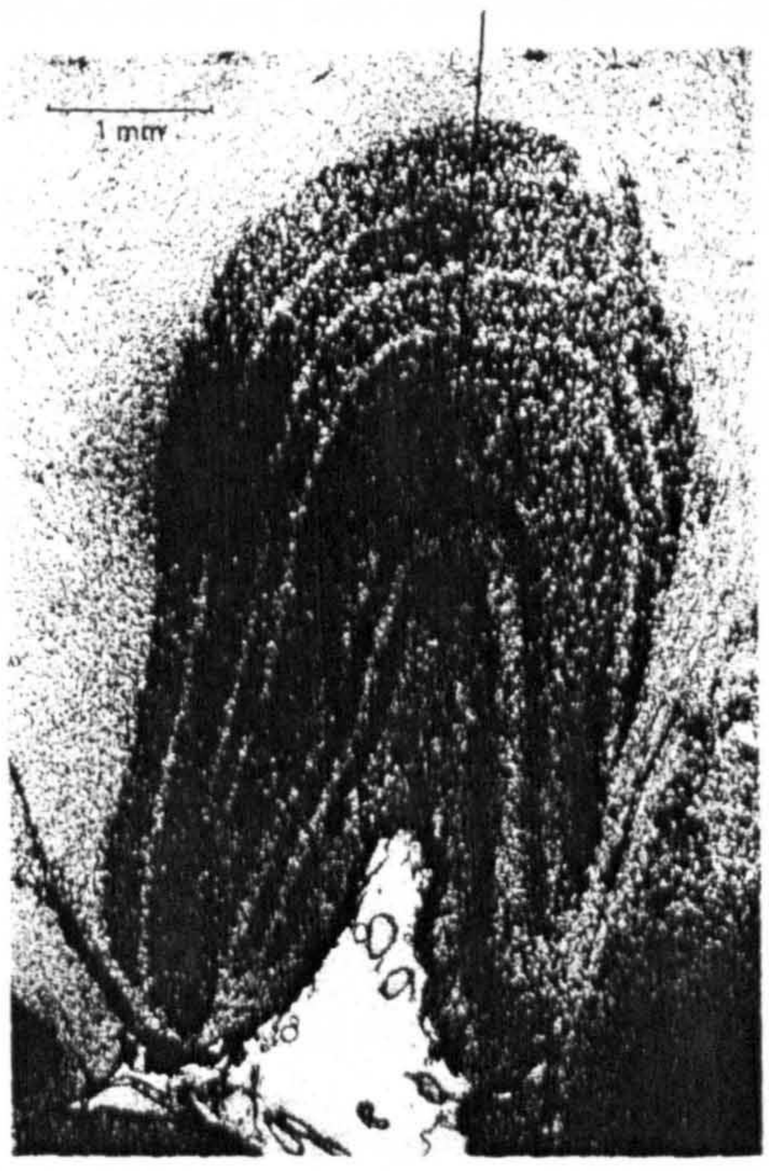

Figure 1-11. The layered structure of the lateral geniculate nucleus (LGN), reproduced from (Zeki 1993).

Mapping of the retina onto the LGN retains the spatial organisation of the ganglion cells, with the fovea and parafovea given an enlarged spatial representation compared to the periphery of the retina. Thus the LGN contains overlapping representations of the visual field arising from different types of ganglion cells. Representations in different layers of the LGN are in register (aligned), so that a single point in the visual field is mapped in up to six points in different layers of the LGN, falling along a single dorsoventral projection line through the LGN (Walls 1953).

b. Receptive fields, and the magnocellular and parvocellular pathways

Receptive fields of LGN cells may be made up of inputs from several ganglion cells, but the response properties of LGN cells are very similar to those of their retinal inputs. The majority of neurons in the lateral geniculate nuclei have antagonistic centre-surround receptive fields. Cells in the magnocellular layers do not have wavelength-specific responses, but have receptive field centres with summed input from L- and M-cones. Cells with centre-surround receptive fields in the parvocellular layers may be wavelength-specific or respond to a broadband of wavelengths. The parvocellular layers 5 and 6 consist predominantly of cells with ON centre receptive fields, while those in layers 3 and 4 consist of mostly OFF centre cells (Schiller and Malpeli 1978). In the magnocellular layers there is no segregation of ON and OFF centre cells. LGN cells appear to be less sensitive than ganglion cells to illumination of both centre and surround of their receptive fields, leading to an enhancement of the antagonistic signal (Hubel and Wiesel 1961). The parvocellular layers also contain Type II cells, which exhibit wavelength-specific responses. The coding of colour by midget and small bistratified ganglions, which project to the parvocellular LGN, is discussed in section 1.2.2 below.

M-cells are tuned to achromatic modulation and P-cells chromatic modulation, although P-cells can also respond to appropriate spatiotemporal input. M- and P-cells have comparable responses to their ideal stimuli (Lee 1996). The size of the receptive field centre of an M-cell is related to the spread of its dendrites (Dacey and Lee 1994a). The centre size of a P-cell 's receptive field may be determined by

dendritic spread, but the centre size of a midget ganglion in and around the fovea is determined by the size of a single cone. Anatomically there is a large difference between the receptive field centre size of M- and P-cells. Thus, the retina is sampled over two spatial scales. M- and P-cells also differ in their temporal responses, with M-cells exhibiting a band-pass response to luminance modulation, peaking at 20-40 Hz under photopic conditions, compared to the low-pass temporal response of P-cells to chromatic modulation, which falls off above 20-30 Hz (Lee et al. 1989; Lee et al. 1990).

c. Other nuclei that receive ganglion cell input

Other destinations of the 10% of optic tract fibres that do not terminate in the LGN include the superior colliculus, the pretectal nuclei, the accessory optic system, and the suprachiasmatic nucleus. The superior colliculus is also a layered structure, within which the retinal projections provide a representation of the contralateral visual field in the right and left portions of the structure. These inputs originate from ganglion cell types other than parasol or midget cells. The interaction of these inputs along with inputs from the cortex and subcortical areas, including signals from other sensory systems, is thought to be involved in the onset of saccadic eye movements. The pretectal nuclei also receive input from ganglion cell axons, in particular the nucleus of the optic tract and the pretectal olivary nucleus. The activity of the nucleus of the optic tract appears to be linked to eye movements and possibly has a role in optokinetic nystagmus (alternating fast and slow eye movements associated with movement). The pretectal olivary nucleus forms part of the pupillary light reflex. The bilateral projection of axons of the pretectal olivary to other nuclei in the light reflex pathway is responsible for constriction of the pupil in both eyes in response to light shone in one eye (the consensual reflex). There are also small retinal inputs to what is termed the accessory optic system, which is thought to be involved in the coordination of eye and head movements. The suprachiasmatic nucleus is involved in the regulation of the body's biological clock that is responsible for generating the circadian rhythms of certain bodily functions. The suprachiasmatic nucleus also receives input from retinal ganglion cell axons.

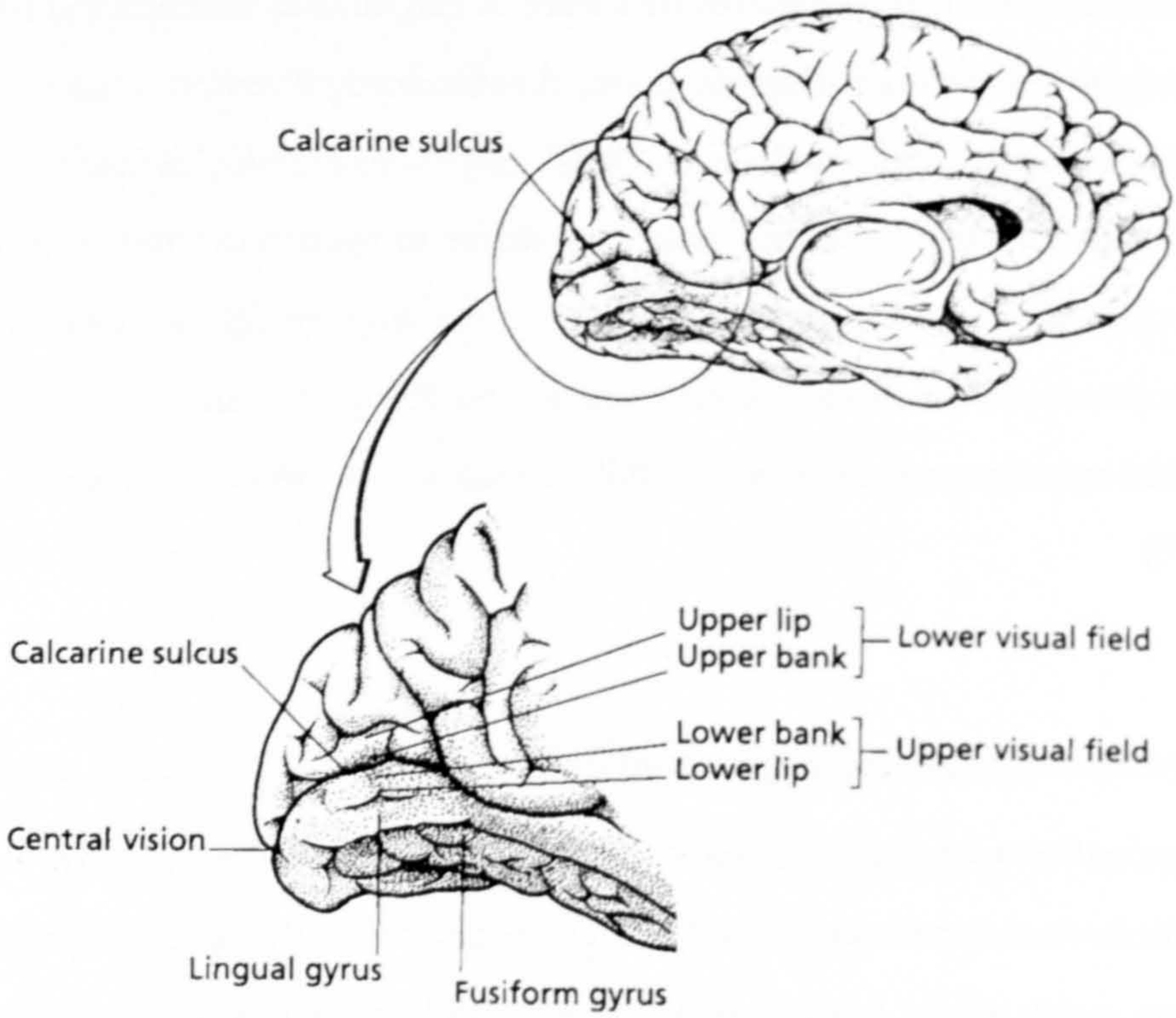

Figure 1-12. The visual cortex, reproduced from (Zeki 1993).

1.1.5 The visual cortex

The destination of neuronal axons originating in the lateral geniculate nucleus is the primary visual cortex, otherwise known as the striate cortex due to its striped appearance. The bundle of fibres linking the LGN with the cortex are termed the optic radiations. The primary visual cortex, otherwise known as V1, is located in the occipital lobe of the cerebral cortex (shown in Figure 1-12). It is found on the medial side of each cerebral hemisphere deep within what is known as the calcarine sulcus, see Figure 1-13. There are two main types of cortical neurons, pyramidal cells and granule cells (otherwise known as stellate cells), named after their cell body shape and spread of their dendrites. Pyramidal cells often project to distant cortical sites or subcortical targets, whereas stellate cells tend to make intracortical connections. The cerebral cortex consists of six layers of cell bodies, collectively termed grey matter. White matter, consisting of axons carrying input and output signals, underlies these cellular layers.

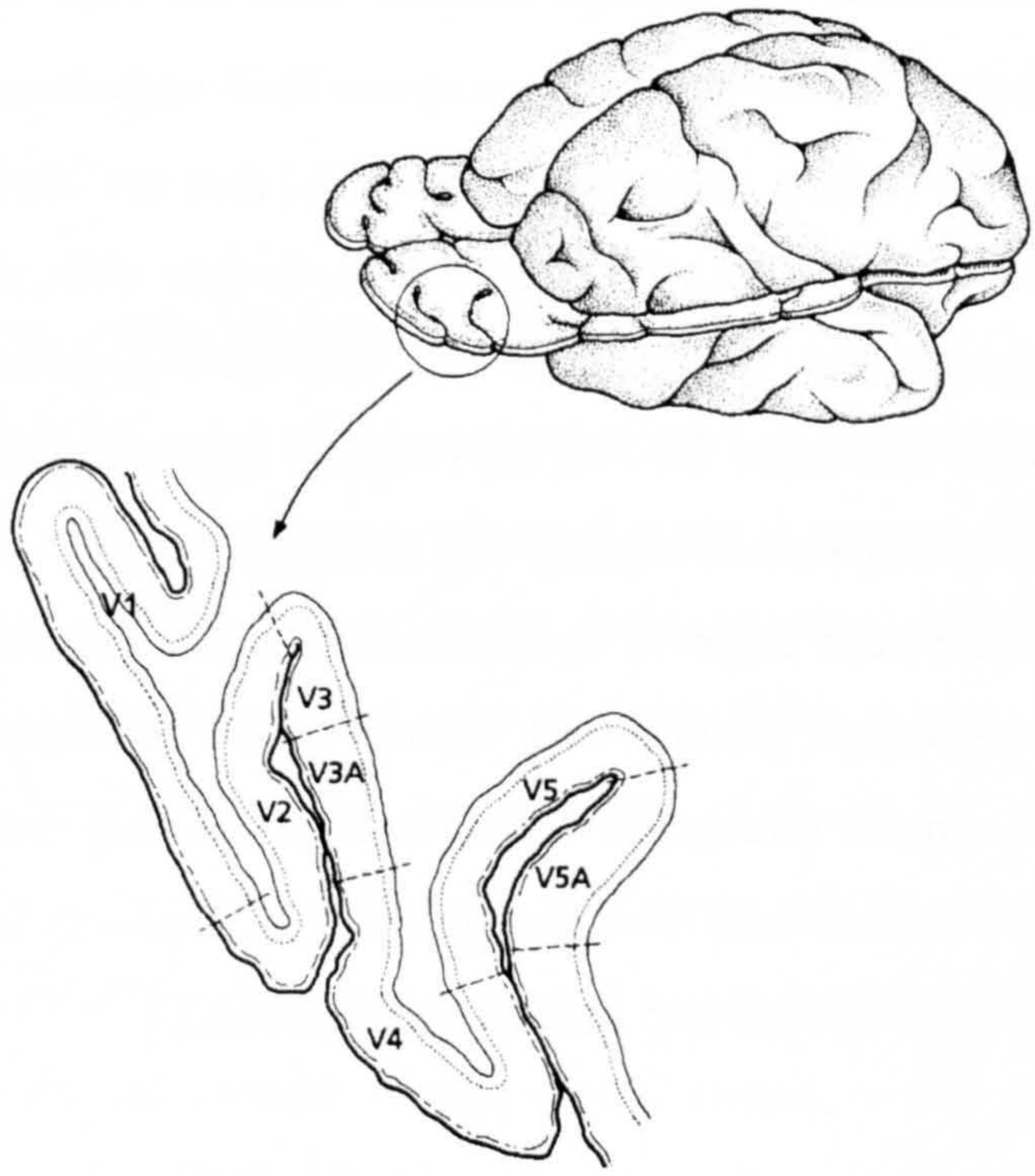

Figure 1-13. Location of the primary visual cortex, V1, and extra striate areas V2-V5a. Reproduced from (Zeki 1993).

Separate subdivisions of layer 4 (4Cα, 4Cβ) in the primary visual cortex receive the main input from the magnocellular and parvocellular layers of the LGN. This layer consists mainly of granule cells, whereas the other cortical layers consist mainly of pyramidal cells. The right LGN projects to layer 4 in the right hemisphere and the left LGN to layer 4 in the left hemisphere, in this way the right and left hemispheres contain a complete representation of the contralateral halves of the visual field. These representations retain the enlarged spatial weighting given to the fovea with respect to the periphery, found in the LGN. This change of spatial organisation from the retina to the cortex is described as the cortical magnification factor. The cells of layer 4 project to more superficial layers in V1 (layers 2 and 3) and other cortical areas. Cells in the remaining layers of the visual cortex connect to specific targets either within the cortex or in subcortical areas.

a. Receptive fields of cortical neurons

The response characteristics of cortical neurons are generally more complex than those of ganglion cells or geniculate cells. Cortical cells have been categorised by

their receptive fields into concentric, simple, complex and hypercomplex cells. Concentric cells have a centre-surround receptive field organisation. These cells are found in layer 4 of V1, they respond monocularly, and are likely to receive direct input from the LGN (Hubel and Wiesel 1968). Simple cells also have receptive fields that are arranged into antagonistic ON and OFF regions, but organised in parallel bands. There are often ON or OFF bands separating an opposing central strip, or there may be adjacent excitatory and inhibitory bands, an example is shown in Figure 1-14. These cells respond to an incremental or decremental bar of light with a specific orientation (Hubel and Wiesel 1962). A moving bar of correct orientation may be a more effective stimulus than a stationary one, but the direction and velocity of movement may also be critical. The majority of simple cells are located in layer 4 of V1, but are also present in other layers..

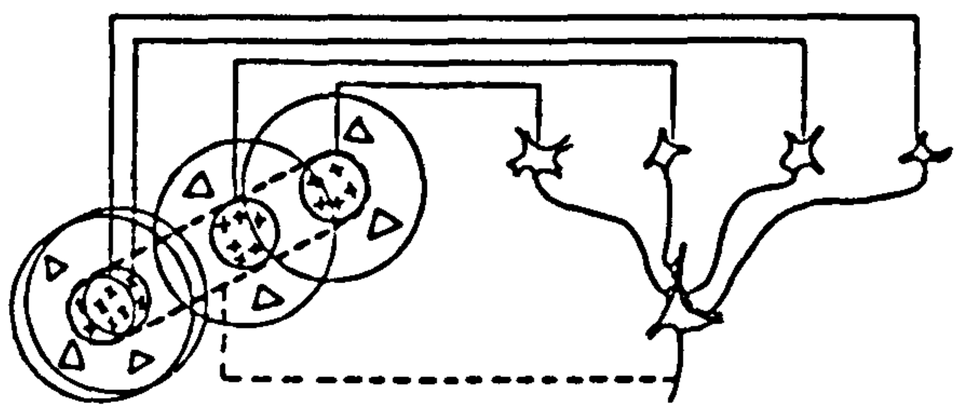

Figure 1-14. Diagram of the receptive field structure of simple cells in the visual cortex. Inputs from ON centre LGN cells make up the ON centre region of the simple cell. Reproduced from (Hubel and Wiesel 1962).

Complex cells do not have receptive fields that can be characterised by excitatory and inhibitory regions. These cells respond to a stationary or moving bar of preferred orientation throughout their receptive field (Hubel and Wiesel 1962). Complex cells are rare in layer 4, but are found in more superficial and deeper layers. These cells often receive input from both eyes. Hypercomplex cells are similar to complex cells, but respond optimally to a bar of specific length (Hubel and Wiesel 1965). These cells are only found outside V1. Hubel and Wiesel (1962; 1965) suggested that cortical neurons increase their required stimulus specificity the further they occur along the path of information processing. They proposed that simple cells were constructed from a linear arrangement of concentric cell receptive fields, and that complex cells receive inputs from several simple cells with the same orientation preference. These authors further proposed that hypercomplex cell

input originates from two or more complex cells with identical orientation preferences.

b. Orientation and ocular dominance columns

The orientation specificity of simple, complex and hypercomplex cells lead to an important feature of the organisation of visual cortical neurons. Cells of a particular orientation are grouped together within the cortex in what are known as orientation columns that travel perpendicular to the surface of the cortex. Adjacent columns differ in orientation systematically, by an angle of about 10° (Hubel and Wiesel 1974). Cells within a column correspond to a particular region of the visual field, and cells in neighbouring columns correspond to neighbouring areas of visual field. A further organisational feature of the visual cortex is the presence of ocular dominance columns. Cortical cells that have binocular input have receptive fields that are identical for the two eyes in terms of size and specificity, and correspond to contralateral areas of the visual field, but usually receive a stronger input from one eye. This leads to an arrangement of cortical cells in columns that correspond to the ocular dominance (right or left) of their input (Hubel and Wiesel 1968).

c. Further functional segregation in the cortex

Within the primary visual cortex there are zones that have been called blobs, which differ from their surrounding regions, labelled interblobs. These zones were identified by cytochrome staining; they are located within the centre of ocular dominance columns and are in register throughout the layers of the cortex. Some neural cells within the blobs have concentric centre-surround receptive fields, which appear to code both form and colour, and others respond to all wavelengths of light, but neither show orientation specificity (Livingstone and Hubel 1984). Cells in the interblob regions have orientation but no wavelength specificity (Livingstone and Hubel 1984). Cells receiving inputs from parvocellular neurons in the LGN connect to cells in the blob and interblob regions, whereas magnocellular projections appear to be routed to layer 4B in V1. Fibres within the blob and interblob zones project to distinct thin striped regions in the cortical area adjacent to V1, known as V2 (Livingstone and Hubel 1984). Neurons from layer 4B, on the

other hand, project to distinct thick striped regions in V2 (Livingstone and Hubel 1987). These thick and thin stripes in V2, in turn, connect with different visual areas in the cortex (Shipp and Zeki 1989b; Shipp and Zeki 1989a). In this way the magnocellular and parvocellular pathways remain largely distinct from the retina to the cortex. This functional segregation is illustrated in Figure 1-15.

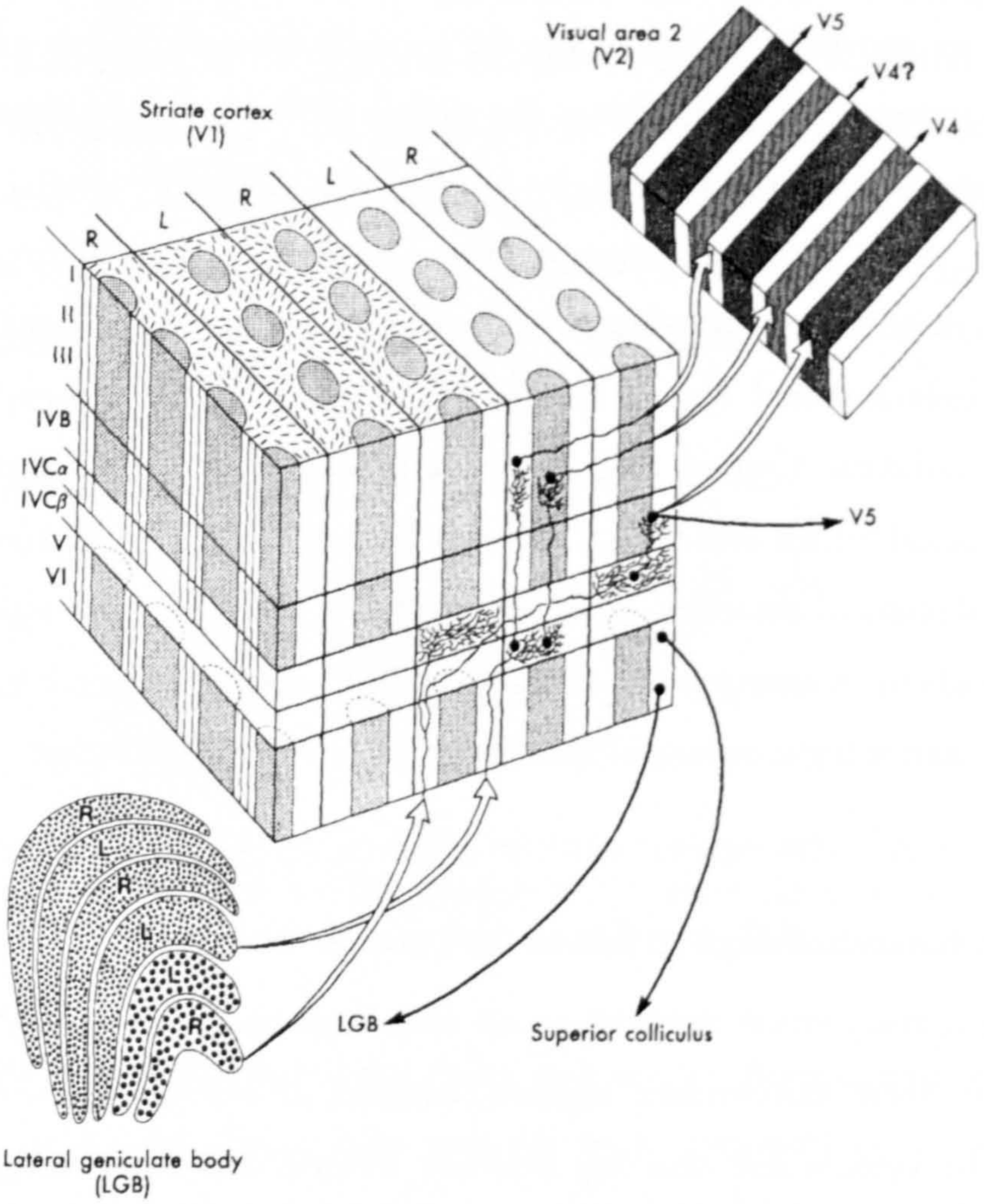

Figure 1-15. Structural organisation of V1. The figure depicts orientation columns and blobs in V1, and illustrates that input signals from the LGN to layers 4Cα and 4Cβ are transported to other layers in V1 and either onto prestriate cortical areas, or return to the LGN, or project to other subcortical nuclei. Reproduced from (Hart Jr. 1992).

The cortex of the occipital lobe, anterior to V1, contains many representations of the contralateral visual field in areas that are part of what is known as the prestriate cortex. These areas extend into the parietal and temporal lobes of the brain. Some of these areas appear to be tuned for processing particular aspects of visual information. The area immediately anterior to the primary visual cortex is V2, which

was introduced above. V2 receives major input from V1 and has the same retinotopic organisation, with the vertical meridian of the visual field forming the border between these two areas. V2 neurons extract more specific information from the visual field map than V1 neurons, as they consist mostly of complex cells with some hypercomplex cells. As described above, the distinct areas (stripes) in V2 continue the functional segregation of information in the visual pathway. Area V3, which surrounds V2, also contains a topographical map of the retina. V3 receives projections from layer 4B in V1 and the thick striped regions in V2. V3 consists mainly of orientation-specific cells and is likely to be associated with the processing of form (Zeki 1978). V4 receives its major input from the thin stripes in V2, with a small input from V1 (DeYoe and Van Essen 1985; Shipp and Zeki 1985). V4 consists mostly of complex cells, and appears to be involved in the processing of colour and form, with most of the cells being colour selective (Zeki 1973). Area V5, otherwise known as MT, is thought to be involved in motion processing as its cells exhibit a strong preference for movement in a particular direction (Zeki 1974). Neurons in layer 4B of V1 project to V5, along with neurons in the thick stripes of V2 (DeYoe and Van Essen 1985; Shipp and Zeki 1985). The segregation of neurons on the basis on physiological function that begins in the LGN appears to diverge in the visual cortex, forming the first stages of information extraction from the visual field.

1.2 Colour vision

The current understanding of human colour vision has developed over the last three and a half centuries. It was Isaac Newton in the late 17th and early 18th century who first realised that colour is a sensation not a property of the electromagnetic radiation that we refer to as light. He also realised that the sensation of colour associated with an object is related to the spectral reflectance of the object. The next major advancement was made by Thomas Young, which he presented in 1801. He believed that it was inconceivable for the number of receptors in the eye to equal the number of colours seen, and proposed that there were only three colour receptors in the eye, which could be differentially activated by the light stimulus.

This idea later became known as the trichromatic theory of colour vision. James Clerk Maxwell took up Young's trichromatic theory in the mid 19th century, carrying out colour mixing experiments, which formed the basis of modern colour specification and colorimetry. Further support for trichromacy came at about the same time from Hermann von Helmholtz, who proposed that trichromacy was possible if there were three receptors within the eye with overlapping spectral sensitivity curves. Trichromatic theory, however, was thought to be at odds with the subjective appearance of colours, which led Edwald Hering in the 1870s to propose his opponent colour theory. Hering noted that there were four primary colour sensations: red, green, yellow and blue, but that yellowish blues and reddish greens were never seen. He suggested, therefore, that colour sensations arose from colour-opponent processes, with red opponent to green and yellow opponent to blue. These two colour vision theories were thought to be incompatible, but reconciliation came with the suggestion that both theories could be accommodated in a zone model of colour vision; with trichromacy holding at the receptor level, and the opponent colour theory holding at some later stage of processing.

1.2.1 Trichromacy and cone spectral sensitivities

The coding of colour in the visual system begins at the level of the cone photoreceptors. Colour vision is only possible over the operating range of the cones, i.e., under photopic or mesopic conditions. Under scotopic conditions humans have no colour vision, and it is generally believed that rods play little or no part in colour vision throughout the mesopic range (see section 1.3.3, however, for a further discussion of this topic). The probability that a photon is absorbed by a photoreceptor is wavelength dependent, but the response of an individual photoreceptor relates only to the number of photons absorbed and signals no information about the wavelength of light; this is known as the principle of univariance. The basis of trichromacy is the existence of three photoreceptors in the eye with overlapping spectral sensitivities; hence, the probability of absorption of a photon of a particular wavelength differs for the three types of cone.

A number of different methods have been employed to verify the existence of, and determine the spectral sensitivities of the three types of cone photoreceptor (L-, M-, and S-cone). Direct measurements of photopigment absorption spectra have been carried out using retinal densitometry, microspectrophotometry and suction electrode recordings. The method of retinal densitometry involves passing light into the eye and measuring the intensity that is reflected back through the pupil. From such measurements the amount of light absorbed by the photopigments as it travels into and back out of the eye, can be inferred, once losses due to absorption by the pigment epithelium are accounted for. Rushton's investigations using retinal densitometry (Rushton 1963; Rushton and Baker 1964; Baker and Rushton 1965) confirmed the existence of the rod photopigment, plus both a middle-wavelength sensitive and a long-wavelength sensitive cone photopigment in the normal human eye, and the absence of the long-wavelength sensitive cone photopigment in protanopia; a particular type of human colour vision deficiency thought to arise from an absence of L-cones (see section 1.2.10). The technique has shortfalls in determining photopigment spectral sensitivity curves, however, because it does not permit measurement of photopigment spectral sensitivity in the tails of the curves where sensitivity is low. Microspectrophotometry involves measuring the spectral transmission of a small beam passed through the outer segment of an individual cone in vitro, compared to a reference beam. Results of measurements using microspectrophotometry have verified the presence of three types of cone photoreceptor in the normal human eye plus the rod receptors, containing photopigments with peak sensitivities in different regions of the visible spectrum (Dartnall et al. 1983). The procedure was also used to provide evidence in support of the belief that the colour vision deficiency deuteranopia arises from an absence of the middle-wavelength sensitive photopigment. Although microspectro-photometry allows relatively accurate measurement of photopigment peak sensitivity (λ_{max}), measured curves differ in the tails from those determined from indirect methods (Stockman and Sharpe 2000). The procedure for measuring the electrical response of a single cone to light by drawing its outer segment into a tiny electrode, is known as suction electrode recording. Suction electrode recordings have been obtained from L-cones (Kraft et al. 1998), and found to agree with cone spectral sensitivity curves derived from indirect methods.

Prior to successful physical measurements, indirect estimates of cone spectral sensitivities were achieved, based on psychophysical data. The spectral sensitivity of the three cone types can be derived from the results of colour matching experiments. Colour normal observers are termed normal trichromats. A trichromat can match one half of a bipartite field filled with a monochromatic test light, by altering the intensities of three primary lights presented in the opposite half of the field. For some test wavelengths a proportion of one or two primaries must be added to the test field to achieve a match. Any set of colour stimuli constitutes a set of primaries if each primary cannot be matched by an additive mixture of the other two; primaries are typically red, green and blue. The relative proportions of three monochromatic primary lights required to match monochromatic test lights taken from the equal energy spectrum (unit radiant power at every wavelength), constitute colour matching functions (CMFs). Any set of CMFs based on three primaries can be linearly transformed into CMFs for any other set of primaries; the fundamental CMFs are equivalent to the cone spectral sensitivity functions measured at the cornea. In 1931 the Commission Internationale de L'Eclairage (CIE) defined a standard colorimetric observer with colour matching properties representative of normal trichromats. The CIE colorimetric observer is discussed in more detail in section 1.2.3 below. The CMFs of the 1931 standard colorimetric observer were based on the colour matching data of Wright (1928-1929) and Guild (1931) obtained over a 2° field, and the photopic spectral luminous efficiency function $V(\lambda)$ defined by the CIE in 1924 (standard spectral luminous efficiency functions are discussed in more detail below in section 1.2.5). It was later thought that the 1924 $V(\lambda)$ function underestimated sensitivity below 460 nm, and modifications by Judd (1951) and Vos (1978) were proposed to CIE 1924 $V(\lambda)$ and the CIE 1931 CMFs, leading to the Judd-Vos modified CIE 1931 CMFs. Other sets of CMFs have been proposed by Stiles and Burch for a 2° field (Stiles and Burch 1955), a 10° field (Stiles and Burch 1959), and by Speranskaya (1959) for a 10° field. The CIE incorporated Speranskaya's colour matching data with Stiles and Burch's 10° measurements to produce CMFs of the CIE 1964 supplementary colorimetric observer for a 10° field. A frequently used estimate of the cone spectral sensitivities was derived from a transformation of the Judd-Vos modified CIE 1931 CMFs (Smith and Pokorny

1975), but several other estimates of the cone fundamentals have been based on different sets of CMFs, listed above (Vos and Walraven 1971; Vos et al. 1990; Stockman et al. 1993; Stockman et al. 1999; Stockman and Sharpe 2000).

Cone sensitivities may also be measured using psychophysical techniques under conditions that aim to isolate the response of a particular cone type (see section 1.3.1 b. below). This type of measurement is difficult in colour normals, but more successful in colour deficient observers lacking in one or two cone types. To compare measurements for colour deficient observers with those of colour normals, the colour deficient observers must have cone sensitivities in their remaining cones that match those in normals. Appropriate observers can be selected from genetic analysis of the photopigment gene array. Recent measurements in S-cone monochromats (who have only S-cones and rod photoreceptors), and in protanopes and deuteranopes of known genotype, have highlighted differences between several estimates of the cone fundamentals and cone spectral sensitivity data from colour deficient observers (Sharpe et al. 1998). This has led Stockman and Sharpe (2000) to propose new cone fundamentals based on a 2° conversion of the Stile Burch 10° CMFs, which the authors suggest are an improvement on the Smith-Pokorny cone fundamentals. The Stockman and Sharpe fundamentals are shown along with those of Smith and Pokorny in Figure 1-16.

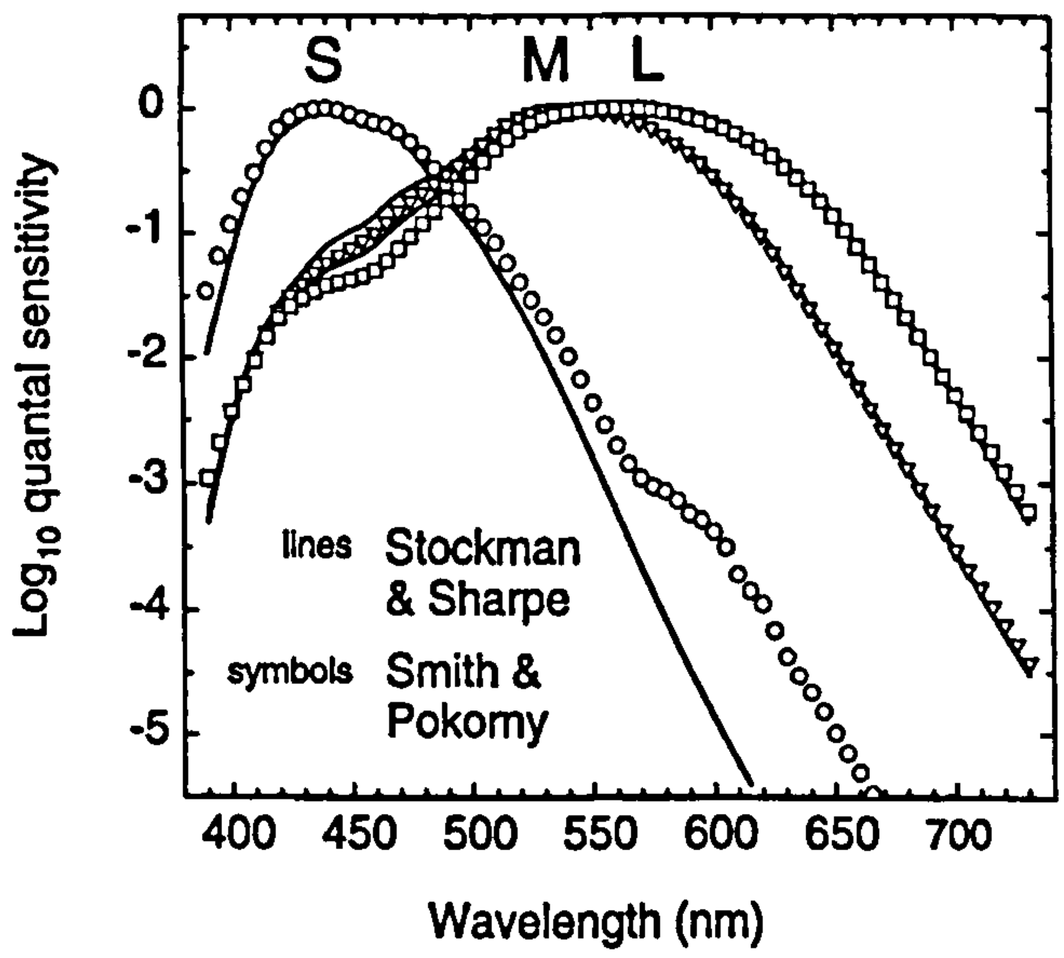

Figure 1-16. Estimates of the cone fundamentals, reproduced from (Gegenfurtner and Sharpe 1999). The open symbols represent the Smith and Pokorny fundamentals, and the lines represent the Stockman and Sharpe fundamentals, see text for details.

1.2.2 The coding of colour in the visual system

To extract information about both the intensity and wavelength of light from the output of the cone photoreceptors, signals from the three types of cone must be compared. This comparison of cone signals is carried out by neural elements in the visual pathway beyond the photoreceptors. Cells that perform the differencing operation between cone signals exhibit what is termed spectral opponency. A spectrally opponent cell might respond in an excitatory manner to input from one cone type and in an inhibitory manner to input from another cone type. It is generally believed that there are two channels along which signals from cells with opposing cone inputs are transmitted: the red-green channel in which signals from L- and M-cones are compared, and the blue-yellow channel in which signals from the S-cones are compared to a combined signal from L- and M-cones. These channels are thought to pertain to the parvocellular pathway. Ganglion cells displaying spectrally opponent behaviour have been found in the primate retina, which serves as a good model for the human retina; but the retinal circuitry subserving such cells is not fully understood.

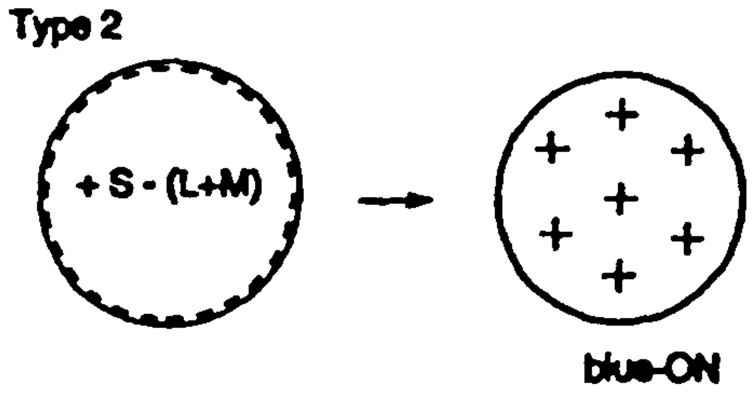

Figure 1-17. The receptive field structure of Wiesel and Hubel's type II cell. Reproduced from (Dacey 1996).

Investigations into the origins of blue-yellow spectral opponency have revealed that a distinct type of ganglion cell is involved. The small bistratified ganglion cell receives input from S-cones, and is excited by blue light and inhibited by yellow light across its receptive field with a blue-ON/yellow-OFF configuration (+B –Y cell) (Dacey and Lee 1994b). These authors suggested that the blue-ON response originates from S-cone ON-bipolar input, and the yellow-OFF response may be attributable to input from an OFF-cone bipolar with connections to both M- and L-

cones. Small bistratified ganglion cells exhibit the properties of Wiesel and Hubel's (1966) type II cells; cells that exhibit spectral opponency with spatially coextensive fields, see Figure 1-17. The identification of a +Y –B ganglion cell, although not confirmed, has also been hinted at (Lee 1996).

The retinal circuitry underlying red-green opponency is presently unclear. The midget ganglion cell is the primary candidate for supplying spectral opponency because these cells are the only cells identified thus far, that selectively make connections with either L- or M-cones (via ON or OFF midget bipolars). Parasol ganglion cells carry no wavelength specific information as they make connections with diffuse bipolars, which in turn, receive input from all three types of cone. The specificity of the midget ganglion system only appears to hold, however, over the central retina, where midget ganglions receive input from a single L- or M-cone. In the periphery, where midget ganglion cells make connections with more than one cone, these connections do not appear to be exclusive to a particular cone type (Dacey 1996). This lack of wavelength specificity in the peripheral retina may explain the well documented degradation of red-green colour vision in the periphery (Weale 1953; Moreland and Cruz 1959; Noorlander et al. 1983; Nagy and Doyal 1993). The midget ganglion cell system in the central retina will supply an excitatory or inhibitory response to red or green light, but an opponent input to the surround is required to form red-green spectrally opponent cells. The origins of such an opponent signal are also unclear. H1 and H2 horizontal cells receive input from more than one cone type and, therefore, cannot provide cone-specific input to the surrounds of receptive fields. Recordings from AI amacrines show that these cells also receive additive input from L- and M-cones, excluding them from a role in the generation of cone-specific receptive field surrounds, also. There may be other, as yet uncharacterised amacrines, with a role in cone-specific spectral opponency. Horizontal cells and the AI amacrine could, however, provide a mixed-surround input. The mixed-surround receptive field model predicts that spectral opponency arises from the greater weighting given to the cone-specific centre compared to the surround receiving input from more than one type of cone (DeValois and DeValois 1993). The circuitry for such a model is shown in Figure 1-18.

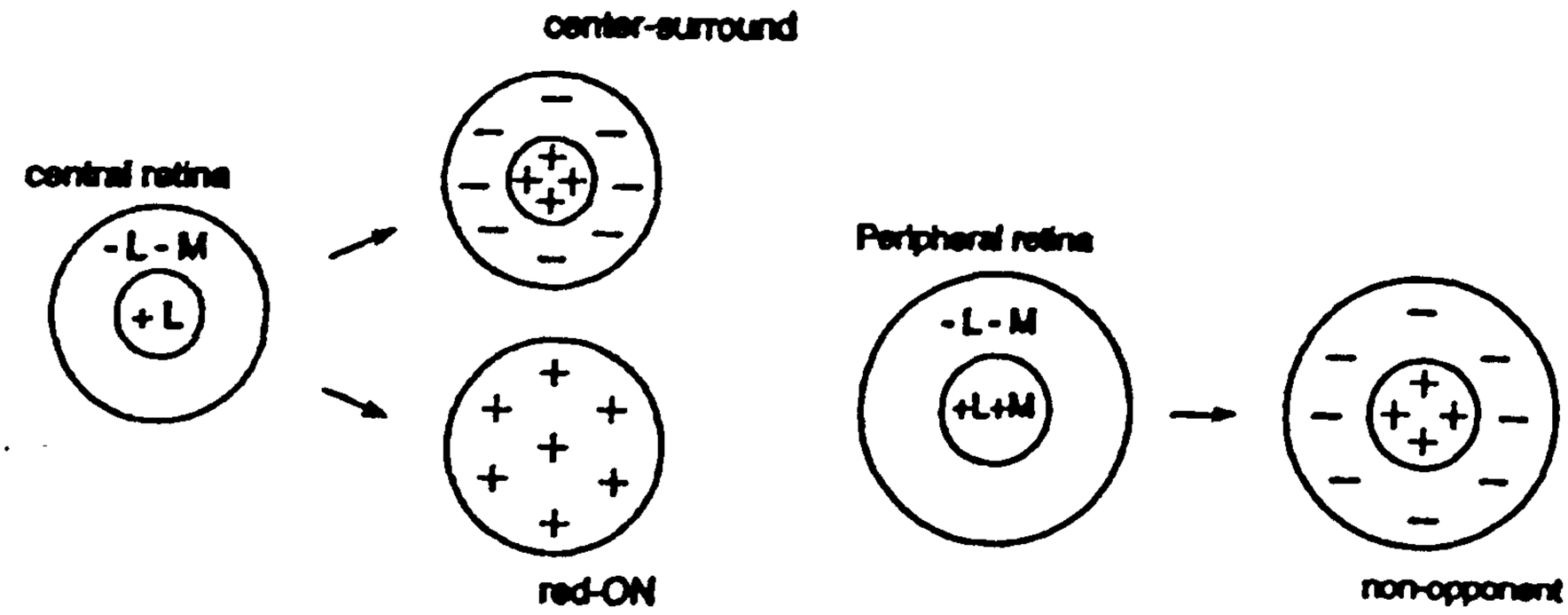

Figure 1-18. Diagrammatic representations of receptive field structure for colour coded cells according to the mixed-surround model, both in the central retina and the periphery. Reproduced from (Dacey 1996).

The receptive field structure evident in retinal ganglion cells is preserved in cells of the LGN; therefore, the next major stage of colour processing takes place in the cortex. Colour coding in the cortex is poorly understood, and mainly restricted to the response properties of cells in the primary visual cortex and prestriate areas V2 and V4. In these regions colour information appears to be utilised in highly colour specific pathways, and also in the extraction of colour-defined structure. There are cells found in V1 that have similar colour response properties to LGN cells, but in V1 of the monkey, doubly-opponent cells have also been identified (Wiesel and Hubel 1966). These cells exhibit spectral opponency with an antagonistic spatial receptive field organisation. They are mostly simple cells and respond maximally to oriented bars defined by specific colour differences, such as a red bar with a green surround. There are also cells in the primary visual cortex of the monkey that respond to colour contrast, independent of the colours involved (DeValois and DeValois 1975). Such cells might be excited by a specifically oriented red bar with a green surround and also a green bar with a red surround, for example. These cells, termed multiple colour cells, appear to respond to structure, whether it is luminance or colour based. The thin stripes of V2 consist mainly of cells with wavelength selective responses (DeYoe and Van Essen 1985). V4 is known to consist of predominantly colour specific cells (Zeki 1973). V4 appears to be arranged in colour columns, where the cells in each column respond to a specific colour. Cells within a column may differ in their demands on the shape of stimulus that will produce an optimum response, but require the same stimulus colour.

1.2.3 Colorimetry and the CIE standard colorimetric observers

The foundation of the field of colour science known as colorimetry, is the trichromatic generalisation. The trichromatic generalisation describes the properties of trichromatic colour matching, and states that given a set of three primary stimuli, all colour stimuli can be matched by an additive mixture of these three primaries, where matches may involve addition of a negative amount of one or two of the primaries. In colorimetry, the relative proportions of the three primaries required to match a colour stimulus are known as tristimulus values. Two stimuli with the same tristimulus values under identical viewing conditions look alike to normal trichromats. Colour matching functions consist of the tristimulus values for monochromatic stimuli of equal radiance, for a given set of primaries. In colorimetry, colour matching functions can be used as weighting functions to determine the amounts of the primaries, for which they are defined, that will match any colour stimulus. If **P** is a colour stimulus with spectral radiant power distribution $P(\lambda)$ and **A, B, C** are a set of primaries so that a match is expressed by

$$\mathbf{P} = A\mathbf{A} + B\mathbf{B} + C\mathbf{C} \qquad \textbf{Eq. 1-1}$$

then the tristimulus values A, B, C are given by

$$A = K\int P(\lambda)\bar{a}(\lambda)\,d\lambda \qquad \textbf{Eq. 1-2}$$

$$B = K\int P(\lambda)\bar{b}(\lambda)\,d\lambda \qquad \textbf{Eq. 1-3}$$

$$C = K\int P(\lambda)\bar{c}(\lambda)\,d\lambda \qquad \textbf{Eq. 1-4}$$

where $\bar{a}(\lambda), \bar{b}(\lambda), \bar{c}(\lambda)$: appropriate colour matching functions, and K: scaling constant.

The CIE 1931 standard colorimetric observer was introduced in that year to provide the first international standard for the specification and measurement of colour stimuli, for use in industry and science. The standard was based on the average colour matching properties of a set of normal trichromats, as there were no reliable estimates of the cone spectral sensitivities at that time. The CIE defined two

equivalent sets of colour matching functions based on the colour matching experiments of Wright (1928-1929) and Guild (1931) and the CIE 1924 spectral luminous efficiency function V(λ) (see section 1.2.5 below). Only relative colour matching values were supplied by Guild and Wright, leading the CIE to derive sets of CMFs under the assumption that a linear combination of the colour matching functions should equal V(λ). The first set of CMFs $\bar{r}(\lambda), \bar{g}(\lambda), \bar{b}(\lambda)$ was defined for a set of real primaries, chosen because they could be calibrated accurately. The units of the tristimulus values R, G, B were defined such that equal proportions of the primaries matched an equal energy white (a stimulus with a flat spectral radiance distribution). In this colorimetric specification, known as the RGB system, the tristimulus values were negative over some regions of the visible spectrum; the CMFs for the RGB system are shown in Figure 1-19.

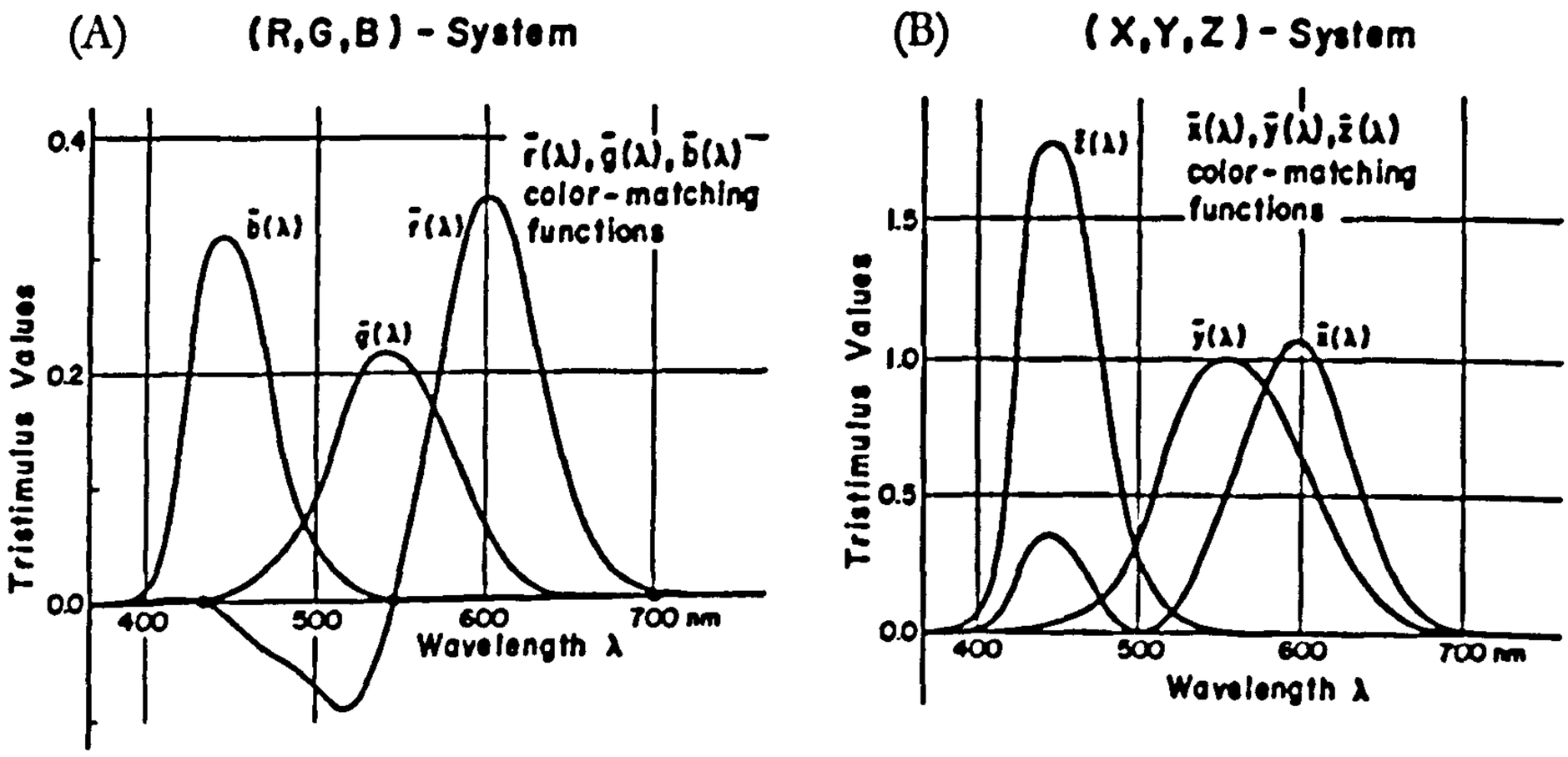

Figure 1-19 (A)-(B). Colour matching functions of the CIE 1931 standard colorimetric observer, for the RGB system (A), and the XYZ system (B). Reproduced from (Wyszecki and Stiles 1982).

The second colorimetric specification defined by the CIE in 1931 was a linear transformation of the RGB system to obtain positive tristimulus values over the whole spectrum. The tristimulus values were denoted X, Y, Z and associated CMFs $\bar{x}(\lambda), \bar{y}(\lambda), \bar{z}(\lambda)$, these are shown in Figure 1-19. The transformed RGB primaries become imaginary primaries in the XYZ system, but equal energy white is still matched by equal proportions of the primaries. The linear transform used to obtain the XYZ system from the RGB was chosen out of the different possibilities

available, to equate the $\bar{y}(\lambda)$ colour matching function with the CIE 1924 photopic spectral luminous efficiency function V(λ); linking colorimetry to the field of photometry. The advantages of the XYZ system led to the global community adopting it as an international standard for colour specification.

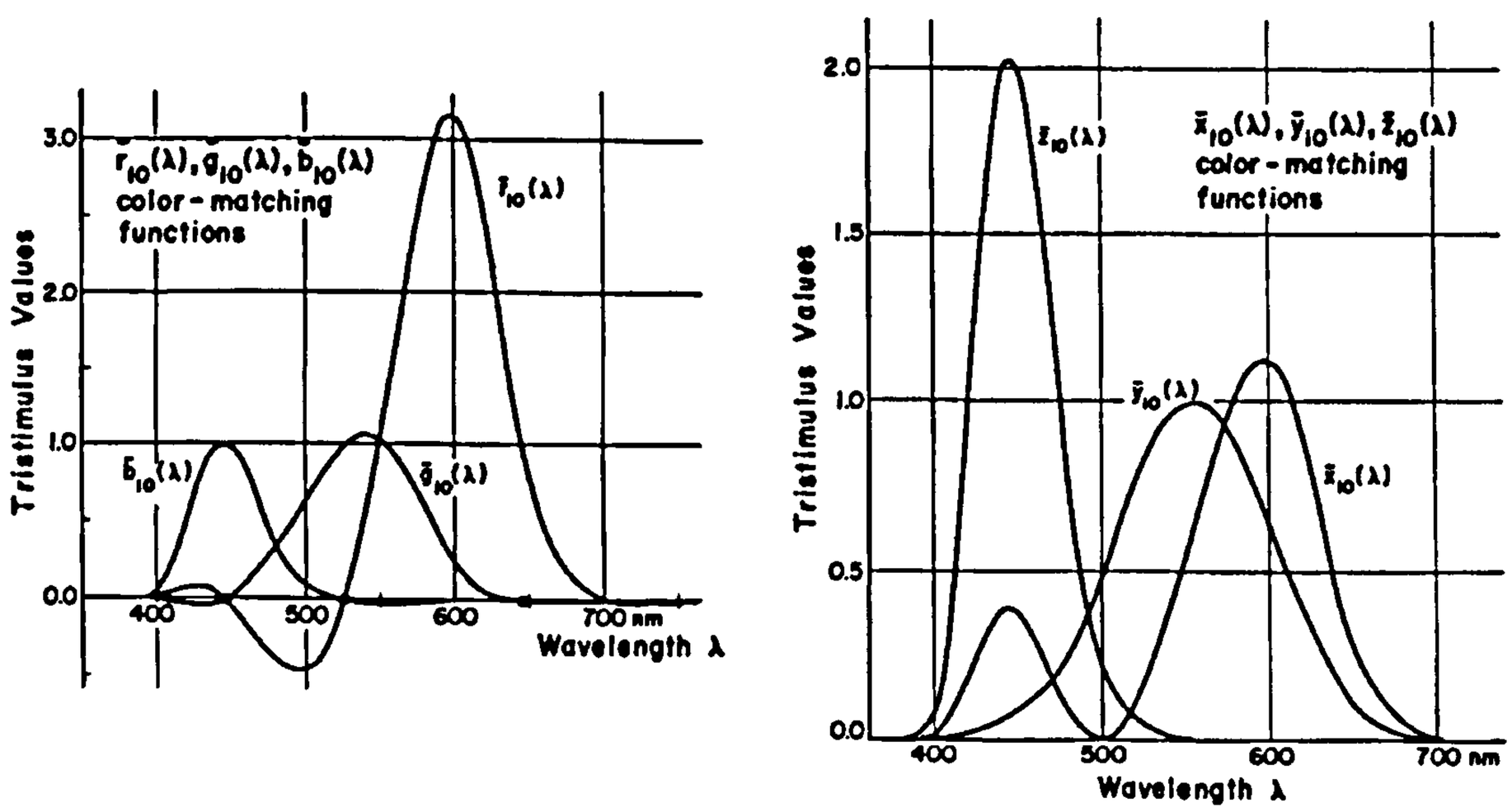

Figure 1-20. Colour matching functions of the CIE 1964 standard colorimetric observer, for the RGB system (A), and the XYZ system (B). Reproduced from (Wyszecki and Stiles 1982).

The colour matching data of Guild and Wright, on which the 1931 standard colorimetric observer was based, were obtained for a centrally viewed field of size 2° angular subtense. This small field size was chosen to limit the influence of rods in colour matching. Later investigations suggested that colour matches for larger field sizes were not adequately predicted by the 1931 observer, and so an alternative set of colour matching functions were defined by the CIE in 1964. The 1964 supplementary standard colorimetric observer was based on the data of Stiles and Burch (1959), and of Speranskaya (1959), who obtained colour matching data for a 10° field. The supplementary CMFs $\bar{x}_{10}(\lambda), \bar{y}_{10}(\lambda), \bar{z}_{10}(\lambda)$ (shown in Figure 1-20) also purport to describe rod free colour-matches, for the constituent data were either obtained at high stimulus luminances or were corrected for rod intrusion. A further complication of large field colour matching is the presence of the Maxwell spot - an area of roughly 4° around the point of fixation that differs in colour

appearance to the remainder of the field, which is attributed to the macular pigment. Colour matches from which the 10° colour matching functions were derived, were made for the area extraneous to the Maxwell spot.

The two CIE standard colorimetric observers define the colour matching characteristics of an ideal observer, based on the colour-matching data of real observers. The CIE 1931 standard observer is recommended for field sizes up to 4° angular subtense and the 1964 supplementary colorimetric observer is recommended for large-field colour matches under photopic viewing conditions. The colour matching properties of individual normal trichromats often differ from those of the CIE standard observers. This is in mainly due to individual differences in the optical density spectra of the lens and macular pigment (see sections 1.1.1 a and 1.1.2 h). Individual differences in lens density can be large even between young observers (van Norren and Vos 1974). Large variations in macular pigment density have also been found between individuals (Werner et al. 1987). These differences account for much of the variation in individual colour matching data and deviations from the properties of the CIE standard colorimetric observers.

1.2.4 Chromaticity diagrams

For either the CIE 1931 or the CIE 1964 colorimetric system, colour stimuli can be represented on a two-dimensional diagram. Such diagrams were first introduced by Maxwell and are referred to as chromaticity diagrams. In a chromaticity diagram two normalised tristimulus values are plotted as Cartesian coordinates, known as chromaticity coordinates. For the CIE 1931 XYZ system the chromaticity coordinates x, y, z are given by

$$x = \frac{X}{(X+Y+Z)} \qquad \textbf{Eq. 1-5}$$

$$y = \frac{Y}{(X+Y+Z)} \qquad \textbf{Eq. 1-6}$$

$$z = \frac{Z}{(X+Y+Z)} \qquad \textbf{Eq. 1-7}$$

Hence

$$x + y + z = 1 \qquad \text{Eq. 1-8}$$

Chromaticity coordinates for the CIE 1964 standard colorimetric system are calculated in a similar way from the tristimulus values X_{10}, Y_{10} and Z_{10}.

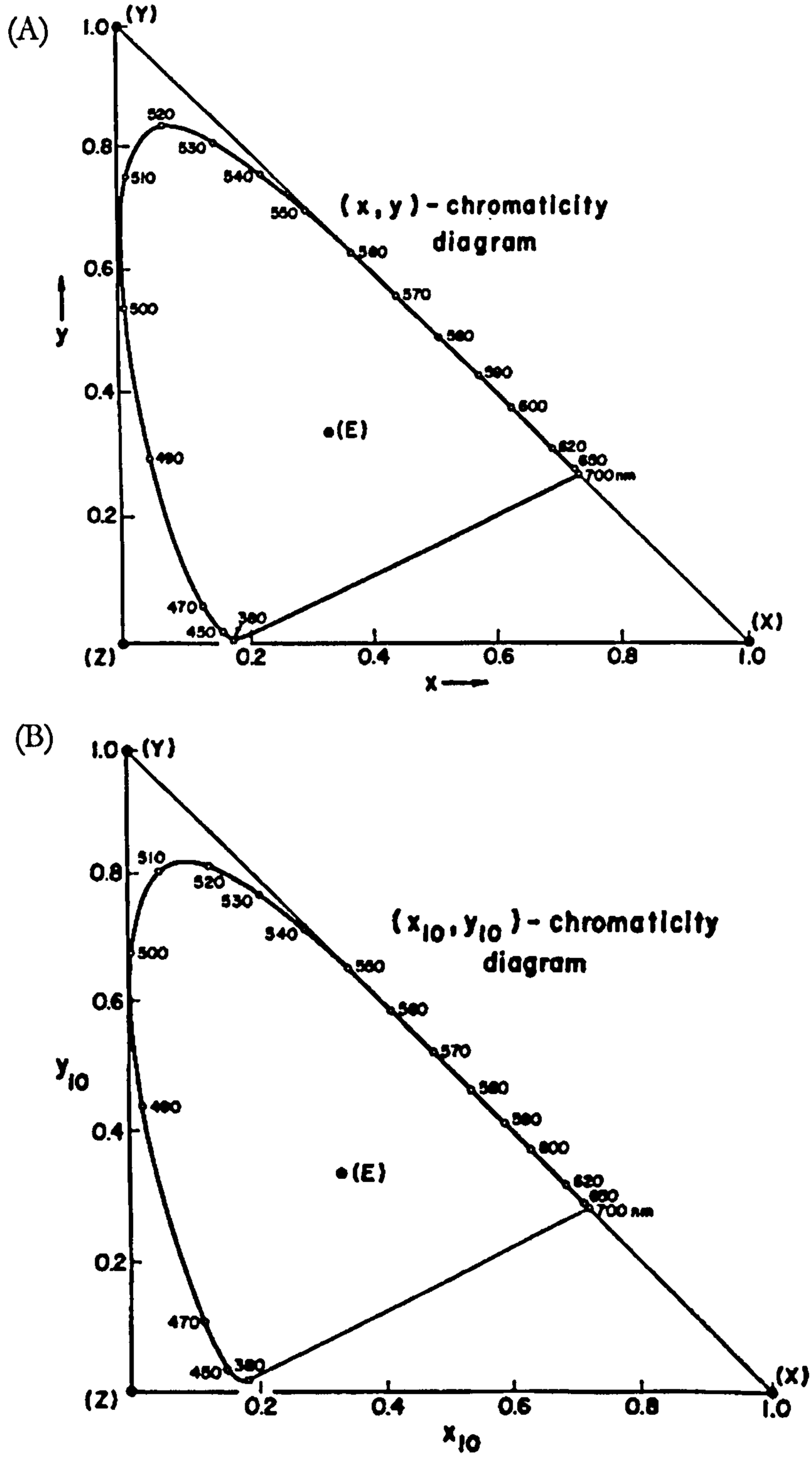

Figure 1-21 (A)-(B). Chromaticity diagrams associated with the XYZ systems of the CIE 1931 (A) and CIE 1964 (B) standard colorimetric observers. Reproduced from (Wyszecki and Stiles 1982).

Equation 1-8 highlights that only two chromaticity coordinates are independent, which is why they can be represented on a two dimensional diagram. It is usual to plot the x and y coordinates. The chromaticity diagrams associated with the XYZ systems of the CIE 1931 and 1964 standard colorimetric observers are shown in Figure 1-21. The chromaticity coordinates of monochromatic stimuli plot as a curve, known as the spectral locus. The line joining the wavelengths at either end of the visible spectrum is known as the line of non-spectral purples. The chromaticity of all real colour stimuli fall with the boundary created by the spectral locus and the line of non-spectral purples.

Chromaticity diagrams are useful for illustrating the relationships between colour stimuli, but they do not define how a colour stimulus will be perceived by a colour normal observer. Colour perception is more complicated, and depends on many factors including stimulus luminance, the conditions of observation, and inter-observer differences such as those discussed in section 1.2.3. It should also be noted that equal distances between chromaticity coordinates of colour stimuli plotted on the CIE 1931 (x, y)-chromaticity diagram and the CIE 1964 (x_{10}, y_{10})-chromaticity diagram do not necessarily relate to equal perceptual colour differences between stimuli.

1.2.5 Photometry and the CIE standard photometric observers

Photometry is the field of colour science used to measure the visual effectiveness of light relative to its spectral radiant power distribution. Photometry is analogous to the field of radiometry, but takes into account the spectral response of the human eye. Photometry is governed by the laws of proportionality and additivity, often referred to as Abney's laws, which state that in terms of brightness, if stimulus A matches stimulus B and if the radiant power of both stimuli are altered by a factor α then α A will match α B (proportionality law), and that for stimuli A, B, C and D, if A matches C and B matches D then (A+B) will match (C+D) (additivity law). These laws also govern colorimetry, where the matching operation is colour matching instead of brightness matching.

The spectral luminous efficiency of the eye, also referred to as the V_λ response, may be described as something akin to the brightness response of the eye for monochromatic lights across the visible spectrum. Measurement of spectral luminous efficiency varies in complexity depending on the viewing conditions. Under scotopic conditions the V_λ response is simply the spectral sensitivity curve of the rod photoreceptors measured at the cornea. Under photopic conditions the V_λ response is determined from activity of the three types of cone. The photopic response curve is dependent on the method of measurement, but is relatively stable over a large range of intensity. The mesopic case is more complicated still; spectral luminous efficiency curves are dependent on the relative activity of the three types of cone and the rods, and not only depend on the method of measurement, but also on the level of retinal illumination.

A number of different methods have been used to measure photopic spectral luminous efficiency, including direct heterochromatic brightness matching, heterochromatic flicker photometry and the minimally distinct border method. In all these methods the reference field is usually chosen to be a white stimulus of broad spectral power distribution, or a monochromatic stimulus of fixed wavelength, while the test field is a monochromatic stimulus of variable wavelength. In direct heterochromatic brightness matching (HBM) two halves of a field of different spectral composition (the test and reference) are matched for brightness by alteration of the radiant power of the test half of the field. Such measurements are difficult because they require the observer to isolate the perception of brightness from hue and saturation, attributes that can differ substantially between the two halves of the field. A variant of HBM is the step-by-step method, where the test and reference field are both monochromatic and the reference field is varied in wavelength to be constantly separated from the test wavelength by a fixed number of nanometres. The main problem with HBM is that it does not obey the photometric law of additivity. For example, if two monochromatic stimuli are matched with a fixed reference stimulus, the sum of the monochromatic stimuli will often produce a stimulus that is less bright than the reference stimulus with double the radiant power. This phenomenon is known as subadditivity, and is thought to be due to cone-cone interactions. A method that satisfies the law of additivity to a

close approximation, is flicker photometry (Ives 1912). In heterochromatic flicker photometry (HFP) two spatially coextensive fields are rapidly alternated, and the flicker frequency plus the radiant power of one field is altered to minimise the perception of flicker. The perceptual attribute that is matched is analogous to brightness, but is usually referred to as flicker brightness. The procedure known as the minimally distinct border method (MDB) produces results that are comparable to HFP (Wagner and Boynton 1972). In this method the test and reference field are juxtaposed and the radiant power of the test field is altered to minimise the appearance of the border between the two halves of the whole field. The method requires optical correction of the chromatic aberration of the eye. For HBM, HFP and MDB the reciprocal of test stimulus radiant power required to match the reference stimulus, is plotted against wavelength, and the curve normalised to unity at its maximum value to obtain the spectral luminous efficiency curve. For step-by-step HBM, the spectral luminous efficiency function is derived from the integral of the function $dV_\lambda/d\lambda$.

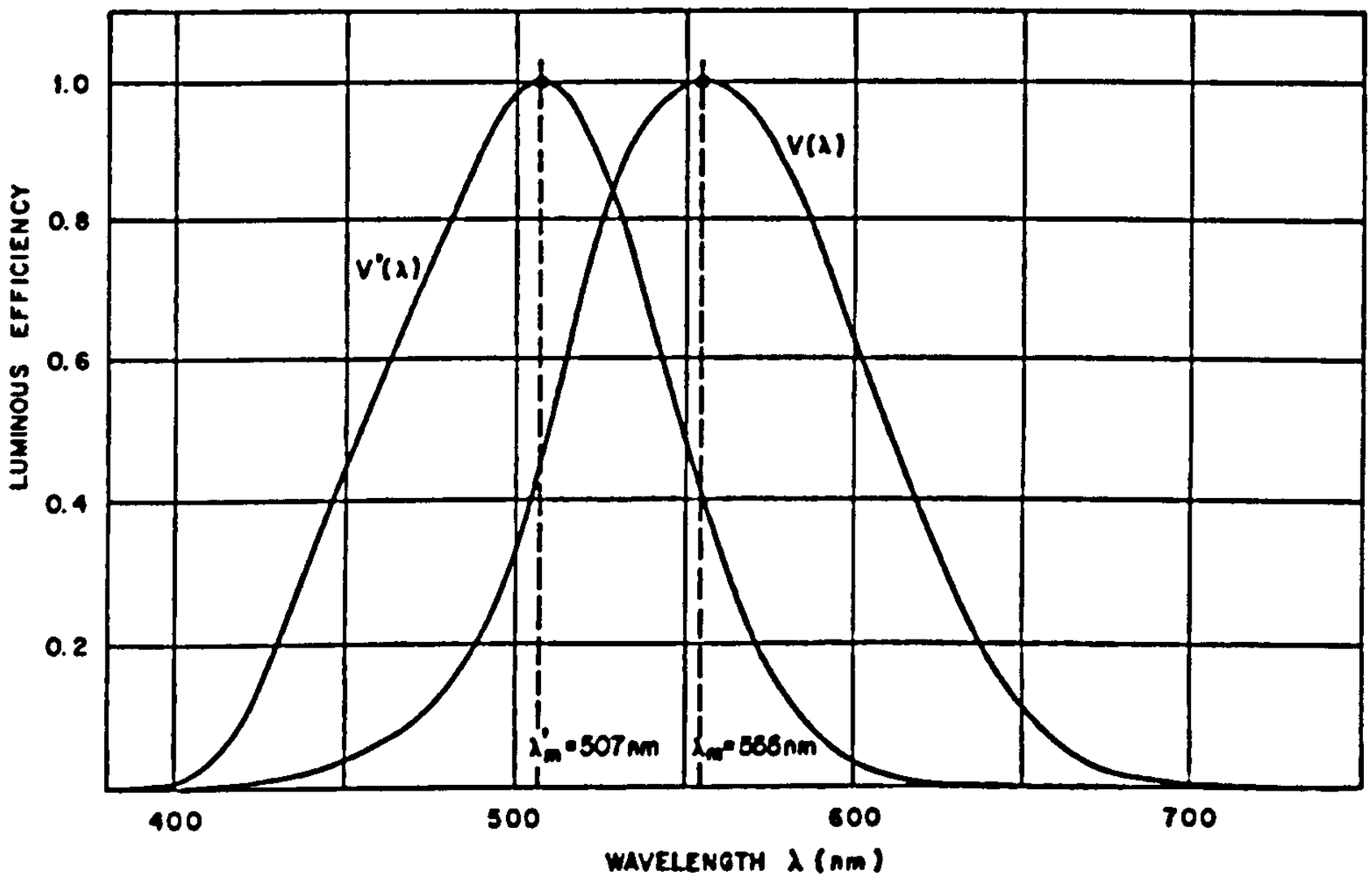

Figure 1-22. The CIE standard luminous efficiency functions for photopic ($V(\lambda)$) and scotopic vision ($V'(\lambda)$). The $V(\lambda)$ curve peaks at 555 nm and maximum sensitivity of the $V'(\lambda)$ function is at 507 nm. Reproduced from (Wyszecki and Stiles 1982).

In 1924 the CIE defined the standard photometric observer for photopic vision, described by the photopic spectral luminous efficiency function $V(\lambda)$. The $V(\lambda)$

function was based on the measurements of Coblentz and Emerson (1918), Hyde, Forsythe and Cady (1918), Gibson and Tyndall (1923), and Hartman (1918), amalgamated into a smooth function by Gibson and Tyndall (1923). The experimental data were acquired for a central 2° field using a number of the methods described above, but was predominantly based on HFP measurements. For this reason, $V(\lambda)$ is generally considered to represent flicker photometric matches. The CIE standard photometric observer for scotopic vision was established in 1951, defined by the scotopic spectral luminous efficiency function $V'(\lambda)$. The $V'(\lambda)$ curve was constructed from the data of Wald (1945b) and Crawford (1949). Wald measured absolute thresholds for monochromatic test stimuli at eccentric locations i.e., the minimum radiance to just detect a flashing stimulus, whereas Crawford's dark adapted observers obtained direct brightness matches for a centrally viewed 20° field. Figure 1-22 shows the standard luminous efficiency functions for both photopic and scotopic vision. The peak sensitivity of the photopic luminous efficiency function is at 555 nm and that of the scotopic function is at 507 nm. This shift is spectral response of the eye towards shorter wavelengths with reduction in illumination is known as the Purkinje shift. The shift in peak spectral sensitivity is evident in mesopic spectral luminous efficiency curves as the adaptation level is reduced from the photopic to the scotopic range. Mesopic spectral luminous efficiency curves and proposed systems of mesopic photometry are discussed in more detail in section 1.3.2 below. Due to the difficulties outlined above and other factors considered in section 1.3.2, there is currently no standard photometric observer for mesopic vision.

Measurements of spectral luminous efficiency subsequent to those that formed the basis of the CIE 1924 $V(\lambda)$ function, suggested that the $V(\lambda)$ curve underestimated sensitivity in the short wavelength region of the visible spectrum. Modifications to the curve below 460 nm by Judd (1951) and later alterations by Vos (1978) led to the definition of the Judd-Vos modified $V_M(\lambda)$ function, which is shown in Figure 1-23. Although this function is more representative of the photopic spectral response of colour normal observers it has not replaced the CIE 1924 $V(\lambda)$ function for general photometric applications; all instrumentation is based on $V(\lambda)$. The

Judd-Vos modified $V_M(\lambda)$, however, is often used in vision science. No spectral luminous efficiency function has been formally recommended by the CIE that describes the photometric characteristics of a large-field. In deriving the $\bar{y}_{10}(\lambda)$ colour matching function of the CIE 1964 colorimetric observer, Stiles and Burch (1959) incorporated flicker photometric matches obtained at the wavelengths of each of their primary stimuli. In 1978 the CIE (CIE 1978) reported that the $\bar{y}_{10}(\lambda)$ colour matching function provides a good fit for flicker matches in other regions of the visible spectrum, and, therefore, provisionally advocated use of $\bar{y}_{10}(\lambda)$ as a spectral luminous efficiency curve for large-field photopic vision.

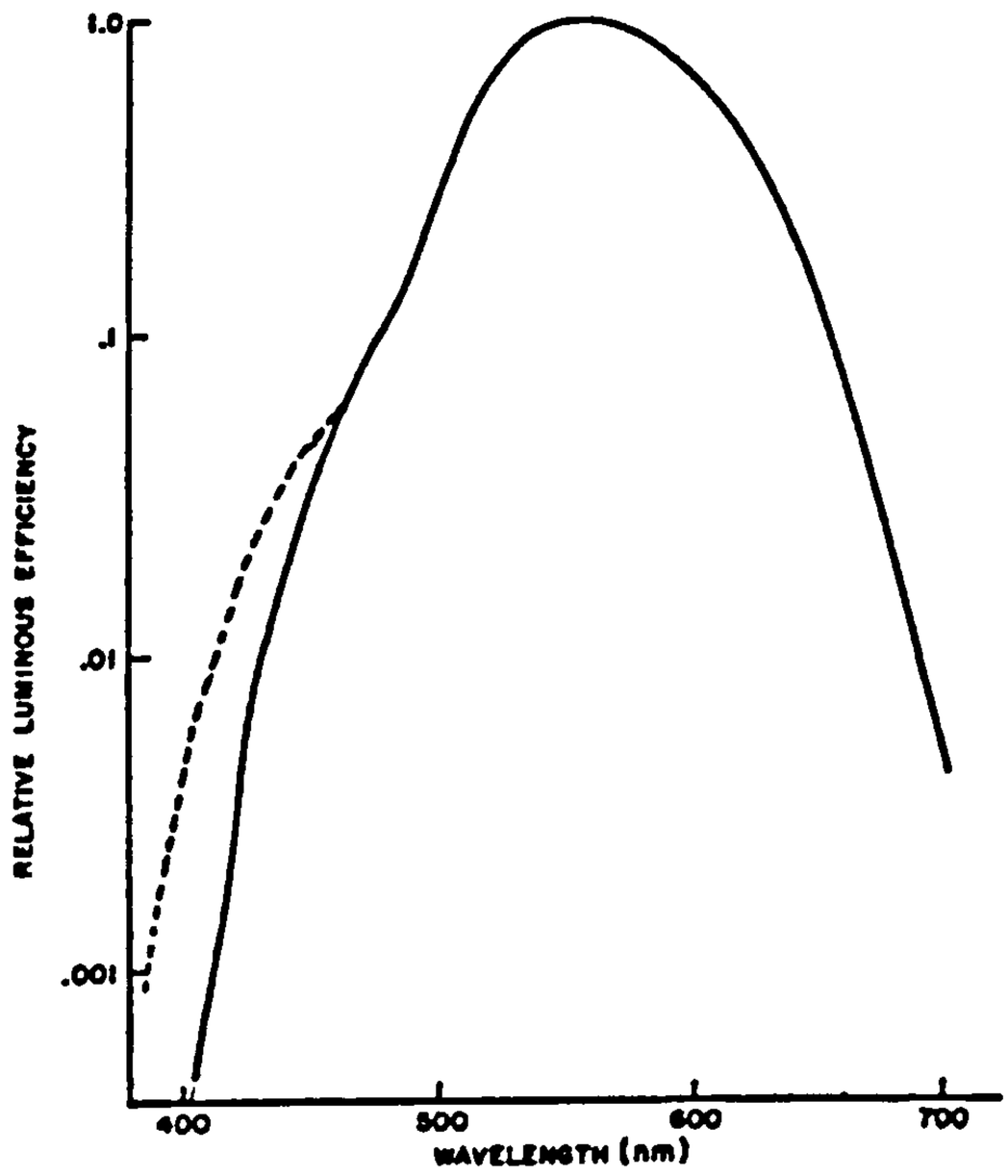

Figure 1-23. The Judd-Vos modified $V_M(\lambda)$ function (continuous line) compared to the CIE 1924 standard luminous efficiency function, $V(\lambda)$ (dashed line). Reproduced from (CIE 1978).

The luminous efficacy of radiation is a quantitative description of the ability of light to elicit a visual response. The photopic ($K(\lambda)$) and scotopic ($K'(\lambda)$) luminous efficacy for monochromatic radiant flux, are defined by equations 1-9 and 1-10, respectively.

$$K(\lambda) = K_m V(\lambda) \qquad \textbf{Eq. 1-9}$$

$$K'(\lambda) = K'_m V'(\lambda) \qquad \textbf{Eq. 1-10}$$

where K_m = 683 lumens per watt (lmW^{-1}) and K'_m = 1700 lumens per watt (lmW^{-1}). Thus, the photopic luminous flux (Φ_v) for a stimulus of radiant flux $\Phi_{e,\lambda}$ is given by

$$\Phi_v = K_m \int \Phi_{e,\lambda} V(\lambda)\, d\lambda \qquad \textbf{Eq. 1-11}$$

and scotopic luminous flux (Φ'_v) is given by

$$\Phi'_v = K'_m \int \Phi_{e,\lambda} V'(\lambda)\, d\lambda \qquad \textbf{Eq. 1-12}$$

The spectral luminous efficiency curves of normal trichromats often differ from those of the CIE standard observers. As mentioned earlier, spectral luminosity curves are highly dependent on the method of measurement, but large variations are also observed between the luminous efficiency functions of colour-normals obtained under identical conditions (Gibson and Tyndall 1923). Deviations from the standard curves and inter-observer variations can be attributed in part to the individual differences in optical density spectra of the crystalline lens and macular pigment, referred to in section 1.2.3. Another source of individual differences in photopic luminous efficiency functions relates to the relative numbers of L- and M-cones in the retina, which are known to vary between colour normals (see Kremers et al. 2000). The photopic spectral luminous efficiency function represents postreceptoral function, and is usually modelled as a linear combination of the activity in the L- and M-cones. The relative weighting of L- and M-cone spectral sensitivity curves required to produce a good fit to the V_λ function for a particular observer varies depending on the relative number of L- and M-cones (Kremers et al. 2000; Brainard et al. 2000).

1.2.6 Chromatic discrimination

The ability of normal trichromats to discriminate between different colour stimuli can be quantified using visual psychophysical techniques. One extensively applied method is the measurement of wavelength discrimination. Given a monochromatic stimulus at fixed wavelength λ, wavelength discrimination ($\Delta\lambda$) is measured by determining the smallest difference in wavelength that produces a just-noticeable change in appearance. Such experiments commonly employ a bi-partite field, one

region of which is filled with light of the fixed test wavelength, and the other region is filled with light of variable wavelength. The just-noticeable difference between the test and variable fields can be found by direct adjustment whilst maintaining a brightness match between the two fields. Alternatively the dispersion of a series of matches between the two fields can be taken as a measure of discrimination. A wavelength discrimination curve can be obtained by measuring $\Delta\lambda$ for values of λ throughout the visible spectrum. It is usual to plot $(\Delta\lambda_+ + \Delta\lambda_-)/2$ against λ, where $\Delta\lambda_+$ and $\Delta\lambda_-$ are the just-noticeable differences in the direction of longer, and shorter wavelengths, respectively. Wavelength discrimination curves characteristically indicate poor discrimination at the ends of the visible spectrum and have two maxima and three minima. An example of a wavelength discrimination curve is given in Figure 1-24. Wavelength discrimination is dependent on field size, eccentricity, presentation duration, light adaptation and stimulus intensity.

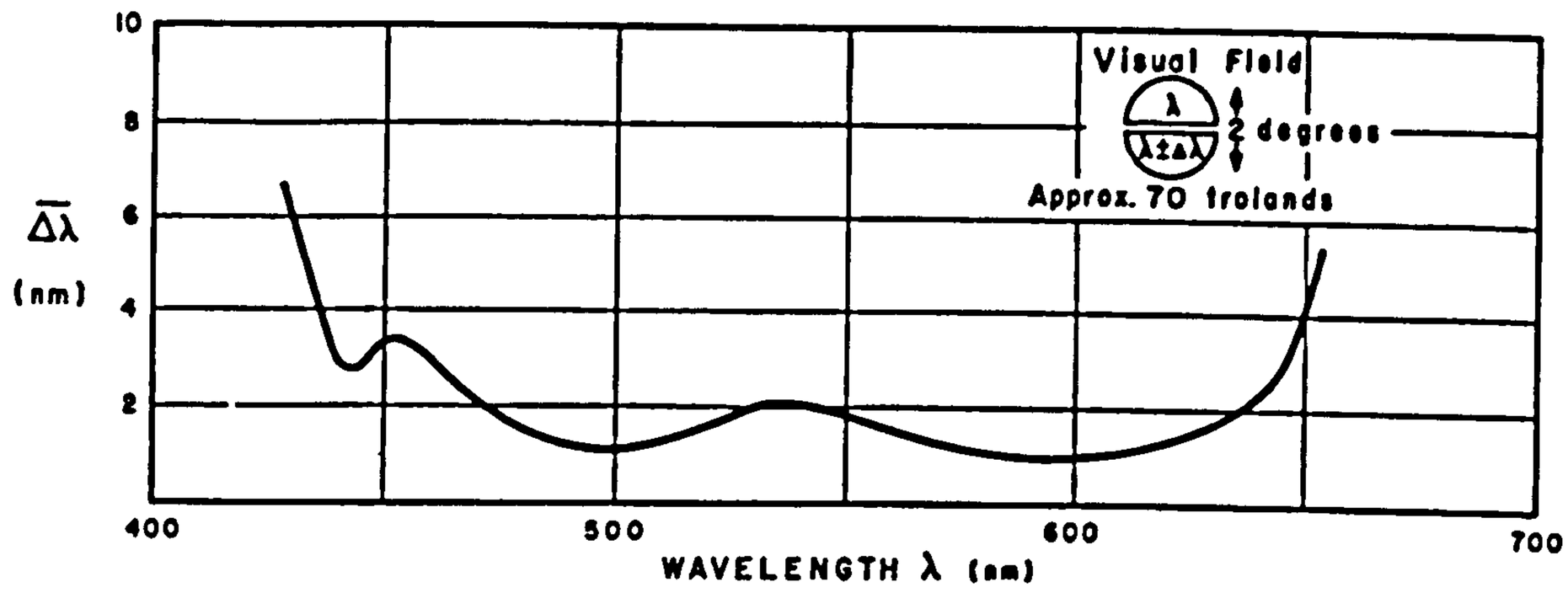

Figure 1-24. Wavelength discrimination curve showing data obtained by Wright and Pitt (1934). Reproduced from (Wyszecki and Stiles 1982).

Chromatic discrimination has also been extended to measurements of just-noticeable differences throughout chromaticity space. Wright (1941) performed such an investigation using mixtures of pairs of either two monochromatic stimuli, or one monochromatic stimulus and one nonspectral purple. In one half of a 2° bipartite field the mixture of the two lights could be varied, while the other half consisted of a test mixture. Observers were required to adjust the variable field so that it differed from the test field by a constant amount, whilst maintaining a brightness match between the two fields. Wright asked his observers to choose a

criterion difference larger than the just-noticeable difference to lessen task difficulty. The results of Wright's experiment are shown in Figure 1-25. The bars indicate criterion differences in perception, which vary considerably in length in different regions of the CIE 1931 chromaticity diagram.

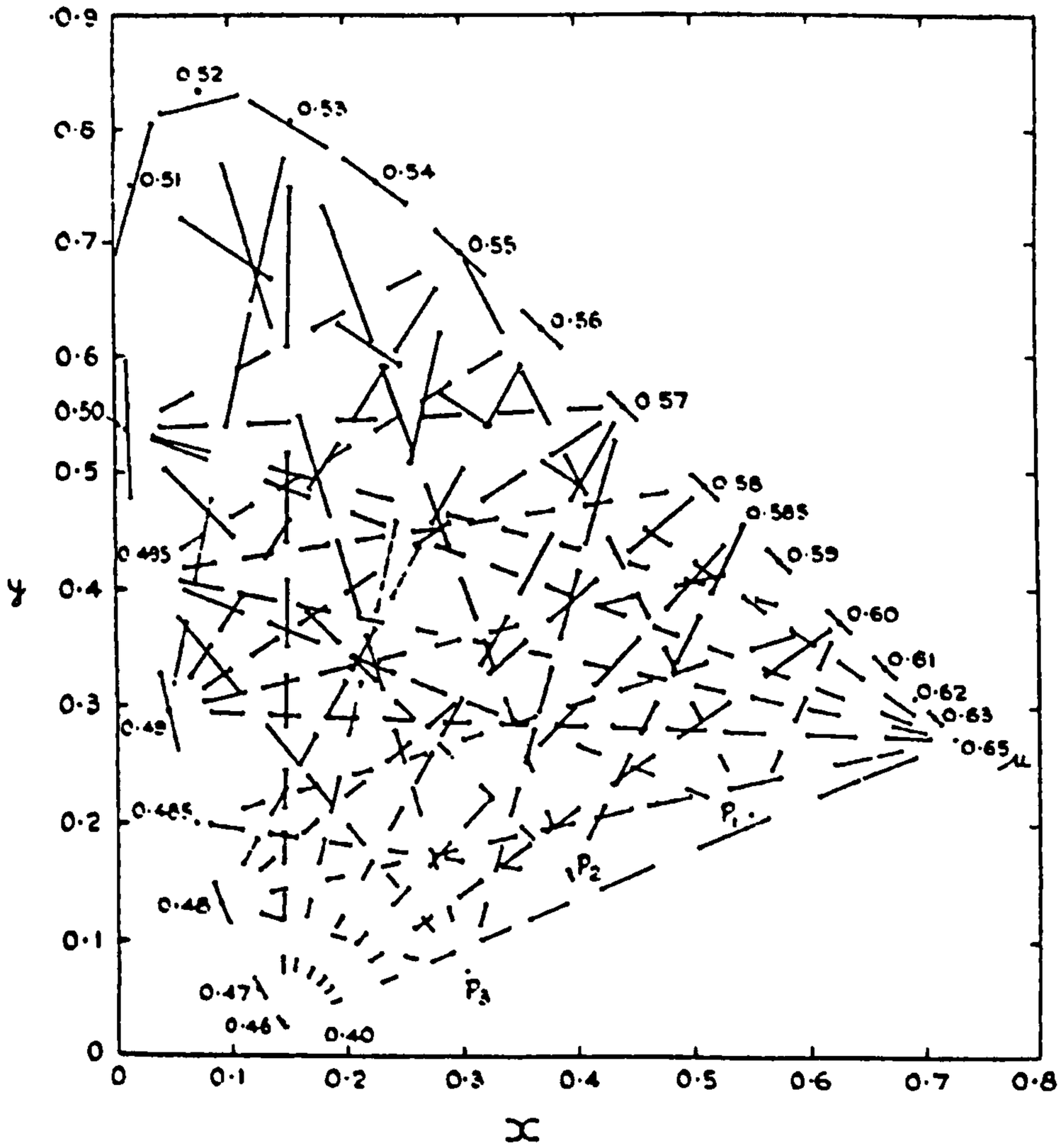

Figure 1-25. The results of Wright's measurements of just noticeable differences in chromaticity, plotted in CIE 1931 chromaticity space. Reproduced from (Wyszecki and Stiles 1982), after (Wright 1941).

MacAdam (1942) carried out a related experiment in which he measured the dispersion of a series of colour matches made by a normal trichromat. In the instrument MacAdam designed, the variable half of a 2° bipartite field could be altered in colour along a line in CIE 1931 chromaticity space, while the luminance of the field was automatically held constant. Starting with the variable field differing in chromaticity from the test field along a particular direction of chromaticity space, MacAdam's observer repeatedly made colour matches between the test and variable fields. The dispersion of a number of such matches was taken as one standard deviation of the distance in the CIE 1931 chromaticity diagram between the variable

and test field settings. MacAdam determined in a further experiment that this measure was equivalent to one third of the just-noticeable difference. For each test chromaticity investigated, MacAdam fitted an ellipse to the discrimination data from different directions of chromaticity space, which were constrained to be symmetrical about the test chromaticity. These ellipses, which have come to be known as MacAdam's chromatic discrimination ellipses, are shown in Figure 1-26, with axes plotted 10 times their actual length. Figures 1-25 and 1-26 illustrate that Wright's and MacAdam's data are broadly comparable.

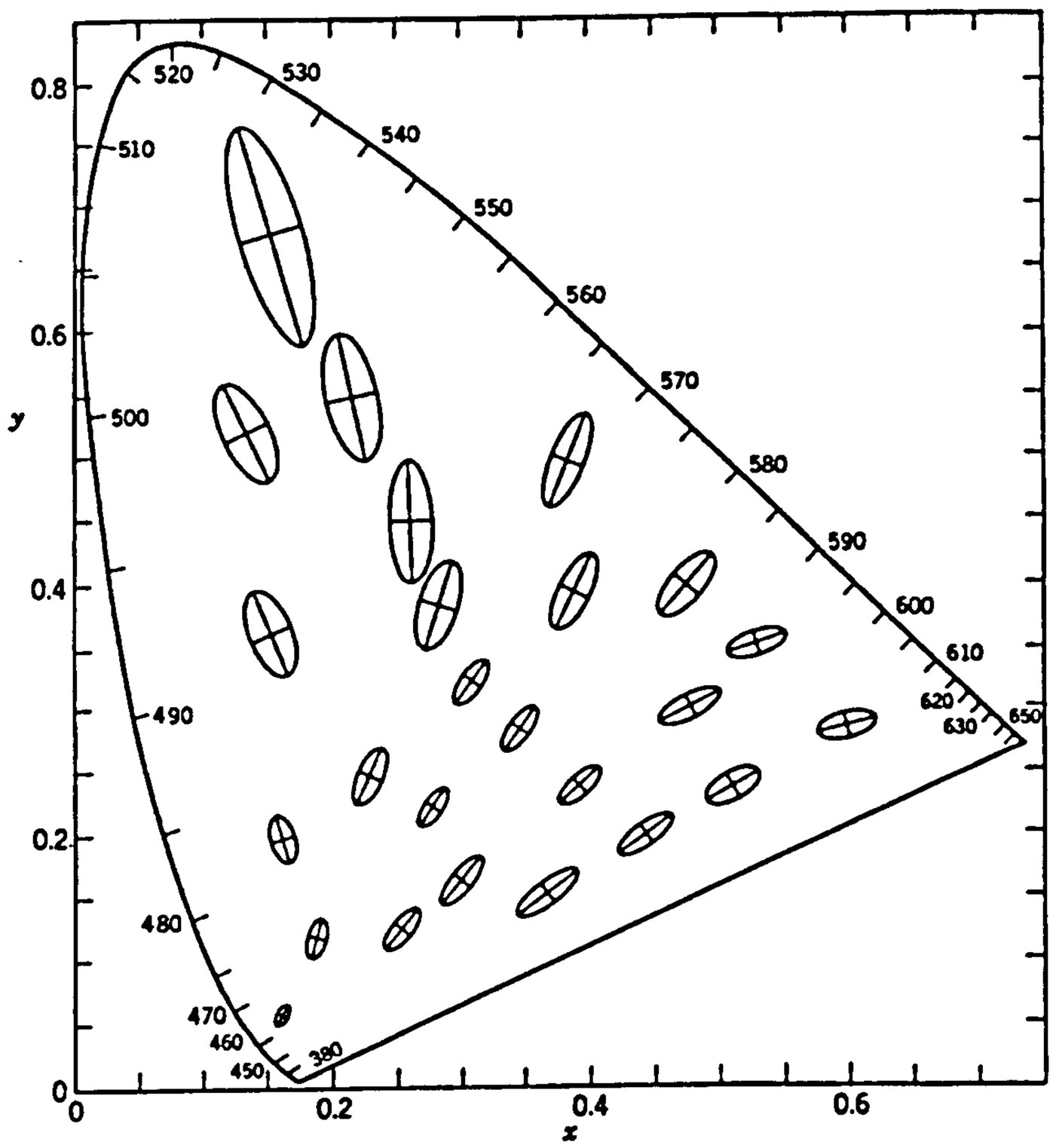

Figure 1-26. The results of MacAdam's measurements of chromatic discrimination based on the dispersion of a series of colour matches, showing MacAdam's ellipses plotted in CIE 1931 chromaticity space, with ellipse axes 10 times their actual length. Reproduced from (Wyszecki and Stiles 1982), after (MacAdam 1942).

Further colour matching experiments were carried out by Brown and MacAdam (Brown and MacAdam 1949; Brown 1957), for which the luminance of the matching field was allowed to vary in addition to the chromaticity. From such data, discrimination ellipsoids can be fitted. Cross sections of Brown and MacAdam's ellipsoids in the plane of constant luminance, were comparable to MacAdam's

original chromatic discrimination ellipses, but showed large variations in the ratio of the major to minor axes between observers. Wyszecki and Fielder (1971) also measured colour matching ellipsoids, carrying out a comparison of their results with those of MacAdam and Brown. Wyszecki and Fielder also assessed the repeatability of individual observers matches, and found the within-subjects variability could be large. Brown (1951) also investigated the effect of reducing stimulus luminance on the precision of colour matching. Brown noted changes in both the size and orientation of the resulting ellipses; the findings of these experiments are discussed further in chapter 4.

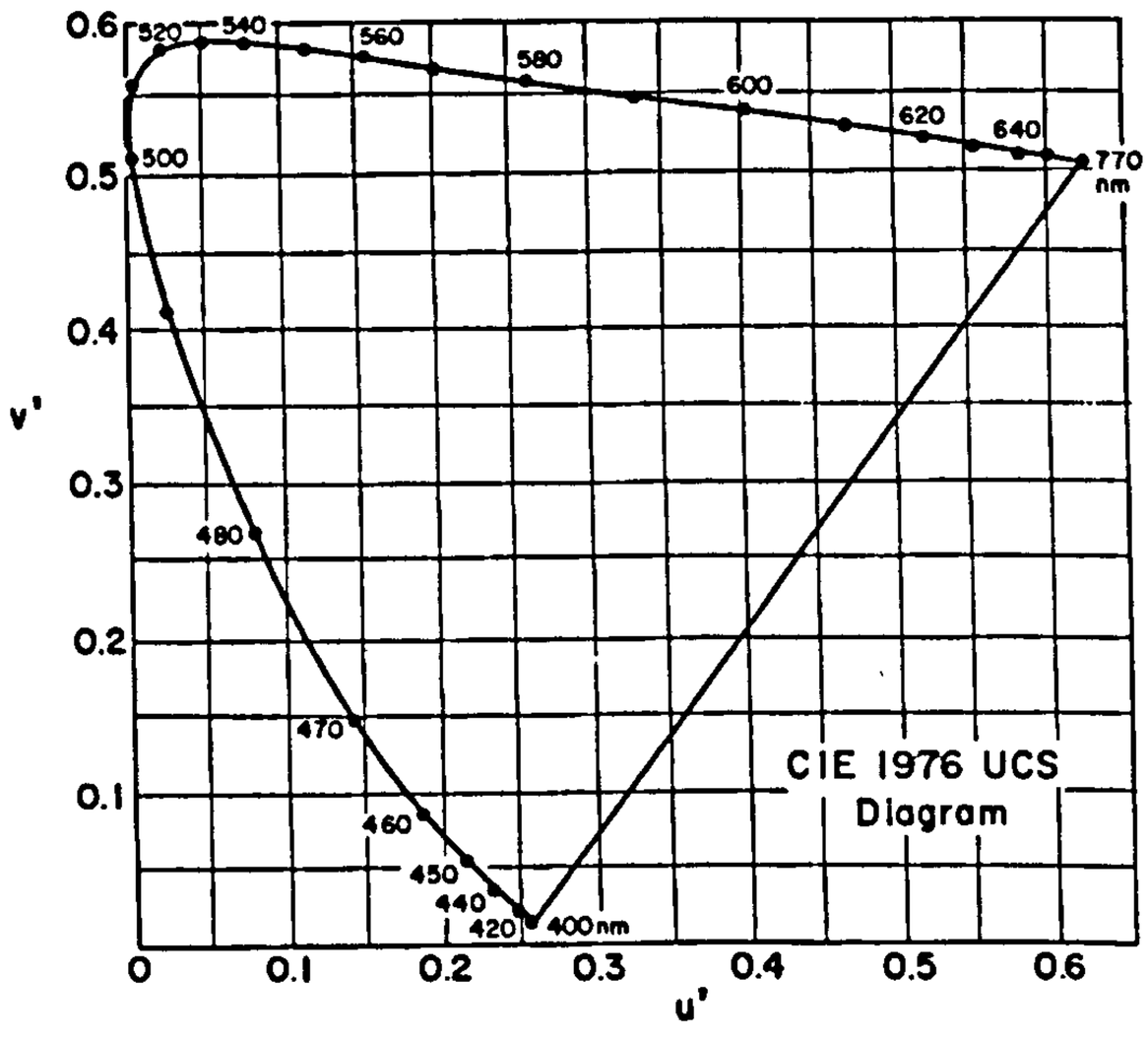

Figure 1-27. The CIE 1976 uniform colour space. Reproduced from (Wyszecki and Stiles 1982).

1.2.7 Uniform chromaticity diagrams and uniform colour spaces

Since definition of the CIE 1931 chromaticity diagram a number of transformations of the diagram have been suggested, which aim to make distances between chromaticities more representative of perceptual differences between colour stimuli of equal luminance. One such transformation, proposed by MacAdam, was recommended by the CIE in 1960, producing what is referred to as the (u, v)-uniform chromaticity-scale (UCS) diagram. The transform of the 1931 (x, y)-chromaticity coordinates into 1960 (u, v)-coordinates is given in Eq. 1-13 below. In

1976 the CIE recommended a modified version of the 1960 UCS diagram, which represented an improvement in uniformity of chromaticity scaling. The transform for the 1976 (u′, v′) UCS diagram is given in terms of the coordinates (u, v) in Eq. 1-14 below and is shown in Figure 1-27.

$$u = \frac{4x}{-2x+12y+3}$$
$$v = \frac{6y}{-2x+12y+3} \qquad \textbf{Eq. 1-13}$$

$$u' = u$$
$$v' = 1.5v \qquad \textbf{Eq. 1-14}$$

To represent perceptual differences between colour stimuli that differ in both chromaticity and luminance, a three-dimensional colour space is required; two approximately uniform colour spaces have been recommended by the CIE, which aim to satisfy this condition. The CIE 1976 (L*, u*, v*)-space (CIELUV) is based on rectangular coordinates and is produced by plotting the quantities L*, u* and v* defined below

$$L^* = 116\left(\frac{Y}{Y_n}\right)^{1/3} - 16 \qquad \text{for } \frac{Y}{Y_n} > 0.008856$$
$$L^* = 903.3\left(\frac{Y}{Y_n}\right) \qquad \text{for } \frac{Y}{Y_n} \le 0.008856 \qquad \textbf{Eq. 1-15}$$
$$u^* = 13L^*\left(u' - u'_n\right)$$
$$v^* = 13L^*\left(v' - v'_n\right)$$

where the Y tristimulus value and (u′, v′)-chromaticity coordinates with the subscript n, refer to the white reference stimulus, which is often taken as one of the standard illuminants defined by the CIE. These standard illuminants are described by their relative spectral radiant power distributions and are representative of different light sources, for example, standard illuminant D65 is representative of a phase of natural daylight. The CIELUV space incorporates a (u′, v′)-chromaticity plane for constant L*. The second uniform colour space recommended by the CIE was the 1976 (L*, a*, b*)-space (CIELAB). In this space the quantities L*, a* and b* defined as in Eq. 1-16, are plotted in rectangular coordinates.

$$L^* = 116\left(\frac{Y}{Y_n}\right)^{1/3} - 16 \qquad \text{for } \frac{Y}{Y_n} > 0.008856$$

$$L^* = 903.3\left(\frac{Y}{Y_n}\right) \qquad \text{for } \frac{Y}{Y_n} \le 0.008856$$

$$a^* = 500\left[\left(\frac{X}{X_n}\right)^{1/3} - \left(\frac{Y}{Y_n}\right)^{1/3}\right] \qquad \textbf{Eq. 1-16}$$

$$b^* = 200\left[\left(\frac{Y}{Y_n}\right)^{1/3} - \left(\frac{Z}{Z_n}\right)^{1/3}\right]$$

If $\frac{X}{X_n}$, $\frac{Y}{Y_n}$ or $\frac{Z}{Z_n} \le 0.008856$, then they are replaced by $7.787\left(\frac{X}{X_n}\right) + \frac{16}{116}$, $7.787\left(\frac{Y}{Y_n}\right) + \frac{16}{116}$ or $7.787\left(\frac{Z}{Z_n}\right) + \frac{16}{116}$, respectively.

Tristimulus values with the subscript n, again refer to a white reference stimulus. The CIELUV space is applicable to sources and the CIELAB space applicable to surface colours. Both spaces are defined for photopic viewing conditions. Associated with these two colour spaces are colour difference formulae, which aim to predict the magnitude of a colour difference between two colour stimuli. These are defined in Eq. 1-17 and 1-18 below.

$$\Delta E = \left[(\Delta L^*)^2 + (\Delta u^*)^2 + (\Delta v^*)^2\right]^{1/2} \qquad \textbf{Eq. 1-17}$$

$$\Delta E = \left[(\Delta L^*)^2 + (\Delta a^*)^2 + (\Delta b^*)^2\right]^{1/2} \qquad \textbf{Eq. 1-18}$$

where ΔE: magnitude of the colour difference, ΔL^*: difference between the two stimuli in the quantity L^*, Δu^*: difference in the quantity u^*, Δv^*: difference in the quantity v^*, Δa^*: difference in the quantity a^*, Δb^*: difference in the quantity b^*.

1.2.8 Colour spaces based on retinal physiology

Colour stimuli can also be represented in colour spaces that relate to the early stages of visual processing. In cone excitation space the activity (relative number of quantal absorptions) of the three cone types is plotted along orthogonal axes. In this

space colour stimuli that fall along any one straight line through the origin have equal chromaticity, but vary in intensity. Cone excitations can be calculated from current estimates of the cone fundamentals (see section 1.2.1 above). By making the assumption that S-cones do not contribute to luminance, MacLeod and Boynton (1979) introduced a chromaticity diagram based on an isoluminant plane of cone excitation space i.e., any plane where the sum of L-cone activity (L) and M-cone activity (M) is constant. In this diagram (shown in Figure 1-28) the quantity l is plotted on the abscissa and s on the ordinate, where l and s are defined in Eq. 1-19.

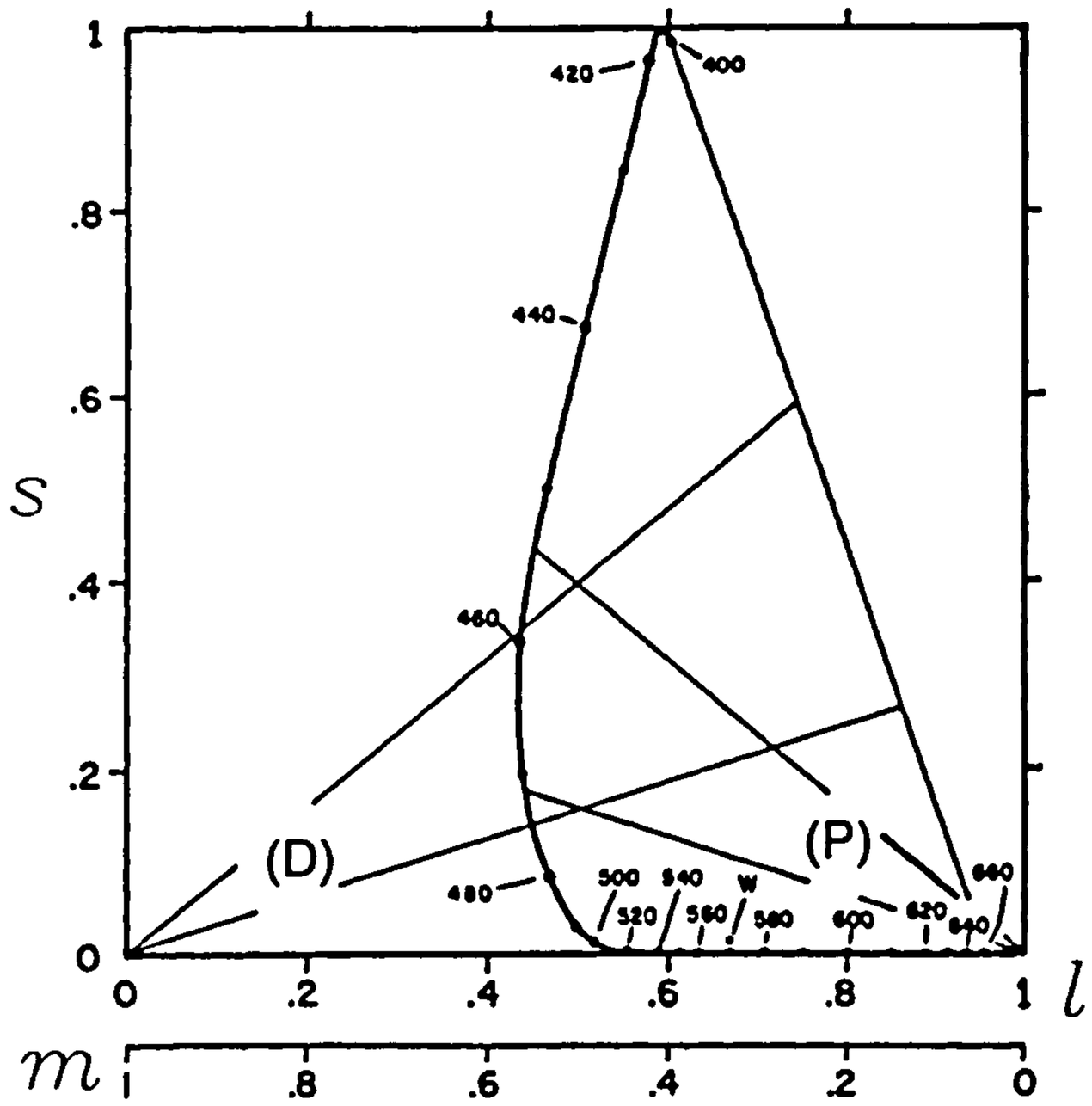

Figure 1-28. MacLeod-Boynton chromaticity diagram. Modified from (Kaiser and Boynton 1996). Lines labelled (P) and (D) show the colour confusion lines of a protanope and deuteranope, respectively.

$$l = \frac{L}{L+M}$$

$$m = \frac{M}{L+M} \qquad \textbf{Eq. 1-19}$$

$$s = \frac{S}{L+M}$$

where S: activity of the S-cones. The quantity m also falls along the abscissa and is equal to (L+M)-l. In this way, horizontal lines in the chromaticity diagram represent constant S-cone excitation and vertical lines represent constant L- and M-cone excitation, i.e. tritanopic colour confusion lines. Protanopic and deuteranopic

isochromatic lines also fall along straight lines in this diagram. It should be noted that steps of equal cone excitations do not correspond to equal perceptions of colour difference in this diagram.

Cone contrast space is based on the premise that cone excitations are recoded in the retina as contrast signals. Such a space is useful for representing colour stimuli relative to a background field, where stimuli can be compared independently of the adaptive state of the cones. It was suggested by Von Kries (1905/1970) that cone signals were normalised individually, and so in cone contrast space the activity of each cone type is computed for an incremental/decremental stimulus relative to the background activity for the same cone type. Contrast is computed according to the Weber-Fechner law, which states that the ratio of an increment stimulus to its adapting level is constant. This relation was first suggested by Weber in relation to sensory discrimination, and Fechner investigated its applicability to visual discrimination. The Weber-Fechner law has been found to hold approximately for almost all sensory receptors. In cone contrast space, cone contrasts C_L, C_M and C_S are calculated according to Eq. 1-20 and plotted on orthogonal axes.

$$C_L = \frac{L - L_0}{L_0}$$
$$C_M = \frac{M - M_0}{M_0} \qquad \text{Eq. 1-20}$$
$$C_S = \frac{S - S_0}{S_0}$$

Where L, M, S: excitations of the L-, M- and S-cones, respectively, for the incremental/ decremental stimulus and L_0, M_0, S_0: excitations of the L-, M- and S-cones, respectively, for the background.

Opponent modulation spaces aim to represent the postreceptoral stage of processing where cone contrast signals are believed to be coded into two opponent colour mechanisms and a luminance mechanism. Derrington, Krauskopf and Lennie (1984) introduced an opponent modulation space (known as DKL space) based on the ideas of MacLeod and Boynton (1979) and Krauskopf, Williams and Heeley (1982).

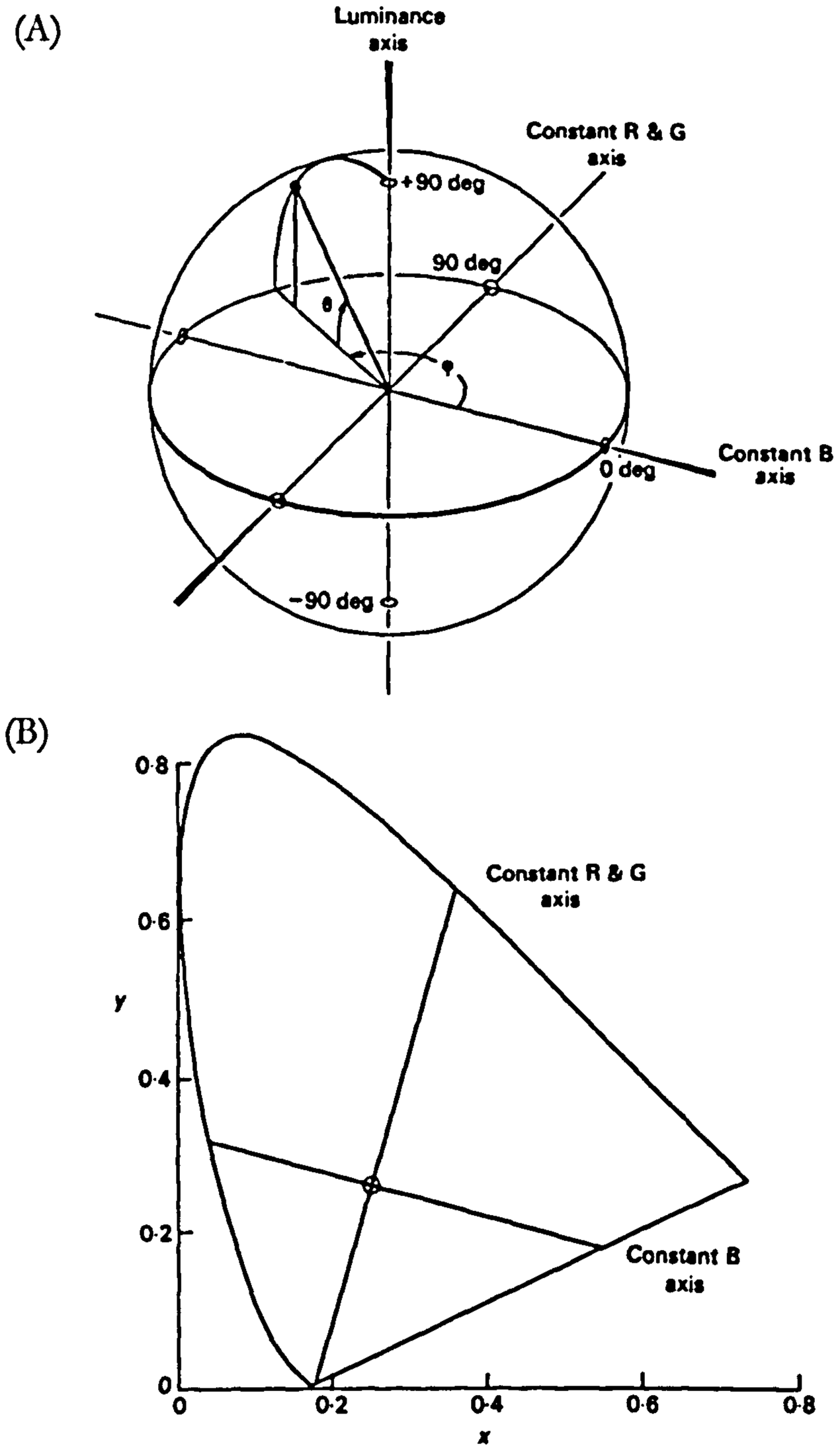

Figure 1-29 (A)-(B). Diagrammatic representation of DKL space (A), and the orientations of the constant L & M-cone axis (labelled constant R & G axis) and the constant S-cone axis (labelled constant B axis) in the CIE 1931 chromaticity diagram (B). Reproduced from (Derrington et al. 1984).

Krauskopf and his colleagues (Krauskopf et al. 1982) suggested from results of their investigations into the nature of colour processing beyond the photoreceptors, that there are three main cardinal axes in colour space that relate to independent visual pathways: a luminance mechanism and two chromatic opponent mechanisms. Based on these findings, Derrington, Krauskopf and Lennie (1984) defined a space with three orthogonal axes: the luminance axis, the axis of constant L- and M-cone excitation and the axis of constant S-cone excitation. A schematic of their space is

shown in Figure 1-29. They considered ganglion and LGN cells with antagonistic receptive fields and defined three "ideal" cells, which would respond maximally to modulation along one of these axes and show no change in response to modulation along the two orthogonal axes (null axes). They recognised that the response of a real cell could then be modelled as linear combinations of these "ideal" cells. They defined an "ideal" luminance cell with summed input from L- and M-cones, and two chromatic "ideal" cells; one with opponent inputs from L- and M-cones and the other with S-cone input opposing input from L- and M-cones. In their electrophysiological recordings from macaque LGN cells they found that all parvocellular cells tested had one null axis that corresponded to either the constant S or the constant L & M axis, indicating that two classes of parvocellular cells exist with uniform response properties to isoluminant chromatic stimuli. Brainard (1996) detailed a method for computing DKL space coordinates for a colour stimulus relative to an adapting background from consideration of the properties of the three cardinal mechanisms. The response of the luminance mechanism can be scaled in terms of photopic luminance, but the choice of scaling constants for the constant S and constant L & M mechanisms are arbitrary. Brainard suggests that each chromatic mechanism should be scaled to give a response of unity for a stimulus with a pooled cone contrast, where pooled cone contrast is the square root of the sum of squared cone contrasts.

1.2.9 Colour order systems

A colour order system is a methodical organisation of object colours, with samples displayed to represent the relationship between all object colours in the given system. One category of colour order system is the colour appearance system. Relationships between colour stimuli in a colour appearance system are based on the visual perception of colours. The only example of a colour appearance system that will be described here is the Munsell system; other examples of this type of system are the Swedish natural colour system, the German DIN (Deusches Institut fur Normung) system and the Optical Society of America system. The Munsell system developed by A.H. Munsell, originated in 1905, and its arrangement of colours produces approximately constant perceptual differences between

neighbouring samples throughout the system in each of three perceptual attributes: hue, value and chroma. Munsell hue has the usual meaning of hue, Munsell value describes the lightness of a sample and correlates with sample reflectance, and Munsell chroma describes the amount by which a colour stimulus differs from an achromatic stimulus of the same lightness. There are 10 hues in the Munsell system; five principal hues (R: red, Y: yellow, G: green, B: blue and P: purple) and five intermediate hues (YR, GY, BG, BP and RP) that are arranged around a circle with equal spacing. The value scale is perpendicular to the hue circle. The grey scale, which runs through the centre of the hue circle, consists of 10 steps with white designated value 10 and black value zero. The scale of Munsell chroma runs radially outwards from the centre of the hue circle; larger numbers indicate stronger colours. A schematic of the system is shown in Figure 1-30. Samples are displayed in the Munsell Book of Color. The book consists of matt or glossy chips arranged with a constant hue on each page and the value scale printed vertically on the page and the chroma scale printed horizontally.

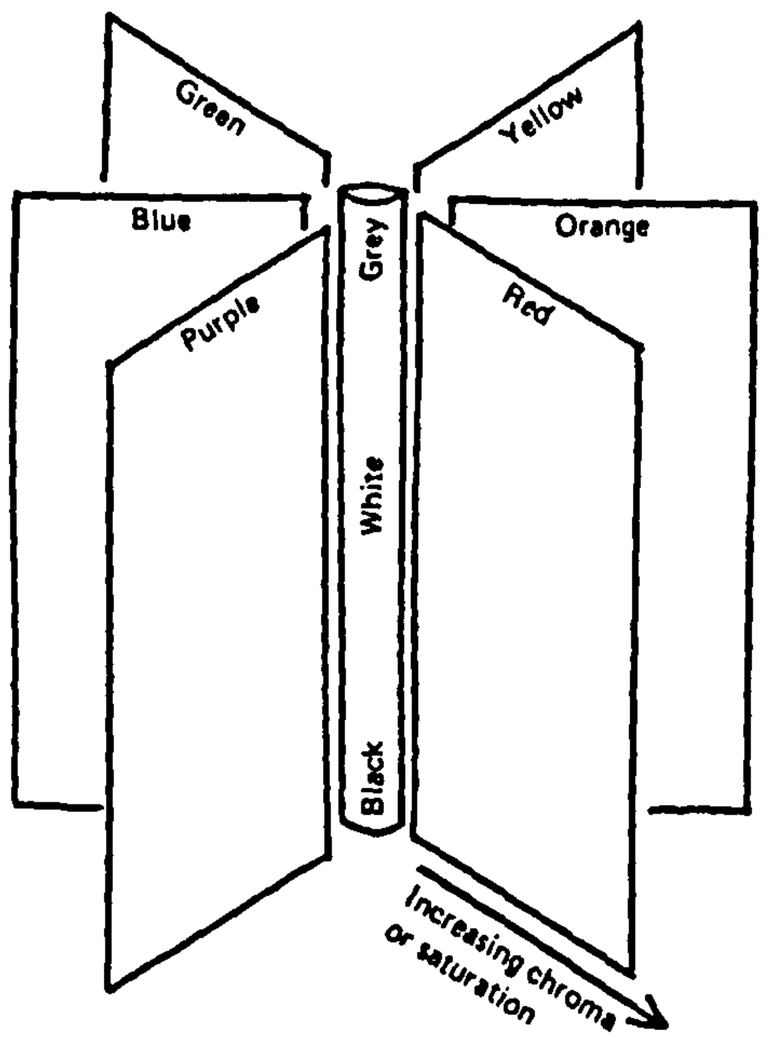

Figure 1-30. Diagram illustrating how the Munsell colour order system is arranged. Reproduced from (Hunt 1987).

1.2.10 Congenital colour vision deficiencies

Congenital colour vision deficiencies arise from inherited photopigment abnormalities. Colour deficient subjects are named in relation to the number of

cone photopigments present in the retina, as anomalous trichromats, dichromats or monochromats. There are three types of anomalous trichromat, termed protanomalous, deuteranomalous or tritanomalous depending on whether there is an abnormality in the long wavelength sensitive (LWS), middle wavelength sensitive (MWS) or short wavelength sensitive (SWS) cone photopigment. The spectral sensitivity of the abnormal photopigment varies markedly among different anomalous trichromats of the same type; thus, the severity of the defect differs greatly. A dichromat lacks one of the three photopigments, and is termed respectively, a protanope, deuteranope or a tritanope if the LWS, MWS or SWS photopigment is absent. The term monochromat refers to subjects lacking two cone photopigments, or subjects with no cone photopigments. A rod monochromat is bereft of all three cone photopigments. The absence of the cone system means that rod monochromats can only detect differences in lightness between colour stimuli, they have poor visual acuity, nystagmus (unsteady fixation) and are photophobic (have an aversion to bright light). Cone monochromats lack two cone types. Cone monochromatism is very rare and is usually characterised by a lack of LWS and MWS photopigments: a condition known as S-cone monochromatism. S-cone monochromats are generally believed to lack the capacity for colour vision, although there are a number of reports of S-cone monochromats requiring two primaries for colour matches, i.e. having dichromatic colour vision, which is thought to arise from interactions between S-cones and rods (Pokorny et al. 1970; Alpern et al. 1971; Hess et al. 1989; Reitner et al. 1991). S-cone monochromats have visual acuity that is lower than normal plus in some cases nystagmus and photophobia.

Both protan and deutan colour vision deficiencies are both more common in males than females because they are defects linked to the X-chromosome (of which females have two and males only one). The incidence of red-green defects also varies with race. Protanopia and deuteranopia are present in the European male population with incidences of 1.01% and 1.28%, respectively, whereas protanomaly and deuteranomaly have an incidence of 1.07% and 4.61%, respectively (Sharpe et al. 1999). The corresponding figures for females are 0.02% (protanopia), 0.03% (protanomaly), 0.01% (deuteranopia), and 0.36% (deuteranomaly) (Sharpe et al. 1999). Tritan colour vision deficiencies are equally likely in males and females.

Estimated rates of incidence in the UK are 1 in 13,000 to 1 in 65,000 (Wright 1952). S-cone monochromacy, like red-green defects, is X-chromosome-linked. It affects approximately one in 100,000 males (Sharpe et al. 1999); all reported cases have been male. Other types of cone monochromacy are extremely rare, making it difficult to estimate the rates of incidence. Estimates of the incidence of rod monochromacy vary, but a Northern European survey in 1990 produced the figure of 1 in 50,000 for both sexes (see Sharpe and Nordby 1990).

Observers with dichromatic and monochromatic vision produce abnormal colour matches compared to normal trichromats, and are unable to distinguish between some colours that appear different to colour normal observers. They also have altered chromatic discrimination and their relative luminous efficiency functions generally also differ from those of colour normals. Anomalous trichromats require three primary stimuli for colour matching, and may have normal chromatic discrimination, but their colour matches differ from those of normal trichromats. Matches to a monochromatic yellow can be obtained from mixing a red and green monochromatic primary, and the relative proportion of red to green (R/G ratio) can be used to differentiate between normal trichromacy, protanomaly and deuteranomaly. This ratio was first used by Lord Rayleigh in 1881 who discovered red-green anomalous observers, and the match is often referred to as a Rayleigh match. Tritanomaly is best distinguished from normal trichromatism by comparison of chromatic discrimination in the green to blue spectral range. Wavelength discrimination curves for anomalous trichromats show characteristics that fall somewhere in between those of normal trichromats and dichromats of the same type. The relative luminous efficiency functions of deuteranomalous and tritanomalous subjects obtained using flicker photometry, are similar to those of normal trichromats, whereas protanomalous subjects exhibit low luminous efficiency for the red end of the visible spectrum (Wright 1946).

Dichromats make colour matches using only two primaries and cannot distinguish between stimuli of certain chromaticities in the absence of brightness cues. For each type of dichromat, stimuli that can be matched by adjustment of intensity only, plot in the CIE 1931 chromaticity diagram on what are termed isochromatic lines,

converging at the copunctual or confusion point. These copunctual points for the three types of dichromat have been measured experimentally and are located outside the spectrum locus (Smith and Pokorny 1975). Figure 1-31 shows examples of isochromatic lines for each class of dichromat, plus the location of the copunctual point for protanopes and tritanopes (the deuteranopic copunctual point falls outside graph (B)).

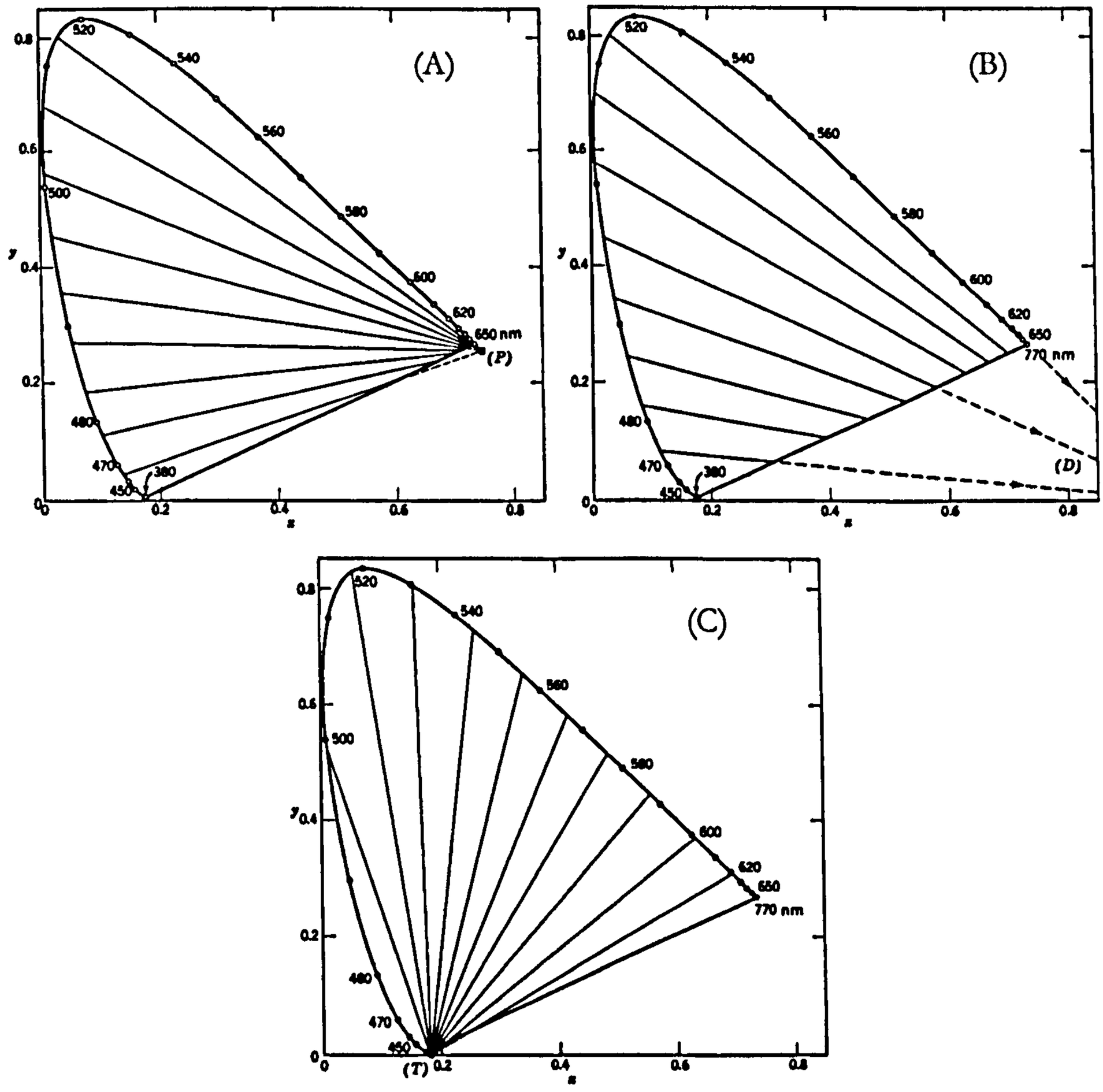

Figure 1-31 (A)-(C). Diagrams illustrating isochromatic lines for each class of dichromat: protanopes (A), deuteranopes (B), and tritanopes (T). Reproduced from (Wyszecki and Stiles 1982).

Protanopes and Deuteranopes cannot discriminate between wavelengths from the red end of the spectrum to about 520 nm and 530 nm, respectively and their wavelength discrimination curves consist of a single minimum at about 495 nm. Wavelength discrimination for tritanopes is absent from about 445 to 480 nm. Dichromatic relative luminous efficiency curves differ from those of normal

trichromats in shape and peak sensitivity, leading to notable differences in sensitivity over particular regions of the visible spectrum. Protanopes exhibit a marked shift in peak sensitivity towards shorter wavelengths compared to colour normals, from 555 nm to about 540 nm, and sensitivity at the red end of the spectrum is greatly reduced (Pitt 1935). The peak sensitivity of a deuteranope's relative luminous efficiency curve is marginally shifted towards longer wavelengths and is located at around 560 nm (Pitt 1935). Tritanopes have the same peak sensitivity as normals, but their relative luminous efficiency functions display reduced sensitivity at short wavelengths (Wright 1952). Examples of luminous efficiency curves for dichromatic observers are illustrated in Figure 1-32.

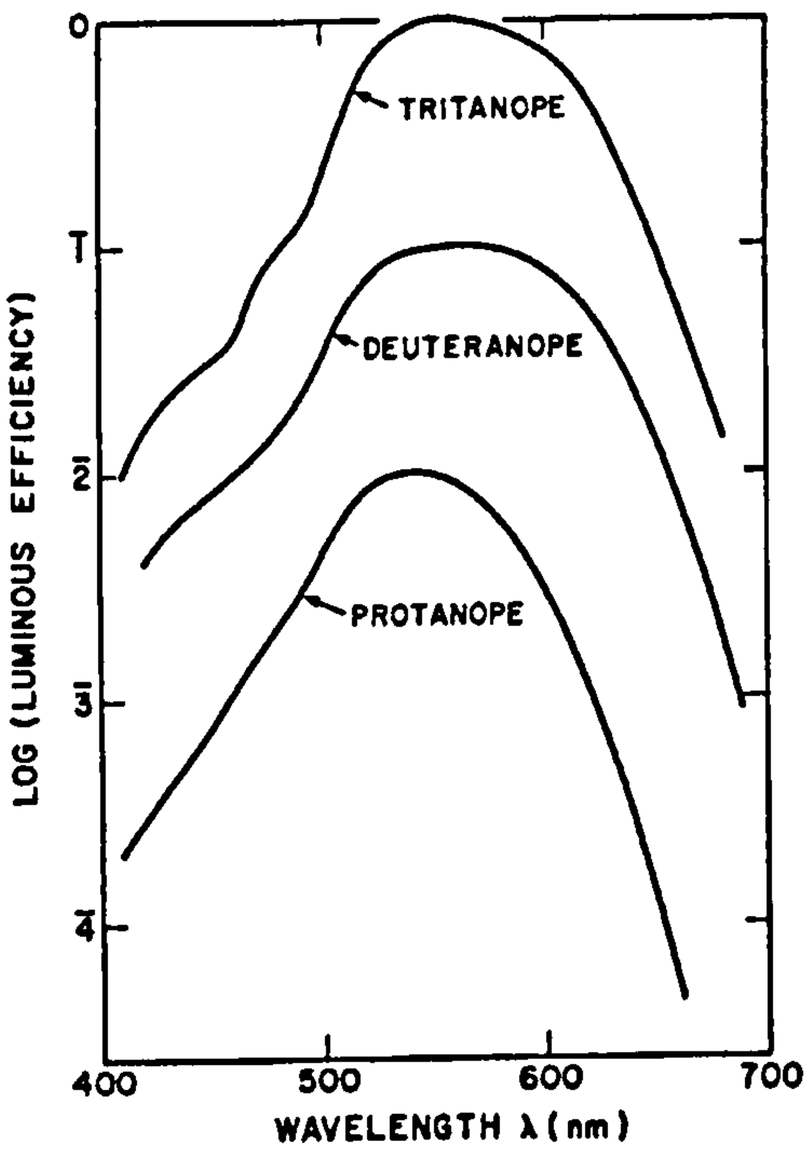

Figure 1-32. Spectral luminous efficiency functions for the three classes of dichromat, after (Pitt 1935) (protanope and deuteranope), and (Wright 1952) (tritanope). The curves are displaced vertically for clarity. Reproduced from (Wyszecki and Stiles 1982).

Rod monochromats can only make matches in terms of relative intensity. The relative luminous efficiency curve of a rod monochromat peaks between 500 and 510 nm and is similar to the standard spectral luminous efficiency curve for scotopic vision (Nordby et al. 1984; Sharpe et al. 1988). Cone monochromats are generally believed to only make matches between colour stimuli by adjustment of their relative intensities. S-cone monochromats have relative luminous efficiency functions similar to the S-cone spectral sensitivity function, with a maximum at around 440 nm. There is some evidence to suggest that in S-cone monochromats

under mesopic conditions, the rods and S-cone interact, resulting in dichromatic colour perception (Reitner et al. 1991). The nature and characteristics of L- and M-cone monochromatism are still poorly understood.

1.2.11 Tests for colour vision deficiencies

There are many different colour vision tests used to detect and/or classify colour vision deficiency, based on different psychophysical methodologies. Three widely used tests will be discussed here: the Ishihara pseudoisochromatic plates, the Farnsworth-Munsell 100-hue test and the Nagel anomaloscope. Pseudoisochromatic plates utilise the fact that dichromats cannot discriminate between certain chromaticities when luminance cues are absent. The Ishihara plates are a screening test for red-green colour deficiencies, i.e. protanopia, protanomaly, deuteranopia and deuteranomaly, but also aim to distinguish between protan and deutan defects. The test pattern (a numeral or pathway) and background are divided into circular patches that vary in luminance, which has the effect of removing edge cues and luminance cues, forcing the observer to discriminate between the test and background solely using colour signals. To overcome the problem of reproducing exact chromaticities in the printing of the plates the chromaticity of the test and background patches are also varied about given coordinates. The average spectral reflectances of the test and background stimulus are chosen to lie approximately along isochromatic lines for protanopes and deuteranopes when viewed under an illuminant representative of average daylight, such as CIE standard illuminant C. The plates consist of four different designs: in the first design normal trichromats (NTs) see a particular number and red-green deficient observers (RGs) see another, in the second NTs see a number and RGs do not, in the third RGs see a number that NTs cannot see, and the fourth is used to distinguish between protan and deutan defects and consists of two numerals, one of which is the only one detected or appears brighter and clearer for protan defects, and the other numeral is the only one detected or appears brighter and clearer for deutan defects, and both are seen by colour normals.

The Farnsworth-Munsell 100-hue test (F-M 100-hue) was developed by Farnsworth in 1943. It is a test of hue discrimination ability and only detects colour vision deficiency if it is moderate or severe. The test consists of 85 Munsell sample papers mounted in black cylindrical housings known as caps, which form a hue circle of fixed chroma. The caps are numbered and arranged contiguously in four boxes with two caps fixed at the ends of the boxes at appropriate intervals in the hue circle (numbers 1, 22, 43 and 64). Subjects are required to arrange the caps within each box between the two fixed samples to form a continuous series of colour. The test should be undertaken using an illuminant that approximates average daylight (usually CIE standard illuminant C). Hue discrimination error scores for each cap are obtained from the sum of the differences between the numbers of neighbouring caps as arranged by the subject. The total error score is equal to the sum of cap error scores minus 170, and is a measure of overall hue discrimination ability. Cap error scores are also plotted on a polar diagram where the distribution of errors may indicate a protan, deutan or tritan defect; specific ranges of cap numbers encompass dichromatic colour confusion axes.

The Nagel anomaloscope utilises the different Rayleigh match characteristics of red-green colour deficient subjects and normal trichromats to classify red-green defects. In the Nagel anomaloscope a 3° bipartite field is presented to the observer, the bottom half of which is filled with yellow light (589 nm) that can be adjusted in intensity, and the top half is filled with a variable mixture of red (670 nm) and green (546 nm), which is maintained at a constant luminance. Observers are firstly required to make a match between the two halves of the field by adjusting the mixture of red and green primaries and the intensity of the yellow light. Secondly, the observer is required to make a match by altering the intensity of the yellow light to a red-green mixture set by the experimenter. Normal trichromats are able to make a precise match within a small range of R/G ratios. Anomalous trichromats make matches outside the range of colour normals, with a precision that can be equivalent to that of colour normals, but their repeated matches are often more variable. Protanomalous subjects have larger R/G ratios than normal trichromats, and deuteranomalous subjects have smaller R/G ratios than NTs. The matching range of both protanopes and deuteranopes encompasses all R/G ratios, i.e., they

can make a match for any R/G ratio by adjusting the intensity of the yellow light. Protanopes and subjects with protanomaly must lower the intensity of the yellow light to make a match with a high proportion of red, reflecting their reduced sensitivity at long wavelengths. This characteristic is utilised to differentiate between protanopes and deuteranopes.

1.3 The dual nature of the retina and aspects of visual function under mesopic conditions

The human visual system can operate over a range of intensities spanning almost 10 log units. Changes in pupil size account for about 1.3 log units of this range of adaptation, but the majority is due to the operating characteristics of the rod and cone photoreceptors. As mentioned in section 1.1.2 b. the cones function at intermediate to high intensities, whereas the rods function when photons are less abundant; but their operating ranges overlap over a region of three to four log units.

It was stated above in section 1.1.2 b. that the term mesopic is used to describe vision under conditions where both rods and cones contribute to the visual response. The mesopic range encompasses levels of intensity from rod saturation to the absolute threshold of the cones, but the relative contribution made by rods and cones in mesopic vision varies as a function of light adaptation, stimulus size, eccentricity, duration, and spectral content. The rod and cone systems are generally considered to operate independently. This is a good approximation under many conditions, but the literature contains several reports suggesting deviation from rod and cone independence; these are discussed in section 1.3.3.

1.3.1 Differences between rod and cone mediated vision

a. Absolute threshold

Threshold is defined as the probability that a change in a particular stimulus attribute is detected. Visual thresholds are often taken as 50% probability of seeing a change. Absolute threshold defines the minimum stimulus for vision when the eye

is fully adapted to the dark, and depends on the size, duration and location of the test stimulus. Rod threshold is usually measured at a peripheral retinal location where there is a high density of rod receptors. Cone threshold can be measured by utilising the fact that rods are absent from the centre of the fovea. Absolute thresholds measured using small, brief stimuli are dependent on the number of quanta entering the eye during a single presentation. Marriott (1963) obtained measurements using such stimuli of wavelength 555 nm (the wavelength of maximum sensitivity for cone vision) imaged within the foveal centre, and found a mean threshold of 602 quanta (range 490-872 quanta). The absolute threshold measured in this way for rods using stimuli of wavelength 507 nm presented in the periphery, is of the order of 80 quanta (Baumgardt 1972). These results indicate that rod vision is about 7.5 times more sensitive than cone vision for stimuli of small area. Absolute thresholds measured using long presentation times and large stimuli are expressed in terms of retinal illuminance. Absolute rod threshold measured in this way for a 6° diameter 200ms stimulus has a mean of -3.46 log scotopic trolands with a range of -3.22 to -3.97 log scotopic trolands (Sharpe et al. 1989). A lower mean value of absolute rod threshold was obtained by Pirenne et al. (1957) using a large field, which corresponded to -4.36 log scotopic trolands. Under such conditions, where spatial and temporal summation is possible, Barlow (1972) determined that cones require a stimulus of 4 log units greater intensity than that required by rods at absolute threshold.

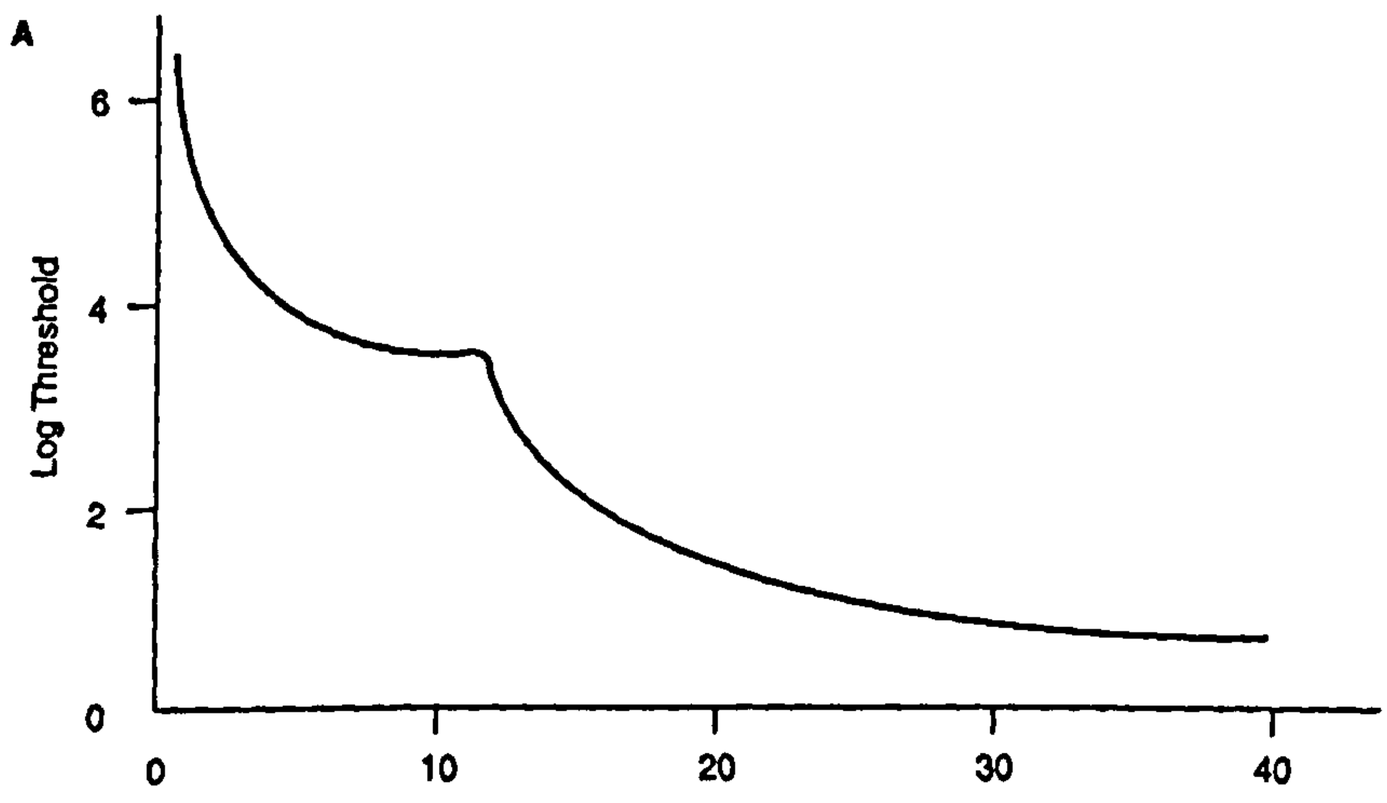

Figure 1-33. An example of a typical dark adaptation curve, reproduced from (Schwartz 1994).

b. Dark adaptation and increment thresholds

The process of recovery of rod and cone sensitivity following adaptation to high ambient illumination is known as dark adaptation. A typical dark adaptation curve is illustrated in Figure 1-33. Usually a broadband, white light is used to provide light adaptation, also known as the bleaching stimulus. After the white adapting stimulus is extinguished, detection thresholds are measured for a brief stimulus presented against a totally dark background. Within a few minutes following the initial rapid fall in threshold a plateau is reached, which represents the cone detection threshold. After a further few minutes threshold falls for a second time until the level of rod absolute threshold is reached, which takes approximately 30 to 40 minutes. The second fall of threshold begins at what is termed the rod-cone break, and marks the point at which the rods become more sensitive than the cones. Above the rod-cone break the stimulus is detected by the cones and below the break it is detected by the rod system.

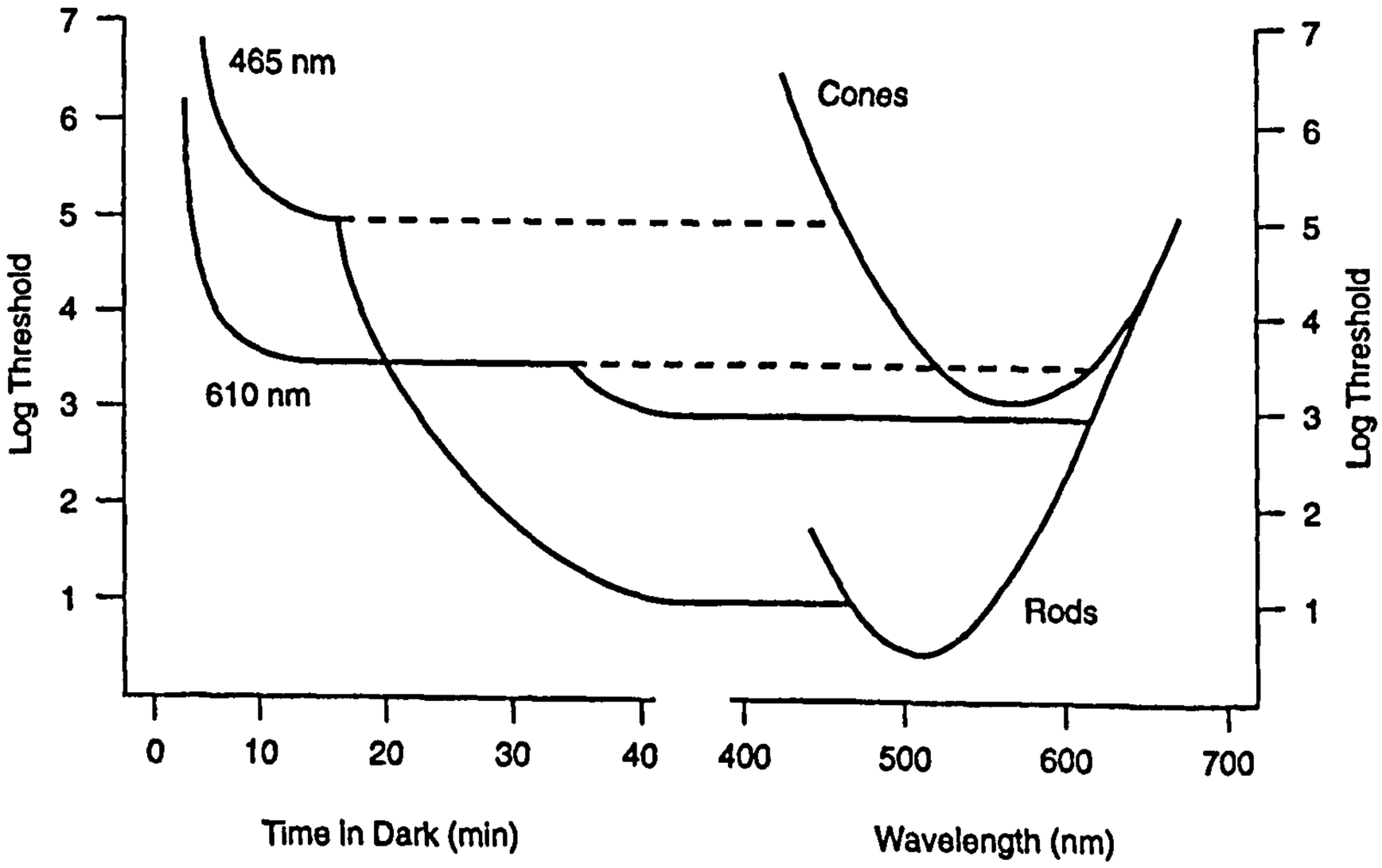

Figure 1-34. Graph to illustrate, for a monochromatic test stimulus, the effect of cone spectral sensitivity on the rod-cone break in the dark adaptation curve, and the effect of rod spectral sensitivity on absolute threshold. Reproduced from (Schwartz 1994).

The shape of dark adaptation curves depends on several factors including the intensity and duration of the bleaching stimulus, the size, duration, location and wavelength of the test stimulus. As the intensity of the bleaching stimulus is

reduced, cone sensitivity becomes less affected and the cone plateau is reached earlier or may no longer be evident (Hecht et al. 1937). Dark adaptation curves obtained with a small stimulus imaged on the rod free area of the fovea also show no rod-cone break and threshold does not fall below the level of the cone plateau (Hecht et al. 1935). Alteration of the test stimulus wavelength results in a change in the level of the cone plateau and absolute threshold, and changes the time at which the rod-cone break occurs. These factors can be approximately related to the spectral luminous efficiency functions of the cones and rods (see Figure 1-34). For long wavelength test stimuli the rods never become more sensitive than the cone system, and again no rod-cone break is present in the dark adaptation curve (Hecht et al. 1942).

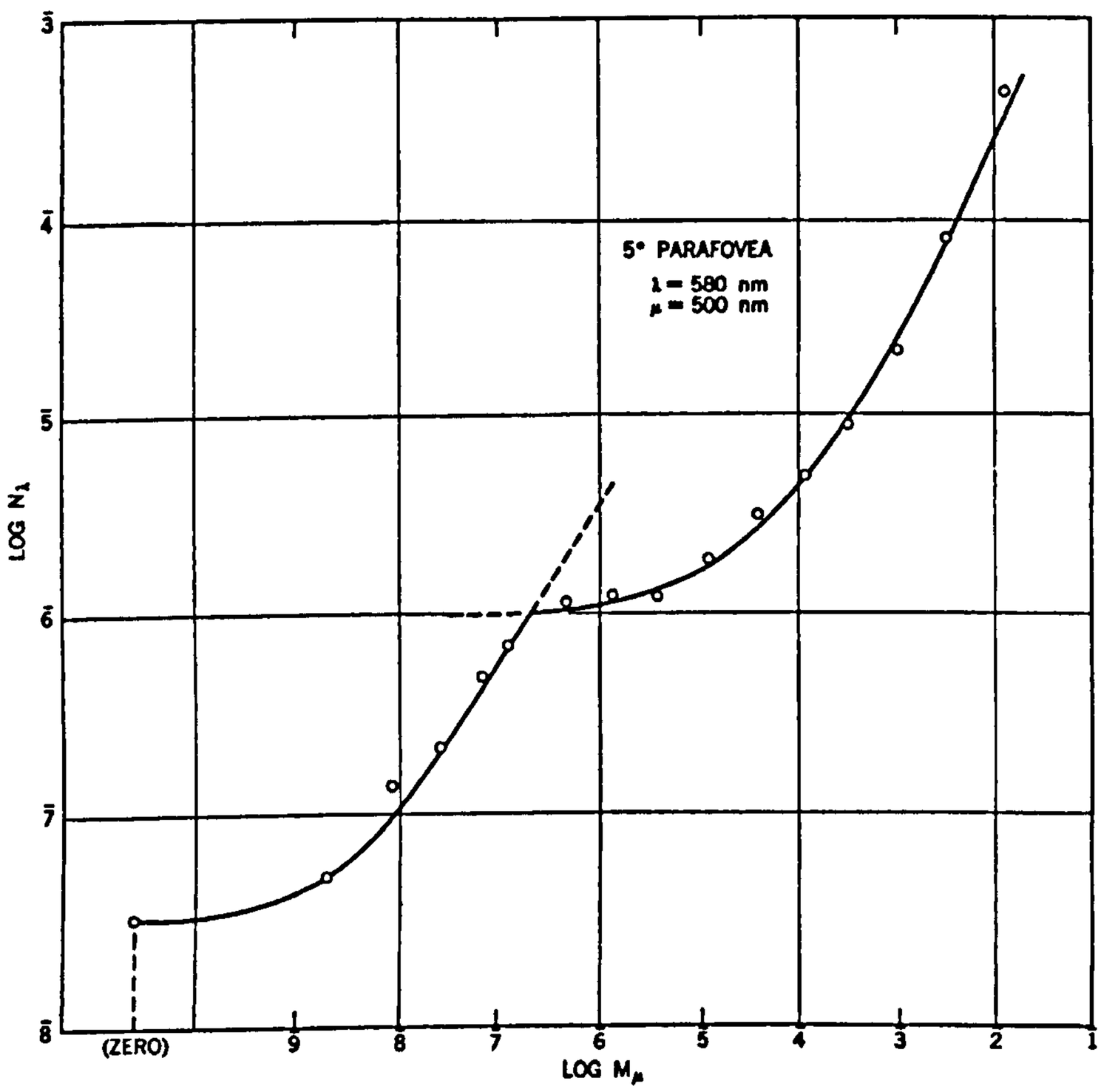

Figure 1-35. Threshold vs. intensity curve obtained using the two-colour method, with a 1° stimulus, showing a rod and cone branch. N_λ denotes the increment threshold and M_μ denotes the radiance of the background field. Reproduced from (Wyszecki and Stiles 1982) after (Stiles 1939).

The threshold for detection of a test stimulus added to a uniform adapting background is described as an increment threshold. Such threshold measurements

may be used to investigate the process of light adaptation. The spectral properties of the background and test are often chosen with the aim of isolating different visual mechanisms such as the rod system from that of the cones. This is achieved by selecting a chromatic adapting background (usually monochromatic) to which the mechanism under investigation is not sensitive and an incremental test stimulus (also usually monochromatic) to which it is sensitive, a scheme known as the two-colour threshold method. If increment thresholds are measured for increasing background intensities, threshold vs. intensity (TVI) curves can be plotted. TVI curves obtained using the two-colour method in the extrafoveal retina typically consist of a rod branch and cone branch, see Figure 1-35.

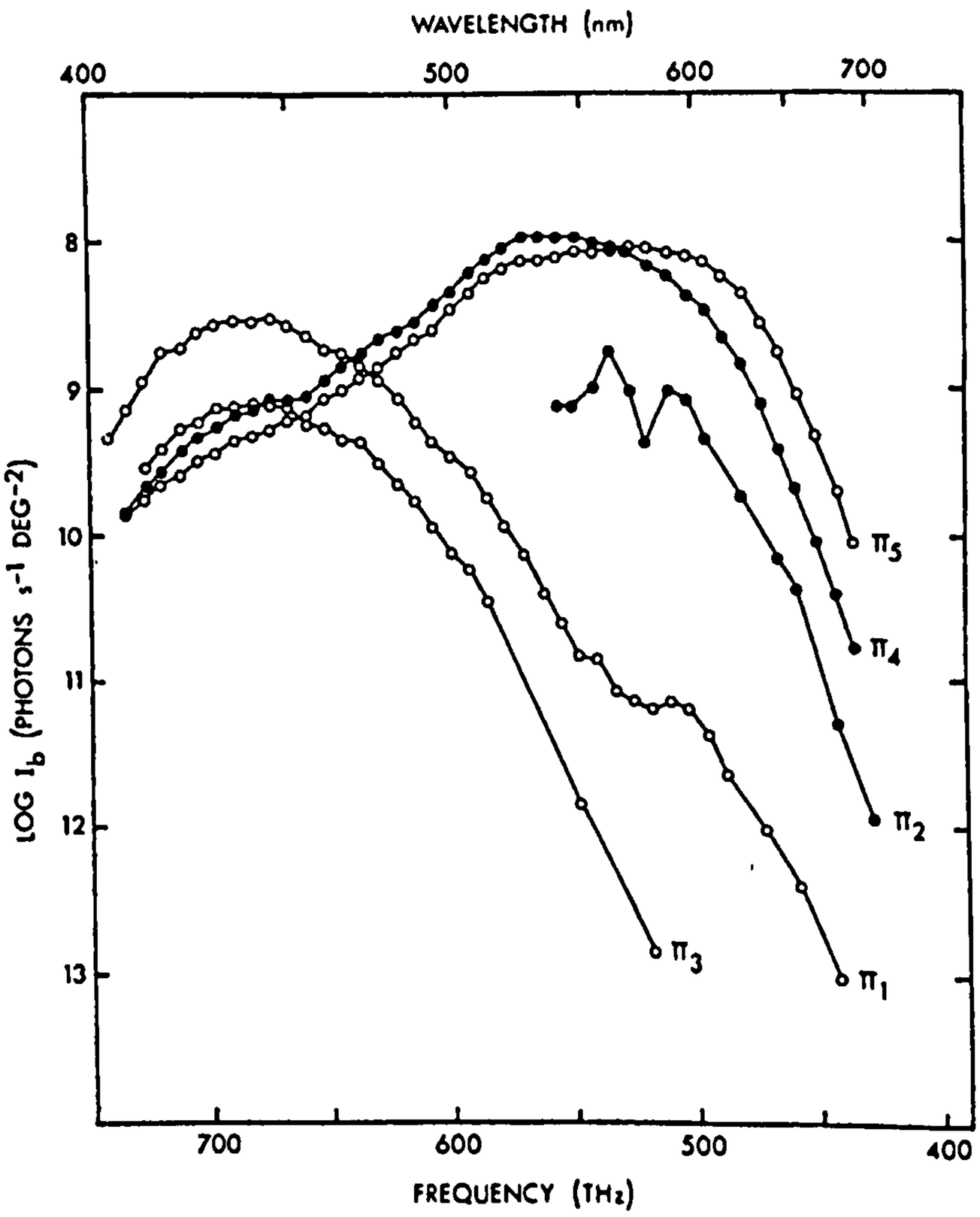

Figure 1-36. Five of Stiles π-mechanisms: π_1-π_5 measured using Stiles' two-colour threshold technique. Reproduced from (Boynton 1979), after data tabulated in (Wyszecki and Stiles 1967).

Stiles used the two-colour threshold method (often referred to as Stiles' two-colour threshold technique) to measure foveal thresholds and TVI curves for test

wavelengths across the visible spectrum against different chromatic adapting backgrounds. Stiles investigations led to the discovery of seven cone-mediated mechanisms with different spectral sensitivity curves, known as the π-mechanisms (Stiles 1959), five of which are shown in Figure 1-36. The π-mechanisms are generally broader than the spectral sensitivity curves of the three cones types, and are thought to represent the behaviour of channels that the cone signals feed into; however, the three mechanisms π_1, π_2, and π_3 appear to be associated primarily with the S-cones, π_4 and π_4' the M-cones, and π_5 and π_5' the L-cones.

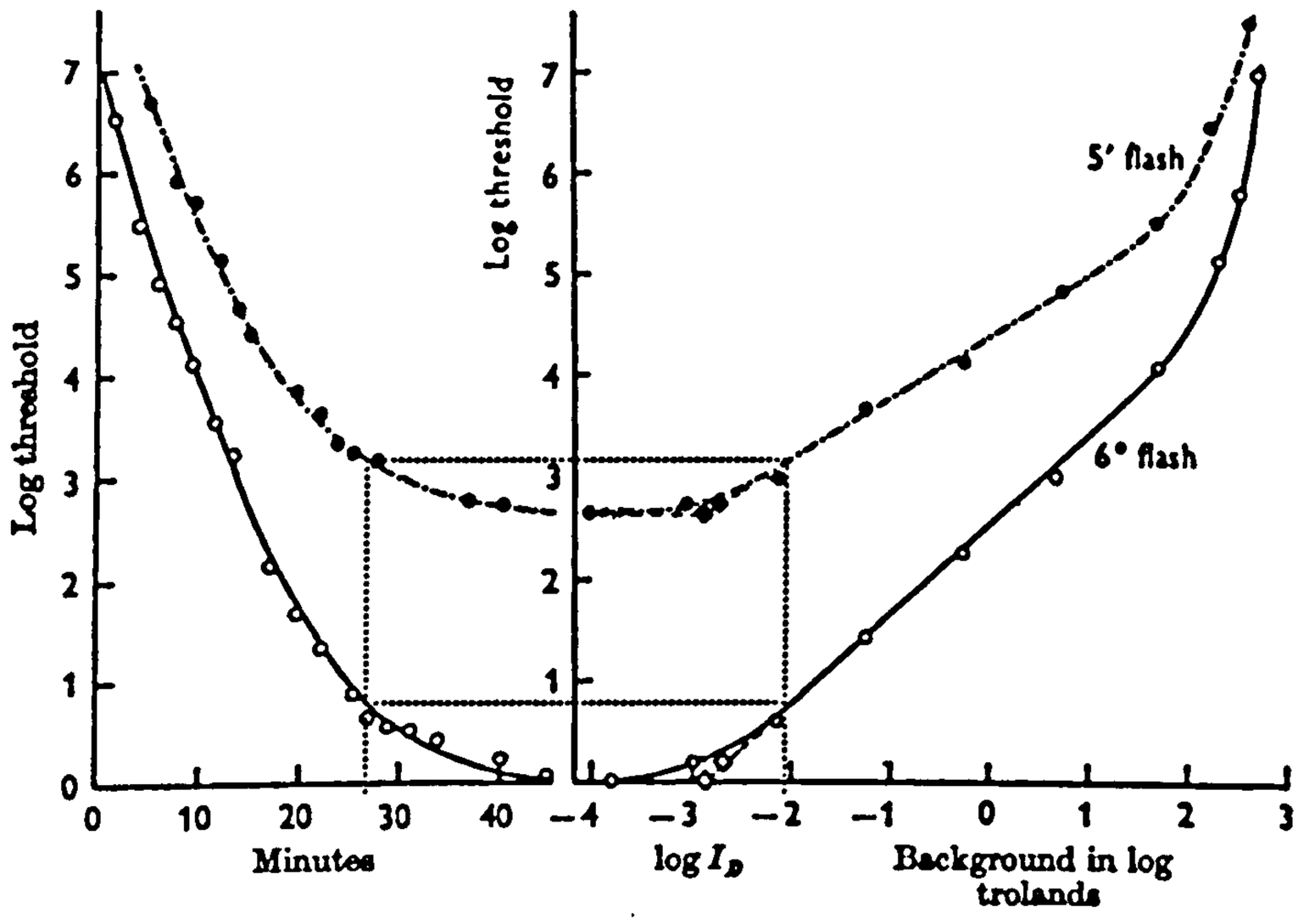

Figure 1-37. Dark adaptation curves (on the left) and increment threshold curves (on the right) for a rod monochromat, modified from (Blakemore and Rushton 1965a). The filled symbols represent measurements for a stimulus 5′ in diameter, and the open symbols represent measurements for a stimulus 6° in diameter. The dashed lines indicate how to find the equivalent background luminance at any stage during dark adaptation (see text for details).

The mechanisms of dark adaptation and light adaptation are closely related. One of the most important factors in visual adaptation is the bleaching and regeneration of photopigments in the rod and cone photoreceptors. Following exposure to light, a proportion of retinal photopigment is bleached, and these molecules take time to resynthesize. The bleaching and recovery of the rod photopigment rhodopsin was studied by Rushton (1961) in a rod monochromat using retinal densitometry (see section 1.2.1). Rushton discovered that log threshold during dark adaptation is

proportional to the amount of bleached rhodopsin. He also noted, however, that measurements of threshold after bleaching depended on the parameters of the test stimulus. Rushton suggested, therefore, that threshold was related to, but not entirely determined by the recovery of rod photopigment. The results of ideas and investigations by Crawford (1937; 1947) indicated that adaptation could be explained in terms of an equivalent background luminance. Further evidence in support of Crawford's suggestion was obtained by Blakemore and Rushton (1965a). At any stage during dark adaptation, the equivalent background luminance is the luminance of the background that produces an increment threshold equal to that of threshold measured in total darkness; this concept is illustrated in Figure 1-37.

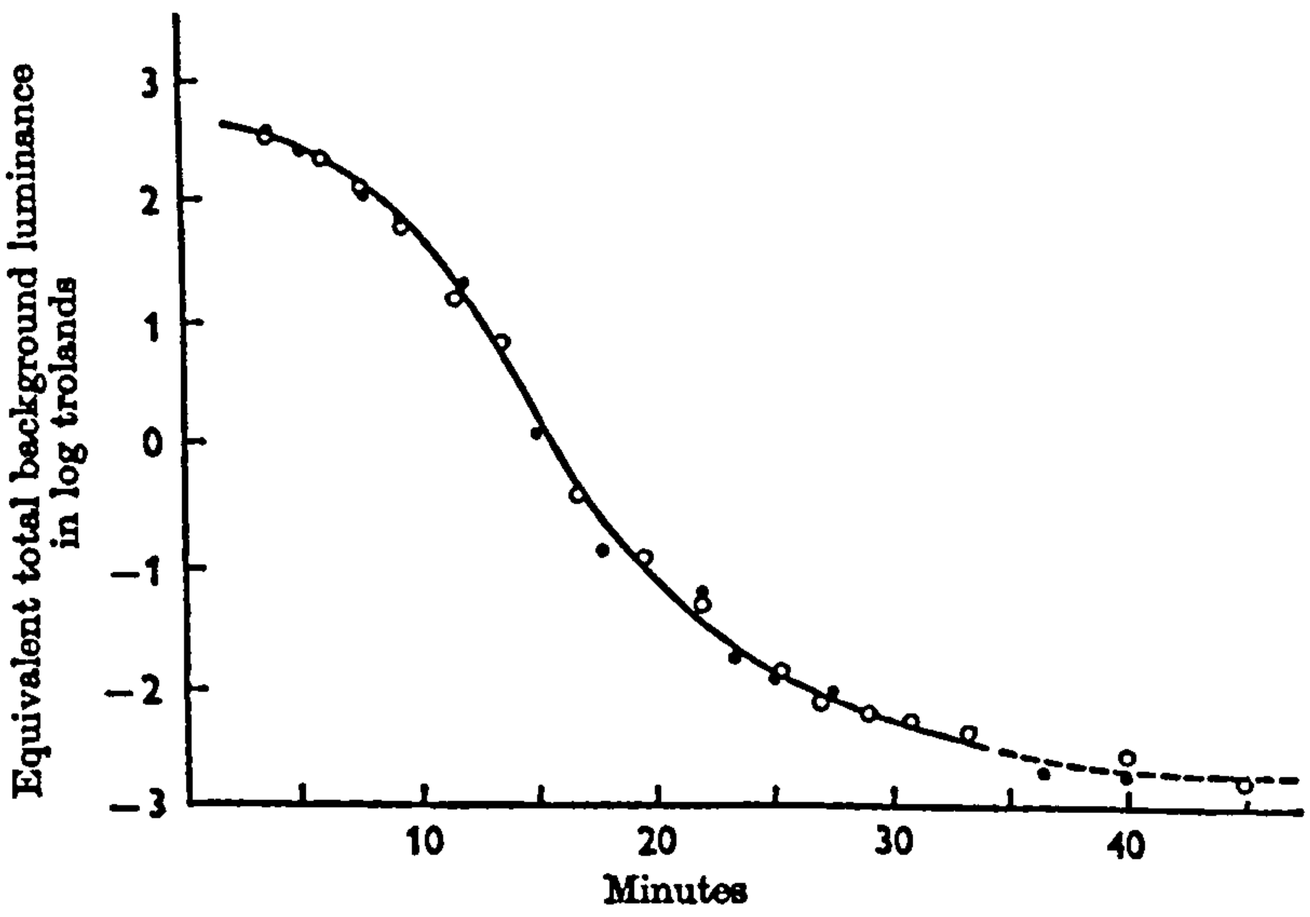

Figure 1-38. Graph illustrating that equivalent background luminance is independent of stimulus size, reproduced from (Blakemore and Rushton 1965a). Data points represent equivalent background luminances found from dark adaptation and increment threshold measurements in a rod monochromat, for a stimulus 5′ in diameter (filled symbols) and for a stimulus 6° in diameter (open symbols).

Blakemore and Rushton (1965a) obtained dark adaptation curves for a rod monochromat after 50% of rhodopsin was bleached, followed by measurement of increment threshold curves. They obtained measurements for two test stimuli differing in area: one test stimulus 5′ in diameter and the other 6° in diameter. For each test stimulus, at intervals during the period of dark adaptation they found the equivalent background luminance. From these results, Blakemore and Rushton showed that equivalent background luminance was independent of test stimulus area over an extended range of threshold variation (see Figure 1-38). This result

implied that the amount of available rhodopsin was related to equivalent background luminance, and that the equivalent background luminance along with the spatial attributes of the test stimulus, determined threshold. These findings compliment the view of Barlow (1964), that the neural noise (or dark-light) of photoreceptors containing a proportion of bleached pigment, produces a signal equivalent to that in response to a real light of equivalent background luminance when almost all the photopigment is regenerated.

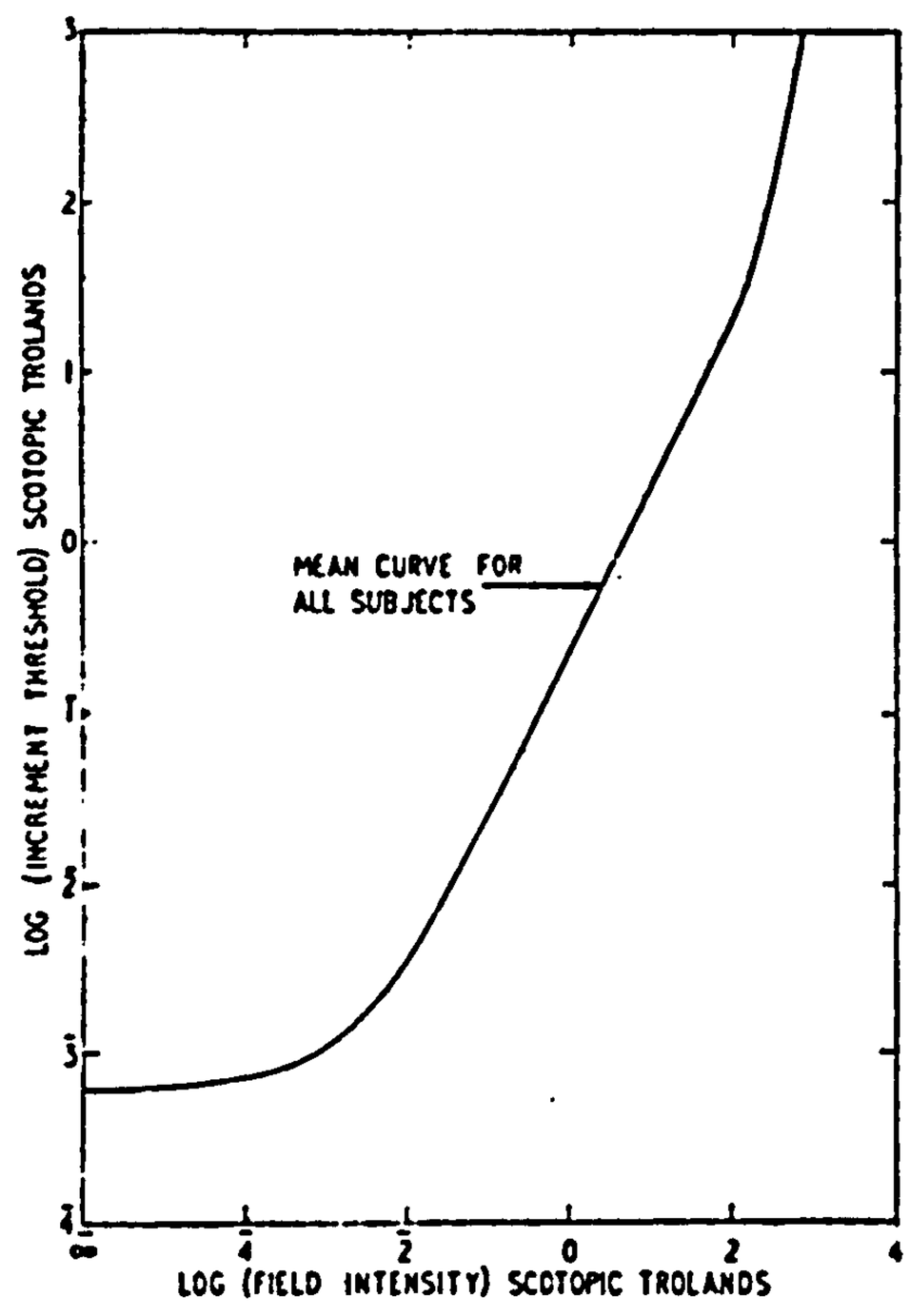

Figure 1-39. Rod increment threshold curve showing rod saturation. Reproduced from (Aguilar and Stiles 1954).

c. Saturation of the rod and cone systems

Aguilar and Stiles (1954) obtained a measure of rod saturation from increment threshold data. They measured the threshold for detection of a 9° diameter incremental test field flashed at 9° eccentricity, as a function of background intensity. By using a green test light on a red adapting background and taking advantage of the difference in the Stiles-Crawford effect for rods and cones, they were able to favour detection by the rod system. Figure 1-39 shows their results. The TVI curve rises from the flat region indicating the level of absolute threshold,

to a region from about -1 to 2 log scotopic trolands where the rods obey the Weber-Fechner law i.e., where $\Delta I/I$ is constant (I: intensity). At high intensities the rod system fails to respond to the incremental stimulus and the system is said to be saturated. Aguilar and Stiles estimated the intensity at which rods saturate from the point at which $\Delta I/I$ became greater than 100 times the value at moderate intensities, where $\Delta I/I$ was approximately constant. This produced an estimate for rod saturation between 2000 and 5000 scotopic trolands.

Cone saturation has been investigated through measurement of increment threshold curves for the π mechanisms. Stiles found that TVI curves for the π_4 and π_5 mechanisms did not appear to saturate even at very high levels of intensity, but there is evidence that the blue sensitive π_1, π_2, and π_3 mechanisms do exhibit saturation (Mollon and Polden 1977). If the chromatic adapting background is presented as a flash to which the test stimulus is added rather than as steady state adaptation, however, TVI curves for the M-cone and L-cone mediated π_4 and π_5 mechanisms indicate that saturation does occur (Shevell 1977).

d. Spatial and temporal characteristics of rod and cone pathways

There are notable differences between the rod and cone system in relation to their spatial and temporal resolution. In general terms, the rods comprise a very sensitive system for the detection of light incident on the retina, whereas the cone system allows resolution of spatial and temporal detail. Properties of the rod system that contribute to its high sensitivity are its ability to sum responses over time and over a relatively large retinal area. Cone pathways, on the other hand, are able to signal information relating to small areas of the retina and brief events in time. It is mainly the L- and M-cones via the achromatic postreceptoral channel that are responsible for high spatial and temporal resolution. The S-cones do not facilitate good spatial vision because of their scarcity in the retina. There is also evidence to suggest that the temporal response of the S-cones is inferior to that of the L- and M-cones (Boynton and Baron 1975).

The spatial summation characteristics of the retina can be investigated by considering the area over which Ricco's law (total spatial summation) holds. Ricco's law states that the number of quanta required for detection threshold does not vary with stimulus size up to a critical size, known as Ricco's area, i.e. the product of stimulus area and intensity is constant. Ricco's area depends on test wavelength, duration and retinal location, and background luminance, and is typically of the order of a few minutes to one degree of visual angle in diameter. Estimates of Ricco's area obtained by Barlow (1958) indicate that Ricco's area for the rods is roughly 10 times that for the cones (Hess 1990). The temporal equivalent to Ricco's law is Bloch's law, which states that the product of intensity and stimulus duration determines threshold up to a critical duration of presentation. Complete temporal summation is dependent on stimulus size, wavelength and retinal location. Bloch's law holds for cones up to durations of the order of 30-50 ms, and for rods up to durations of the order of 100 ms (Hess 1990).

The properties of spatial vision are often investigated by measuring the threshold contrast for detection of sinusoidal gratings. If reciprocal thresholds are obtained for gratings of different spatial frequency, the resulting curve is referred to as the contrast sensitivity function. Contrast sensitivity reaches a peak at intermediate spatial frequencies and falls off sharply at high frequencies. Measurements under conditions that approximately isolate the rod and cone systems at 10° eccentricity (D'Zmura and Lennie 1986) and those acquired for a rod monochromat (Hess et al. 1987), reveal that under mesopic conditions the two systems have comparable contrast sensitivity at low spatial frequencies, but that the high frequency cut-off for the rod mechanism is much lower than that of the cones. This leads to acuities of 6 cycles deg^{-1} and 15 cycles deg^{-1} at 20 scotopic trolands for the rod and cone systems, respectively.

Critical flicker frequency (CFF) is the frequency of presentation of a stimulus modulated in intensity either sinusoidally or with a square wave profile, at which the perception of flicker can no longer be detected and the stimulus appears continuous (a sensation described as flicker fusion). Critical flicker frequency is dependent on retinal illuminance (Hecht and Verrijp 1933). For predominantly cone-mediated

flicker detection (a small stimulus presented at the fovea), CFF peaks at about 45 Hz in the region of 10,000 photopic trolands. For a peripheral target at low retinal illuminances, where flicker is detected by rods, CFF peaks at about 10 Hz. If, however, flicker is investigated under conditions that favour detection by rods at high levels of illuminance, up to 30Hz flicker can be detected (Conner and MacLeod 1977). There is evidence to suggest that rod vision in fact comprises two temporal channels (also see section 1.1.2 g), a slow channel that operates at low intensities and a second fast pathway that is able to detect greater rates of flicker at higher intensities (Conner 1982; Hess and Nordby 1986).

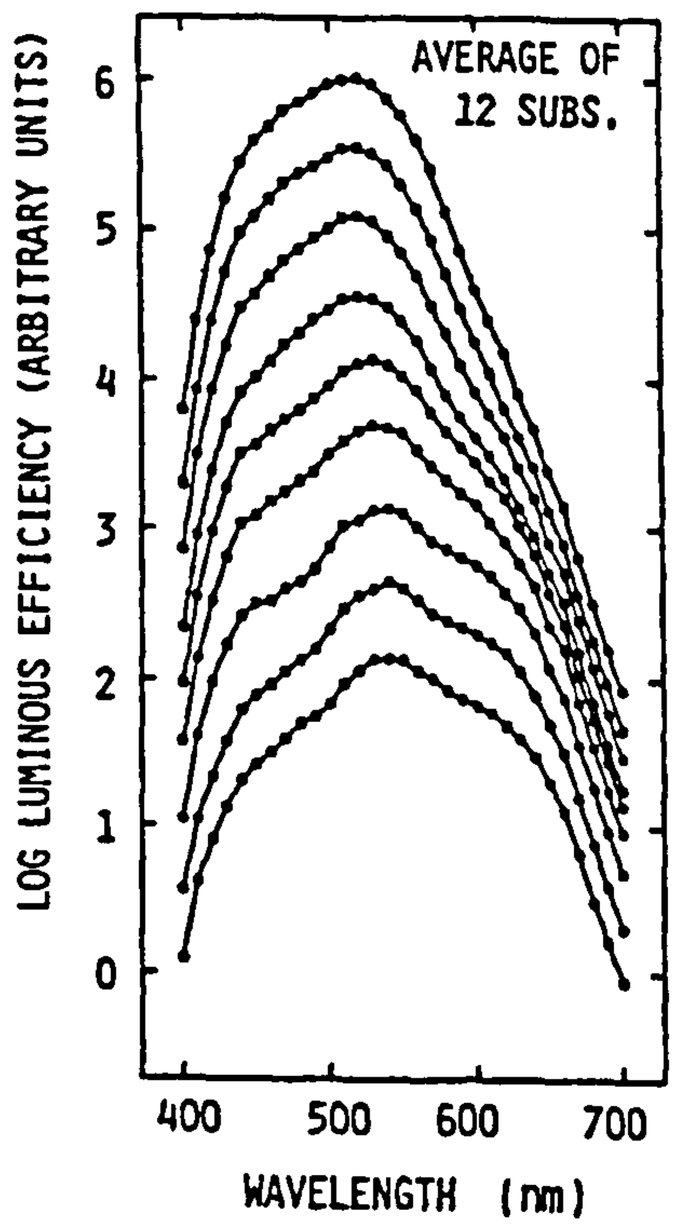

Figure 1-40. Mesopic luminous efficiency curves obtained using heterochromatic brightness matching. Retinal illuminance is lowest for the curve at the top of the figure and highest for the curve at the bottom. The curves are displaced vertically for clarity. Reproduced from (Sagawa and Takeichi 1986).

1.3.2 Mesopic spectral luminous efficiency

As stated in section 1.2.5 there is currently no standard luminous efficiency function for mesopic vision. There are, however, many examples of mesopic spectral luminous efficiency functions in the literature, and several proposed systems of mesopic photometry. Direct heterochromatic brightness matching (HBM) has been

the most widely used method of obtaining spectral luminous efficiency curves in the mesopic range (Kinney 1958; Sagawa and Takeichi 1986; Sagawa and Takeichi 1987; Ikeda and Shimozono 1981; Yaguchi and Ikeda 1984; CIE 1989; CIE 2001). Examples of mesopic luminous efficiency curves obtained using HBM are shown in Figure 1-40. The method of flicker photometry, which has been successfully applied to the measurement of photopic spectral luminous efficiency, has also been investigated in the mesopic range. Vienot and Chiron (1992) compared mesopic flicker photometric measurements to those obtained using HBM. They found that unlike the brightness matching results, the flicker data did not exhibit a continuous function with adaptation level, but were found to lie on one of two branches of a discontinuous curve. They reported that judgements of minimum flicker became very difficult close to the break in the curve. These results indicate that more than one mechanism is involved in detecting flicker under mesopic conditions. Vienot and Chiron reported that at the discontinuity, one observer was able to make minimum flicker judgements for a 445 nm test stimulus with two radiance settings, depending on the flicker frequency. These findings suggest that the method of flicker photometry is inappropriate for measurement of mesopic spectral luminous efficiency curves.

The majority of currently proposed systems of mesopic photometry are based on HBM. Six systems based on brightness matches for 10° diameter fields have recently undergone assessment by the CIE (Palmer 1968; Sagawa and Takeichi 1987; Sagawa and Takeichi 1992; Nakano et al. 1988; Trezona 1991; CIE 2001). In section 1.2.5 the phenomenon of subadditivity was discussed in relation to HBM under photopic conditions. In the mesopic range a second type of additivity failure occurs, known as superadditivity (Yaguchi and Ikeda 1983). In this case if two monochromatic stimuli are matched with a fixed reference stimulus, the sum of the monochromatic stimuli will often produce a stimulus that is brighter than the reference stimulus with double the radiant power. A number of systems of mesopic photometry based on brightness matching have been designed to specifically address the problems of subadditivity and superadditivity. An alternative method of obtaining mesopic spectral luminous efficiency curves has been employed by He et al. (1997; 1998), based on measurements of reaction times. The authors claim that reaction time

measurements reflect processing of the magnocellular channel and, therefore, obey the laws of additivity within a given level of adaptation for criterion reaction times. He et al. (1998) have developed a system of mesopic photometry from reaction time measurements, which they report overcomes the problems associated with photometry based on HBM.

1.3.3 Rod-cone interactions

Psychophysical investigations under mesopic conditions have revealed effects that indicate interactions between the rod and the cone systems and thus, a break down of rod and cone system independence. Rod-cone interactions have been reported to alter detection thresholds, the perception of flicker, and colour processing. These effects are discussed below.

There is evidence that rod sensitivity is altered by stimulation of cones in the surrounding background field (Makous and Boothe 1974; Frumkes and Temme 1977; Latch and Lennie 1977; Makous and Peeples 1979; Buck and Makous 1981; Shapiro 2002). Shapiro (2002) investigated the effects of backgrounds that isolated the L-cone and S-cone system, respectively, and found that the L-cone system, but not the S-cone system contributed to the reduction of rod sensitivity. There are also reports in the literature of scotopic background stimulation raising increment thresholds for the cones (Latch and Lennie 1977; Temme and Frumkes 1977; Buck 1985a; Buck 1985b). The magnitude of both these rod-cone interaction effects is dependent on the size of the background field.

Under conditions where rods and cones are both able to detect a flickering stimulus, constructive and destructive interference of rod and cone signals can occur (MacLeod 1972; van der Berg and Spekreijse 1977). MacLeod showed that it is possible for rod and cone signals to cancel exactly, producing a null point in the perception of flicker. Several studies have reported that cone mediated detection of flicker (greater than 18 Hz) may be raised at the fovea and in the periphery as a results of rod-cone interactions (Goldberg et al. 1983; Alexander and Fishman 1984; 1986; Coletta and Adams 1984; 1986). The threshold luminance for flicker detection

is increased under dark adapted conditions, and reduced for rod saturating backgrounds or during the recovery of rod sensitivity following a bleach. The interaction appears to be laterally mediated, and is thought to be a consequence of rod modulation of horizontal cell feedback mechanisms in flicker detection (Arden and Hogg 1985). Frumkes et al. (1986) found that the opposite interaction also occurs: their results indicated that stimulation of neighbouring cones has an influence on rod-mediated flicker.

Reported effects of rod-cone interactions on colour processing are summarised here, but are described in more detail in chapter 4. Rod signals are known to disrupt large field colour matches (Trezona 1970; Shapiro et al. 1994). Rod activity has been associated with the impairment of wavelength discrimination (Stabell and Stabell 1977), and changes in the hue and saturation of colour stimuli (Stabell and Stabell 1996) in the periphery compared to the fovea. Rod impairment of chromatic discrimination has also been documented (Nagy and Doyal 1993; Knight et al. 1998; Knight et al. 2001), and the interaction between rods and L-cones has been reported to produce colour sensations (McCann and Benton 1969; McKee et al. 1977). The phenomenon of superadditivity (see section 1.3.2 above) that occurs for brightness matching under mesopic conditions is also thought to be a consequence of rod-cone interactions.

1.4 A summary of the investigations

The investigations that constitute this body of work are described and the ensuing results discussed, in the following six chapters.

- In chapter 2 the experimental equipment is detailed, and calibration procedures described. The methodology employed in each experiment is also included in this chapter.
- Chapter 3 consists of an investigation into the effects of different spatial attributes of the visual stimulus on chromatic sensitivity, carried out under photopic conditions. The results that are described and discussed within chapter 3 include those obtained from colour-normals, and subjects with congenital

colour vision deficiency, and those with acquired colour vision deficiency. The data from colour normals obtained as part of this study allows the changes in chromatic sensitivity arising from changes in spatial parameters to be compared with changes due to factors such as retinal illuminance, investigated in chapter 4.

- Chapter 4 describes a study of chromatic sensitivity in colour-normals under mesopic conditions, where changes in chromatic sensitivity are investigated as retinal illuminance is reduced. This chapter also includes an assessment of the influence of rod signals on chromatic thresholds in the mesopic range.
- In chapter 5, the concept of a stimulus conspicuity metric is discussed, and the development of an empirical model for describing the conspicuity of a target defined by colour and luminance contrast at different levels of illumination is reported. The results of a comparison between this model of conspicuity and other models of mesopic vision are discussed.
- Chapter 6 contains an investigation into the characteristics of visual search performance under mesopic conditions, both for achromatic targets and targets defined by colour and luminance contrast. The application of the conspicuity model developed in chapter 5, to predict mesopic visual search performance is assessed in this chapter.
- The results of all these investigations are discussed collectively in chapter 7.

The major findings are as follows:

- The threshold for detection of colour is dependent on the spatial attributes of the stimulus, but to a much greater degree is dependent on the level of illumination as it is reduced into the mesopic range. Differences are evident in the behaviour of the red-green and blue-yellow chromatic mechanisms to changes in parameters of the stimulus.
- At chromatic threshold in the mesopic range, chromatic signals and rod signals appear to be processed independently.
- As defined in this study, stimulus conspicuity in the mesopic range is a function of stimulus photopic and scotopic contrast, the chromatic content of the stimulus and retinal illuminance. Conspicuity is predominantly dependent on photopic contrast and chromatic difference to the immediate background at low

photopic/ high mesopic light levels, whereas scotopic contrast is the major determinant of conspicuity in the low mesopic range.

- The relationship between visual search time and luminance contrast changes as background luminance is reduced, reflecting the increase in contrast thresholds, and also a reduction in the effectiveness of a unit change in physical contrast.
- In the low mesopic range, visual search performance is predominantly dependent on the scotopic contrast of the stimulus. At low photopic/ high mesopic light levels colour is an important determinant of visual search performance, particularly when luminance contrast is low. In addition, for the stimulus conditions employed in the visual search procedure, scotopic contrast appears to be an important determinant of search time, even in the low photopic range.
- The conspicuity model developed chapter 5 can successfully be used to predict visual search performance, and represents a better predictor of performance in the mesopic range than either stimulus photopic or scotopic contrast.

2 Equipment and methods

All the experiments in this body of work consisted of visual stimuli presented to human subjects using a cathode-ray tube (CRT) display. For the major part of the experimental work, a single set of equipment comprising a CRT display, control computer and pupil measurement system was used. For the experiments in chapter 5, a second almost identical experimental system was also used; these are referred to as system-1 and system-2, respectively. For the experiments in chapter 4, a single channel Maxwellian view optical system was used in addition to system-1.

All the experiments, which are described in detail in the sections below, were conducted using common psychophysical techniques; these included the staircase method, the method of adjustment and the measurement of search time. In the staircase method, an attribute of the stimulus is either increased or decreased in a step-wise fashion in accordance with the observer's response to the stimulus. With well chosen staircase parameters (start value, step size and determination of end point where a plateau in the response is reached) the staircase method is an efficient procedure, and by randomly interleaving a number of staircases response bias due to knowledge of the procedure can be reduced (Cornsweet 1962). Staircase procedures were used in chapters 3, 4 and 5. In the method of adjustment, the observer has direct control over setting the level of a particular stimulus attribute. The method of adjustment is fast, but highly subjective. It is ideally suited to record the rapid change in sensitivity that occurs immediately following light adaptation, and for this reason was used to measure dark adaptation curves in chapter 4. Measurement of response time is a common method of recording visual performance for a given task, and was employed in the experiments in chapter 6, where the reponse time recorded was search time. As search time may be related to the accuracy with which the task is performed, response accuracy was monitored by classifying stimuli following detection (see section 2.6).

2.1 CRT display-based systems

The display used in both system-1 and system-2, was a 20″ CRT monitor (system-1: Sony trinitron multiscan SFII, model CPDSF2T; system-2: Sony trinitron, model GDM-400PST). Control programs ran on a PC (Hewlett Packard Vectra) under MS-DOS, with the monitor driven by an 8-bit graphics card (system-1: Hercules Graphite Terminator, system-2: Videologic GraphixStar 560), with a resolution of 1280 x 1024 pixels. Observer responses were recorded via a button box attached to an input/output board (Amplicon PC30AT).

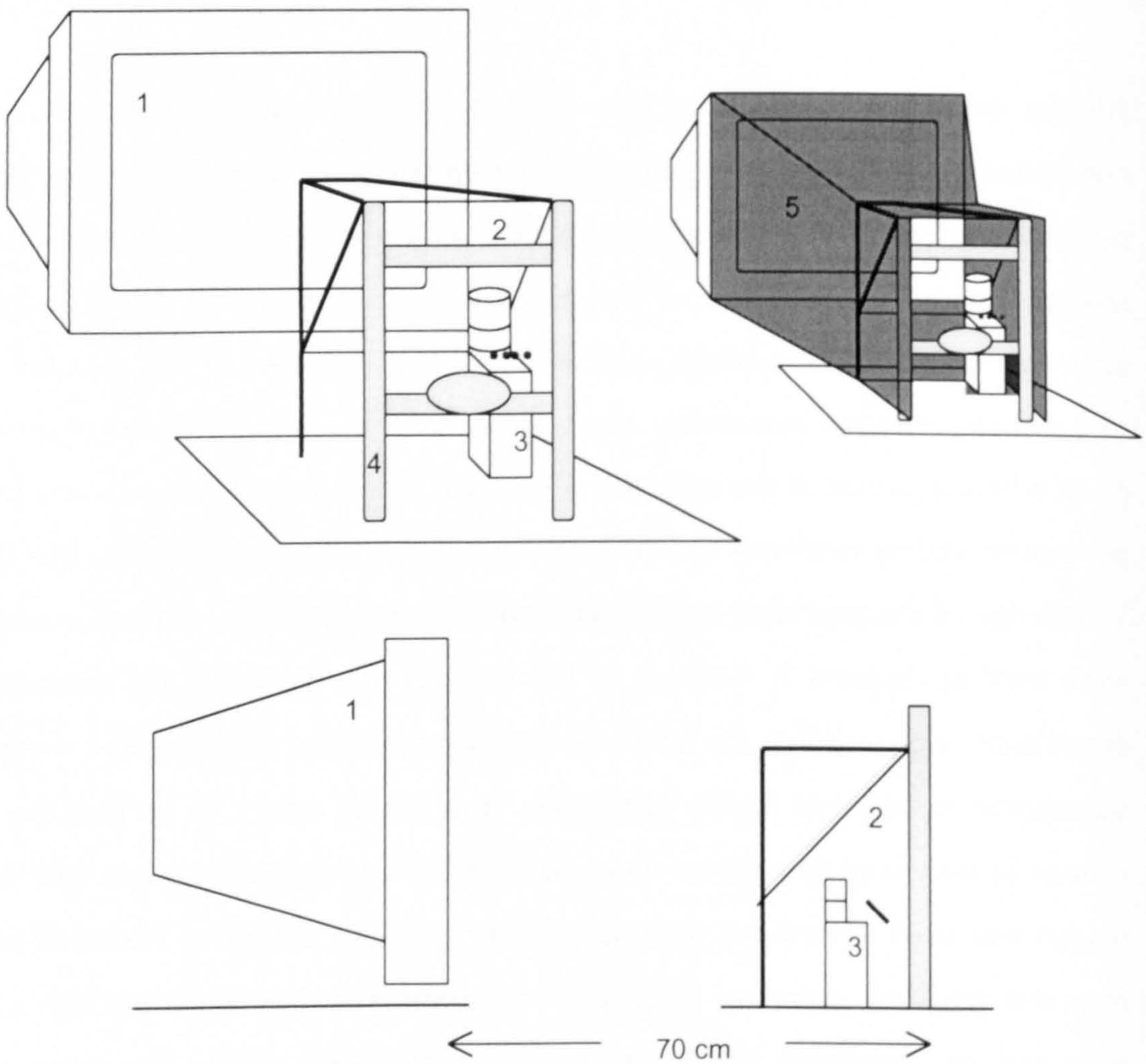

Figure 2-1. CRT monitor-based system. 1: 20″ colour CRT monitor; 2: infrared mirror mounted at 45°, on which a neutral density filter can be fixed at 45° (shown by the dotted line); 3: infrared camera and near infrared LED's to diffusely illuminate the front of the eye; 4: chin and forehead rest; 5: hood to restrict light from the screen reaching the observer without first passing through the filter.

Observers' head movements were restricted by use of a chin rest and forehead support. The viewing distance was 70 cm throughout, producing a display area of 22° by 27° visual angle. Each experimental room was made sufficiently light proof to allow dark adaptation to the lowest stimulus luminance used in any of the experiments. A diagram of the equipment is shown in Figure 2-1.

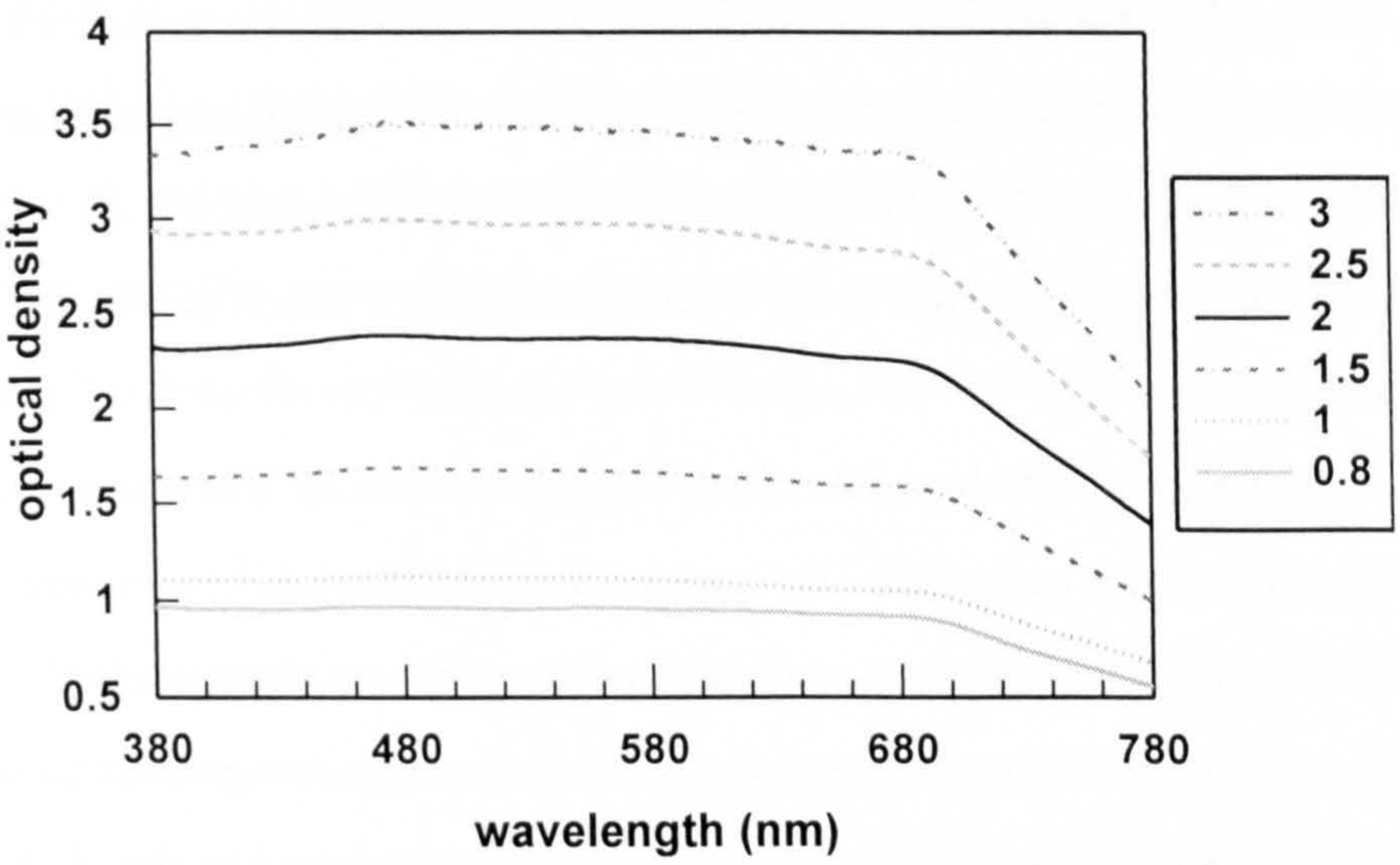

Figure 2-2. Spectral profile of the neutral density filters calibrated at 45° incidence, labelled with their nominal density at normal incidence. All the filters show an increase in transmittance from 680 to 780 nm.

2.1.1 Neutral density filters

An operating range of stimulus luminance spanning 4 log units was achieved using neutral density filters. The spectral transmittance of a sample from each filter was measured with a spectrophotometer (Cary 05). Measurements were made between 380 and 760 nm at 2 nm intervals. These data were extended to 780 nm by lengthening a regression line fit to the data between 720 and 760 nm, and then converted to points at 5 nm intervals. These data were then transformed to optical densities and entered into the control programs. The filters were calibrated either at 45° incidence, or at normal incidence, depending on their mounted position when in use. The optical density profile of each filter calibrated and used at 45° incidence is shown in Figure 2-2. The optical density spectrum for each filter was used in the control program of every experiment to modify the effective spectral power

distribution of each of the three phosphors of the display when combined with the filter.

Neutral density filters were used to reduce stimulus background luminance in the study of chromatic sensitivity described in chapter 4, the measurements of conspicuity detailed in chapter 5, and the visual search experiments described in chapter 6. For all three studies a tunnel was built between the monitor and the chin rest to prevent light from reaching the observer without passing through the filter, which was mounted at 45°. The mounting angle was dictated by the orientation of the infrared mirror (see Figure 2-1), which provided a support for the filters. For background luminances of 10 cd m^{-2} and above, no filter was used. For all background luminances below 10 cd m^{-2} a neutral density filter was used, and the display luminance was maintained at approximately 10 cd m^{-2} to ensure that a large gamut of chromaticities and range of luminance contrasts were available. Mean filter densities and effective stimulus background luminances are given in each relevant chapter. The filters calibrated at normal incidence were used in the dark adaptation experiments described in chapter 4. The filters were mounted in a pair of light-tight goggles. Filter density was increased at intervals during the experiment to extend the range through which stimulus luminance could be gradually lowered.

2.1.2 Pupil measurements

Measurements of natural pupil diameter were made in chapter 5 from video images of the pupil. The front of the eye was diffusely illuminated with near-infrared radiation and images obtained with an infrared camera. The two experimental systems: system-1 and system-2, employed different methods of extracting pupil sizes from these images. System-1 incorporated the pupillometer developed by Barbur (1987), in which best circles are fitted to video images of the pupil every 20 ms. System-2 incorporated a frame grabber (ArcSoft Zipshot PA-10) to capture the video images, and pupil diameters were obtained by averaging the number of pixels in the vertical and horizontal diameters of each pupil image, using a calibration to convert to millimetres. The calibration between image pixels and millimetres was obtained by measuring the pixel diameter of two artificial pupils of known physical

diameter, positioned in place of the observer's eye. This calibration was performed at the beginning and end of each experimental session.

2.1.3 CRT monitor calibration

In order to generate stimuli with a specific photopic luminance and chromaticity on a CRT monitor, it is necessary to know the chromaticity of the red, green and blue phosphors, and the relationship between electron gun voltage and luminance for each of the red, green and blue guns. The experiments in chapter 5 required that stimuli with a specific photopic luminance and scotopic luminance be generated, where the photopic luminance was calculated according to the $\bar{y}_{10}(\lambda)$ colour-matching function of CIE 1964 supplementary standard observer, which is generally accepted to represent the photopic luminous efficiency for a 10° field. In this case, the spectral radiance of the three phosphors must also be entered into the control program in addition to the luminance versus gun voltage data. It is then possible to convert the luminance calibration data specified in terms of the CIE 1924 luminous efficiency function $V(\lambda)$, to equivalent calibration data with luminance specified in terms of $\bar{y}_{10}(\lambda)$. Thus, the following calibrations were required for each monitor: First, the radiance of each of the phosphors was measured using a calibrated telespectroradiometer (either Gamma Scientific model RD2 or the National Physical Laboratory's visual displays spectroradiometer, which is based on a commercially available double-grating monochromator, manufactured by Bentham). Radiance data were acquired at 5 nm wavelength intervals from 380 nm to 780 nm, with each of the guns set at maximum voltage. These data for the two monitors are shown in Figure 2-3. Second, the luminance versus gun voltage relationship was measured for each of the three electron guns with a calibrated photometer (either LMT L1003 or LMT L1009). Measurements were acquired every 2 voltage steps of the 256 steps available for the 8-bit graphics card and polynomials were fit to the data to obtain values for all 256 steps, an example can be seen in Figure 2-4. The chromaticities of the three phosphors were calculated from the phosphor radiance data according to the following equations (Eq. 2-1 - Eq. 2-5). The phosphor chromaticities are plotted for the two monitors (system-1 and system-2) in Figure 2-5.

$$x = \frac{X}{(X+Y+Z)} \qquad \textbf{Eq. 2-1}$$

$$y = \frac{Y}{(X+Y+Z)} \qquad \textbf{Eq. 2-2}$$

$$X = k\int L_{e,\lambda}\,\bar{x}(\lambda)\,d\lambda \qquad \textbf{Eq. 2-3}$$

$$Y = k\int L_{e,\lambda}\,\bar{y}(\lambda)\,d\lambda \qquad \textbf{Eq. 2-4}$$

$$Z = k\int L_{e,\lambda}\,\bar{z}(\lambda)\,d\lambda \qquad \textbf{Eq. 2-5}$$

where x, y: CIE 1931 chromaticity coordinates; X, Y, Z: CIE 1931 tristimulus values; k: normalising factor; $L_{e,\lambda}$: phosphor radiance; $\bar{x}(\lambda)$, $\bar{y}(\lambda)$, $\bar{z}(\lambda)$: CIE 1931 colour matching functions. The luminance versus gun voltage relationship of a CRT monitor does not remain constant during its lifetime, with maximum luminance decreasing marginally over time. The luminance versus gun voltage calibration, therefore, was carried out at a frequency of roughly once a month for the duration of the experimental work.

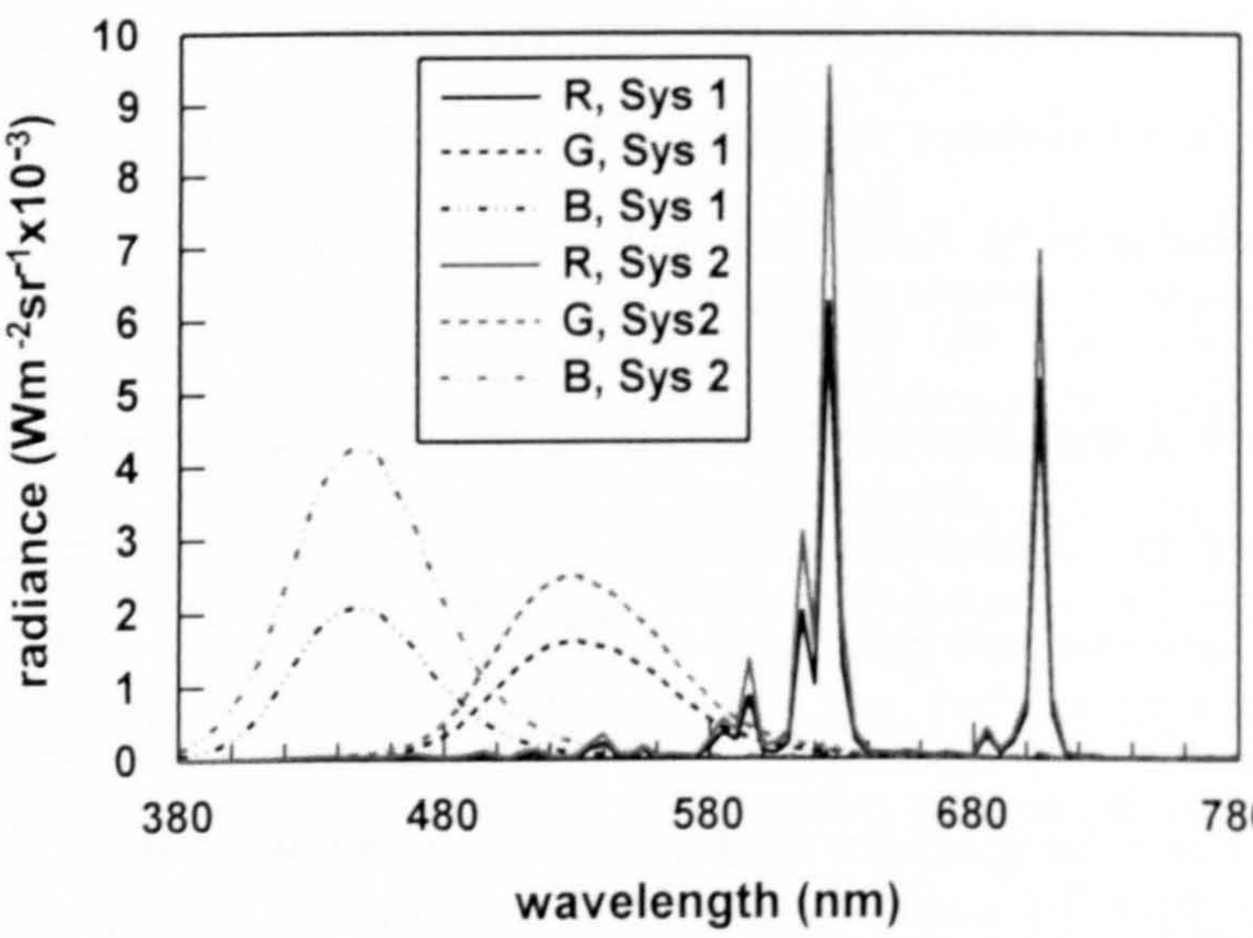

Figure 2-3. Monitor calibration. Phosphor radiance data for the red (R), green (G) and blue (B) phosphors for system 1 and system 2. The phosphors of the two monitors have similar spectral power distributions, but differ in absolute radiance.

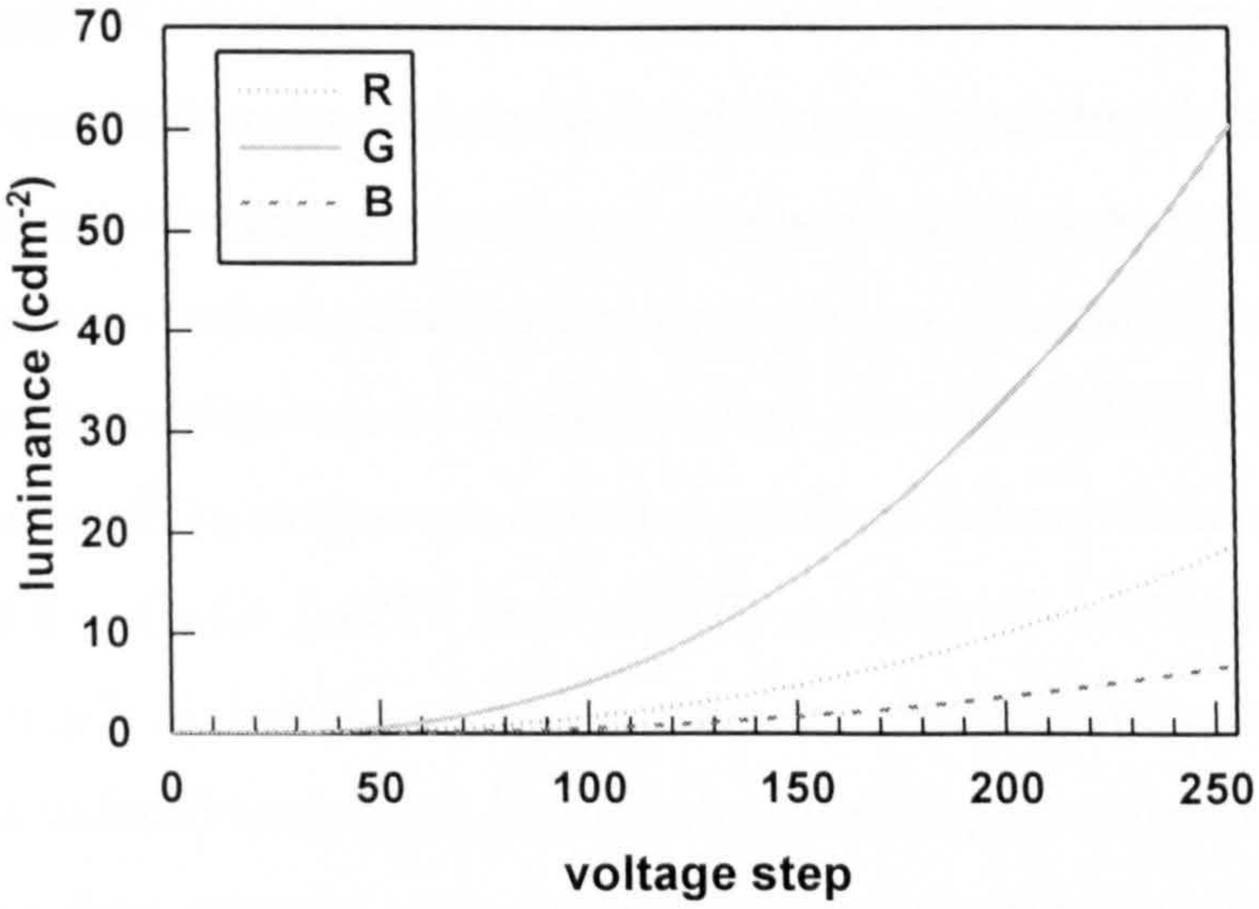

Figure 2-4. Luminance versus gun voltage calibration for the red (R), green (G) and blue (B) phosphors of the CRT monitor for system-1. For an 8-bit graphics card there are 256 voltage steps, measurements are acquired every 2 voltage steps and polynomials fit to the data to obtain values for all 256 steps.

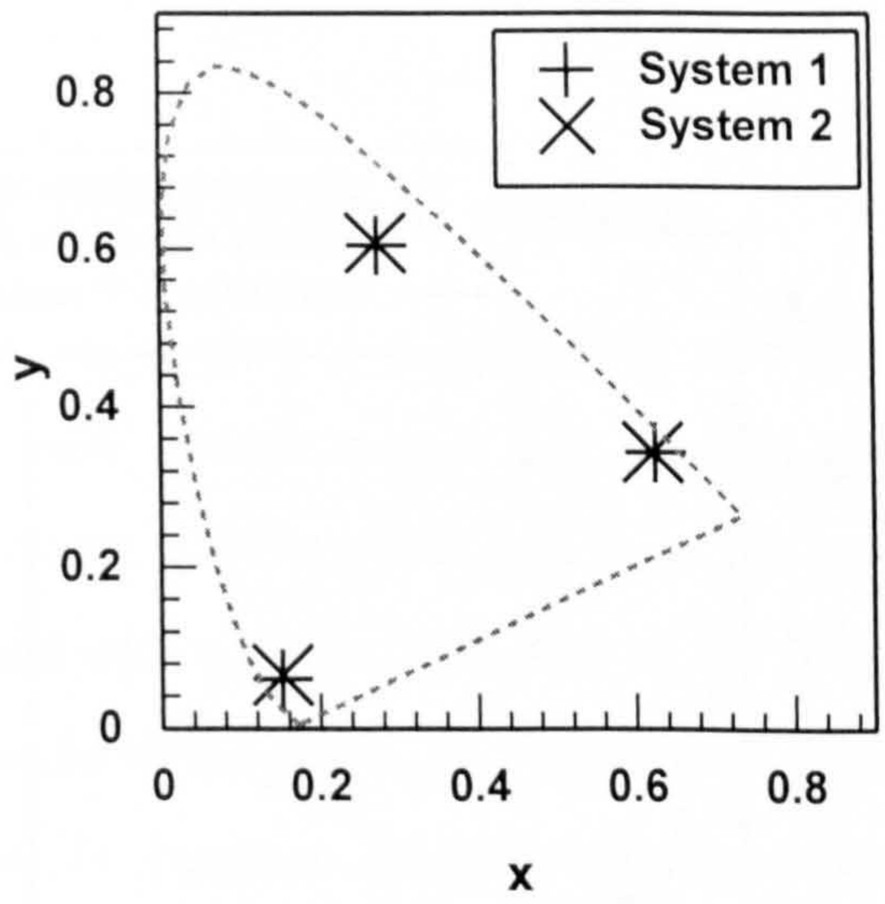

Figure 2-5. Phosphor chromaticities for system-1 and system-2, calculated from the measured spectral power distribution of the phosphors, plotted in the CIE 1931 (x, y)-chromaticity diagram. The phosphor chromaticities for the two monitors were very similar.

2.1.4 Colorimetric transformations

For a three primary system display system such as a CRT monitor, stimulus chromaticity is restricted to a gamut of chromaticities, which at its largest, consists of the triangular region bounded by the chromaticities of the three phosphors, but

which diminishes in size with increasing stimulus luminance. Within the bounds of chromaticity and luminance set by the display's characteristics, any combination of photopic luminance and chromaticity can be generated. A stimulus specified by both its photopic luminance and scotopic luminance, however, is restricted further in its chromaticity. Stimuli with the same ratio of scotopic to photopic luminance have chromaticities that fall on a single line in the region of chromaticity space that can be reproduced on the monitor (Barbur et al. 1998a), which will be referred to as the S-by-P line. An example of such a line is plotted in Figure 2-6. For the experiments in chapter 5, previously developed algorithms (Barbur et al. 1998) were applied to calculate the available chromaticities for a stimulus with a given photopic-scotopic luminance pair. Errors present in the calculations were reflected in the generated values of scotopic luminance, which differed from the specified values. However, it was possible to compute to within rounding errors, the actual scotopic luminances of the stimuli used from radiance data generated by the program for each stimulus computed using the settings of the three electron guns and the calibration data.

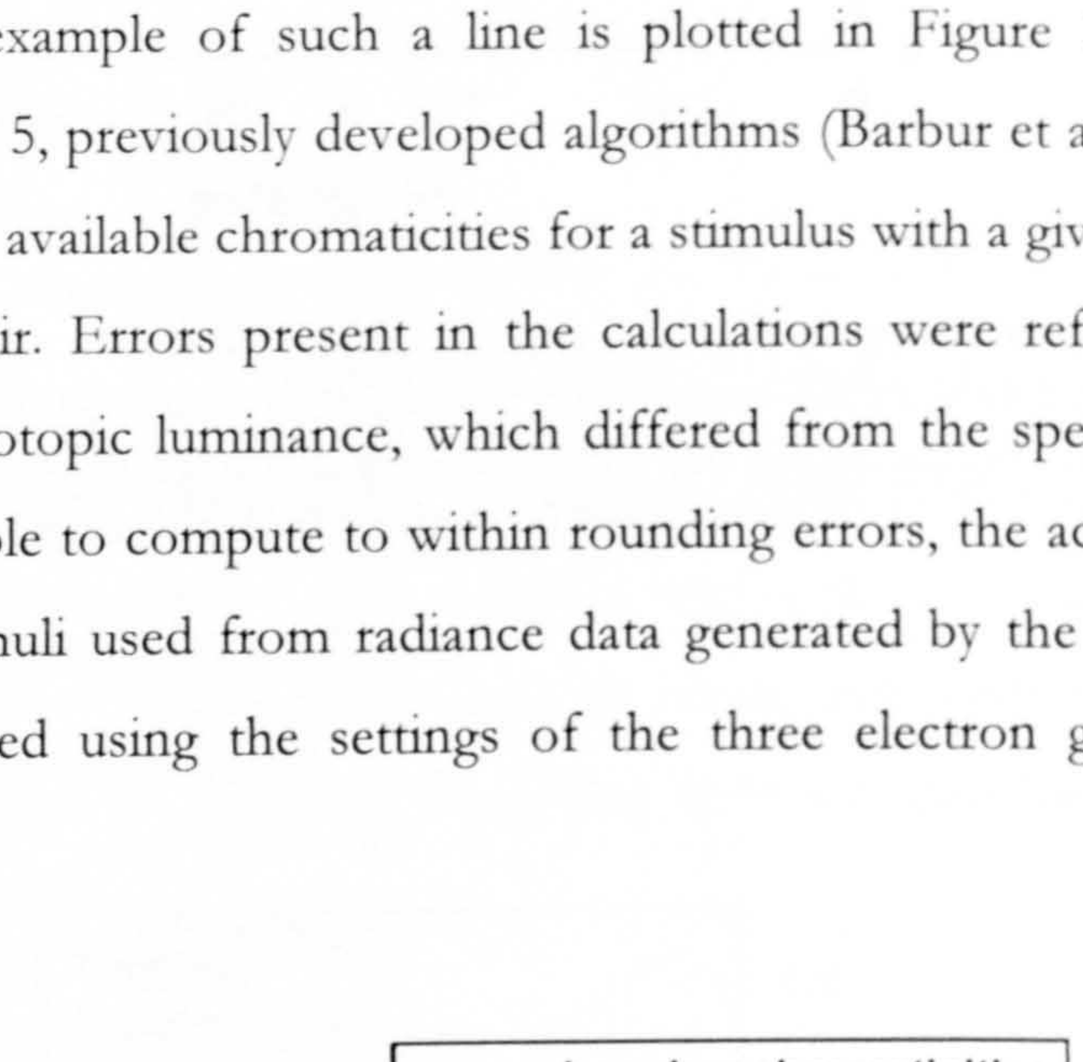

Figure 2-6. Example of the region of (x, y)-chromaticity space that can be reproduced on a typical CRT monitor (shown by the dashed line) and a line of chromaticities within that region that can be generated for stimuli with a particular ratio of scotopic luminance to photopic luminance (constant S:P ratio, or S-by-P line; shown by the continuous line).

Following the initial display calibration, the ability of the experimental system to accurately reproduce stimuli of a given luminance and chromaticity, or a given

photopic luminance contrast, scotopic luminance contrast and chromatic difference (CD) was assessed (contrast was defined according to Eq. 2-8 and CD according to Eq. 2-11). The colorimetric properties of sample stimuli were measured using a calibrated telespectroradiometer (Gamma Scientific model RD2) and compared to parameter values specified in the control program. All measured values were within 5% of those specified, even when neutral density filters were used.

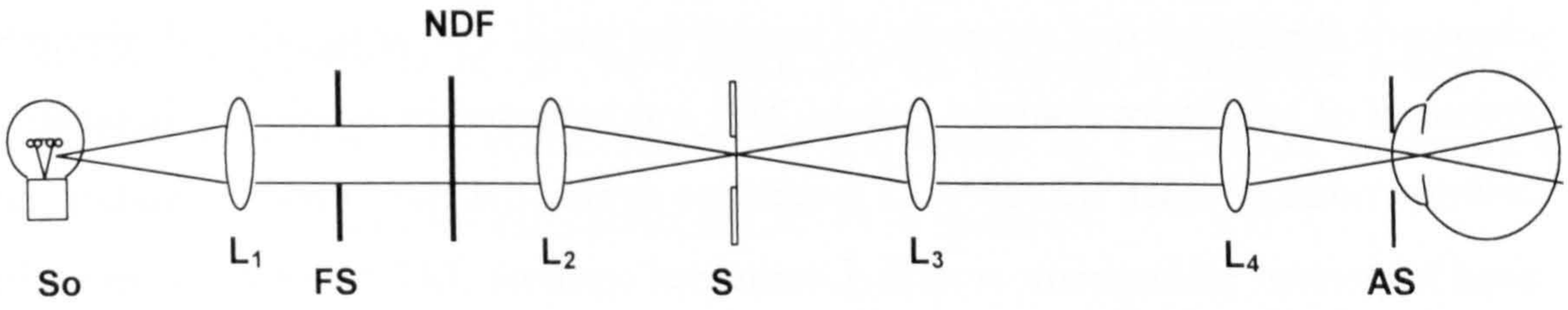

Figure 2-7. Diagram of the single channel Maxwellian view optical system. So: source (tungsten-halogen lamp); L_{1-4}: lenses; FS: field stop; NDF: neutral density filter; S: shutter; AS: aperture stop.

2.2 Maxwellian view optical system

For the experiments in chapter 4 a bleaching stimulus was required. A single channel Maxwellian view optical system was used to provide light adaptation. A diagram of the equipment is shown in Figure 2-7. The source was a 12 V tungsten-halogen lamp, supplied with a constant current of 8.2 Amps from a stabilised power supply. An electromechanical shutter was connected to a computer to control the shutter opening time. To measure the conventional retinal illuminance or Troland Value provided by the system, a white reflectance standard ($BaSO_4$) was positioned in the exit beam at a fixed distance from the pupil plane.

The luminance of the reflectance standard was measured using a calibrated photometer (LMT L1003) aligned at 45° to the surface, and the Troland Value calculated from the following formula

$$T = \frac{10^6 \pi d^2 L}{\beta} \qquad \textbf{Eq. 2-6}$$

where T: Troland Value, d: distance from the pupil plane to the reflectance standard, L: luminance of the surface of the reflectance standard, β: reflectance of the white standard. The size of the bleaching field was 30°.

2.3 Colour vision test employing luminance contrast noise

In chapters 3 and 4, a colour vision test was used to investigate chromatic sensitivity under photopic and mesopic conditions, respectively. In order to measure chromatic thresholds it is necessary to extract the use of colour signals and eliminate detection of luminance contrast signals. This was achieved by employing luminance contrast noise to mask detection of luminance contrast signals, thus eliminating the need to present isoluminant stimuli. Luminance contrast (LC) noise was created by dividing the stimulus and surround into small patches, and allowing the luminance of neighbouring patches to vary while maintaining a constant mean luminance, Figure 2-8 shows an schematic of this procedure, where the patches make up an array of checks. The magnitude of the noise was varied by increasing or decreasing the range of luminances incorporated.

The colour vision test used in chapters 3 and 4 was based on the test designed by Barbur et al. (1992). Stimuli consisted of a 15 x 15 array of checks generated in a uniform, achromatic background. A single stimulus presentation began with the chromaticity of the whole array equal to that of the background, then a selection of checks underwent a change in chromaticity forming the test target, and finally returned to the achromatic background chromaticity. The change in chromaticity was in any one of a number of specified directions away from the background chromaticity towards the spectrum locus. Chromatic changes were isoluminant with respect to the CIE 1924 standard observer for photopic vision V(λ). The difference in chromaticity from the background (CD) was measured as a Euclidean distance in CIE 1931 (x, y)-chromaticity space and controlled by a randomly interleaved multiple-staircase procedure (one staircase corresponding to each direction of colour space tested).

$$CD = \sqrt{(x_t - x_b)^2 + (y_t - y_b)^2} \qquad \textbf{Eq. 2-7}$$

where, x_t, y_t: CIE 1931 chromaticity coordinates of the test target; x_b, y_b: CIE 1931 chromaticity coordinates of the background. The value derived from each staircase gave the chromatic threshold measured for one colour direction. Staircase step sizes were adjusted in relation to the final threshold value to maximise the efficiency of the measurement procedure. Chromatic difference was measured in CIE 1931 chromaticity space because the control program was originally developed to obtain results for comparison with those of MacAdam (MacAdam 1942). The results in chapter 3 are presented graphically in CIE 1931 space and those in chapter 4 are presented in graphically in CIE 1976 space. For the purpose of statistical analysis in chapters 3 and 4, chromatic thresholds expressed in CIE 1931 units were transformed to equivalent thresholds in CIE 1976 space.

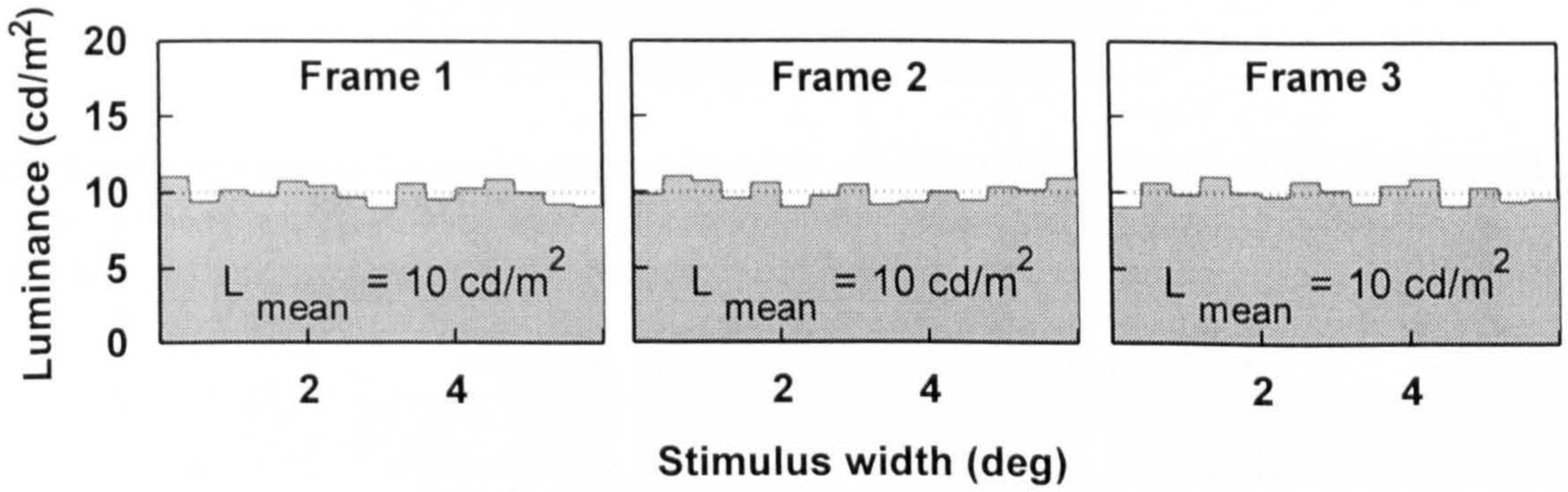

Figure 2-8. An example of dynamic luminance contrast noise. The luminance profile of the checks that make up the array is shown across the width of a 6° stimulus, for three sequential frames. The frame duration for the photopic experiments was 53 ms. In this example the mean luminance remains constant at 10 cd m^{-2} across the whole stimulus while individual checks vary in luminance with each frame within a specified percentage of the background luminance.

2.3.1 Colour vision testing under photopic conditions.

Two different stimulus configurations were used to investigate the effect of stimulus parameters on chromatic thresholds in chapter 3. In the first configuration the test target consisted of vertical bars defined only by colour, which popped-up in the middle of each presentation as they underwent a change in chromaticity. This stimulus was designed to measure thresholds for detection of a colour defined spatial pattern, and will be referred to as the pattern test. An example of the pattern

test stimulus is shown in Figure 2-9. For the second stimulus configuration the test target was formed by a square block, which was defined at all times by a luminance contrast pedestal. This stimulus was designed to measure thresholds for detection of pure colour changes independent of structure, and will be referred to as the colour test. An example of the colour test stimulus is shown in Figure 2-10.

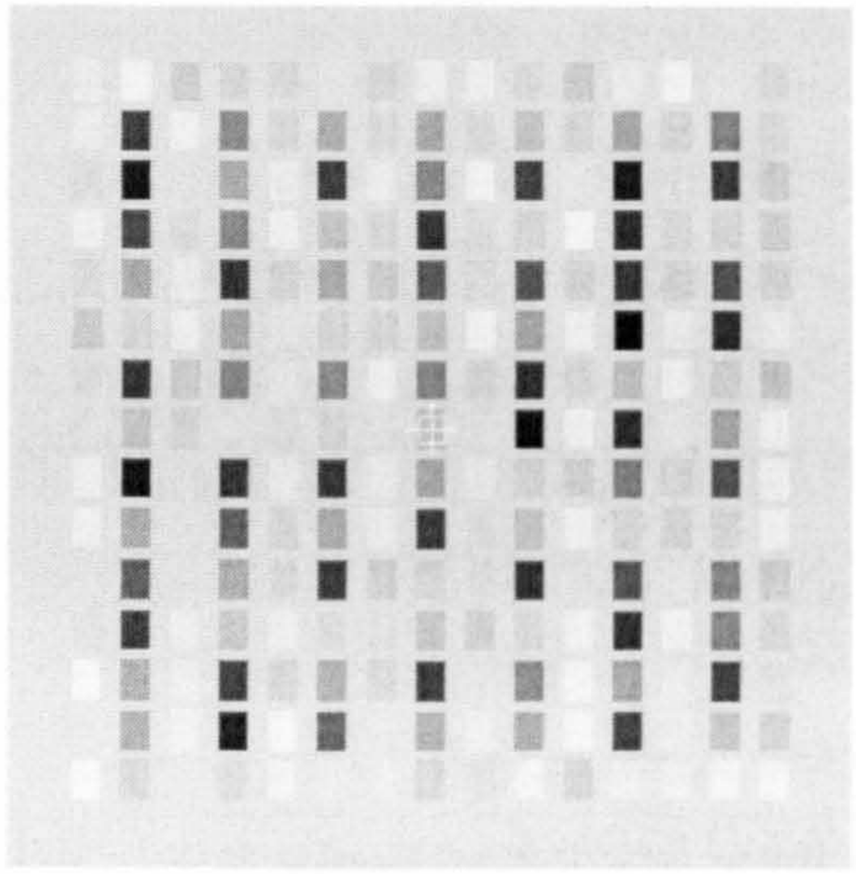

Figure 2-9. Example of the stimulus for the pattern test, designed to measure thresholds for detection of a colour defined spatial pattern. In the middle of each presentation a selection of the checks underwent a change in chromaticity forming coloured vertical bars.

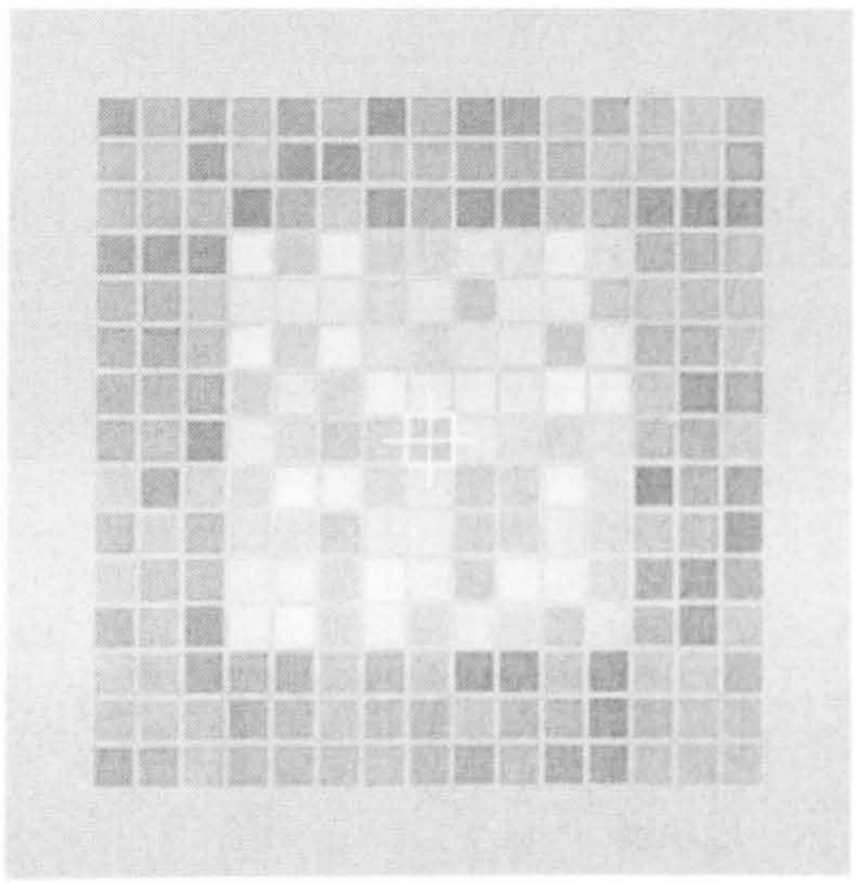

Figure 2-10. Example of the stimulus for the colour test, designed to measure thresholds for detection of colour changes, independent of structure. The central block was defined by a luminance contrast pedestal and underwent a change in chromaticity in the middle of each presentation.

For both stimulus paradigms, the duration of presentation was 1500 ms, divided into achromatic, chromatic, and achromatic periods of length 600, 300, and 600 ms. Dynamic changes in luminance contrast noise occurred every 53 ms, and took values of ± 16% of the mean luminance of the stimulus. The achromatic background chromaticity was chosen as the chromaticity of MacAdam white: x = 0.305, y = 0.323 (MacAdam 1942). When testing normal trichromats and patients with acquired colour vision deficiency, 12-16 colour directions were investigated, equally spaced in (x, y)-chromaticity space. When testing dichromats, directions close to the particular dichromatic colour confusion line passing through the background chromaticity were preferentially selected, with a total of 16-18 directions investigated. For the pattern test the luminance of the background and array was 24 cd m^{-2}. For the colour test the luminance of the background and test target was 24 cd m^{-2} and the luminance of the surrounding array was 18 cd m^{-2}, thus creating a luminance pedestal for the target.

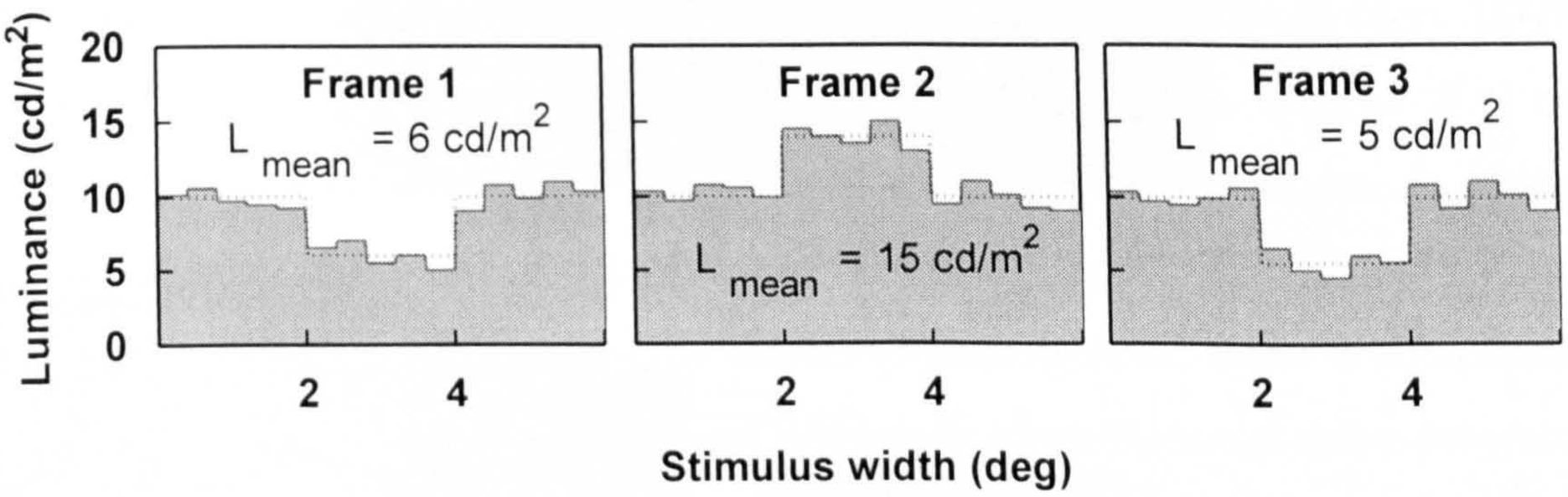

Figure 2-11. A graphical representation of the combination of dynamic luminance contrast and light flux noise used in the mesopic colour vision test. The luminance profile of checks that made up the array is shown across the width of a 6° stimulus, for three sequential frames. The frame duration in the mesopic experiments was 107 ms. The mean luminance of the central five checks was modulated in addition to the random variation in luminance of each individual check.

2.3.2 Colour vision testing under mesopic conditions

To measure chromatic sensitivity under mesopic conditions it is necessary to eliminate detection of both photopic and scotopic luminance contrast signals. The colour vision test employed in chapter 4 incorporated three types of masking: luminance contrast (LC) noise, large field light flux (LF) noise and a luminance

contrast pedestal (LCP). Similar to the way in which LC noise masks photopic luminance contrast signals, LF noise was introduced to mask spatially pooled rod signals (Barbur et al. 1994a). LF masking was provided by the random modulation of the mean luminance of the test target within a percentage range of the mean luminance of the stimulus. Figure 2-11 shows a schematic of luminance contrast noise and light flux noise combined. The presence of a luminance contrast defined pedestal helped further to mask the detection of luminance contrast changes associated with the onset of a chromatic stimulus.

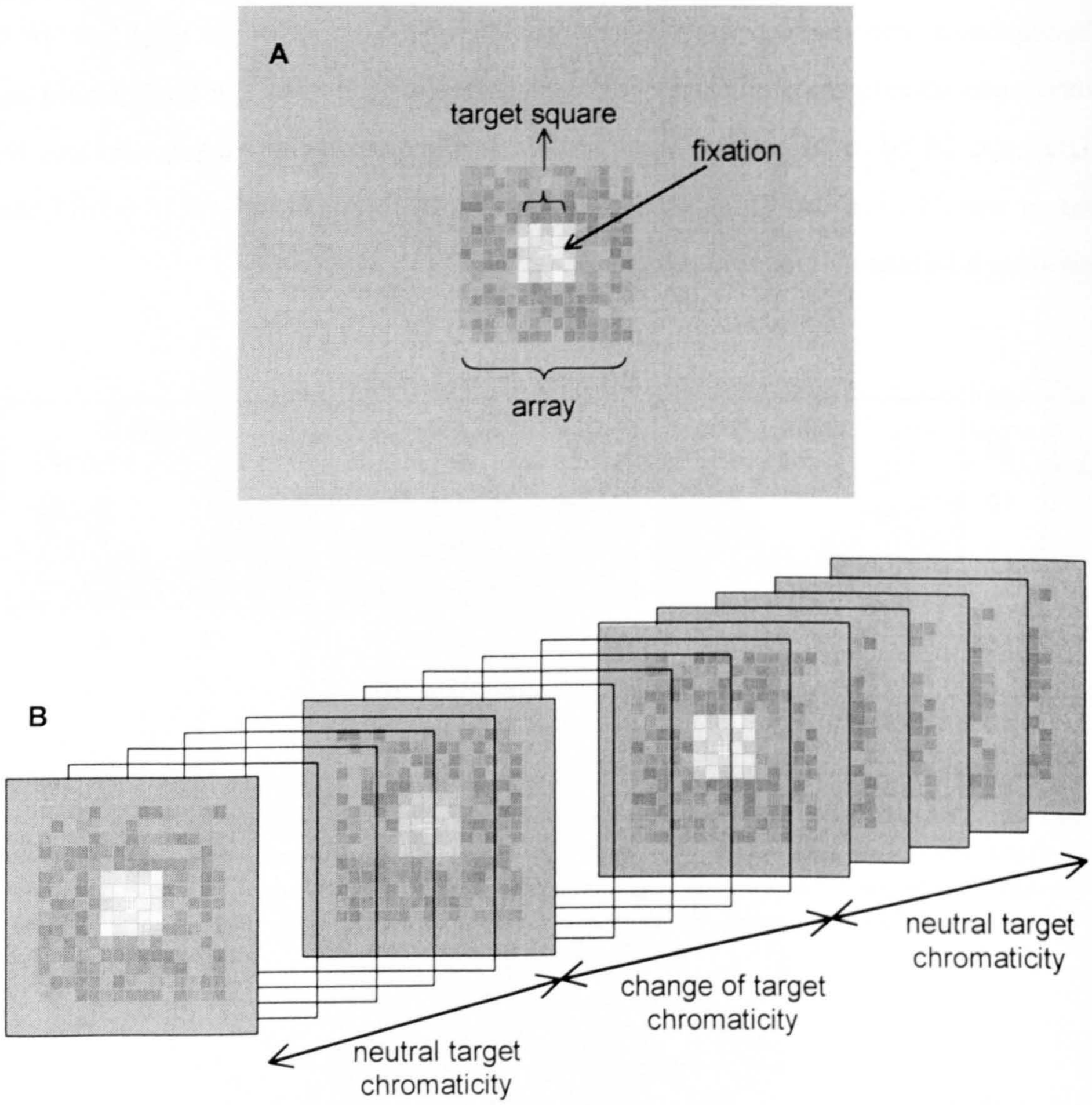

Figure 2-12 (A)-(B). Example of the stimulus used to measure chromatic thresholds under mesopic conditions, with the array centred at the fovea. The target square was defined by a luminance contrast pedestal and underwent a change in chromaticity in the middle of each presentation (B).

target dimensions	size of array	check dimensions
2° x 2°	6° x 6°	24′ x 24′
4° x 4°	12° x 12°	48′ x 48′

Table 2-1. Dimensions for the two sizes of stimulus used to measure chromatic thresholds under mesopic conditions.

Two stimulus sizes were used, providing test targets of diameter 2° and 4° angular subtense, the stimulus dimensions of which are shown in Table 2-1. In both cases the central 5 x 5 check square was defined by an LCP, forming the test target. All stimuli were presented on a uniform, neutral background. Figure 2-12 shows an example of this stimulus. Measurements were carried out using the two stimulus sizes at different retinal eccentricities. For the eccentric measurements the stimulus was always presented in the right hemi-field. Monocular viewing with the right eye was used for all these measurements, therefore, the results show changes in the sensitivity of solely the nasal retina at different eccentricities.

Dynamic changes in luminance contrast and light flux noise occurred every 107ms to ensure that rod generated luminance contrast signals were masked. For the majority of the measurements a single stimulus was 1500 ms in duration, divided into achromatic, chromatic, and achromatic periods of length 500, 500, and 500 ms. The timing was adjusted for the experiments in section 4.3.6, where a comparison was made between thresholds measured after dark adaptation and those measured on the cone plateau of the dark adaptation curve. The new timing consisted of achromatic, chromatic, and achromatic periods of 500, 600, and 100 ms, respectively.

2.4 Dark adaptation experiments

Dark adaptation curves were measured in chapter 4 to determine the duration of the cone plateau. Light adaptation was provided using the single channel Maxwellian view optical system described in section 2.2. Immediately after a 2 minute period of light adaptation of retinal illuminance (Troland Value) 5 log tds, detection thresholds were measured over a 25 minute period using the method of adjustment.

A white-light stimulus presented on a CRT display was used to measure threshold variation with time. Target luminance was reduced over a range of more than 3 log units using neutral density filters mounted in a pair of goggles. In this way the optical density could be increased rapidly, at intervals during the experiment. The target was a modified Landolt ring with a ratio of outer to inner diameter of 5:3 and with a 10° sector removed. The target was flashed on for 120 ms and off for 400 ms in a repetitive cycle, and was presented randomly in one of three different positions on an arc to the right of fixation (see Figure 2-13 for an illustration of the stimulus). The subject could increase or decrease the luminance of the target in steps by pressing a button. The size of each increment/decrement was 30% of the target luminance. Threshold values were recorded by pressing a third button when the target was judged to be just barely visible.

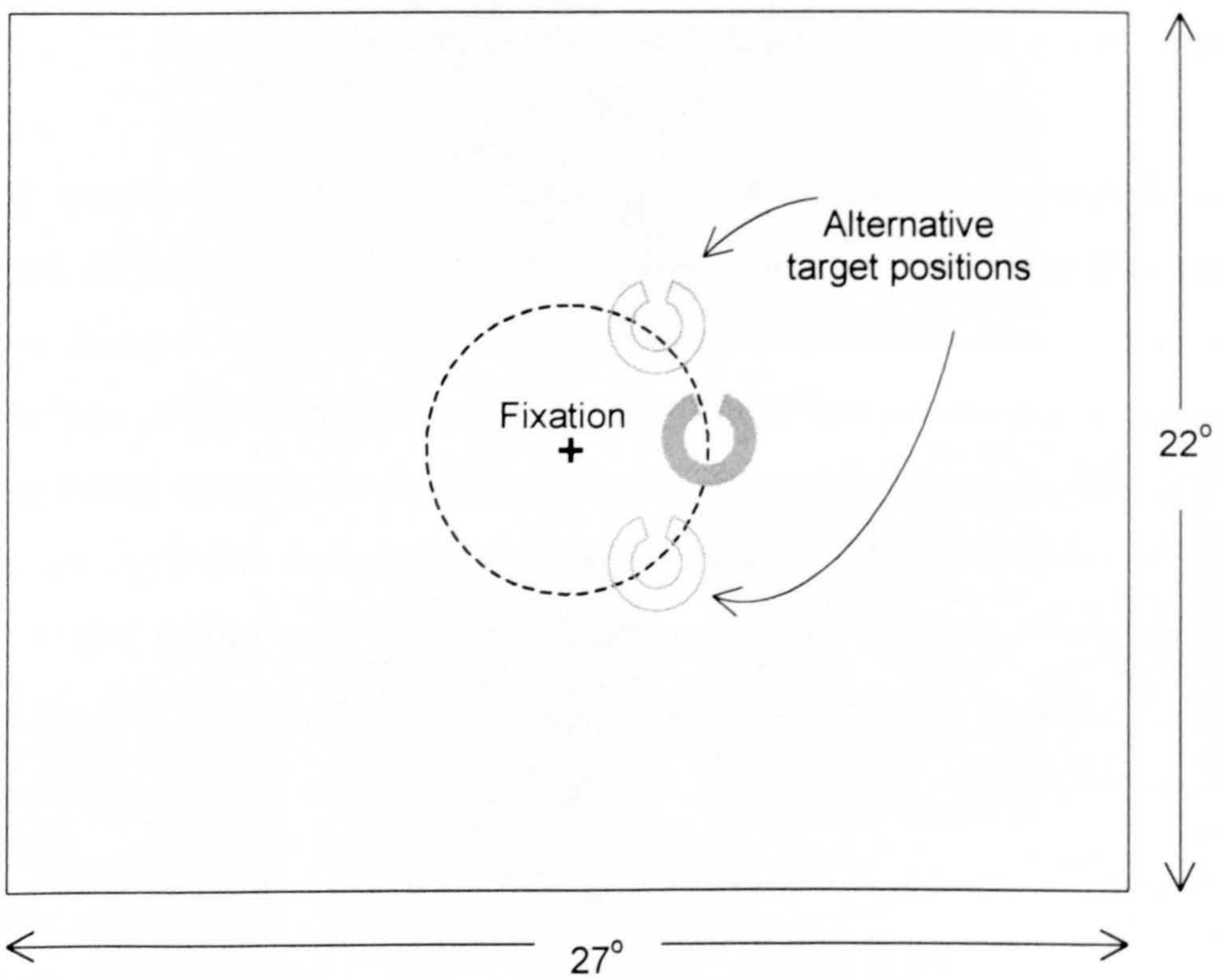

Figure 2-13. The stimulus used in the dark adaptation experiments. The white-light target was presented to the right of fixation in one of three positions on arc of fixed eccentricity.

2.4.1 Calculation of appropriate dark adaptation times

For all experiments performed at a background luminance of 10 cd m^{-2} or lower, observers were adapted to the level of the background prior to beginning

measurements. For backgrounds of 10 cd m^{-2} and above, an adaptation time of 5 min was used. Adaptation times for lower background luminances were calculated by assuming an exponential function between log luminance and adaptation time, using the minimum value of 5 min at 10 cd m^{-2} and setting the adaptation time for the lowest background luminance used as 30 min.

2.5 Visual matching procedure

In chapter 5, a matching procedure was used to relate the conspicuity of a test target defined by luminance contrast and colour, to the conspicuity of a similar reference target (match target) defined by achromatic contrast. The test and match targets were based on Landolt rings; they had an outer to inner diameter ratio of 5:3, but a sector removed to provide the gap. The test target was defined by its photopic contrast (C_p) value, scotopic contrast (C_s) value and chromatic difference (CD) with respect to the background. The match target had the same spectral power distribution as the background, but differed in luminance to create a target of achromatic contrast. Defined in this way the match target had equal values of photopic and scotopic contrast. The two rings were presented briefly at a fixed eccentricity. The observer was asked to indicate by pressing buttons on a response box, whether the test or match target was the most conspicuous; this was alternatively explained as choosing the target that was the most noticeable, the most obvious, or the most clearly visible. A psychophysical staircase was employed to vary the contrast of the match target. The output of the staircase procedure gave the contrast value (C_m), for the achromatic match target that appeared equally conspicuous as the test target. Matches could then be obtained in this way for different test target combinations of photopic contrast, scotopic contrast and CD value. Initially, a pilot study was carried out to investigate the conspicuity of targets with zero photopic and scotopic contrast. Following the pilot study, amendments were made to the design of the matching procedure before collection of an extensive data set of test-match pairs.

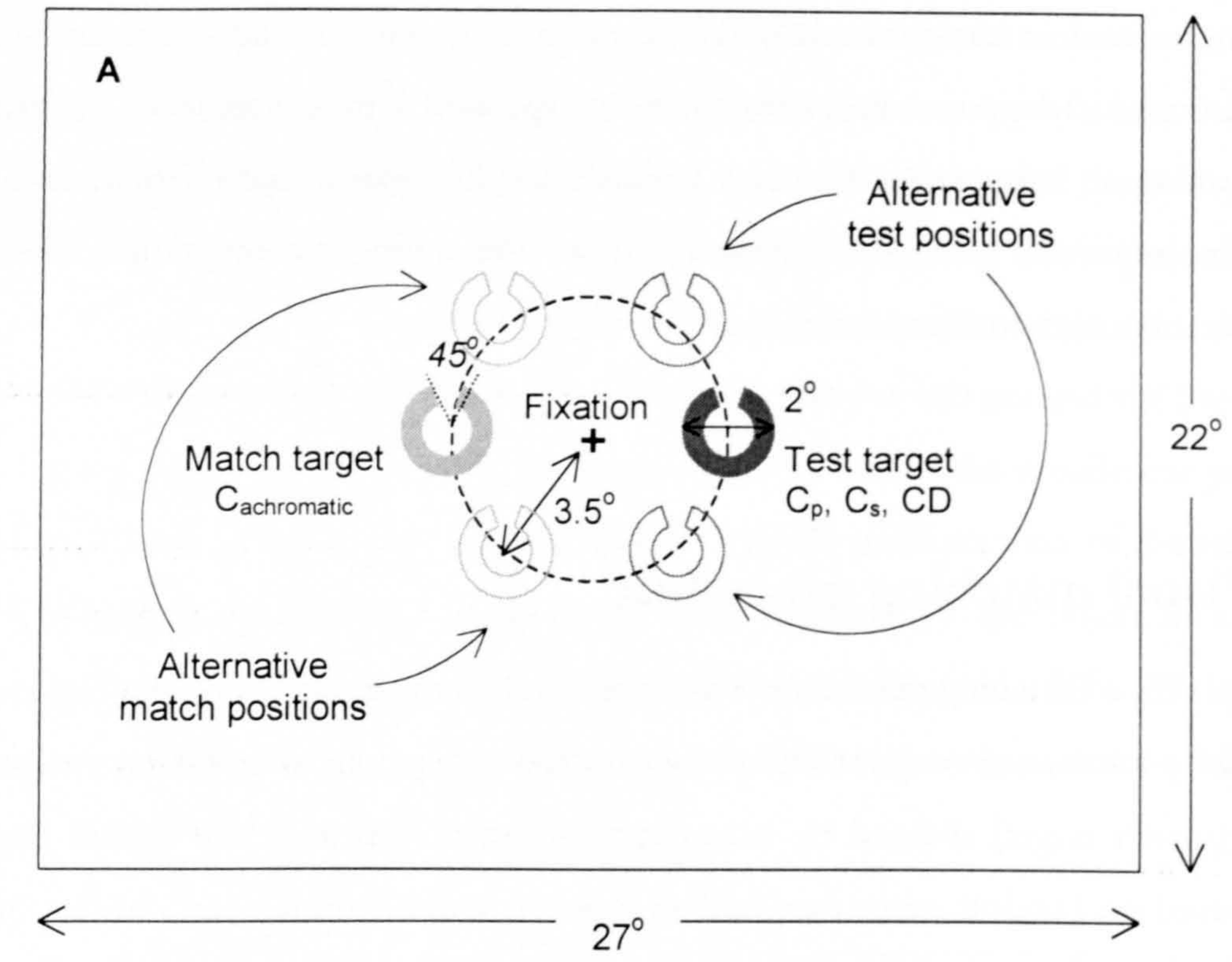

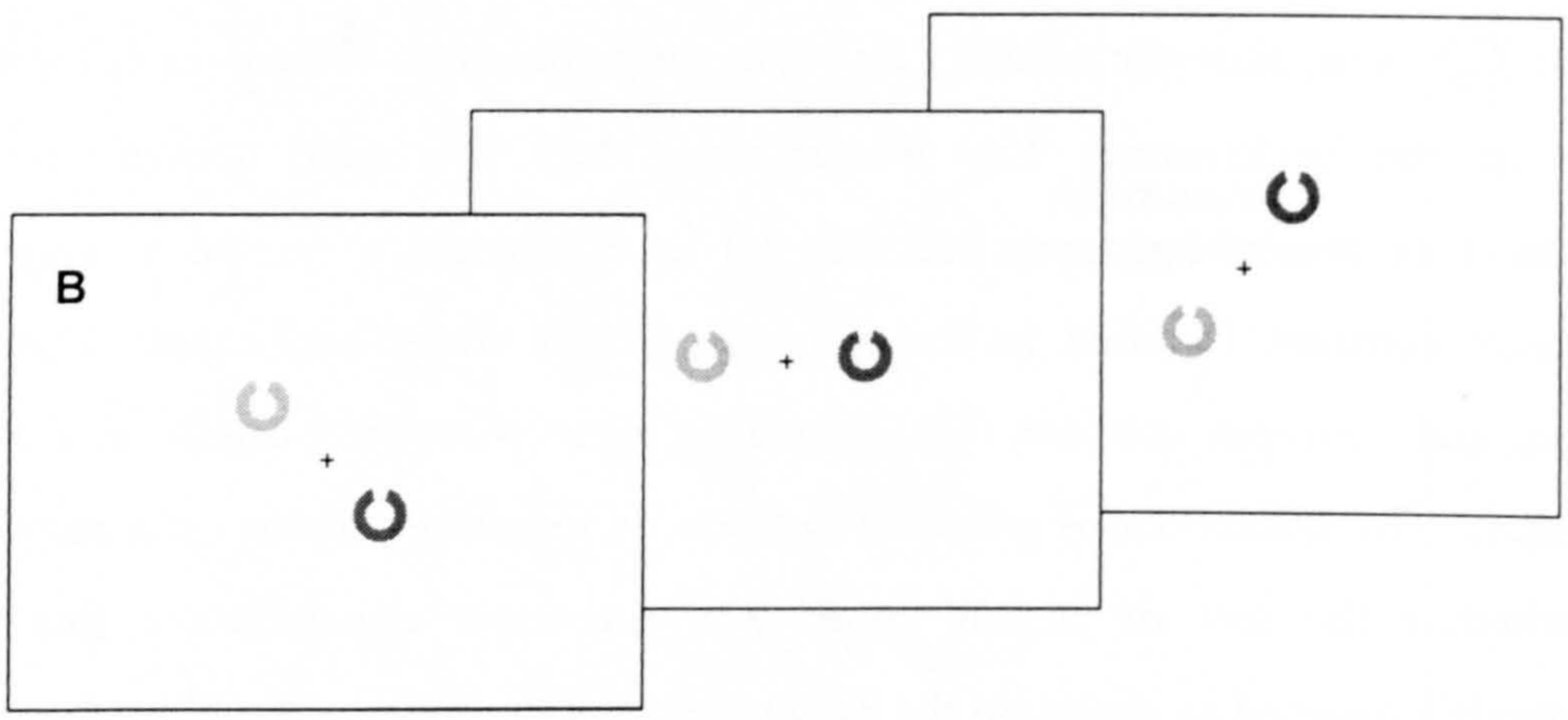

Figure 2-14 (A)-(B). Diagrams of the stimulus used in the pilot matching experiments. Angles in normal type refer to angles subtended at the eye; angles in italic type refer to angles in the plane of the display (A). The test target was defined by C_p, C_s, and CD. The match target was defined by positive achromatic contrast. The test target was presented to the right of fixation and the match target is presented to the left of fixation (A)-(B). Separation of the test target and match target was fixed and the pair of rings is presented randomly in any one of three positions on a 3.5° arc (B).

2.5.1 Design of the matching procedure for the pilot study

For the pilot study, the test and match rings were 2° angular subtense in diameter, with a 45° sector removed, and were presented at an eccentricity of 3.5°. The test target was always flashed to the right of fixation and the match target always to the

left. The two targets were constantly separated by 180° in the plane of the display, and were presented randomly in one of three different positions to minimise the effects of adaptation at a single location, see Figure 2-14 for an example of the stimulus.

The background field was chosen to have the chromaticity of MacAdam white: x = 0.305, y = 0.323. During a single presentation the rings were flashed simultaneously for 500 ms. Observers were asked to indicate by pressing a button, whether the test or the match ring was the most conspicuous. Six values of match contrast were obtained in a single experiment by running six interleaved staircases concurrently.

In the pilot study photopic luminance was calculated using the CIE 1924 luminous efficiency function for photopic vision, and scotopic luminance was calculated using the CIE 1951 luminous efficiency function for scotopic vision. Contrast was calculated according to Eq. 2-8,

$$C = \frac{L_t - L_b}{L_b} \qquad \textbf{Eq. 2-8}$$

where C: contrast (photopic or scotopic), L_t: luminance of the target (photopic or scotopic), and L_b: luminance of the background (photopic or scotopic). Photopic and scotopic luminance were calculated according to Eq. 2-9 and Eq. 2-10, respectively.

$$L = K_m \int L_{e,\lambda} V(\lambda)\, d\lambda \qquad \textbf{Eq. 2-9}$$

where L: photopic luminance, K_m: maximum photopic luminous efficacy, $L_{e,\lambda}$: radiance of the target or background, $V(\lambda)$: CIE 1924 standard photopic luminous efficiency function,

$$L' = K'_m \int L_{e,\lambda} V'(\lambda)\, d\lambda \qquad \textbf{Eq. 2-10}$$

where L′: scotopic luminance, K_m': maximum scotopic luminous efficacy, $L_{e,\lambda}$: radiance of the target or background, $V'(\lambda)$: CIE 1951 standard scotopic luminous efficiency function. The chromatic difference (CD) was measured as a distance in the CIE 1976 (u′, v′)-chromaticity diagram,

$$CD = \sqrt{\left(u'_t - u'_b\right) + \left(v'_t - v'_b\right)} \qquad \textbf{Eq. 2-11}$$

where u'_t, v'_t: CIE 1976 chromaticity coordinates of the target; and u'_b, v'_b: CIE 1976 chromaticity coordinates of the background.

2.5.2 Re-design of the conspicuity matching procedure

Following the pilot study, amendments were made to the conspicuity matching procedure before collection of an extensive data set. The diameters of the test and match rings were increased to 3°, to increase the possible area of receptor signal summation. The eccentricity of presentation was increased to 7°, corresponding to a retinal location with increased rod density, to increase possible effects of rod intrusion. Photopic luminance was calculated using the CIE 1964 $\bar{y}_{10}(\lambda)$ colour matching function, according to Eq. 2-12,

$$L_{10} = K_m \int L_{e,\lambda} \bar{y}_{10}(\lambda)\, d\lambda \qquad \textbf{Eq. 2-12}$$

where L_{10}: 10-degree photopic luminance, K_m: maximum photopic luminous efficacy, $L_{e,\lambda}$: radiance of the target or background, $\bar{y}_{10}(\lambda)$: CIE 1964 colour matching function. Scotopic luminance was calculated using Eq 2-10, and contrast according to Eq. 2-8. Chromatic difference values were measured as distances in a transformed version of the CIE 1964 (x_{10}, y_{10})-chromaticity space, using the transform that converts CIE 1931 (x, y)-space into CIE 1976 (u′, v′)-space, which is given in Eq. 2-13,

$$u' = \frac{4x}{(-2x + 12y + 3)}; \quad v' = \frac{9y}{(-2x + 12y + 3)} \qquad \textbf{Eq. 2-13}$$

where u′, v′: CIE 1976 chromaticity coordinates, and x, y: CIE 1931 chromaticity coordinates. Coordinates in this transformed colour space will be referred to as (u_{10}', v_{10}')-coordinates. CD values were calculated using Eq. 2-11, but with (u'_t, v'_t) and (u'_b, v'_b) replaced by ($u_{10}'_t$, $v_{10}'_t$) and ($u_{10}'_b$, $v_{10}'_b$). The CIE 1964 supplementary colorimetric observer was used in this case as it is representative of the colour matches of normal observers over a large field and was, therefore, considered to be more suitable for a stimulus location of 7° eccentricity than the CIE 1931 2° observer. However, the 10° colour matching functions were derived from

measurements made at photopic luminances and exclude effects of rod intrusion in the matches. It is unlikely, therefore, that they will predict colour matches at mesopic levels, but it is probable that prediction errors would be smaller for the 10° colour matching functions than for the CIE 1931 2° colour matching functions.

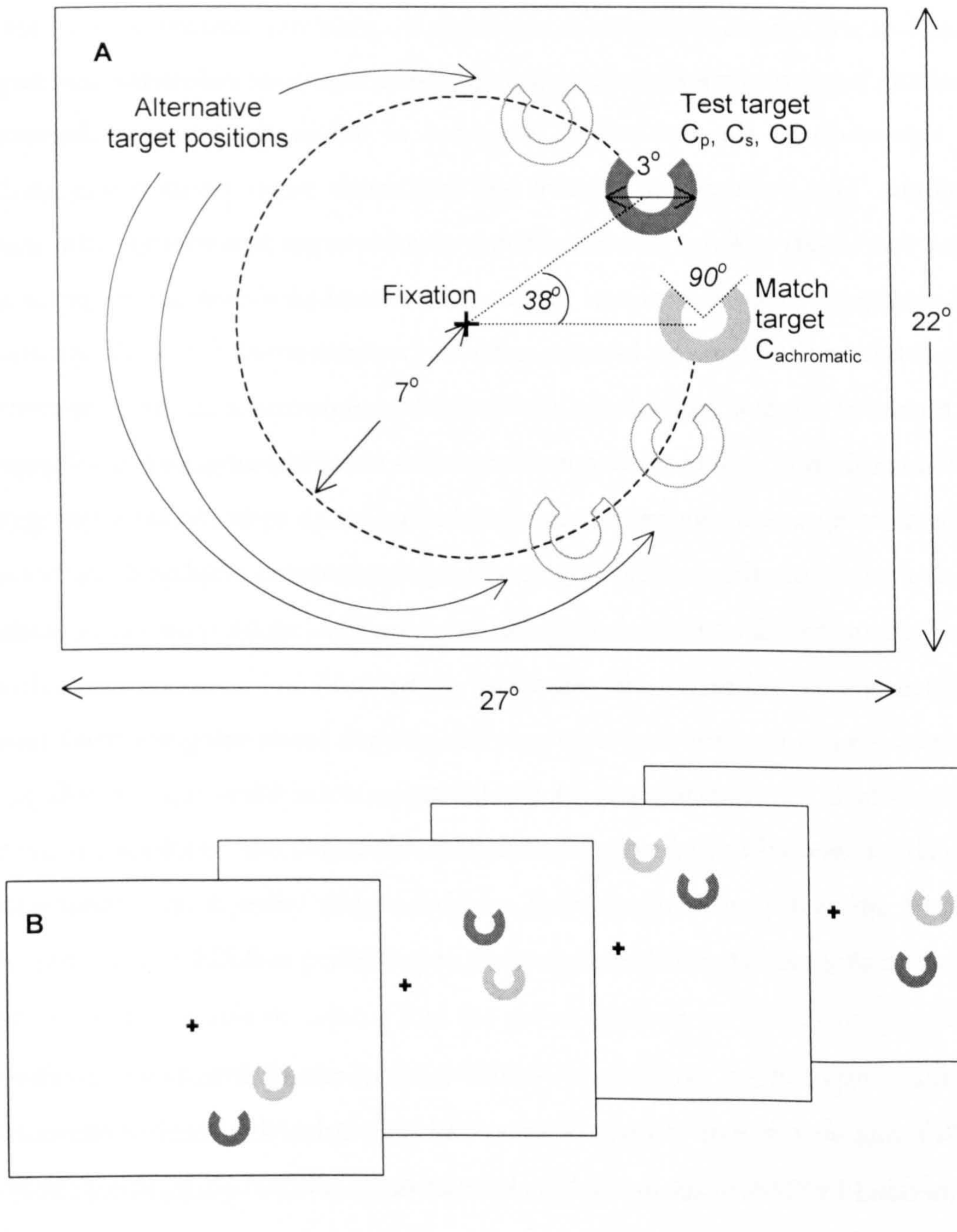

Figure 2-15 (A)-(B). Diagram of the stimulus used in the conspicuity matching experiments. Angles in normal type refer to angles subtended at the eye; angles in italic type refer to angles in the plane of the display (A). The test target was defined by C_p, C_s, and CD. The match target was defined by positive achromatic contrast. Separation of the test target and match target is fixed (A)-(B). The pair of rings was presented randomly in any one of four positions on a 7° arc to the right of fixation (B).

A presentation time of 500 ms was retained, which was chosen as a compromise between a transient and sustained presentation time. The two rings were presented in one of four different positions on a 7° arc to the right of fixation. Figure 2-15 shows an example of the stimulus. The four positions were used to reduce the effects of adaptation at a single location.

The match target was presented on the arc either above or below the test target, while separation of the two targets remained at 38° in the plane of the screen throughout. This switching of relative test and match target position was used to prevent the observer from attending solely to one target, for example the match target, during an experimental run. Observers were asked to indicate by pressing a button, whether the higher or lower target was the most conspicuous. Presentations were restricted to one half of the visual field to reduce the required spread of attention, and thus reduce task complexity. Binocular viewing was employed to simulate viewing conditions in the real world. The switch to binocular viewing (the original design of the conspicuity matching procedure employed monocular viewing) meant that a combined response from the right and left eye was obtained, which is subject to differences in sensitivity of the nasal and temporal retina. It did eliminate the need to compare conspicuity judgements made using the nasal vs. the temporal retina. The chromaticity of the background field was $x_{10} = 0.306$, $y_{10} = 0.326$. This chromaticity, specified for the 10° observer, was calculated from the combined spectral power distribution of the display phosphors, when set to produce the chromaticity of MacAdam white, $x = 0.305$, $y = 0.323$.

In a single experiment two match results were obtained from two interleaved staircases, one with a high starting contrast and one with a low starting contrast, as recommended by Cornsweet in the "double-staircase method" (Cornsweet 1962). It was found from preliminary measurements performed over a number of days, that there was a significant effect on values of match contrast (C_m) due to the day of measurement. Analysis of variance (ANOVA) performed for four different sample conditions at different light levels, showed the day to be a significant factor ($p<0.05$) in three of the four cases. The most likely reason for this was large variation in observer criterion between different days. Hence, six values of match

contrast were obtained over three days (two values per day); to capture the increased variability of C_m values generated from testing over a number of days.

During each experiment, measurements of natural pupil diameter were made using the methods described in section 2.1.2. For system-1, the mean pupil diameter was taken from a dynamic recording of pupil size, lasting 20 seconds. For system-2, the mean pupil diameter was calculated from a number of static images of the pupil, acquired during the experiment.

The staircase procedure was also redesigned to allow the most efficient measurement of matching contrast, for a large range of possible contrasts. Ideally, the step sizes of the staircase procedure should relate to the just noticeable difference (jnd) in contrast for successive presentations of the achromatic match target. Just noticeable differences in contrast for successive presentations of the achromatic match target were estimated from the spread of matches obtained for two simultaneously presented achromatic targets (an achromatic test target and an achromatic match target). The spread of C_m values was taken as two standard deviations of a series of 36 matches made by two observers. The spread of C_m values for a test target of high achromatic contrast was much greater than the spread of C_m values for a test target of low achromatic contrast. The spread of C_m values divided by test target contrast, however, was found to be approximately constant across a number of light levels in the mesopic range. From the finding that the jnd for simultaneous presentation was proportional to the contrast of the target, it is not unreasonable to assume that the jnd in contrast for successive presentations would also be proportional to the contrast of the target. As the potential range of match contrast was large, the possible range of jnds was also large. Hence, the staircase design had to be a compromise over all the conditions to be tested. Estimates of the range of jnds were made from the measurements of two observers. The values of contrast used were those judged to be the largest and smallest likely values of match contrast for the test target specifications used in the experiment. The largest step size was chosen to be 5 times the largest estimated jnd and the smallest step size was set at the smallest estimated jnd. This lead to some

redundancy in the staircase procedure for targets of very high or very low conspicuity.

2.6 Visual search task

A visual search procedure was employed in chapter 6 to measure the search time needed to find a target presented amongst a scene of distracter elements. The stimulus elements were designed to be similar to those used in the conspicuity matching experiments. Each stimulus consisted of a single target and 19 distracters, which were rings with an outer to inner diameter ratio of 5:3 and with a sector removed. Distracters were displayed with the missing sector (gap) oriented either upwards or downwards, whereas the gap in the target ring was oriented obliquely in one of four positions shown in Figure 2-16. Stimulus elements were constrained to a central, circular region within the background field. The target could be displayed at any position within this region to simulate visual search across the central visual field in a real scene. The circular region was divided into cells and the target and distracters were arranged in random cells within the field and positioned randomly within the cells. The test target and distracters were defined by their photopic contrast (C_p) value, scotopic contrast (C_s) value and chromatic difference (CD) to the background, in the same way as the targets used in the conspicuity matching experiments. Photopic luminance, scotopic luminance and chromatic difference were calculated according to Eq. 2-12, Eq. 2-10 and Eq. 2-11, respectively.

In a single presentation the stimulus was displayed until detection was recorded or until the maximum allowable visual search time limit was reached. The subject was required to fixate the centre of the field preceding each presentation, but was not restricted in his/her eye movements whilst searching for the target. The subject was asked to press a response button immediately that he/she detected the target, and the display was simultaneously replaced with a uniform grey. Manual reaction times were recorded with a precision of 1 ms. The subject was then required to specify by means of a four-choice response box, the orientation of the gap in the target ring, to verify correct target identification. If the target was not detected during the

presentation time, it was represented with the stimulus elements rearranged, up to five times. If a target was not detected after five presentations it was omitted from the remainder of the experiment. Search times were recorded in milliseconds. The percentage that each test target stimulus went undetected during a single presentation (time-out rate) was recorded for each target, and the percentage that each target was incorrectly identified (response error rate) was also recorded in order to assess the accuracy of the observers' responses.

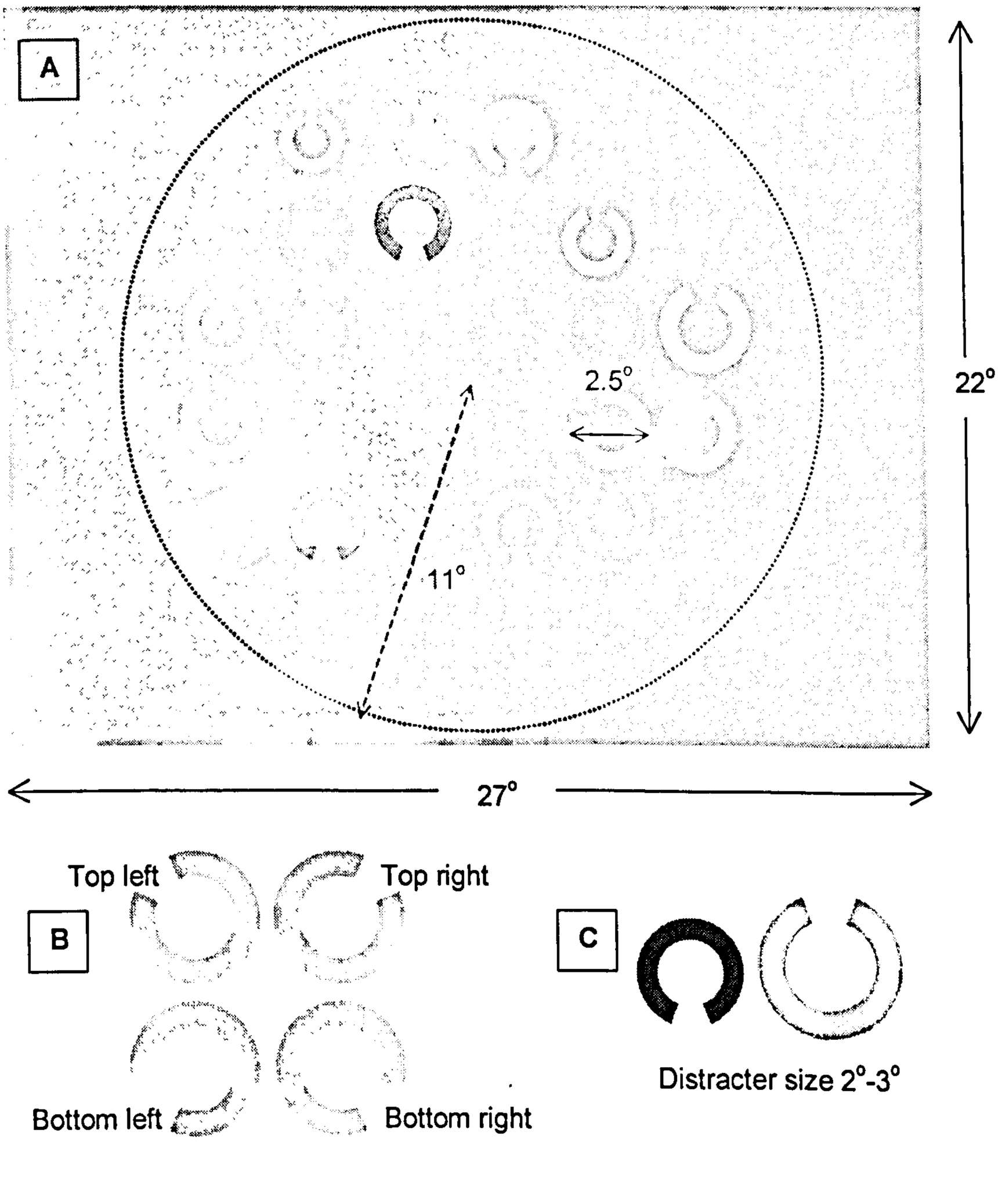

Figure 2-16 (A)-(C). Stimulus used in the visual search experiments (A). Ten of the rings were defined by colour and luminance contrast, 10 were defined by achromatic contrast. The target took one of 12 specifications at random; six defined by colour and luminance contrast and six defined by positive achromatic contrast. The target was presented with the gap oriented in one of four oblique positions (B). Distracter rings were presented with the gap oriented either upwards or downwards (C).

The central circular field was 22° in diameter. The target diameter was 2.5° visual angle, and distracter elements ranged in size from 2°-3° angular subtense. Both target and distracters had a 45° sector removed to provide the gap; see Figure 2-16 for illustrations of the target and distracters, and a typical stimulus. The target size was reduced from the 3° used in the conspicuity matching experiments to allow for a greater number of distracters in the search stimulus. The gap size was reduced in comparison with the 90° gap used in the conspicuity matching experiments to increase task difficulty. The chromaticity of the background field was that of MacAdam white: (x = 0.305, y = 0.323), which was equivalent to that used in the conspicuity matching experiments. The maximum duration of a single presentation was 8 sec. Each target was presented 48 times and the search times averaged over the whole circular stimulus field.

3 Effect of stimulus parameters on chromatic sensitivity

3.1 Introduction

In order to test for colour vision deficiency or to investigate chromatic sensitivity, one needs to isolate the use of colour signals. Modulation of wavelength or chromaticity is usually accompanied by changes in luminance contrast, so to elicit responses to colour alone, detection of luminance contrast signals must be avoided. There are at least two possible approaches for minimising the involvement of luminance contrast signals; one is to establish complete isoluminance, and the other is to mask the detection of luminance contrasts that may be present in a coloured stimulus. The second approach can be achieved to some extent by superimposing stimuli on a luminance pedestal, thus raising the local luminance difference threshold. A more elegant solution of raising the luminance contrast threshold is to bury stimuli in luminance contrast noise.

To present stimuli of equal luminance, one must consider the luminous efficiency response of the observer one wishes to test. There are large differences between the luminous efficiency functions of normal trichromats and subjects with congenital colour vision deficiencies (Wright 1946), and significant variations amongst normal trichromats themselves (Gibson and Tyndall 1923). These variations between individuals mean that isoluminance must be set for each observer to ensure isolation of colour signals. Luminance matches between two stimuli are usually made using flicker photometry: the two stimuli are imaged on the same retinal location and rapidly alternated, and by adjusting the frequency of alternation and radiance of the stimuli a criterion of minimum flicker can be met. However, if isoluminance is set in this way, and the "isoluminant" stimulus is presented with a temporal modulation

that differs from the condition under which minimum flicker was achieved, the isoluminance condition may no longer be valid.

The use of luminance contrast noise to mask detection of luminance contrast signals has long been employed in colour vision testing, being the principle behind the design of pseudoisochromatic plates. In plates such as the Ishihara pseudoisochromatic plates, the target and surround differ in colour, but are both divided into patches that vary in lightness. In the presence of this spatial luminance noise it is only possible to distinguish the test from the surround by a difference in the chromatic signal. The modulation of luminance in a cimputer generated stimulus may be purely spatial (static), or may be varied temporally as well as spatially (dynamic). Static luminance contrast noise (LC noise) incorporated in a CRT display-based test, has been demonstrated to mask detection of static patterns defined by photopic luminance contrast signals, in normal trichromats, dichromats and anomalous trichromats (Regan et al. 1994). Static LC noise does not, however, mask detection of transient luminance contrast signals, or luminance contrast defined motion signals. Temporal modulation of the background field has been used to selectively reduce the sensitivity of visual mechanisms tuned to detection of luminance contrast defined motion (Barbur et al. 1986). Use of a dynamic background perturbation technique is also thought to achieve better isolation of the chromatic signal by masking transient luminance contrast signals. In another CRT display-based test, dynamic LC noise has been shown to successfully mask photopic luminance contrast signals in normal trichromats and dichromats (Barbur et al. 1992). Results from normal trichromats have shown that luminance contrast thresholds are markedly increased with increasing amplitude of dynamic LC noise, whereas chromatic thresholds remain relatively unaffected by the increase (Barbur et al. 1994b). Chromatic discrimination ellipses (see section 1.2.6) obtained by normal trichromats using these two CRT display-based tests (Barbur et al. 1992; Regan et al. 1994), differ in size. There are many stimulus differences between the tests, which could be responsible for the difference in ellipse size. In this study, the effects of the spatial extent and distribution of the stimulus on measurements of chromatic sensitivity have been investigated.

Impaired colour vision may accompany lesions of the visual pathway from the retina to the visual cortex. Acquired colour vision deficiency is typically characterised by onset after birth, nature and severity that change over time, and differentially affected right and left eyes. Acquired colour vision deficiency is a common consequence of visual pathology and detection of colour vision abnormalities is often used as a diagnostic tool, for example, in conditions such as glaucoma. Assessment of acquired colour vision loss may also be used to monitor progression of the underlying condition e.g., in optic neuritis, and where the mechanisms of the pathology are understood, provide information on how colour is processed in the visual system.

Patients with acquired colour vision deficiency often exhibit other abnormalities of visual function, and lesions can cause nonuniform defects over the visual field. Also, marked variations in spectral sensitivity may be elicited in response to different temporal frequencies (Alvarez and King-Smith 1984). It is questionable, therefore, whether stimulus luminance can be equated using flicker photometry in these patients, making it more desirable to mask detection of stimulus specific luminance contrast signals in other ways. Dynamic LC noise has been shown to mask photopic luminance contrast signals in patients with acquired colour vision deficiency (Barbur et al. 1994b; Barbur et al. 1997).

Acquired colour vision deficiencies do not typically follow the patterns of congenital colour vision loss, so investigation of chromatic discrimination restricted to dichromatic isochromatic zones, for which many colour vision tests are designed, is of limited benefit. A better characterisation of colour vision deficiency can be obtained by measuring chromatic discrimination spread throughout different directions in chromaticity space. This is an advantage of the computer-controlled test, which can be tailored to probe chromatic sensitivity along different axes in colour space. In addition, the flexibility of such tests also allows the use of stimuli with different spatial configurations.

This chapter contains an investigation into the effects of the size and spatial distribution of the test stimulus on measurements of chromatic sensitivity under

photopic conditions. In particular, whether changes in these stimulus characteristics produce similar effects in normals, subjects with congenital colour vision deficiency and subjects exhibiting acquired colour vision defects. The investigation was carried out using a colour vision test similar to that reported by Barbur et al. (1994b), employing dynamic LC noise. Two test stimuli were employed, which differed in spatial arrangement and could be manipulated in size. One stimulus was designed to elicit thresholds for detection of a spatial pattern defined only by its difference in chromaticity to the surround, and the second stimulus was designed to measure chromatic discrimination thresholds for a spatially defined block i.e., colour changes independent of structure.

3.2 Subjects and Methods

The experimental technique used to measure chromatic discrimination was described in section 2.3.1. The two stimulus configurations were also described in section 2.3.1. The pattern test was used to measure thresholds for detection of a spatial pattern that was defined solely by chromatic signals, buried in a pattern defined by luminance contrast. For this test, subjects were required to respond when they detected coloured vertical bars. The stimulus for the colour test consisted of a large square defined by luminance contrast, and was used to measure detection thresholds for pure colour changes independent of structure. For the colour test, subjects were required to respond when they detected the presence of any colour change in the square stimulus, which was superimposed on a pattern defined by luminance contrast.

3.2.1 Subjects

Of the subjects involved in this investigation, six were normal trichromats, two were dichromats, and two were subjects with acquired colour vision deficiency. The colour normal observers were tested with the Ishihara plates. The mean age of the colour normal observers was 22 yrs, range 20-26 yrs; four were male and two were female. The dichromats were diagnosed using the Nagel anomaloscope. Both

dichromats were deuteranopes, and will be referred to as d-1 and d-2. The two subjects with acquired colour vision deficiency have been labelled Subject A and Subject B. Subject A was female, and was diagnosed with optic neuropathy of unknown aetiology. Subject B was also female, and was diagnosed with toxic optic neuropathy. The data for Subject B was kindly donated by Dr. Janet Wolf.

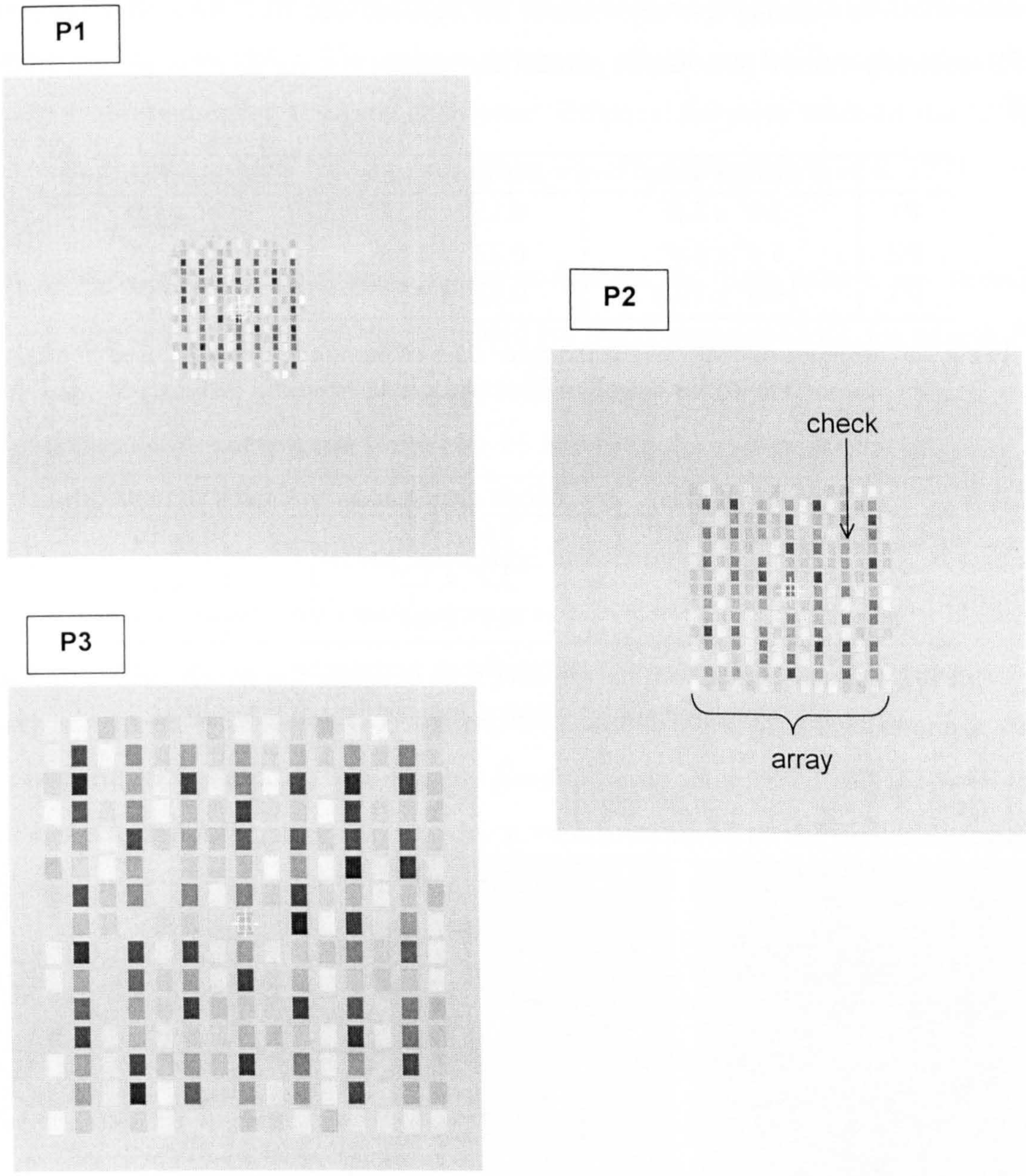

Figure 3-1. The three pattern test stimuli P1, P2 and P3, designed to measure thresholds for detection of a colour defined spatial pattern. In the middle of each presentation a selection of the checks underwent a change in chromaticity forming coloured vertical bars. The relative scaling of the bars was maintained for all three stimulus sizes.

3.2.2 Methods

Chromatic discrimination thresholds were measured for the pattern and colour test over different spatial scales. Three sizes of pattern test (P1, P2 and P3) and three sizes of colour test (C1, C2 and C3) were investigated. Dimensions of the pattern and colour test stimuli are given in Table 3-1 and Table 3-2, and the stimuli are displayed in Figure 3-1 and Figure 3-2. Stimuli P2 and C2 had equal array dimensions and similar test target areas: 7.2° squared and 10.2° squared, respectively. Parameters common to both the pattern and colour test are given in section 2.3.1.

	Size of array	Bar dimensions	Check dimensions
P1	3.6° x 3.6°	0.15° x 3.12°	9′ x 12′
P2	5.4° x 5.4°	0.22° x 4.68°	13′ x 17′
P3	10.8° x 10.8°	0.43° x 9.37°	26′ x 35′

Table 3-1. Stimulus dimensions for the three sizes of pattern test stimuli, used to measure thresholds for detection of a colour defined spatial pattern.

	Size of array	Block dimensions	Check dimensions
C1	5.4° x 5.4°	1.8° x 1.8°	19′ x 19′
C2	5.4° x 5.4°	3.2° x 3.2°	19′ x 19′
C3	5.4° x 5.4°	4.7° x 4.7°	19′ x 19′

Table 3-2. Stimulus dimensions for the three sizes of colour test stimuli, used to measure thresholds for colour changes, independent of structure.

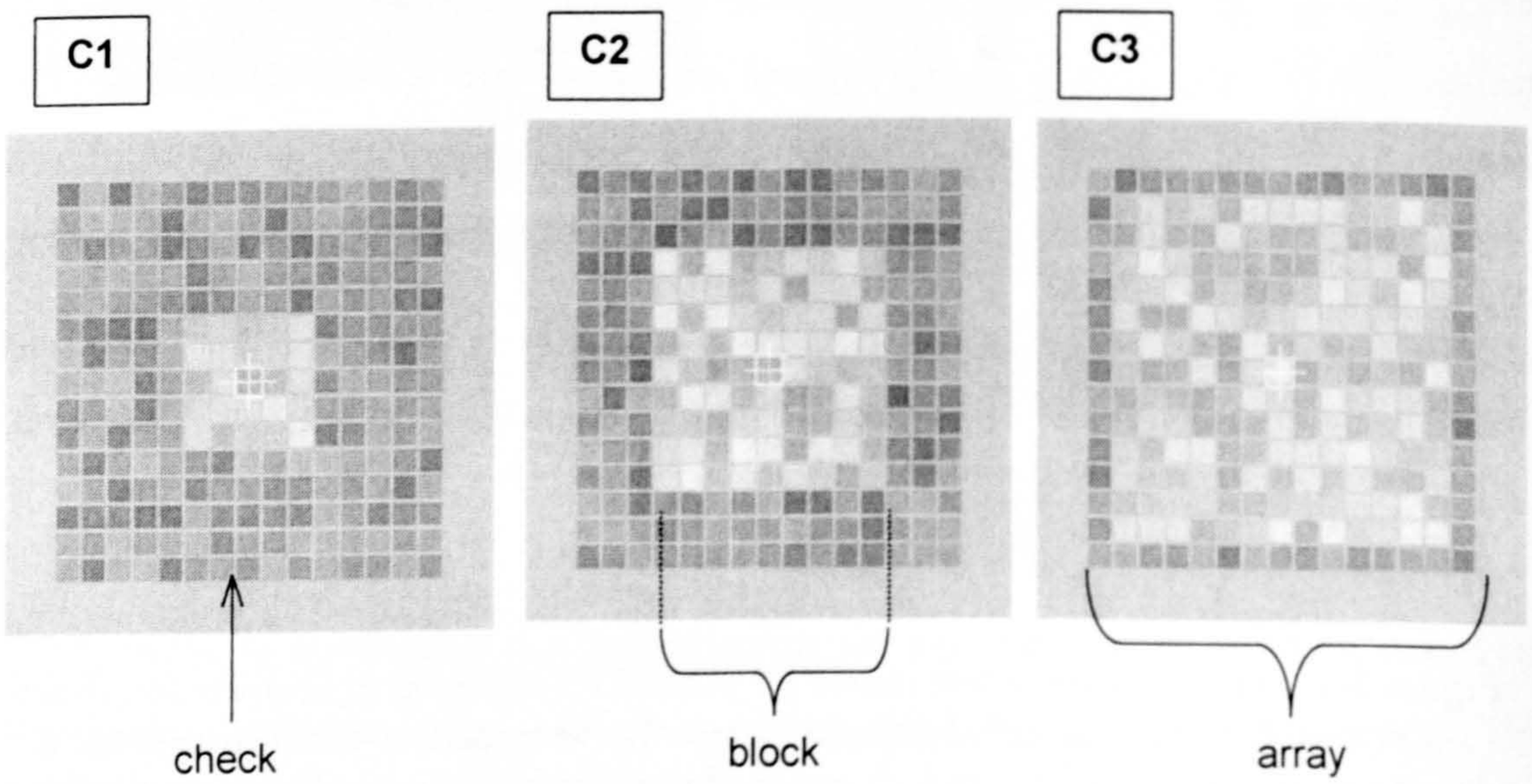

Figure 3-2. The three colour test stimuli C1, C2 and C3, designed to measure thresholds for detection of colour changes, independent of structure. The test square was defined by a luminance contrast pedestal and was always seen by the subject. The square underwent a change in chromaticity in the middle of each presentation.

Six normal trichromats carried out measurements for the three versions of the pattern test, acquiring two sets of thresholds for each stimulus. Three of the colour normal observers also performed measurements for the three versions of the colour test. Measurements were made monocularly with the dominant eye. The results were obtained as polar coordinates in CIE 1931 (x, y)-chromaticity space, which when plotted form what have come to be known as MacAdam discrimination ellipses (MacAdam 1942). The region within an ellipse can be thought of as the isochromatic region for a normal trichromat. Elliptical fits were made to the (x, y)-coordinates using a direct least squares fitting algorithm (Fitzgibbon et al. 1999).

The deuteranope, d-1, performed measurements for the three pattern test stimuli, P1-P3. Chromatic thresholds were acquired for the deuteranope, d-2, for stimuli P2 and C2, only. Both subjects with acquired colour vision deficiency carried out measurements for pattern test stimuli P1-P3 and the colour test stimulus C2.

Subjects A and B were affected bilaterally; hence, measurements by all observers were made monocularly with the dominant eye. Subject A exhibited what is likely to be a defect in her light adaptation mechanism, reporting discomfort from glare at moderate to high luminance, with structured stimuli appearing uniform. For this reason, the background luminance was lowered from 24 to 8 cd m^{-2} for both the pattern test and colour test, and a pedestal luminance of 16 cd m^{-2} was used for the colour test.

In order to make size comparisons between the chromatic discrimination ellipses obtained for the normal trichromats, the (x, y)-coordinates for each individual ellipse were transformed into points in the CIE 1976 (u′, v′)-uniform chromaticity space. The fact that equal differences in perception do not relate to equal differences in distance on the (x, y)-chromaticity diagram, makes it difficult to compare differences in ellipse dimensions in this space. In particular, caution should be taken in applying parametric statistical tests to ellipse dimensions in (x, y)-space, which assume that the data are of interval scaling. The (u′, v′)-chromaticity space, although still nonuniform, is a better approximation of a uniform colour space, and

over small regions of the space one can consider that differences in distance approach interval scaling. Elliptical fits were made to the (u′, v′)-coordinates of each set of thresholds, for each observer, to obtain the lengths of the major and minor semi-axes. A one-way analysis of variance (ANOVA) was used to compare individually, the major and minor axes lengths, for the three pattern test stimuli and the three colour test stimuli. To compare differences between the pattern test stimulus P2 and the colour test stimulus C2, the stimuli with most similar array dimensions and test target areas, a t-test was used to assess differences in major and minor axis lengths. For all the statistical analyses, the level of significance was taken at $\alpha = 0.05$.

3.3 Results

3.3.1 Normal trichromats

Figure 3-3 shows the mean thresholds obtained by the six normal trichromats for stimuli P1-P3, along with the elliptical fits for these data, plotted in (x, y)-chromaticity space. As the stimulus size was increased, the mean thresholds decreased. The reduction in thresholds, however, was not uniform in all directions tested; sensitivity along the major axis (the blue and yellow colour directions) appeared to be more affected than that along the minor axis (the red and green colour directions). The ellipses fitted to the mean thresholds in (u′, v′)-chromaticity space, also exhibited this nonuniform reduction in threshold with increase in stimulus size, see Table 3-3. The change in length of the minor semi-axis with stimulus size, was less than the change in length of the major semi-axis. The result of the statistical analysis of the change in minor semi-axis length with stimulus size is displayed in Table 3-4, the full table can be found in appendix A. The ANOVA established that the reduction in minor semi-axis length with increase in pattern test stimulus size was highly significant. It was not possible to perform a similar ANOVA for the major axis, as the variance of the semi-axis lengths differed considerably for the three pattern sizes (Levene's test $p<0.001$, (Levene 1960)).

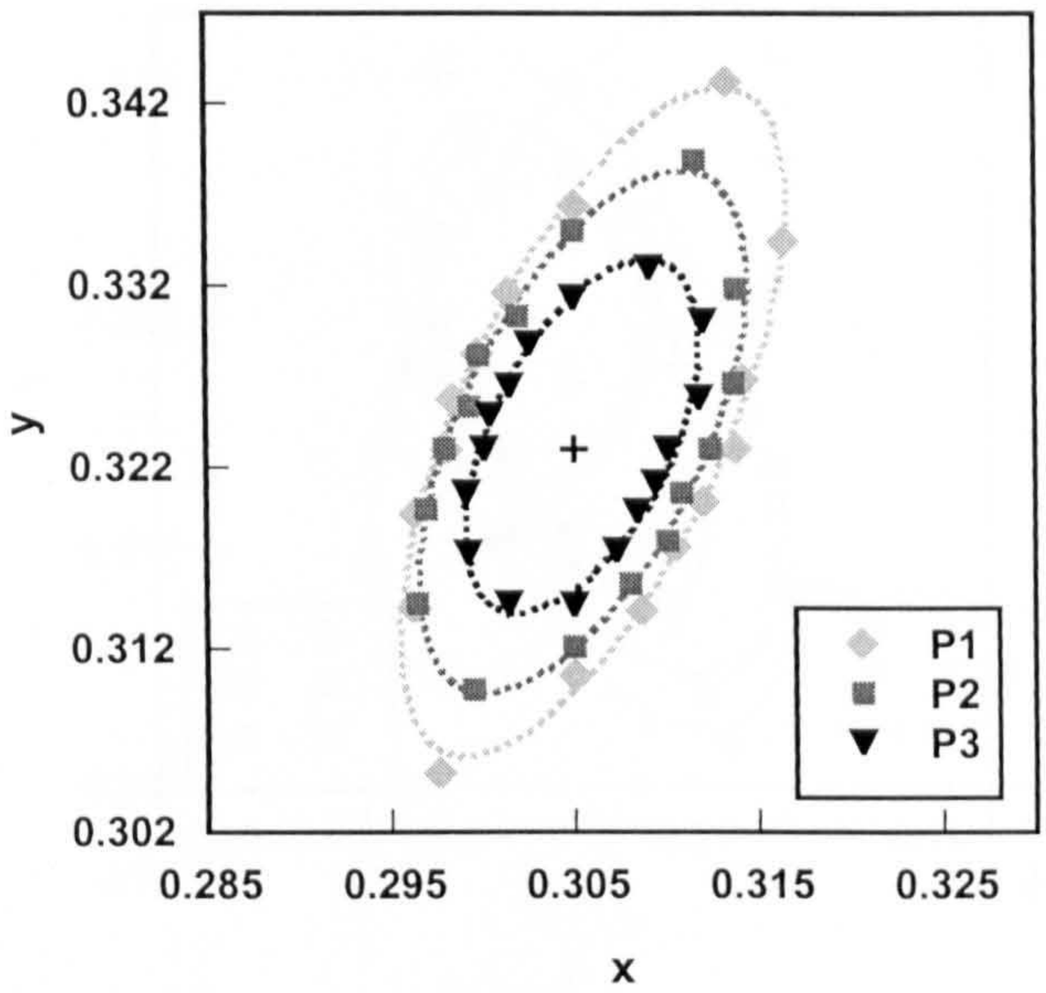

Figure 3-3. Average thresholds for the six normal trichromats for the three pattern test stimuli P1-P3, plotted in (x, y)-chromaticity space. Symbols represent data points and dotted lines represent fitted ellipses. The cross indicates the background chromaticity.

	P1	P2	P3	C1	C2	C3
Major semi-axis	11.1	8.8	6.0	4.8	4.2	3.3
Minor semi-axis	5.7	5.2	3.8	3.1	2.5	2.0

Table 3-3. Major and minor semi-axis lengths for ellipses fitted to the mean data for six observers in (u′, v′)-chromaticity space, for the three sizes of the pattern test and the colour test. Units are distances in the CIE 1931 chromaticity diagram x 10^3.

	Major semi-axis	Minor semi-axis
Pattern test	N/A	***
Colour test	NS	*
P2 vs. C2	***	***

Table 3-4. Results of the statistical analysis of the change in major and minor semi-axis length with stimulus size, for the pattern test, the colour test and a comparison of the two tests for normal trichromats. The semi-axis lengths were for ellipses fitted to the mean data in (u′, v′)-chromaticity space. Significance levels are given as ***: $p<0.001$, **: $p<0.01$, *: $p<0.05$, NS: not significant.

The mean results for three colour normal observers who performed measurements for stimuli C1, C2 and C3 are shown in Figure 3-4, along with the respective elliptical fits, plotted in (x, y)-chromaticity space. Similar to the pattern test results, thresholds for the colour test decreased with increasing test target size.

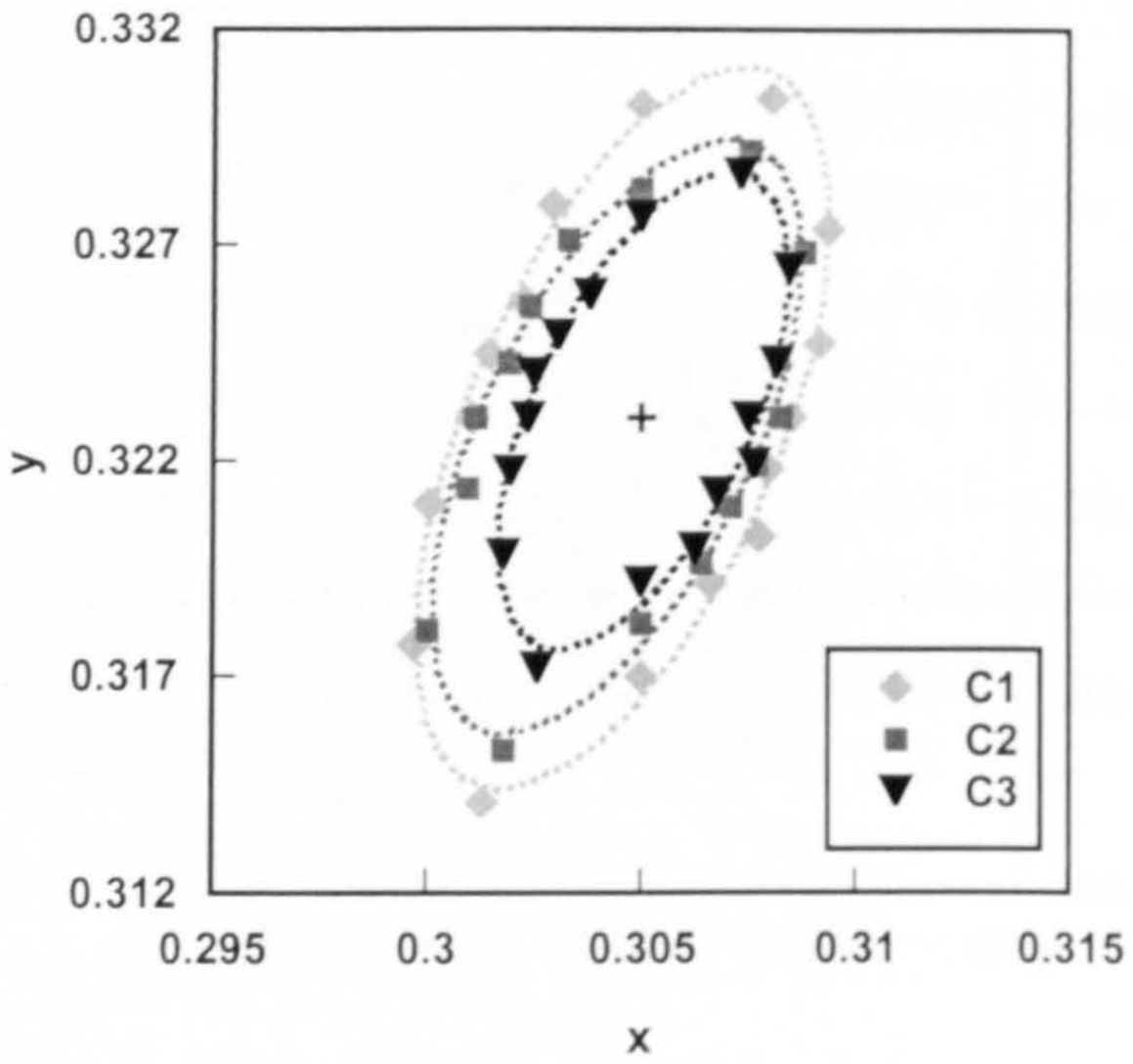

Figure 3-4. Average thresholds for the three normal trichromats for the three colour test stimuli C1-C3, plotted in (x, y)-chromaticity space. Symbols represent data points and dotted lines represent fitted ellipses. The cross indicates the background chromaticity.

The change in sensitivity for different sizes of the colour test, however, appeared to be more uniform across colour directions than for the pattern test. The lengths of the major and minor semi-axes of the ellipses fitted in (u′, v′)-space are shown in Table 3-3, and the results of the statistical comparisons of the major and minor semi-axis lengths for the colour test are displayed in Table 3-4 (the full statistical table is shown in appendix A). The ANOVA for the colour test demonstrated that the reduction in semi-axis length with increase in block size was not significant for the major axis, but a significant change was found for the minor axis.

Figure 3-5 shows the comparison of chromatic thresholds obtained for the pattern test and the colour test for the stimulus configurations P2 and C2, which had similar test target areas. It is clear that the two stimulus arrangements produced a substantial difference in thresholds, with larger thresholds arising for the pattern test. The statistical comparison of the major and minor semi-axes for the pattern test vs. the colour test showed the differences in axis length to be highly significant, see Table 3-4.

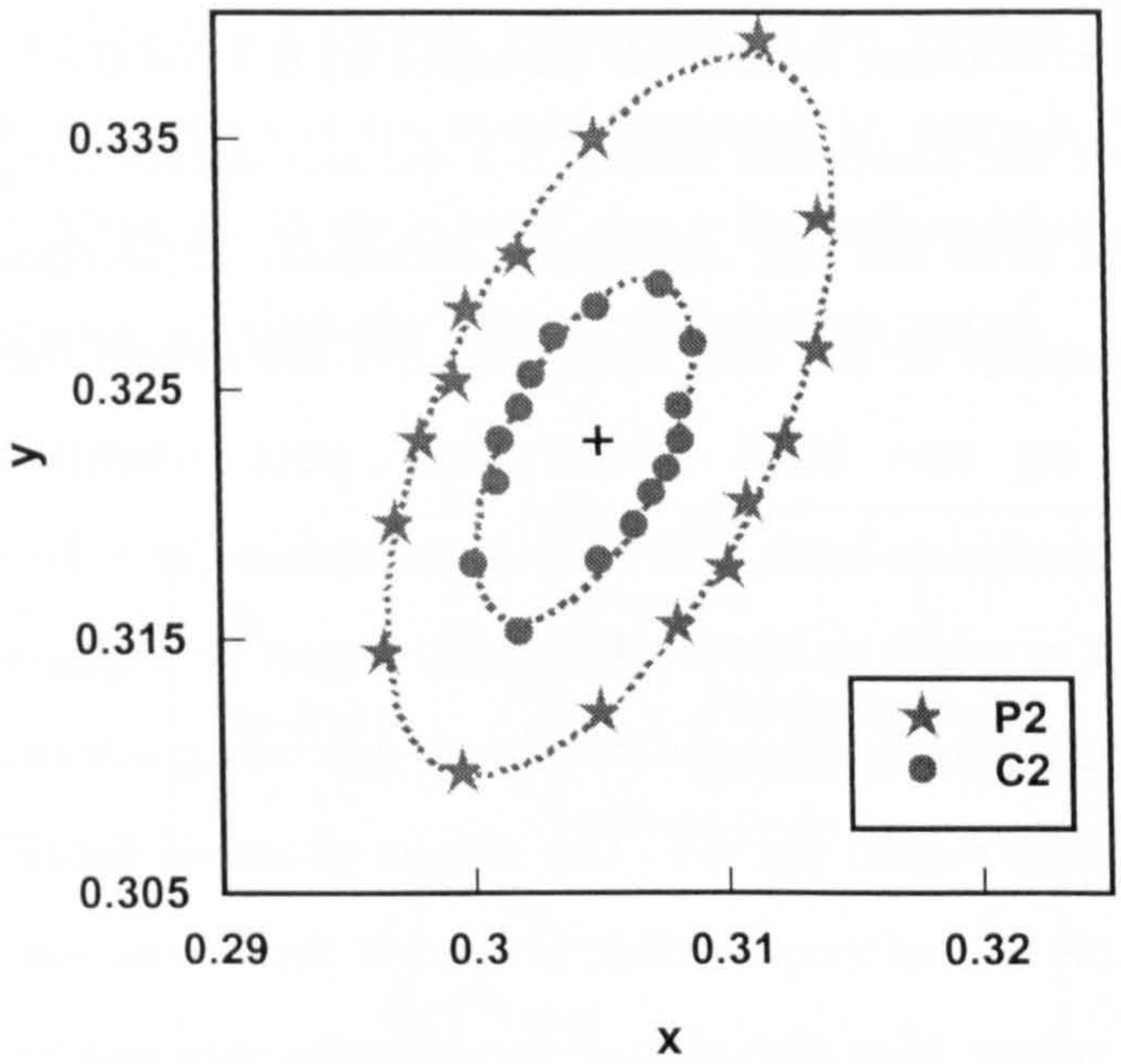

Figure 3-5. Average chromatic thresholds for three normal trichromats for the pattern test stimulus P2 and the colour test stimulus C2, plotted in (x, y)-chromaticity space. The symbols represent data points and the dotted lines represent fitted ellipses. The cross indicates the chromaticity of the background.

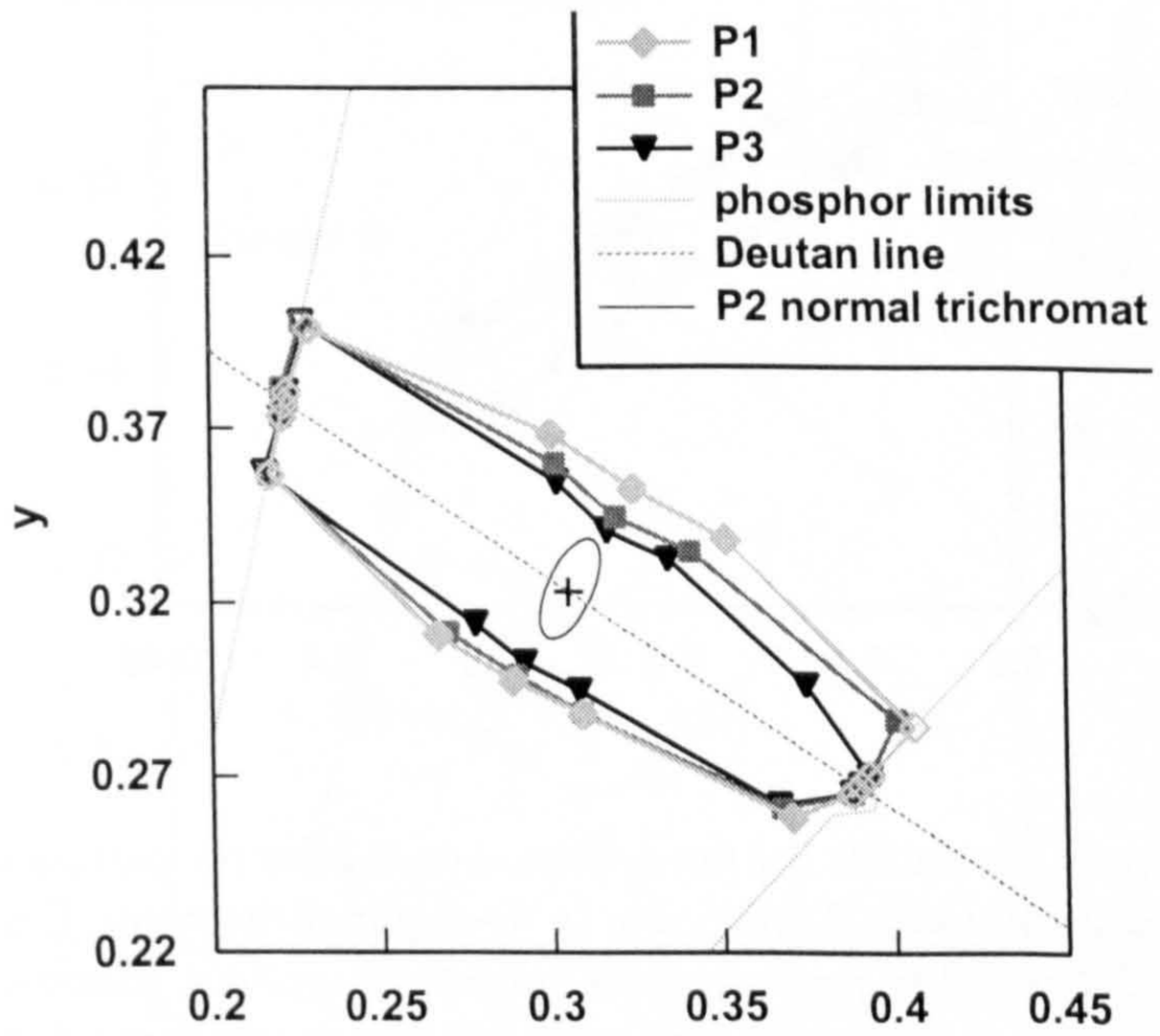

Figure 3-6. Chromatic thresholds for the deuteranope d-1 for the three pattern test stimuli P1-P3, plotted in (x-y)-chromaticity space. Closed symbols indicate measured thresholds, open symbols indicate an arbitrary maximum value (see text). The dotted line indicates the deuteranopic confusion line that passes through the background chromaticity.

3.3.2 Dichromats

Figure 3-6 shows the chromatic thresholds obtained by d-1 for the three pattern test stimuli. For several of the directions tested, d-1 did not detect the presence of the coloured vertical bars even for the maximum chromatic difference that could be reproduced on the display. In the directions that d-1 did detect the coloured bars, the thresholds fell on two lines. These lines were oriented roughly with deuteranopic colour confusion lines, and were separated in the yellow-blue direction by a region equivalent in width to the isochromatic region of a normal trichromat in this direction. The region formed by the two lines, extending towards the spectrum locus, is the isochromatic region for d-1. The results obtained for the three sizes of the pattern test stimulus were very similar, although there was some reduction of the thresholds in the yellow-blue direction as the stimulus size was increased.

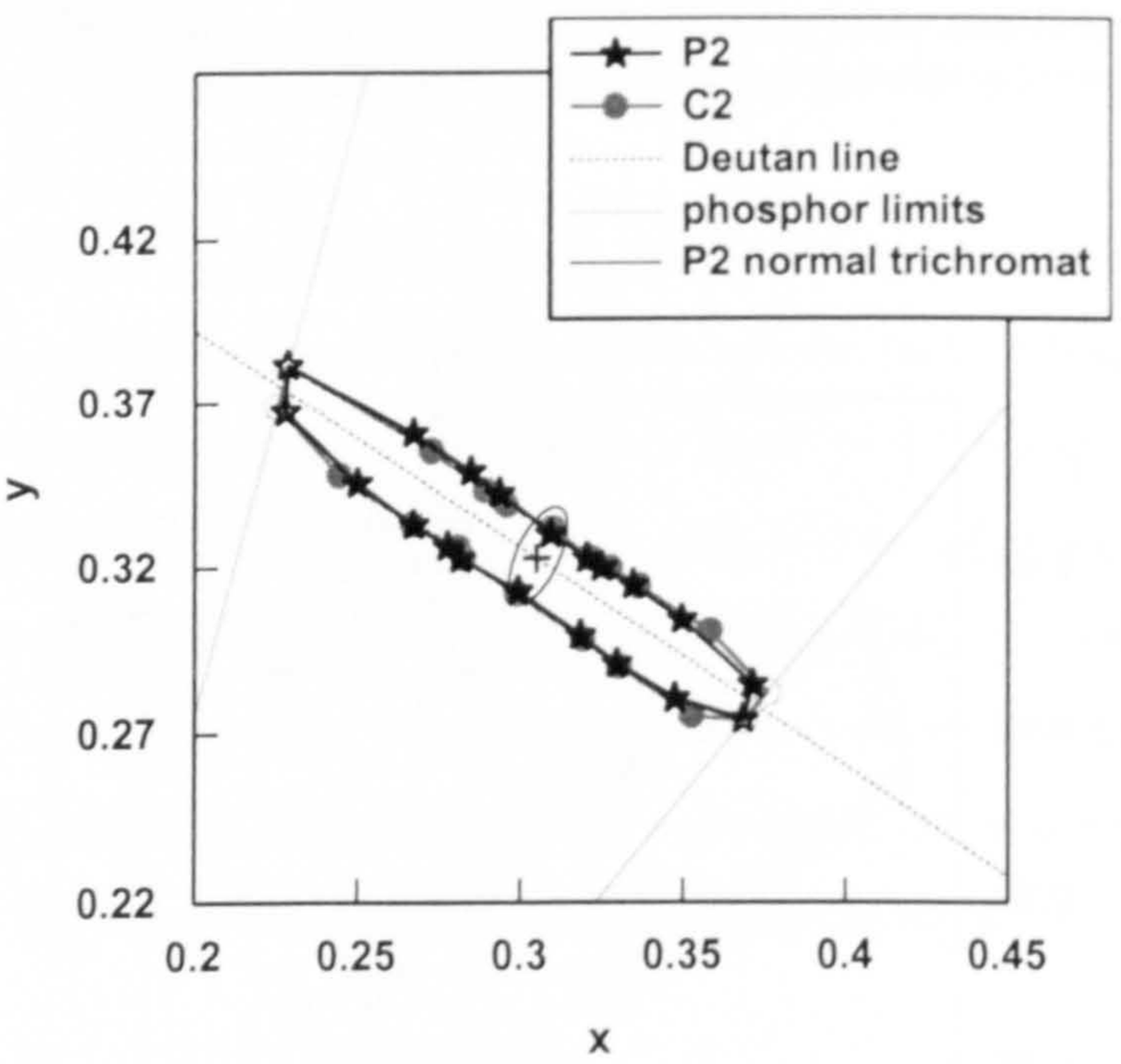

Figure 3-7. Chromatic thresholds for the deuteranope d-2 for the pattern test stimulus P2 and the colour test stimulus C2, plotted in (x, y)-chromaticity space. Closed symbols indicate measured thresholds, open symbols indicate an arbitrary maximum value. The dotted line indicates the deuteranopic confusion line that passes through the background chromaticity.

Measurements made by d-2 for both the pattern test and the colour test are shown in Figure 3-7. Thresholds were obtained for the two dimensions of the pattern test and the colour test with similar target areas: P2 and C2. The isochromatic region for

d-2 was similar to that for d-1, although the separation between the two deutan lines was narrower, indicating a greater sensitivity in the yellow-blue direction for d-2. There was little difference in the results acquired for stimuli P2 and C2; in fact d-2 exhibited less difference in thresholds along the yellow-blue direction for the two stimulus configurations, than the normal trichromats tested.

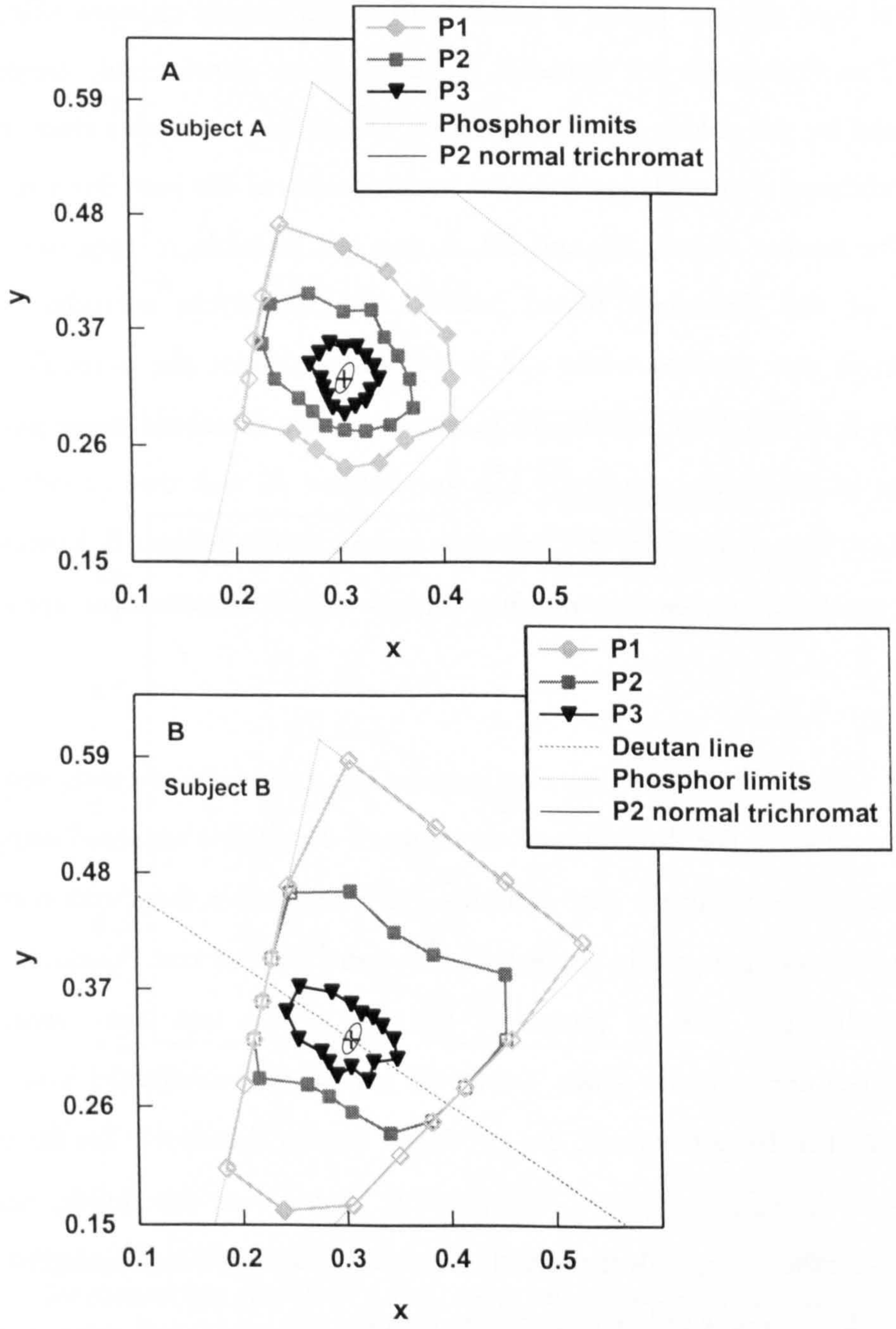

Figure 3-8 (A)-(B). Chromatic thresholds in subjects with acquired colour vision deficiency for the three pattern test stimuli P1-P3, plotted in (x, y)-chromaticity space. Results for Subject A, a patient with optic neuropathy of unknown aetiology (A). Results for Subject B, a patient with toxic optic neuropathy (B). Closed symbols indicate measured thresholds, open symbols indicate an arbitrary maximum value (see text). In (B), the dotted line shows the deuteranopic colour confusion line that passes through the background chromaticity.

3.3.3 Patients with acquired colour vision deficiency

The results of Subjects A and B for the three stimulus sizes of the pattern test are shown in Figure 3-8, plotted in (x, y)-chromaticity space. Subject A's Snellen visual acuity was 6/18 in each eye, and although she could not discriminate coloured vertical bars she still found it possible to detect colour changes using the pattern test. The thresholds for Subjects A and B were considerably larger than those obtained by the colour normal observers for all three stimulus sizes. Both subjects also exhibited a much larger increase in thresholds as the stimulus size was reduced. For the smaller stimuli P1 and P2, it was not possible to measure thresholds in many of the directions tested because the maximum reproducible chromatic difference was reached while still below threshold for the particular subject. For Subject B, it was only possible to measure a single threshold using pattern P1. The pattern of chromatic sensitivity loss for Subject A, was that of diffuse loss in all directions tested. The loss of chromatic sensitivity for Subject B, however, appeared to be greater along an axis roughly aligned with a deuteranopic colour confusion line.

Figure 3-9 shows the results obtained by the two subjects with acquired colour vision deficiency for the comparison between thresholds obtained using colour test stimulus C2 and pattern test stimulus P2. Subject A's threshold contour for the colour test was marginally smaller than for the pattern test. Similar to her pattern test results, the loss of sensitivity for the colour test was evenly distributed throughout chromaticity space. Subject B exhibited a substantial loss of chromatic sensitivity for the pattern test, but produced smaller thresholds for the colour test in all colour directions where it was possible to measure thresholds, except for the blue/violet directions. B's thresholds for the colour test were oriented roughly along a deutan line, similar to her pattern test results.

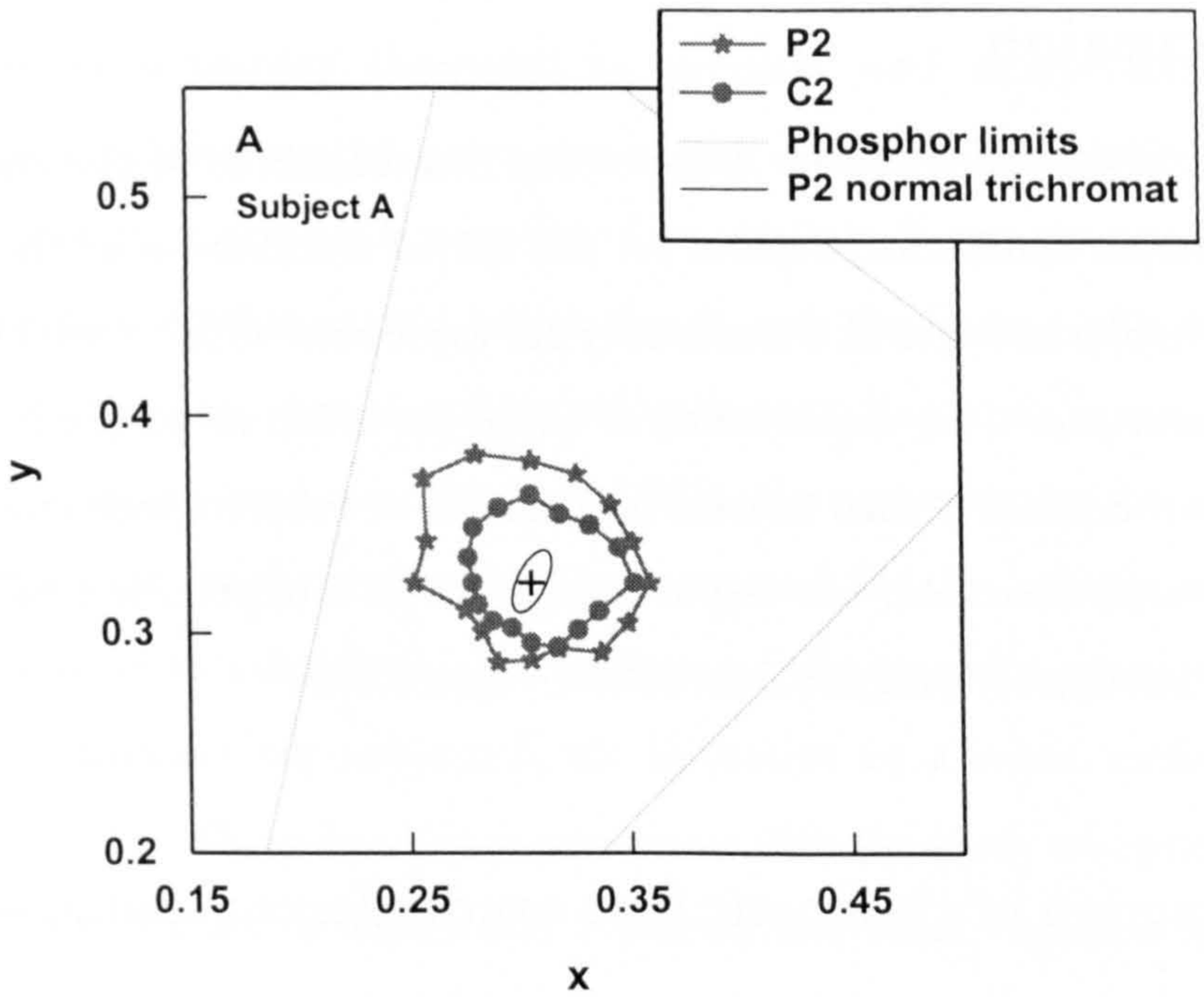

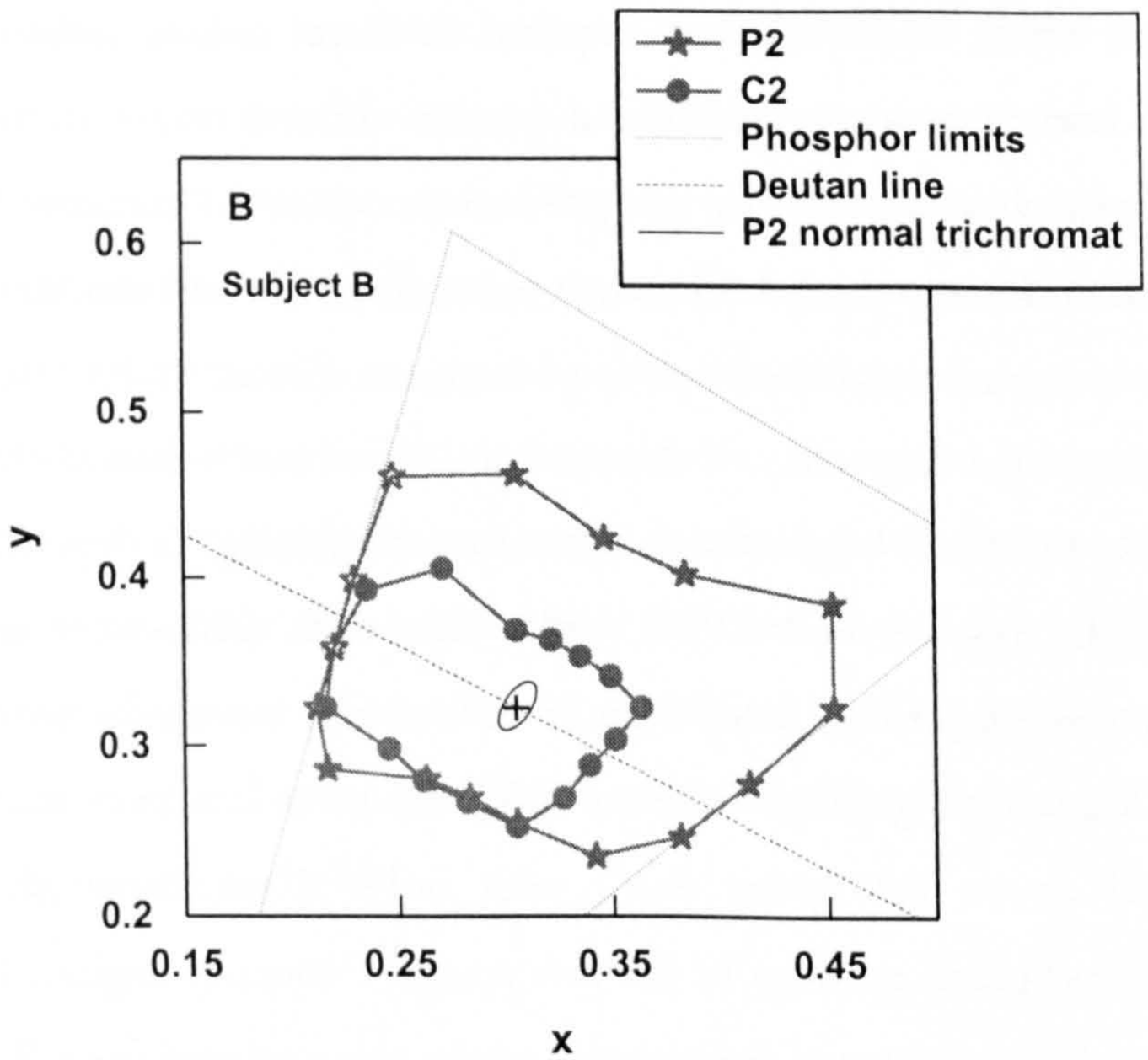

Figure 3-9 (A)-(B). Chromatic thresholds for subjects with acquired colour vision deficiency for pattern test stimulus P2 and colour test stimulus C2, plotted in (x, y)-chromaticity space. Results for subject A, a patient with optic neuropathy of unknown aetiology (A). Results for subject B, a patient with toxic optic neuropathy (B). Closed symbols indicate measured thresholds, open symbols indicate an arbitrary maximum value (see text). In (B), the dotted line shows the deuteranopic colour confusion line that passes through the background chromaticity.

3.4 Discussion

The results of this investigation indicate that measurements of chromatic sensitivity under photopic conditions, depend on the spatial distribution of the test stimulus and also whether changes in chromaticity are associated with, or are independent of stimulus structure. This dependence is more apparent in subjects with acquired colour vision deficiency than normal trichromats or subjects with congenital colour deficiency, and, therefore, has implications for the interpretation of colour vision test results in subjects with acquired colour vision losses.

3.4.1 Detection of chromatic bars over different spatial scales

For all observers, differences were seen in the results for the three sizes of pattern test stimulus, where observers were required to detect colour defined vertical bars buried in a luminance contrast defined pattern. The decrease in sensitivity with reduced pattern size was greatly exaggerated for the two subjects with acquired colour vision deficiency compared to normal trichromats and the dichromat tested. Differences in sensitivity elicited by the pattern test stimuli P1-P3, may relate to the differences in spatial frequency of the stimuli. It has been reported that wavelength discrimination for equal-brightness monochromatic gratings is dependent on spatial frequency (Hilz and Cavonius 1970), with wavelength differences increasing with increased spatial frequency. Also, a study of contrast sensitivity to red-green and blue-yellow chromatic gratings (Mullen 1985) revealed low pass sensitivity curves that declined above 0.8 cycles deg^{-1}, with reduced sensitivity for blue-yellow compared to red-green gratings in the low spatial frequency region. In the current study, the approximate spatial frequencies of the three stimuli were 2.1, 1.4 and 0.4 cycles deg^{-1}, for P1, P2 and P3, respectively. The observed decline in sensitivity over these spatial frequencies agrees with the findings of Mullen. The greater rise in detection thresholds with spatial frequency in the blue-yellow direction is also consistent with the findings of Mullen over this frequency range. It is suggested that the change in blue-yellow threshold for deuteranope d-1 may also be attributed to a loss in sensitivity with increasing spatial frequency.

The pattern test results for the subjects with acquired colour vision deficiency show marked losses in sensitivity compared to normals, and exaggerated threshold increases with increasing spatial frequency of the stimulus. The smallest and only complete chromatic threshold contour for subject B is elongated along a deuteranopic colour confusion axis, which ties in with the finding of predominantly red-green deficiencies in optic nerve pathologies, including toxic optic neuropathy, using standard colour vision tests (Verriest 1963). No comment can be made on the orientation of results for the remaining pattern stimuli for this subject, as it was not possible to measure thresholds in all directions of chromaticity space investigated. The complete contours for subject A are indicative of a more uniform loss of chromatic sensitivity. These results are consistent with the study of optic neuritis by Mullen and Plant (1986), in which they reported individual variation in chromatic sensitivity losses to red-green and blue-yellow stimuli for 1 cycle deg^{-1} gratings, but on average, equal losses for both colour directions. The large differences in chromatic thresholds for the three stimulus sizes observed for subjects A and B may also be attributed to changes in spatial frequency of the stimulus, but illustrate a much greater dependence for subjects with acquired colour vision deficiencies than for normals and subjects with congenital colour vision loss. A possible explanation for such an enhanced deterioration in chromatic sensitivity for subjects with retinal or optic nerve pathologies is that uniformly distributed cell damage may lead to a reduced ability to summate chromatic signals over receptive fields. This is analogous to the suggestion that poor summation of chromatic signals causes the degradation of colour vision observed in the peripheral retina (Noorlander et al. 1983; Abramov et al. 1991; Nagy and Doyal 1993).

3.4.2 Comparison of chromatic sensitivity inherently associated with and independent of stimulus structure

The results of the pattern test compared to detection of colour changes independent of structure (colour test), reveal differences in chromatic thresholds for the two test stimuli both for normal trichromats and subjects with acquired colour vision deficiency. No significant differences were seen between the two tests for the deuteranope tested. Previous studies have revealed large differences between

chromatic detection thresholds associated with and independent of structure in subjects with cerebral achromatopsia (Barbur et al. 1994b) and a subject with optic neuritis (Barbur et al. 1997). The current study indicates that small differences are also observed for normal trichromats, with the pattern test yielding larger thresholds than the colour test for all three subjects tested. This somewhat unexpected result differs to that reported by Barbur (1994b) for the one trichromat tested under similar conditions, where no changes in sensitivity were observed for the two stimulus paradigms. The lack of agreement between the two studies may stem from differences in the stimulus parameters used; for example, in the current study, a change in the spatial distribution of the pattern test stimulus would be sufficient to eliminate differences in thresholds obtained using the two tests (pattern test and colour test). Other investigations, however, report that the chromatic discrimination of normal trichromats is poorer for stimuli presented in the form of isochromatic plates than for uniform colour stimuli (Lakowski 1966; Watanabe et al. 1998). The authors of these two studies suggest that differences in discrimination can be attributed to task differences, i.e. extracting form information from colour, vs. discriminating changes in hue. Results of the present study support this suggestion, as although both stimuli employ luminance masking similar to the design of pseudoisochromatic plates, the task differs between the two tests - the pattern test requiring detection of form and the colour test requiring detection of hue changes.

The response of normal trichromats to changes in the area of the colour test stimulus produced little difference in sensitivity, although for the mean thresholds of the three subjects, a statistically significant difference was found along a red-green axis. These results indicate that at the fovea, an increase of the area of a uniform stimulus above 1.8° diameter had little effect on chromatic thresholds. It has been reported that hue appearance (Abramov et al. 1991), colour discrimination for temporally modulated red-green and yellow-blue chromatic gratings (Noorlander et al. 1983), and red-green colour discrimination for uniform stimuli (Nagy and Doyal 1993), all reach a plateau for sufficiently large field size, and that the critical field size, beyond which performance asymptotes, increases with eccentricity. Abramov et al (1991) obtained a measure of critical field size for invariant hue perception at different retinal locations. Their results for the periphery agree with

those of Nagy and Doyal (1993), who investigated the effect of field size on red-green chromatic discrimination at 10° and 25°. Abramov et al (1991) also included measurements at the fovea, and found minimal changes in red, green, blue and yellow hue mechanisms for foveal field sizes larger than 0.3° in diameter. These results suggest that measures of foveal colour appearance/ colour discrimination may exhibit little dependence on field size for smaller sizes than those investigated in the present study, where some change in red-green thresholds were seen for field sizes greater than 1.8°. What is apparent from the current results, is that for normal trichromats, changes in the dimensions of a spatially defined block of colour have less effect on chromatic discrimination than changes in spatial scale of a colour defined pattern.

The results for the two subjects with acquired colour vision deficiency also show larger thresholds for the pattern test compared with the colour test. This was not the general finding in the investigation of subjects with cerebral achromatopsia (Barbur et al. 1994b), where two out of three of the subjects investigated, exhibited a greater loss of sensitivity for detection solely of colour changes and the third subject showed reduced sensitivity for detection of a coloured pattern. In Barbur's (1997) study of subjects with optic neuritis, the one subject tested with the two stimulus paradigms, revealed close to normal thresholds for detection of pure colour changes, but greatly reduced sensitivity in all directions of chromaticity space when required to detect coloured vertical bars.

The comparison of results for the pattern and colour test in the present study, support previous findings of different uses of chromatic signals leading to marked differences in chromatic sensitivity for subjects with optic nerve pathology (Barbur et al. 1997). From the results of his study of subjects with cortical deficits, Barbur (1994b) suggested that the cortical representation of form based on chromatic signals and the perception of colour changes in patterns defined by luminance contrast, may have different neural substrates. The results of the current study suggest that it is also possible that mechanisms for processing chromatic signals are affected differently in optic nerve pathologies. Further manipulation of stimulus parameters in an attempt to equate thresholds obtained using the pattern test and

colour test in subjects with such pathologies, may reveal more information about the coding of chromatic signals early in the visual system.

4 Chromatic sensitivity in the mesopic range

4.1 Introduction

Human colour vision extends to relatively low light levels, but as illumination is reduced, sensitivity to differences in wavelength and chromaticity deteriorates. Wavelength discrimination is reduced across most of the spectrum with decreasing retinal illuminance, the greatest loss occurring in the midwavelength region (McCree 1960). An improvement in discrimination around 460 nm may be seen at low retinal illuminances, however, for a small field or flashes of short duration (McCree 1960; Mollon et al. 1992). Normal observers also show increased tritan errors on the FM 100-hue test performed under low illumination (Bowman and Cole 1980; Knoblauch et al. 1987; Smith et al. 1991; Knight et al. 1998). Brown's study of foveal chromatic discrimination (1951) indicated that performance is impaired below about 3 cd m^{-2}, with normal observers becoming tritanomalous at mesopic levels.

Colour vision is also degraded in the retinal periphery. This is evident from studies of wavelength and colour discrimination (Weale 1953; Moreland and Cruz 1959; Noorlander et al. 1983; Nagy and Doyal 1993), although it has been reported that peripheral discrimination may approximate foveal discrimination for sufficiently large fields (Noorlander et al. 1983; Nagy and Doyal 1993). Reported changes to colour vision in the periphery have included shifts in hue and changes in saturation of monochromatic stimuli with eccentricity (Moreland and Cruz 1959; Stabell and Stabell 1976a; Stabell and Stabell 1996; Buck et al. 1998). These changes observed in the periphery have been attributed either to changes in the cone mechanisms, desaturation effects of rod signals, or rod-cone interactions; arguments that could equally be applied to the observed degradation of performance with reduction in retinal illuminance. It has been shown that large field colour matches have a rod contribution, so that four matching primaries are required to characterise colour

matches in order to satisfy the colorimetric laws of additivity (Trezona 1970) (Shapiro et al. 1994). Under conditions that differentially minimise or maximise the stimulation of rods, the Stabells provided evidence for both a cone-based and a rod-based effect on the deterioration of wavelength discrimination (Stabell and Stabell 1977) and the change of hue and saturation of monochromatic lights in the periphery (Stabell and Stabell 1996). Other studies employing differential stimulation of rods suggest that red-green (Nagy and Doyal 1993) and blue-yellow (Knight et al. 1998; Knight et al. 2001) chromatic discrimination is impaired when rods are stimulated. The Stabells (1996) have suggested that the desaturating effects of rods may be a consequence of rod input to spectrally opponent pathways, rather than the action of independent rod and cone pathways. There is evidence from measurements of successive colour contrast that rod signals have access to chromatic pathways when below cone threshold (Stabell and Stabell 1994; Buck 1997), and it has been reported that rods and L-cones can interact to produce colour sensations (McCann and Benton 1969; McKee et al. 1977). Little is known, however, of the possible neural mechanisms for such rod-cone interactions. Although these findings suggest that rod signals affect measures of colour vision in the periphery and may similarly affect colour vision at reduced levels of illumination either through desaturation effects or rod-cone interactions, these effects are stimulus dependent, and it is by no means clear how the influence of these factors changes with light adaptation level and other stimulus conditions.

The objectives of this study were twofold. The first aim was to characterise chromatic discrimination with reduction in light level, for one location in chromaticity space, at two retinal locations: the fovea and the near periphery. The experimental procedure consisted of measuring thresholds for the detection of chromaticity changes against a neutral background, thus constituting a measure of chromatic sensitivity. This was achieved using a psychophysical staircase, unlike many previous measures of chromatic discrimination that have involved either finding by direct adjustment the just noticeable difference between two coloured fields, or determining an estimate of discrimination from the standard deviation of a number of colour matches made between a fixed and variable field. Previous studies of chromatic discrimination have also required the setting of isoluminance, whereas

the experimental procedure used in this study employed dynamic luminance contrast to mask detection of both photopic and scotopic luminance contrast signals, which has the advantage of eliminating the need to set isoluminance. The second aim was to investigate the contribution of rod signals to changes in chromatic sensitivity with reduction in illuminance. In particular, to determine whether the preferential loss of blue-yellow sensitivity at low light levels reported in the literature, can be attributed to rod involvement in chromatic processing.

4.2 Subjects and Methods

The experimental technique used to measure chromatic thresholds under mesopic conditions (mesopic colour vision test) is described in section 2.3.2. The use of local dynamic luminance contrast noise has been shown to mask detection of luminance contrast signals in normal trichromats (Barbur et al. 1992). Barbur et al. (1998b) have also shown that in addition to local LC noise, random changes of mean stimulus luminance (light flux noise) can be used to mask the contribution rod signals make to the pupil response. To ensure adequate masking of both photopic and scotopic luminance contrast signals at the mesopic luminance levels used in the current study, the effect of luminance contrast and light flux noise levels on achromatic and chromatic thresholds was assessed. Chromatic sensitivity measurements were then performed at a number of mesopic light levels, with the stimulus centred either at the fovea, 3.5° or 7° in the periphery. The influence of rod signals on chromatic sensitivity was investigated by performing measurements following light adaptation on the cone plateau of the dark adaptation curve, and after complete dark adaptation to the luminance of the stimulus.

4.2.1 Subjects

Four observers took part in the experiments. All were normal trichromats according to the Ishihara plates and the colour vision test described in section 2.3.1. The age range was 22-49, subjects HA and HW were female, JB and SM were male. All observations were made monocularly with the right eye and with natural pupils.

4.2.2 Assessment of the masking technique under mesopic conditions

Achromatic and colour thresholds were measured by subject HW using the mesopic colour vision test with no random luminance masking, and with luminance contrast (LC) and light flux (LF) noise set at ±20% of the mean luminance of the stimulus. For the achromatic measurements, detection thresholds were obtained for both increments and decrements in target luminance. Colour measurements consisted of determining the threshold to detect a colour change for six directions in chromaticity space. These directions corresponded to the protan, deutan and tritan colour confusion lines passing through the respective dichromatic copunctual points (Smith and Pokorny 1975) and the background chromaticity. For each dichromatic confusion line, thresholds in the two directions away from the background chromaticity have been labelled "1" and "2", for example "protan 1" and "protan 2". Measurements were performed at a low photopic/high mesopic background luminance and a mid-mesopic background luminance, with the stimulus centred either at the fovea, 3.5°, or 7° from fixation in the right hemifield. The masking-present and masking-absent conditions were compared by taking the ratio of the thresholds obtained for each condition. Chromatic thresholds were also measured at the mid-mesopic level, with the stimulus positioned at an eccentricity of 3.5°. In this case, the effect of increasing levels of luminance contrast and light flux noise was investigated, for nine directions in chromaticity space. The ranges of LC and LF noise were set at 0, ±20%, ±40 and ±60% of the mean stimulus luminance.

4.2.3 Investigation of chromatic sensitivity in the mesopic range

Two observers performed measurements for a number of light levels (HA: 6, HW: 7) in the range 45-0.0041 cd m^{-2} following appropriate dark adaptation to the background field (see section 2.4.1 for a description of the calculation of dark adaptation times). Table 4-1 shows the stimulus background luminances used, along with the corresponding mean filter densities for background luminances below 10 cd m^{-2}. Neutral density filters were employed to reduce stimulus luminance while

maintaining the CRT display in the mid to low end of its operating range of luminance (see section 2.1.1). The stimulus was centred either at the fovea, 3.5°, or 7° from fixation in the right hemifield, on the horizontal meridian. Eccentricities of 3.5° and 7° were chosen because in the near periphery it was relatively easy to carry out the measurements, but beyond 7° the test became increasingly difficult. These eccentricities also correspond to retinal locations where there is a reasonable rod density. The achromatic background was chosen to have a chromaticity of $x = 0.305, y = 0.323$ $(u' = 0.195, v' = 0.464)$, the chromaticity of MacAdam white (MacAdam 1942). The level of random luminance modulation was set at ±20% of the mean luminance of the stimulus for testing at the higher light levels, and increased up to ±40% for the lower light levels and more peripheral measurements to compensate for increased luminance contrast thresholds. A luminance pedestal of constant contrast was used over the range of light levels investigated.

Nominal filter density	Mean optical density at 45° incidence	Background luminance (cd m^{-2})	Dark adaptation time (min)
NONE	0	45	5
NONE	0	20	5
NONE	0	10	5
1.0	1.17	0.68	10
2.0	2.25	0.056	16
2.5	2.87	0.013	22
3.0	3.39	0.0041	30

Table 4-1. Filter densities, background luminances and dark adaptation times for photopic and mesopic measurements of chromatic sensitivity.

To fully examine the loss of blue-yellow sensitivity in the mid-mesopic range, thresholds were measured with a change in background chromaticity from the neutral MacAdam white to a chromaticity of $x = 0.26$, $y = 0.23$ $(u' = 0.198, v' = 0.395)$, a bluish grey. This change allowed thresholds to be measured in the yellow direction of colour space at 0.056 cd m^{-2}, which was not possible with the original background chromaticity due to the limits of the display's colour gamut.

Results were obtained as polar coordinates in CIE 1931 (x, y)-chromaticity space, which when plotted formed MacAdam chromatic discrimination ellipses (MacAdam 1942). Before plotting, however, the results were transformed into coordinates in the CIE 1976 (u′, v′)-chromaticity space; one of the colour spaces introduced by the CIE to correct for the nonuniformity in the CIE 1931 chromaticity diagram. Elliptical fits were made to the (u′, v′)-coordinates using a direct least squares algorithm (Fitzgibbon et al. 1999). Ellipses were fitted at all bar the lowest stimulus background luminance. The effects of changes in stimulus luminance on four aspects of the fitted ellipses plotted in (u′, v′)-space were investigated: sensitivity, orientation, ellipticity and asymmetry. Orientation was taken as the alignment of the major axis of each ellipse with the abscissa; the angle measured counter-clockwise from the abscissa in degrees. Ellipticity gave a measure of ellipse elongation. At the lower light levels, using the original background chromaticity, it was not possible to measure thresholds in the yellow direction of colour space due to the limits of the colour gamut of the display. Ellipticity was, therefore, defined as the ratio of the semi-major axis in the blue direction to half the minor axis length, i.e. only half of the fitted ellipse was considered. Asymmetry along either the major or minor axis was taken as the ratio of the longer to the shorter semi-axis. Asymmetry was only computed in cases where it was possible to measure thresholds in all directions investigated.

4.2.4 Investigation of possible rod involvement in chromatic processing

Three observers: JB, SM and HW performed measurements at a single light level, both after dark adaptation to the level of the stimulus, and on the cone plateau of the dark adaptation curve following a white-light bleach. The stimulus was centred either at 3.5° or 7° to the right of fixation. Measurements were obtained for a test target of diameter 2° angular subtense at 3.5° and for a test target of 4° diameter at 7°. The background chromaticity was chosen as x = 0.26, y = 0.23 (u′ = 0.198, v′ = 0.395), to ensure that it was possible to measure thresholds in the yellow direction of colour space. The test target luminance was 0.09 cd m^{-2} with a corresponding background luminance of 0.45 cd m^{-2} (the test target was defined by a luminance

contrast pedestal). This was the lowest stimulus luminance that could be employed for testing during the cone plateau, and was roughly 0.5 log units above cone threshold.

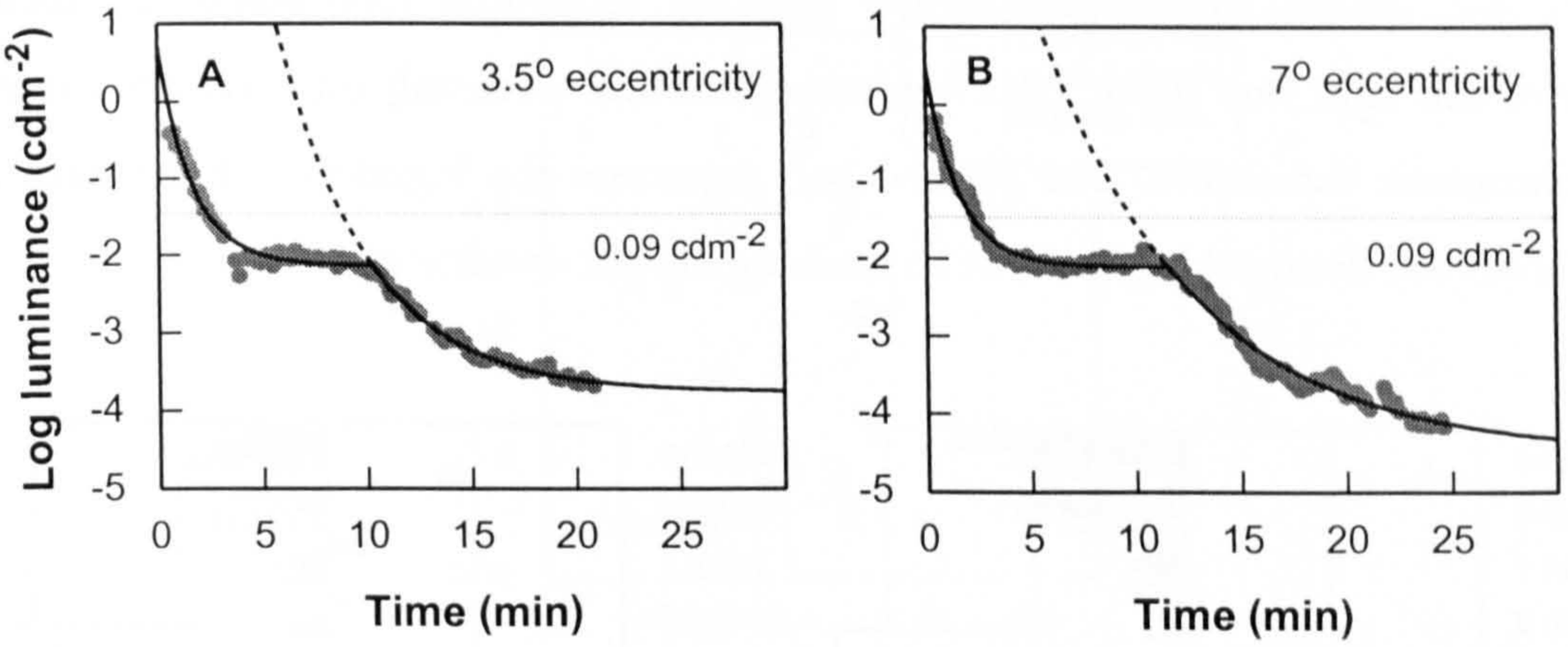

Figure 4-1(A)-(B). Examples of dark adaptation curves measured for subject HW. Filled circles represent measured thresholds, solid lines show curves fitted separately to the cone portion and rod portion of the data, and dotted lines show the fitted rod sensitivity curve extended above the cone plateau. The dashed line at 0.09 cd m^{-2} indicates the luminance of the stimulus used to measure chromatic thresholds. Curve obtained with a 2° stimulus positioned at 3.5° eccentricity (A). Curve obtained with a 4° stimulus positioned at 7° eccentricity (B).

The apparatus used to provide the bleaching stimulus was described in section 2.2. Subjects were light adapted to a 5 log td field for 2 min. Preliminary dark adaptation measurements for subject HW, obtained using the method described in section 2.4, were used to establish the onset and duration of the cone plateau after bleaching. Dark adaptation curves were measured for a 2° ring target presented at 3.5° eccentricity, and for a 4° ring target presented at 7° eccentricity. The onset and duration of the cone plateau for each eccentricity of presentation were estimated from two measured curves at each retinal location, examples of which are shown in Figure 4-1. The timings used for the chromatic sensitivity measurements at 3.5° and at 7°, were chosen to fall within the estimates of the cone plateau location for the two dark adaptation curves obtained at each eccentricity. At 3.5° measurements were started 4 min after the end of the bleach and continued for a further 4.5 min. At 7° measurements were started 5 min after the end of the bleach and continued for a further 3.75 mins.

4.3 Results

4.3.1 Effectiveness of the masking technique

Figure 4-2, shows the effects of the masking technique (combined luminance contrast and light flux noise, plus luminance contrast pedestal) on both achromatic and chromatic thresholds. The plotted bars represent the logarithm of the ratio of thresholds for the masking-present to masking-absent condition.

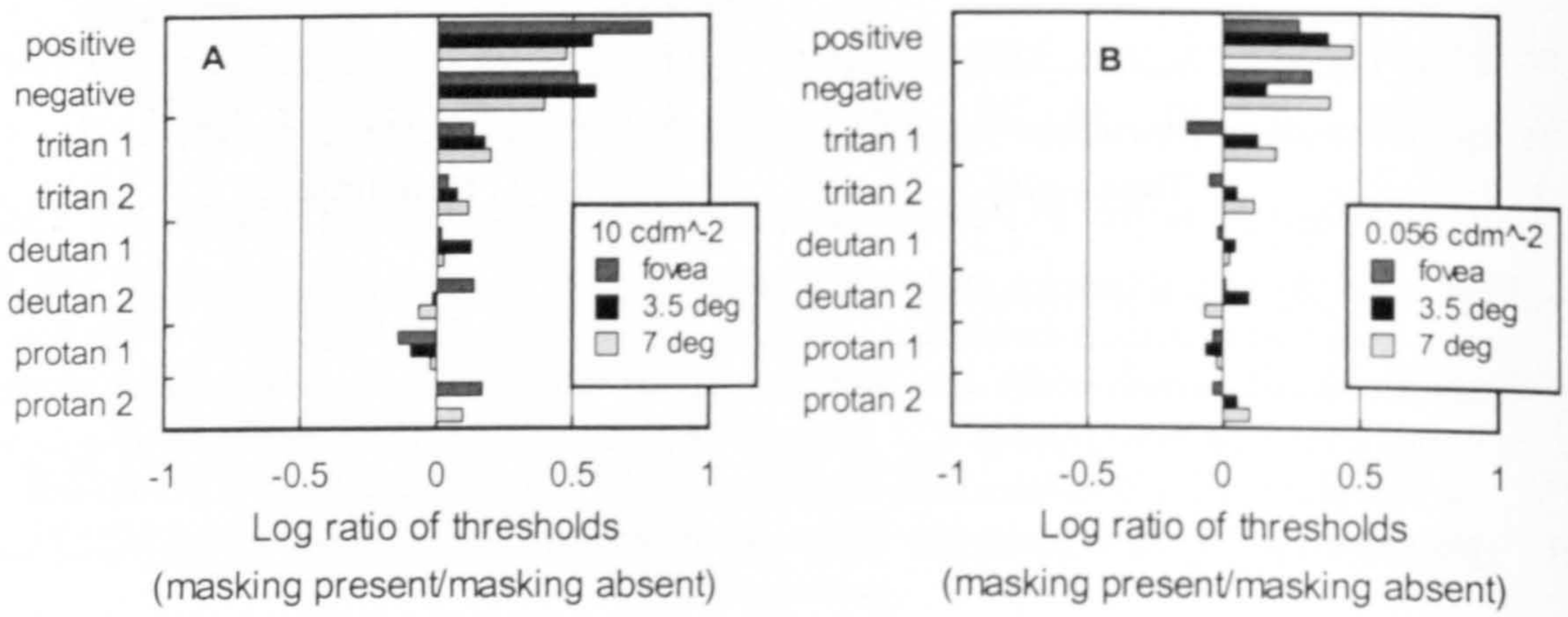

Figure 4-2 (A)-(B). Comparison of the effect of masking to no masking on achromatic and chromatic thresholds obtained at the fovea, 3.5° and 7° eccentricity. Achromatic thresholds were measured for both positive and negative contrast stimuli. Chromatic thresholds were measured along two directions of each of the three dichromatic colour confusion axes, labelled tritan 1, tritan 2 etc. Measurements at 10 cd m^{-2} (A). Measurements at 0.056 cd m^{-2} (B).

The results show that achromatic thresholds were raised in the masking-present condition compared to the masking-absent condition, whereas chromatic thresholds (measured along the dichromatic colour confusion axes) were affected little by the presence of luminance noise. At 0.056 cd m^{-2}, achromatic thresholds were raised less than at 10 cd m^{-2} for a noise level of 20%, hence, noise levels of greater amplitude were employed when testing at the lowest background luminances.

Figure 4-3 illustrates the effect of increasing the amplitude of masking noise on chromatic thresholds in several directions of chromaticity space. The stimulus luminance was 0.056 cd m^{-2}, and the level of masking increased from 0 to 60% of

the mean stimulus luminance. These results show that the magnitude of luminance contrast noise had little influence on chromatic thresholds.

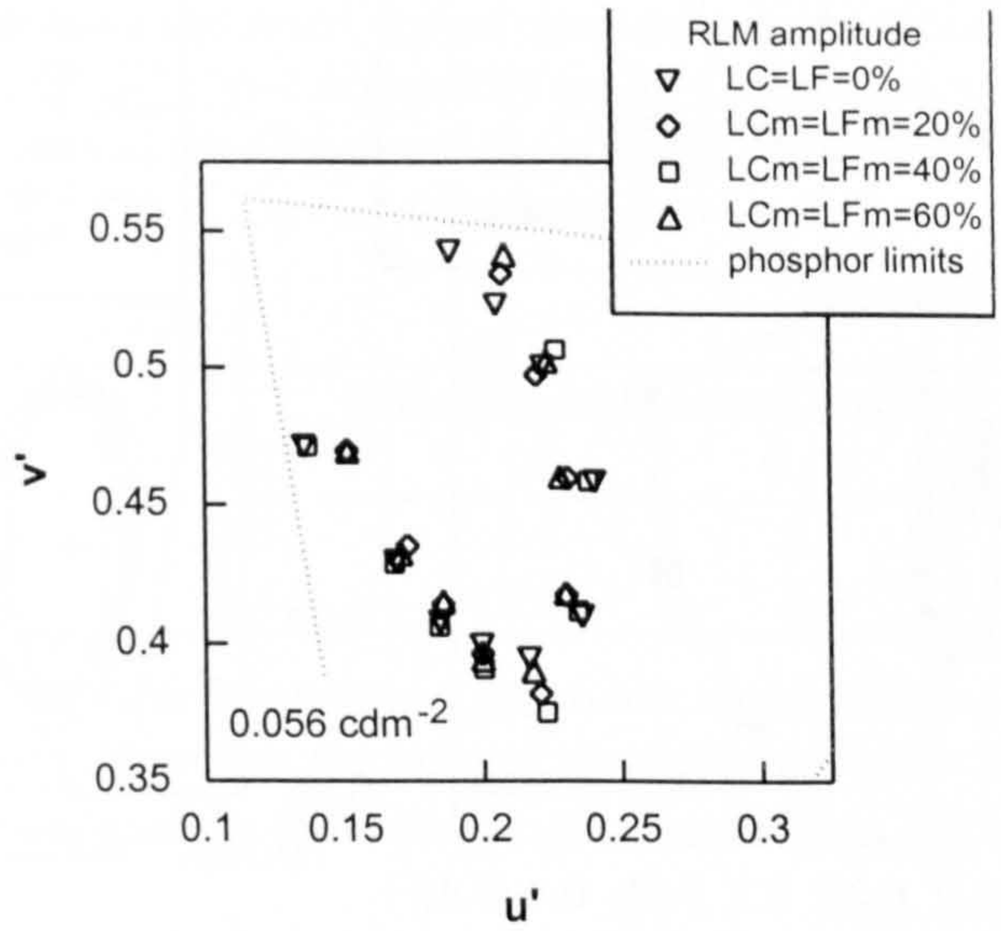

Figure 4-3. Chromatic thresholds measured at 0.056 cd m^{-2} for increasing levels of luminance contrast (LC) and light flux (LF) masking.

4.3.2 Foveal measurements

Chromatic sensitivity measurements for subjects HA and HW obtained with the stimulus centred at the fovea, are shown in Figure 4-4. The results are plotted in the CIE 1976 (u′, v′)-chromaticity space. Threshold contours for the two observers were qualitatively similar. There was little change in sensitivity for test luminances of 45, 20 and 10 cd m^{-2}, but below this level thresholds increased markedly as test luminance was reduced.

Despite the great reduction in sensitivity at the lower mesopic levels, subjects were aware of colour changes and could correctly label the principal hues. The threshold increase for luminances of 0.056 cd m^{-2} and below, was such that it was not possible to measure the threshold in all angles tested. There is a limit imposed by the phosphors of the monitor on the maximum saturation that can be produced at each angle. For some angles the maximum saturation was reached while below the observer's threshold. At the lowest test luminance (0.0041 cd m^{-2}) it was only possible to obtain thresholds at three of the test angles.

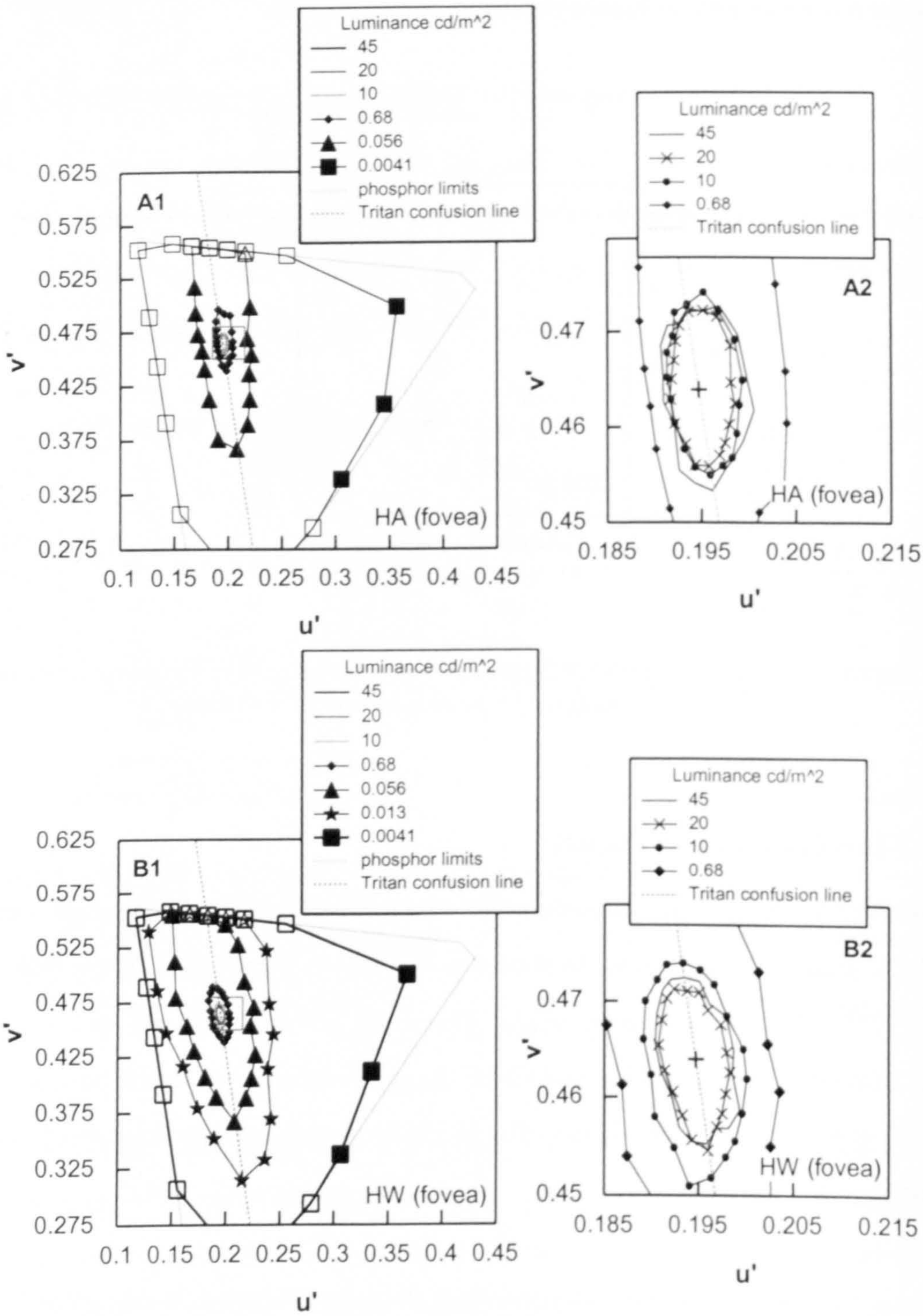

Figure 4-4 (A)-(B). Chromatic thresholds measured with the stimulus centred at the fovea, obtained by subject HA over six light levels (A), and by subject HW over seven light levels (B). A1 and B1 show measurements for all test luminances used, A2 and B2 show an enlarged section (the region indicated by the square on A1 and B1), in which the results for the highest three test luminances can be seen in greater detail. The closed symbols indicate chromatic thresholds. The open symbols indicate that the maximum saturation that could be produced by the monitor was reached while still below threshold for the observer, and an arbitrary maximum value has been assigned.

	Stimulus luminance (cd m^{-2})					
	45	20	10	0.68	0.056	0.013
HA	62	62	64	64	65	
HW	67	67	66	69	71	69

Table 4-2. Orientations of the fitted, foveal chromatic discrimination ellipses for subjects HA and HW, measured in (x, y)-chromaticity space. Orientation was defined as the angle between the major axis of the ellipse and the abscissa, measured in a counter-clockwise direction.

	Stimulus luminance (cd m^{-2})					
	45	20	10	0.68	0.056	0.013
HA	2.0	2.5	2.5	3.7	4.2	
HW	2.2	2.4	2.2	2.9	2.8	2.8

Table 4-3. Ellipticities of the fitted, foveal chromatic discrimination ellipses of subjects HA and HW. Ellipticity was defined as the ratio of the major semi-axis length in the blue colour direction, to the average minor semi-axis length, measured in (u′, v′)-chromaticity space.

		Stimulus luminance (cd m^{-2})					
		45	20	10	0.68	0.056	0.013
Major axis	HA	1.1	1.1	1.2	1.6		
	HW	1.0	1.1	1.2	1.1		
Minor axis	HA	1.3	1.2	1.3	1.3	1.2	
	HW	1.0	1.0	1.0	1.2	1.2	1.1

Table 4-4. Major and minor axis asymmetries for the fitted, foveal chromatic discrimination ellipses of subjects HA and HW. Axis asymmetry was defined as the ratio of the longer to shorter semi-axis length, measured in (u′, v′)-chromaticity space.

The sets of ellipses for both subjects were oriented approximately along the tritan colour confusion line that passes through the background chromaticity (tritan axis), which is also the axis of S-cone modulation (S-cone axis). In (x, y)-chromaticity space this tritan axis makes an angle of 68° with the abscissa. The major axes of the ellipses for subject HA were inclined a few degrees below this angle, and the orientation of HW's ellipses were close to 68°, see Table 4-2. There was no systematic variation of orientation with light level. The values of ellipticity for the fitted ellipses are given in Table 4-3. For subject HA, ellipticity generally increased with reduction in light level, leading to a doubling of ellipticity over the range 45-0.0056 cd m^{-2}. Subject HW showed no systematic increase in ellipticity, although values tended to be greater for measurements obtained at the lower stimulus luminances compared those made at the higher luminances. The values of asymmetry for the fitted ellipses are shown in Table 4-4. The ellipses obtained at 10,

20 and 45 cd m^{-2} were roughly symmetric about the background chromaticity for both subjects. The ellipse obtained at 0.68 cd m^{-2} for subject HW was also approximately symmetric, but the ellipse for subject HA showed a distinct asymmetry along the major axis. For light levels 0.056 cd m^{-2} and 0.013 cd m^{-2}, although thresholds were not obtainable at all angles, the raw data points and fitted data suggest that the complete ellipses would also exhibit asymmetry along the major axis.

4.3.3 Thresholds obtained in the near periphery

Measurements obtained by both HA and HW with the stimulus centred at 3.5° eccentricity are shown in Figure 4-5. Thresholds were generally larger for this stimulus location than for the foveal measurements. Like the measurements obtained at the fovea, thresholds at luminances of 45, 20 and 10 cd m^{-2} were similar, and below 10 cd m^{-2} sensitivity was greatly reduced with the fall in stimulus luminance. Ellipse orientation was again approximately independent of stimulus luminance, but there was a slight change in the orientation of the two sets of ellipses compared to the foveal data sets. The ellipses remained approximately aligned with the tritan axis, but with a tilt in the direction of the deuteranopic colour confusion line passing through the background chromaticity (deutan axis). This lead to increases in the angles of orientation compared to the foveal data, see Table 4-5.

The results obtained at 3.5° show no systematic increase in ellipticity or asymmetry with stimulus luminance for either subject (see Table 4-6 and Table 4-7). Again, it was not possible to measure asymmetries along the major axis below 0.68 cd m^{-2}, but the plotted data for the lower light levels suggested that asymmetries may be present.

	Stimulus luminance (cd m^{-2})					
	45	20	10	0.68	0.056	0.013
HA	66	67	65	68	69	
HW	71	74	71	77	76	73

Table 4-5. Orientations of the fitted chromatic discrimination ellipses for subjects HA and HW, obtained at 3.5° eccentricity. Orientation was defined as the angle between the major axis of the ellipse and the abscissa, measured in a counter-clockwise direction in (x, y)-chromaticity space.

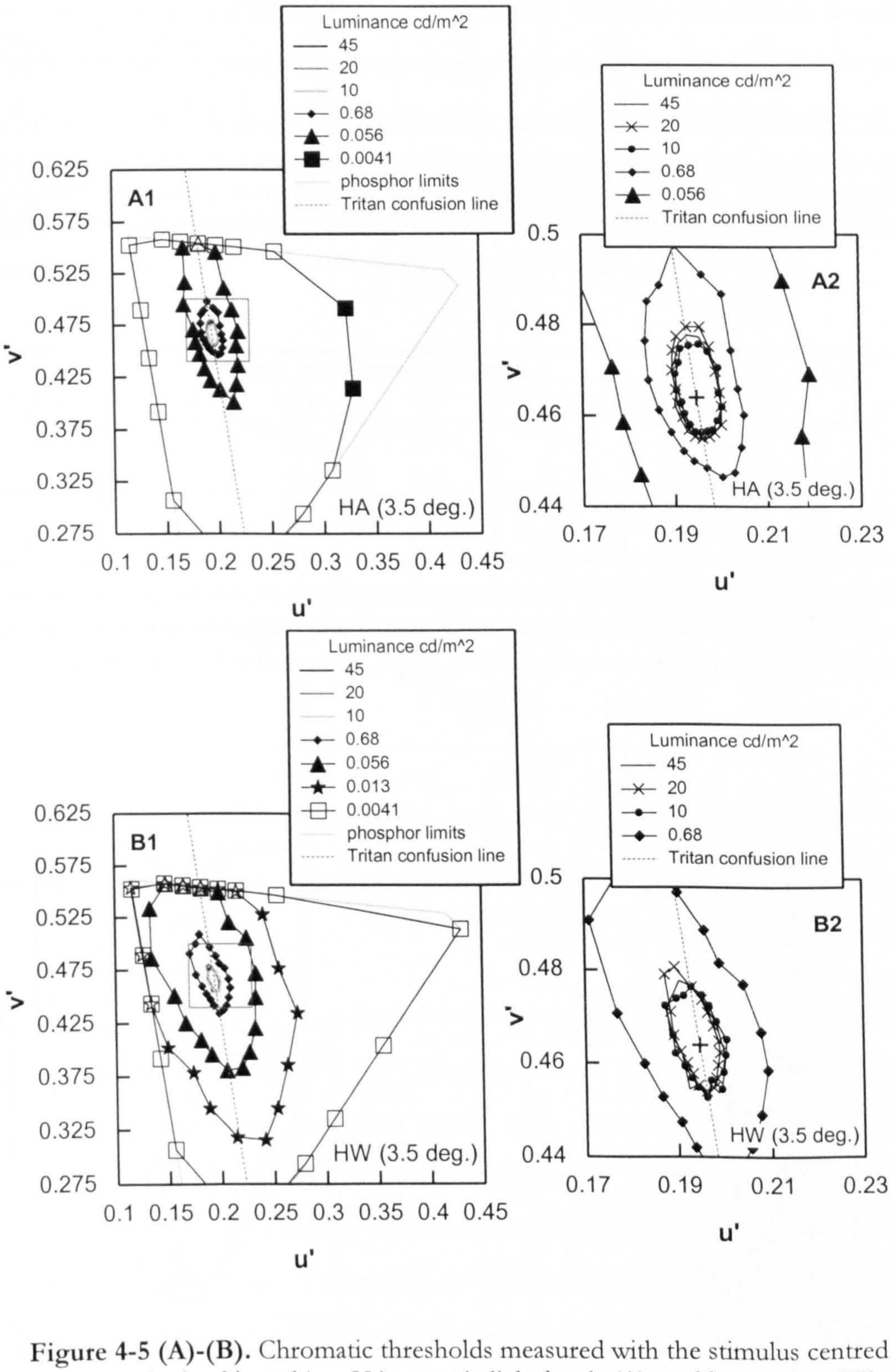

Figure 4-5 (A)-(B). Chromatic thresholds measured with the stimulus centred at 3.5° eccentricity, obtained by subject HA over six light levels (A), and by subject HW over seven light levels (B). A1 and B1 show measurements for all test luminances used, A2 and B2 show an enlarged section (the region indicated by the square on A1 and B1), in which the results for the highest three test luminances can be seen in greater detail. The closed symbols indicate chromatic thresholds. The open symbols indicate that the maximum saturation that could be produced by the monitor was reached while still below threshold for the observer, and an arbitrary maximum value has been assigned.

	Stimulus luminance (cd m^{-2})					
	45	20	10	0.68	0.056	0.013
HA	2.3	2.6	2.1	2.6	2.9	
HW	2.4	3.2	2.1	2.8	1.9	2.3

Table 4-6. Ellipticities of the fitted chromatic discrimination ellipses of subjects HA and HW, obtained at 3.5° eccentricity. Ellipticity was defined as the ratio of the major semi-axis length in the blue colour direction, to the average minor semi-axis length, measured in (u′,v′)-chromaticity space.

		Stimulus luminance (cd m^{-2})					
		45	20	10	0.68	0.056	0.013
Major axis	HA	1.4	1.7	1.6	1.8		
	HW	1.3	1.7	1.2	1.6		
Minor axis	HA	1.1	1.2	1.1	1.2	1.3	
	HW	1.2	1.2	1.0	1.1	1.2	1.1

Table 4-7. Major and minor axis asymmetries for the fitted chromatic discrimination ellipses of subjects HA and HW, obtained at 3.5° eccentricity. Axis asymmetry was defined as the ratio of the longer to shorter semi-axis length, measured in (u′, v′)-chromaticity space.

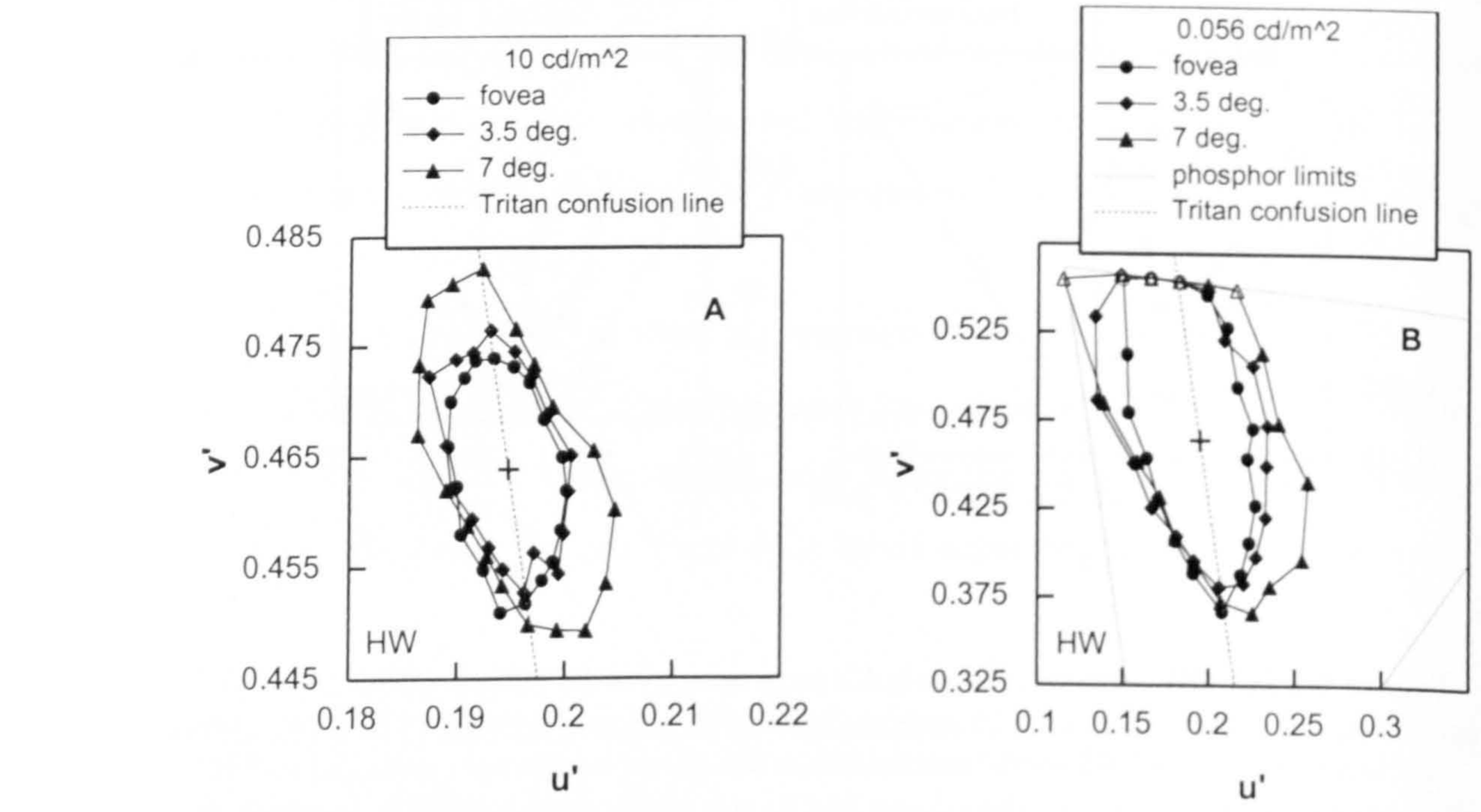

Figure 4-6 (A)-(B). Comparison of chromatic thresholds obtained at the fovea, 3.5° and 7° eccentricity for subject HW. Measurements acquired at 10 cd m^{-2} (A), and at 0.056 cd m^{-2} (B). Closed symbols indicate measured thresholds and open symbols represent an arbitrary maximum value.

Threshold measurements for subject HW with the stimulus positioned at 7° eccentricity are shown in Figure 4-7. For the two stimulus luminances tested, larger thresholds were obtained at this eccentricity than for either the foveal location or at 3.5° eccentricity. These data also showed a more pronounced change of ellipse orientation towards the deutan axis than the results at 3.5°, with the angle of orientation increasing to 77° and 78° (from 71° and 76°) for the 10 and 0.056 cd m^{-2} data, respectively.

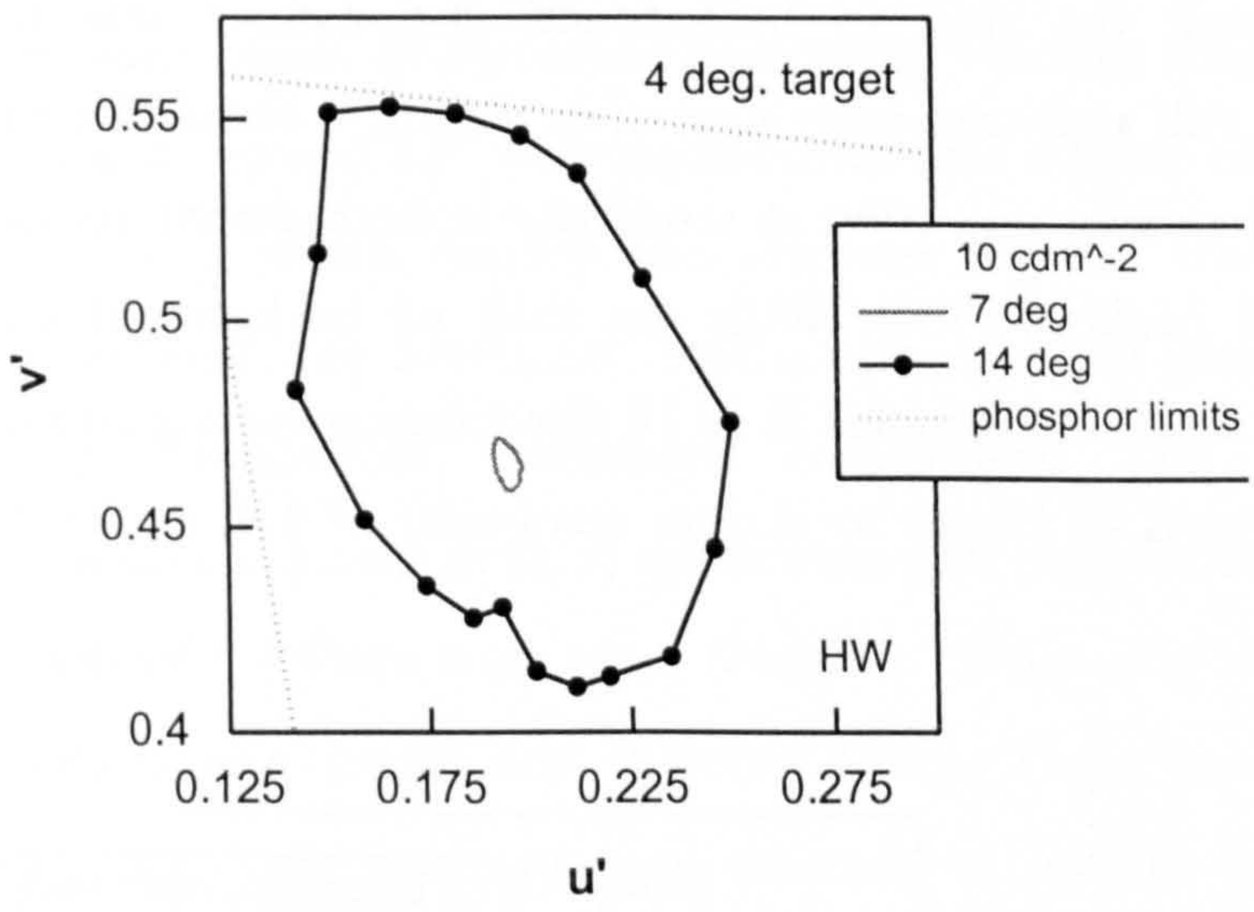

Figure 4-7. Peripheral chromatic thresholds for subject HW obtained for a 4° stimulus at a luminance of 10 cd m^{-2}.

The results of measurements performed by subject HW at 7° and 14° eccentricity are also shown in Figure 4-7, for a stimulus size of 4° at a luminance of 10 cd m^{-2}. The ellipse orientation increased again with eccentricity from 71° to 75° for eccentricities of 7° and 14°, respectively. With this larger field size, however, the angle of ellipse orientation at 7° was less that for the 2° diameter stimulus, the value being 71° compared to 77°. In fact, using the larger field size of 4° diameter, the angle of orientation at 14° eccentricity was less than the angle at 7° eccentricity for a stimulus size of 2° diameter: 75° compared to 77°.

4.3.4 Change of background chromaticity

For the lower mesopic levels, i.e., 0.056 and 0.013 cd m^{-2}, the data obtained at all three stimulus locations appeared to exhibit an asymmetry along the major axis.

This apparent asymmetry corresponds to a reduced sensitivity for S-cone decrements (i.e., towards yellow) and/or an increased sensitivity for S-cone increments (i.e., towards blue). It was difficult to evaluate these possible asymmetries due to the aforementioned limits of the CRT display. To overcome the constraints set by these limits and further investigate any asymmetries, measurements were obtained by subject HA at 0.056 cd m^{-2} and 3.5° eccentricity, with a change in background chromaticity from u′ = 0.195, v′ = 0.464 to u′ = 0.198, v′ = 0.395 (see Figure 4-8). At this chromaticity, the background appeared a bluish-grey. Although the shift in background chromaticity was not large and the background still appeared fairly neutral in colour, it should be noted that this may have caused a slight reduction in sensitivity in both directions along the tritan axis (Polden and Mollon 1980). With the shift of background chromaticity it was possible to measure thresholds in all 18 directions; revealing an asymmetry along the major axis (ratio of longer to shorter semi-axis) of 1.8, in the direction described above.

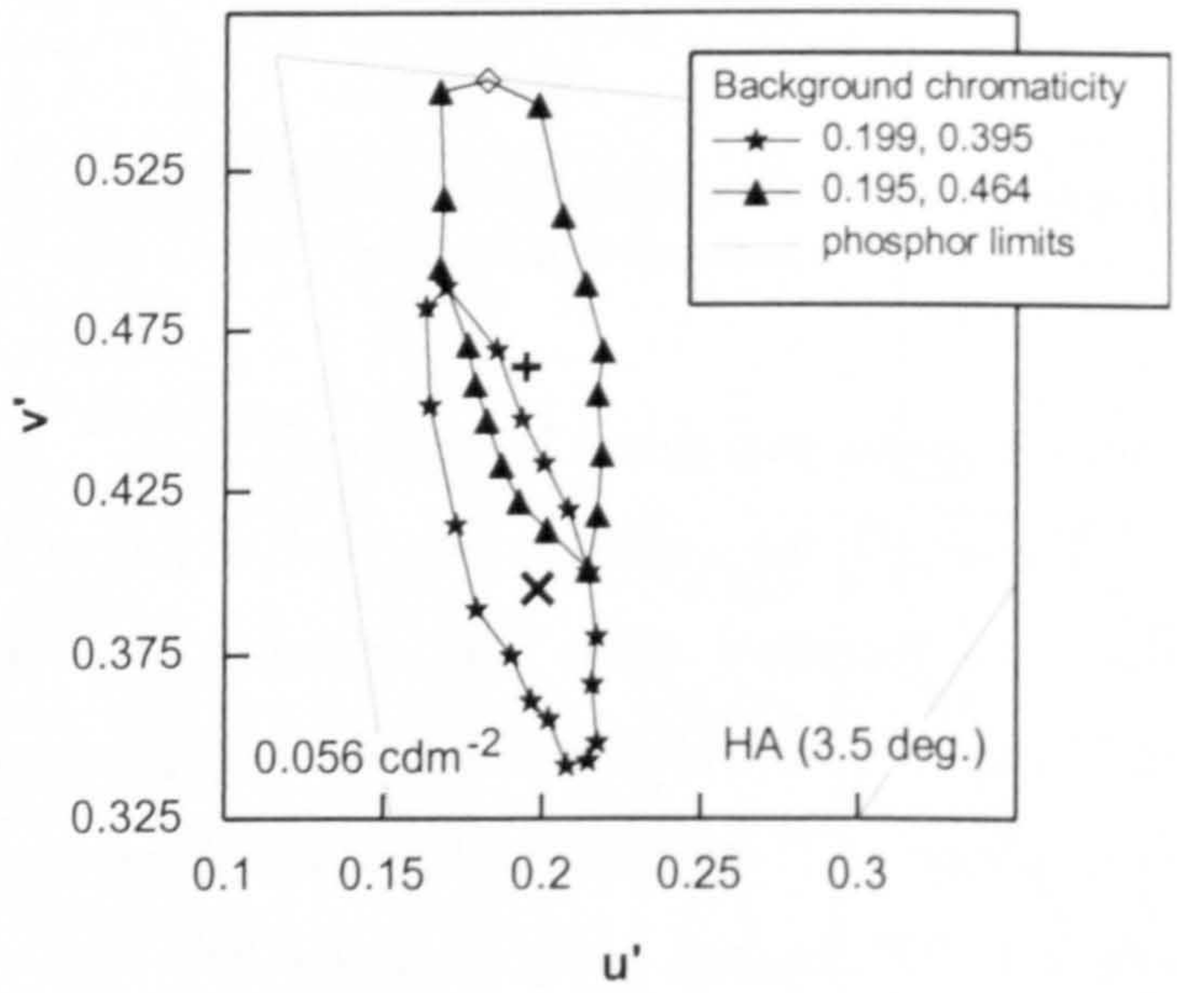

Figure 4-8. Chromatic thresholds for subject HA measured at 3.5° eccentricity at a luminance of 0.056 cd m^{-2}, for two backgrounds of different chromaticity. The first background chromaticity corresponds approximately to daylight at a colour temperature of 6500K. The second is bluish grey in appearance and was selected to allow greater changes of chromaticity for all colour directions tested. Closed symbols indicate measured thresholds, open symbols represent an arbitrary maximum value.

4.3.5 Ellipses plotted in DKL space

The CIE 1976 (u′, v′)-chromaticity space was introduced to correct for the nonuniformity of the CIE 1931 (x, y)-chromaticity space. The (u′, v′)-space is a better approximation of a uniform space, but even at moderate levels of light adaptation the thresholds measured in this study were not independent of the direction tested. This complicates inferences about the ellipticity of the threshold contours and asymmetry of thresholds along a particular axis, e.g., the S-cone axis. A better way to investigate possible asymmetries is to plot the data in a colour space that is related to the early stages of chromatic processing. For this reason the fitted results obtained at the fovea and 3.5° were transformed into a plane of DKL space (Derrington et al. 1984), which models the response of the three proposed postreceptoral mechanisms: the luminance mechanism, the red-green chromatic mechanism and the yellow-blue chromatic mechanism. The chromaticity coordinates of the threshold points in (x, y)-space were first transformed to express the relative activation of the three cone types (Nakano 1996) using the Smith and Pokorny cone fundamentals (Smith and Pokorny 1975). These cone excitations were then transformed to cone contrasts using the cone excitations for the neutral background, and recoded into representations of the three postreceptoral mechanisms according to the DKL space model (Brainard 1996). The scaling of each colour opponent mechanism (L-M and S-Lum) was chosen to produce a unit response when excited in isolation by a stimulus of unit pooled cone contrast (Brainard 1996).

The ellipses plotted in DKL space were examined for changes in symmetry of the thresholds along the colour opponent mechanism axes, with changes in retinal illuminance. Asymmetry was calculated as the ratio of the negative value to the positive value along each mechanism axis. Figure 4-9 and Figure 4-10 show the results obtained at the fovea and 3.5° eccentricity transformed into planes of DKL space. The fitted data have been plotted, with the luminance planes superimposed to compare the symmetry of L-M and S-Lum mechanisms at each light level. This transformation to DKL space was performed for the data acquired at background luminances of 10-0.68 cd m^{-2} only, because below this level the measured data was incomplete and the elliptical fits less reliable.

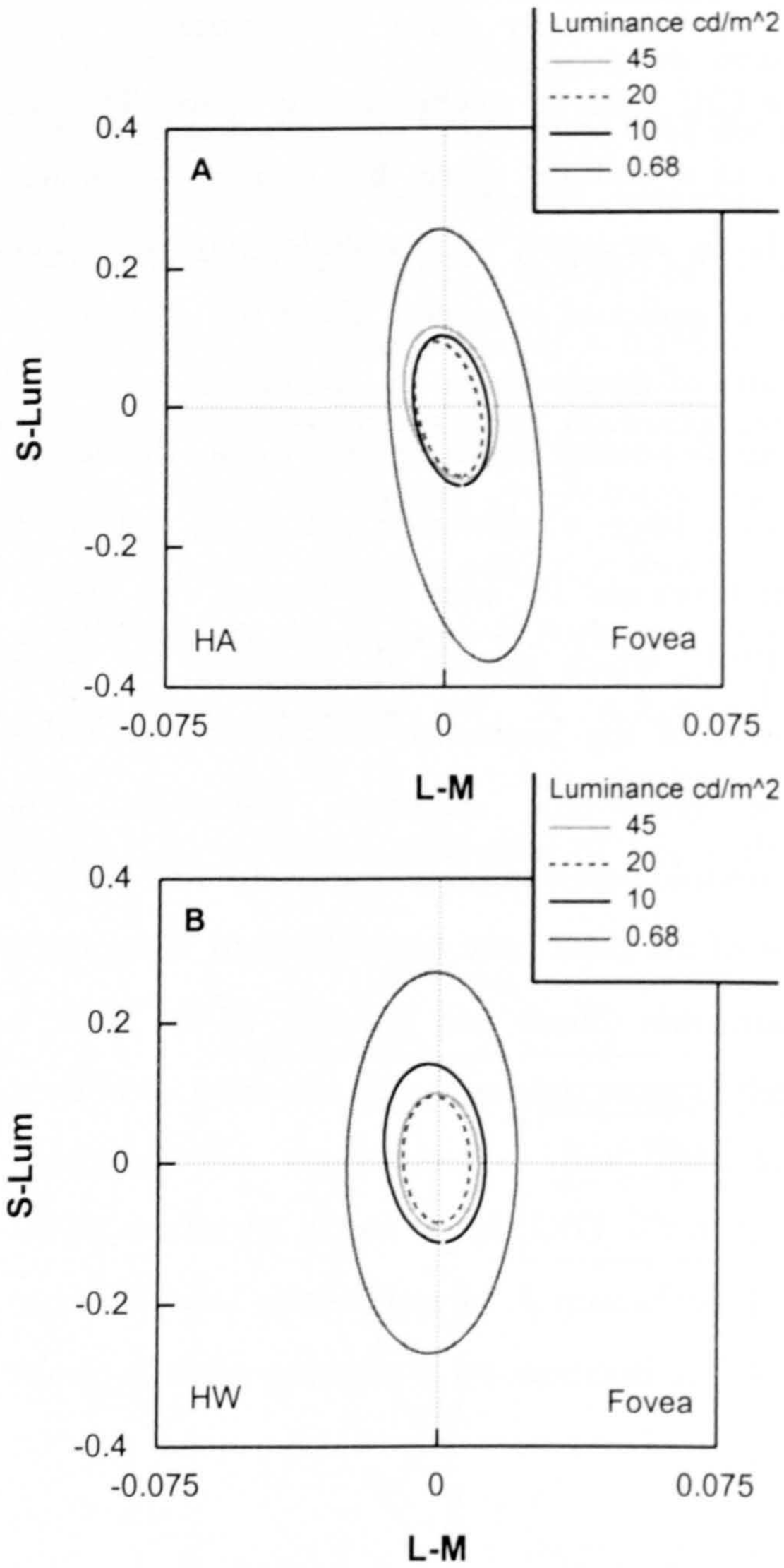

Figure 4-9 (A)-(B). Chromatic discrimination ellipses obtained at the fovea, transformed into DKL space. Luminance planes are superimposed. Results are shown for two subjects (A): subject HA and (B): subject HW.

The values of asymmetry calculated for each mechanism axis are shown in Table 4-8 for the foveal data and Table 4-9 for the data acquired at 3.5° eccentricity. For both stimulus locations, subject HA tended to exhibit asymmetric L-M channel thresholds in the direction of greater sensitivity for M-cone signals, but with more balanced thresholds at 3.5° eccentricity, whereas HW tended to exhibit asymmetric

thresholds in the direction of a relative increase in L-cone sensitivity, and showed more balanced thresholds at the fovea.

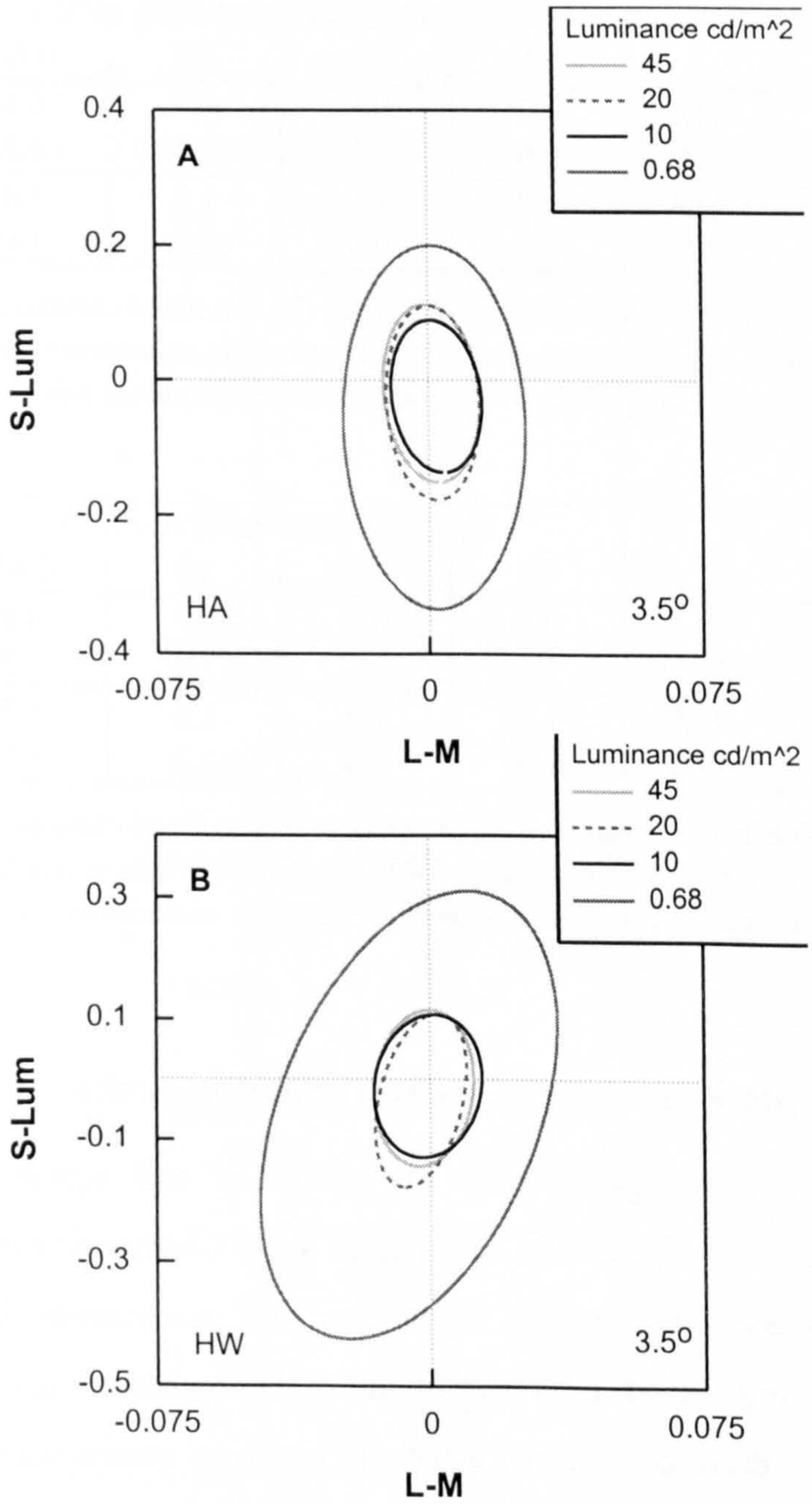

Figure 4-10 (A)-(B). Chromatic discrimination ellipses obtained at 3.5° eccentricity, transformed into DKL space. Luminance planes are superimposed. Results are shown for two subjects (A): subject HA and (B): subject HW.

For the S-Lum mechanism, both subjects exhibited balanced thresholds at the fovea, apart from HA at 0.68 cd m^{-2}, who showed a reduction in relative sensitivity to S-cone decrements. At 3.5° eccentricity both subjects showed asymmetric thresholds with a reduced relative sensitivity for S-cone decrements. This suggests

that the apparent asymmetry along the S-cone axis of results plotted in (u′, v′)-chromaticity space was in fact a true asymmetry for S-cone thresholds.

Fovea		Stimulus luminance (cd m^{-2})			
		45	20	10	0.68
L-M	HA	0.7	0.8	0.7	0.6
axis	HW	1.0	1.0	1.1	1.2
S-Lum	HA	0.9	1.0	1.1	1.4
axis	HW	1.0	0.9	0.8	1.0

Table 4-8. L-M and S-Lum mechanism asymmetries for the fitted chromatic discrimination ellipses of subjects HA and HW, obtained at the fovea. Axis asymmetry was defined as the ratio of the negative to the positive value along each mechanism axis in DKL space.

3.5° ecc.		Stimulus luminance (cd m^{-2})			
		45	20	10	0.68
L-M	HA	0.9	0.9	0.7	0.9
axis	HW	1.2	1.3	1.0	1.2
S-Lum	HA	1.3	1.6	1.5	1.7
axis	HW	1.3	1.8	1.2	1.5

Table 4-9. L-M and S-Lum mechanism asymmetries for the fitted chromatic discrimination ellipses of subjects HA and HW, obtained at 3.5° eccentricity. Axis asymmetry was defined as the ratio of the negative to the positive value along each mechanism axis in DKL space.

4.3.6 Dark adapted vs. cone plateau measurements

The results of the investigation into the effect of rod signals on chromatic thresholds are shown in Figure 4-11 and Figure 4-12. Chromatic thresholds for the three observers measured using the 2° target at 3.5° eccentricity, both after dark adaptation and during the cone plateau of the dark adaptation curve, are shown in Figure 4-11. Under these conditions, threshold contours varied somewhat between the observers. Subjects JB and HW exhibited somewhat larger thresholds than SM, and SM and HW displayed asymmetric thresholds along the S-cone axis, whereas JB did not. However, none of the three observers showed marked differences between their thresholds measured under the two conditions of adaptation.

The measurements were repeated at 7° eccentricity for a 4° target. This eccentricity corresponds to a retinal location with a greater rod density, and the larger target size increases the area for potential rod signal pooling. The results obtained after dark

adaptation and during the cone plateau of the dark adaptation curve, for the same three observers are shown in Figure 4-12. Again there were noticeable differences in thresholds for the three subjects; SM's chromatic sensitivity was superior to that of JB and HW, and only HW exhibited asymmetric thresholds along the S-cone axis. For all three subjects, however, chromatic thresholds measured under the two different conditions of adaptation showed no significant differences.

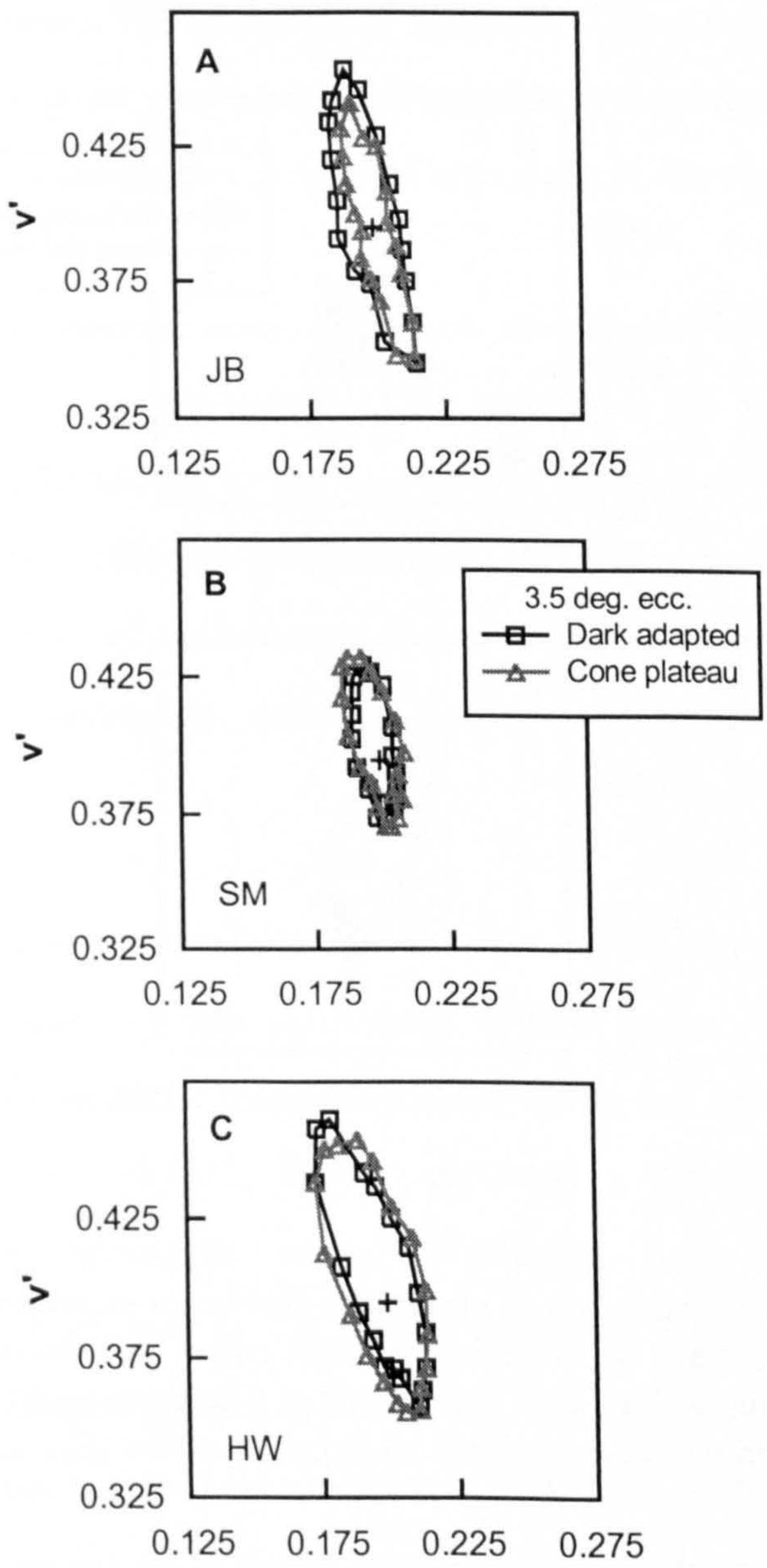

Figure 4-11 (A)-(C). Comparison of chromatic thresholds measured after dark adaptation and during the cone plateau of the dark adaptation curve. The results were obtained with a stimulus of 2° diameter centred at 3.5° eccentricity at a luminance of 0.09 cd m^{-2}. The results are shown for three subjects: subject JB (A), subject SM (B) and subject HW (C).

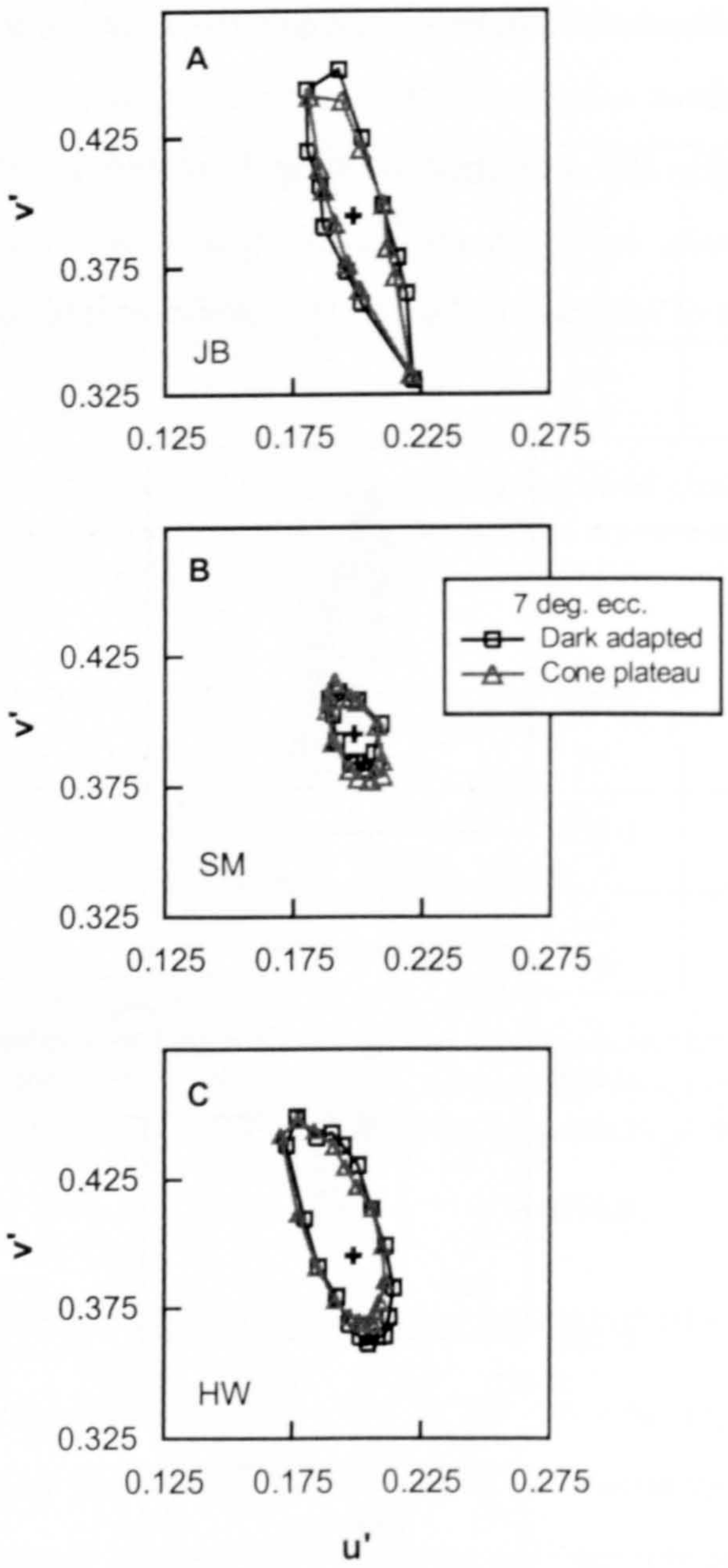

Figure 4-12 (A)-(C). Comparison of chromatic thresholds measured after dark adaptation and during the cone plateau of the dark adaptation curve. The results were obtained with a stimulus of 4° diameter centred at 7° eccentricity at a luminance of 0.09 cd m^{-2}. The results are shown for three subjects: subject JB (A), subject SM (B) and subject HW (C).

4.4 Discussion

It is clear that the lowering of background light adaptation into the mesopic range causes a reduction in chromatic sensitivity. The results of this study show that the loss of chromatic sensitivity is observed both foveally and with the stimulus centred

3.5° and 7° in the periphery, and that there are differences between chromatic threshold contours at each eccentricity. Threshold contour changes that are observed with reduction in light level are discussed below in relation to the loss of cone quantal catches and the difference in response characteristics of S-cones compared to L-and M-cones. It is known that dynamic luminance contrast noise fails to cause any significant increase in chromatic detection thresholds in the photopic range (Barbur et al. 1992) in agreement with Mullen et al.'s (1997) finding of independence between chromatic and luminance detection mechanisms. The results of this study suggest that under the conditions investigated, chromatic and luminance contrast signals are also processed separately in the mesopic range.

A dynamic luminance contrast noise technique was employed to ensure detection was based on purely chromatic signals. This technique has been shown to raise achromatic detection thresholds in the mesopic range, but produce little effect on chromatic thresholds; minimising detection of luminance contrast changes associated with the onset of a chromatic stimulus. It has, therefore, been assumed that the measured thresholds represent solely the sensitivity of chromatic mechanisms.

The background light adaptation level had a marked effect on chromatic sensitivity. The worsening of sensitivity was particularly evident below 10 cd m^{-2}. The non-uniform elevation of chromatic thresholds observed at the fovea is consistent with the findings of Brown (1951). Brown reported a preferential reduction of discrimination along tritanopic colour confusion lines at mesopic retinal illuminances, which is evident in the results presented here from the increase in ellipticity that accompanies the fall in light level, with the ellipses aligned along the S-cone axis. The selective loss of chromatic sensitivity along the axis of S-cone modulation is also consistent with the finding of tritan errors for the FM 100-hue test when performed under mesopic conditions (Bowman and Cole 1980; Knoblauch et al. 1987; Smith et al. 1991; Knight et al. 1998).

4.4.1 Ellipse orientation: inter-observer differences and changes with eccentricity and field size.

Results obtained in the near periphery were qualitatively similar to foveal measurements, but typically showed a reduction in chromatic sensitivity compared to the fovea. The deterioration with light level similarly began below 10 cd m^{-2}, but at larger eccentricities the direction of poorest sensitivity shifted away from the tritanopic axis towards the deuteranopic colour confusion line. In addition, for the thresholds obtained at the fovea and 3.5° in the periphery there were systematic differences in ellipse orientation between the two observers whos' results constituted the major part of the study.

A potential difference between the two subjects leading to the observed differences in ellipse orientation, may relate to the density of their macular pigment, which is known to vary between individuals (Werner et al. 1987).(Hammond et al. 1997) Smith et al (1995) computed that chromatic filtering by the macular pigment theoretically causes a rotation of tritan and red-green axes in chromaticity space, which is dependent on pigment density. An alternative possibility is that small differences in the wavelengths of cone photopigment peak sensitivities between the two observers may cause the differences in orientation. Estimates of macular pigment density were not acquired for the two subjects, and it was not possible to obtain estimates of cone photopigment peak sensitivity, therefore, possible effects of these two factors remain unconfirmed.

The shift in ellipse orientation with eccentricity was observed at 3.5°, 7° and 14° in the periphery, and appeared to depend on stimulus size, as the degree of ellipse tilt at 3.5° was reduced for a field size of 4° diameter compared to that of 2°. Alterations of ellipse orientation seem to imply changes in the orientation of the tritan line along which the major axes of the ellipses appear to align. It is unlikely that changes in macular pigment density with eccentricity could account for these findings because minimal density of pigment is found at the larger eccentricities investigated (Hammond et al. 1997), and the direction of ellipse tilt predicted by the modelling of Smith et al. (1995) is in the opposite direction to that observed here. One possible explanation for the change of ellipse orientation with eccentricity might be

that the increasing density of rods influences chromatic sensitivity, but this idea is rejected in the discussion below (section 4.4.2). It is generally thought that the only factors that can affect the orientation of a tritan line are changes in the wavelength of photopigment peak sensitivity, changes in pre-receptoral filtering, or rod intrusion effects. It is unlikely that any of these factors are responsible for the observed changes in ellipse orientation with eccentricity. The finding of such changes, therefore, challenges the representation of two cardinal post-receptoral colour mechanisms (Krauskopf et al. 1982), and may instead reflect the processing of multiple colour mechanisms. Evidence for the existence of such multiple colour mechanisms has been reported in the literature (Webster and Mollon 1991; D'Zmura 1991). It is suggested that the changes in ellipse orientation with eccentricity observed in this study may be a manifestation of changes in the sensitivity of such multiple mechanisms.

4.4.2 The influence of rods on chromatic sensitivity in the mesopic range

The results of this study have shown that there is a preferential reduction of sensitivity along the S-cone axis, and that asymmetrical S-cone thresholds are observed at mesopic light levels. The contribution of rod signals to this nonuniform and asymmetric sensitivity loss was assessed from measurements obtained under differential levels of rod activation. It is generally believed that the response of dark adapted cones may be isolated during the cone plateau of the dark adaptation curve, following sufficiently high light adaptation. This is due to the different recovery rates of rod and cone photopigments after bleaching and the assumption, therefore, that thresholds during the early part of the dark adaptation curve are set by the cones. During the cone plateau, cone threshold remains constant while rod sensitivity continues to increase; the rod-cone break occurring when the sensitivity of the rods becomes greater than that of the cones. Blakemore and Rushton (1965b) determined indirectly the change in rod sensitivity above cone threshold, and found it to follow an extension of the rod portion of the dark adaptation curve. Thus, it is possible to measure chromatic sensitivity at a level just above the threshold for the cones for a period during the cone plateau, whilst remaining below rod threshold.

On addition there is evidence that measurements of brightness and colour matches performed following the recovery of cones after light adaptation at intensities well above the cone threshold, are not affected by rod activity (Stabell and Stabell 1976a; Stabell and Stabell 1976b). It is certainly the case that differential activation of rods is achieved under the two recovery phases of the dark adaptation curve, without the need to ensure isolation of cone responses during the cone plateau. Rod influences are minimal during the period of constant cone threshold, and after full dark adaptation to the same background level, rod influences are maximal.

The comparison of results obtained for the fully adapted cones with minimal rod influence, and those obtained after full adaptation of the rods, showed no effect of rod activity on chromatic thresholds for either of the two eccentricities investigated. These results suggest that neither the selective loss of chromatic sensitivity along the tritan axis nor the asymmetry in thresholds in the blue and yellow directions can be attributed to rod signals. This would seem to contradict evidence that in the mesopic range both red-green discrimination at 25° eccentricity (Nagy and Doyal 1993) and yellow-blue discrimination at 7° eccentricity (Knight et al. 2001) are impaired by the influence of rods. Wavelength discrimination at 7.5° eccentricity also appears to be impaired by rod intrusion, but with little effect seen at 2.5° (Stabell and Stabell 1977). Knight (1998) also reported a reduction of tritan errors for the FM 100-hue test that are observed at mesopic light levels, when testing was carried out during the cone-plateau stage of the dark adaptation curve. This finding was also interpreted as evidence for rod involvement in chromatic mechanisms. There are a number of differences between these studies and the investigation carried out here, which include differences in eccentricity, stimulus size, and level of illumination. There are also differences in methodology; for example, in this study chromatic discrimination thresholds were measured from a neutral stimulus as opposed to measuring discrimination between suprathreshold chromatic stimuli. Another major difference in methodology relates to the use of different techniques to eliminate detection of luminance contrast signals. Nagy and Doyal (1993) and Knight et al. (2001) used flicker photometry to set isoluminance, Stabell and Stabell (1977) simply stated that a brightness match was maintained for changes in wavelength; whereas in the present investigation, dynamic luminance contrast noise

was employed to mask detection of luminance contrast signals. It is questionable whether reliable matches can be made using flicker photometry at mesopic levels, as matches fall on two branches of a discontinuous curve (Vienot and Chiron 1992). Vienot and Chiron reported that close to the transition flicker matches are difficult and some observers will make matches on both branches at the transition illuminance level. If scotopic luminance contrast signals are not effectively eradicated, they could account for apparent differences between cone plateau thresholds and thresholds acquired after complete rod recovery through a desaturating effect that is independent of cone mechanisms. For their investigation using the FM 100-hue test, Knight et al. (1998) maintained that the caps for which increased errors were seen after dark adaptation, did not coincide with the caps that produced the greatest rod excitation and, therefore, could not be attributed to action of an independent desaturating rod mechanism. A possible explanation for the absence of a rod effect on chromatic discrimination in the current study may be that the effects of rod-cone interactions are masked in the presence of luminance contrast noise. However, the effects of the many differences between the present study and those reporting rod-cone interactions are not clear and require further investigation.

4.4.3 Changes in chromatic sensitivity with reduction of light level, with particular regard to the S-cone system

An alternative explanation for the non-uniform loss of chromatic sensitivity may be found from consideration of the characteristics of the S-cones. The general reduction of relative sensitivity with decreasing light level may be attributed to the reduction in quantal catch of the cone receptors and a corresponding decrease of signal to noise ratio. The greater loss of sensitivity along the S-cone axis could be explained by the scarcity of S-cones in the retina (Curcio et al. 1991), or by S-cones only approaching the Weber region for higher levels of excitation (Boynton and Kambe 1980; Yeh et al. 1993). This explanation can also account for the asymmetry in chromatic sensitivity that is observed for some subjects, which has also been reported for yellow-blue mechanism detection thresholds at photopic levels (Vingrys and Mahon 1998). If the level of S-cone excitation falls below the Weber

region at lower light levels, decrements in S-cone excitation will produce a move further away from the Weber region, leading to a reduction in sensitivity. Similarly, increments in S-cone excitation will produce a move into the Weber region, leading to an improvement in sensitivity. This behaviour would predict the observed asymmetry: reduced thresholds towards the blue and increased thresholds towards the yellow. This hypothesis also predicts that changes in background adaptation level should either enhance or reduce the observed asymmetry in chromatic thresholds when S-cones are involved. DeMarco et al. (DeMarco et al. 1994) observed symmetry in such thresholds at ~ 100 cd m^{-2}, and Shinomori et al. (Shinomori et al. 1999) observed equal sensitivity to both directions of saw-tooth temporal modulation of S-cone excitation at 3 cd m^{-2}, although they were able to produce differences by adaptation to such asymmetrical stimuli. The asymmetry in the thresholds for increments and decrements of S-cone excitation is not observed in all subjects and appears to depend on luminance, eccentricity, stimulus size and probably other factors including filtering by the ocular media. More experimental work is therefore needed to test this hypothesis and to explain why the chromatic threshold asymmetry along the tritan axis is not present in all subjects for the same experimental conditions.

5 A model of conspicuity in the mesopic range

5.1 Introduction

Luminance contrast is a major determinant of performance in different visual tasks. For example, as luminance contrast is increased an improvement is seen in both visual acuity (Ludvigh 1941) and reading speed (Legge et al. 1987). Reaction time to the appearance of luminance contrast gratings, or increment light flux changes, decreases with increasing contrast (Harwerth and Levi 1978), and search times are reduced for increased luminance contrast (Barbur et al. 1991; Nasanen et al. 2001). Performance typically improves with increasing contrast until a plateau is reached after which performance is independent of contrast. The characteristics of such task-specific performance curves, however, are determined by many additional stimulus factors.

Colour can also be an important determinant of performance in a variety of visual tasks, where performance may depend on the combination of saturation and hue. For example, when spatial and transient achromatic signals are masked, reaction times to uniform chromatic stimuli exhibit a wavelength dependence (Ueno et al. 1985), and reaction times to photopically isoluminant red-green gratings are reduced as the colour contrast of the grating is increased (Parry 2001). For both photopically isoluminant chromatic targets and chromatic targets with identical luminance contrast, visual search time differs depending on the hue of the target (Barbur and Forsyth 1990; Nagy and Sanchez 1990; D'Zmura 1991).

Considering this dependence of visual task performance on stimulus contrast and colour, it would be advantageous to obtain a measure of the combined effectiveness of these stimulus parameters. The measure proposed in this study is conspicuity, which describes the discriminability of a target from its surroundings, and takes into account both the colour contrast and luminance contrast of the stimulus. Recent

studies of visual search have proposed that target discriminability/ saliency/ conspicuity is an essential determinant of visual search performance (Verghese and Nakayama 1994; Itti and Koch 2000; Palmer et al. 2000), supporting the need to develop measures of stimulus conspicuity.

The need for a greater understanding of the relative contribution of colour and luminance contrast to conspicuity is perhaps more pertinent in the mesopic range. The absence of a standard luminous efficiency function for mesopic vision means that luminance contrast cannot be computed under these conditions as it can for either photopic or scotopic vision. Hence, when considering the relationship between luminance contrast and visual task performance, performance can only be measured in terms of photopic luminance contrast or scotopic luminance contrast, neither of which describes fully the adaptive state of the eye under mesopic conditions. Even in the achromatic mesopic domain, therefore, one needs to obtain a measure of the relative contribution of photopic contrast and scotopic contrast to task-specific performance. In addition, little is understood of the relationship between visual task performance and colour in the mesopic range. Hence, a measure based on contributions from these three parameters (photopic contrast, scotopic contrast and colour contrast), such as stimulus conspicuity, would be a valuable, practical way of assessing the visual effectiveness of a stimulus in the mesopic range.

Engel (1971; 1974; 1977) developed a measure of conspicuity based on the area within which a target object could be detected, during an exposure that was sufficiently short to preclude eye movements (75 msec). Further studies employed measures of conspicuity based on Engel's definition. Jenkins and Cole (1982; 1984) measured the maximum eccentricity at which a target object could be detected with a fixed probability during a presentation time of 250 ms. Kooi and Toet (1999) defined conspicuity as the largest lateral separation between fixation and the target object, at which the target is just barely noticeable for a 250 ms presentation. These measures were developed to efficiently quantify the ability of a target to attract the attention of an observer during a single glance of the stimulus, such as might occur during visual search. Both Engel (1977) and Kooi and Toet (1999) showed that such a measure of conspicuity correlates well with visual search performance. An

alternative method of measuring stimulus conspicuity was adopted by Barbur and Forsyth (1990). They quantified the conspicuity of a target grating by determining the achromatic contrast of a similar grating that produced an equal perceived conspicuity. Under this definition, conspicuity can be thought of as a measure of effective contrast. In this method, stimulus conspicuity is measured using an achromatic reference scale, which must itself be calibrated for a given visual task. The advantage of this calibration approach is that luminance contrast for stimuli of the same spectral power distribution as the surrounding background, can be defined unambiguously. Using such a calibration Barbur and Forsyth (1990) demonstrated a good correlation of their measure of conspicuity with visual search performance.

In the present study, a matching method similar to that of Barbur and Forsyth (1990) was used to measure the conspicuity of a uniform target defined by colour and luminance contrast by determining the achromatic contrast of a similar target that was equally conspicuous. The target investigated was based on a Landolt C and an intermediate presentation time was used. This method was employed, firstly, on the premise that a local measure of the visibility of a target against its immediate background might make a suitable predictor of performance for a broader range of visual tasks than a conspicuity measure based on the ability to capture attention using brief presentation times. For example, the conspicuity matching method might be expected to provide a better prediction of acuity or reading speed. Secondly, the conspicuity matching method allows direct comparison with a large number of existing models of mesopic vision. These are models that have been proposed as systems mesopic photometry, but at present, have not been accepted by the CIE. Such models aim to predict the mesopic luminance of a stimulus in terms of the luminance of a particular reference stimulus, and can, therefore, be used to predict a measure of mesopic luminance contrast for a stimulus. Such values of mesopic luminance contrast could be compared to the measure of conspicuity provided by the conspicuity matching method, i.e., a value of mesopic luminance contrast predicted by one of the proposed systems of mesopic photometry could be compared to the equivalent achromatic luminance contrast determined using the conspicuity matching method. For scales of conspicuity based on distance or area such as Engel's measure of conspicuity, only an indirect comparison would be

possible between distance/area and luminance contrast predicted by a system of mesopic photometry.

The aims of this investigation were firstly, to develop a matching procedure to equate the conspicuity of a target defined by colour and luminance contrast to a similar target defined by achromatic luminance contrast, and obtain measures of conspicuity for targets with a large range of colour/luminance contrast combinations, throughout the mesopic range. The second aim was to develop a model of the relationship between the measure of conspicuity employed and the physical parameters of the target stimulus, based on the set of acquired conspicuity data. The final aim was to compare the measure of conspicuity developed in this study to measures of mesopic luminance contrast obtained from currently proposed systems of mesopic photometry.

5.2 Subjects and methods

As stated in the introduction, the matching procedure consisted of measuring the conspicuity of a test stimulus by determining the achromatic luminance contrast of a similar stimulus that was judged to be equally conspicuous. Initially, a pilot study was carried out to test the design of the matching procedure and investigate the conspicuity of a restricted sample of target stimuli. A description of the matching procedure was given in section 2.5 and details specific to the pilot study can be found in section 2.5.1. For the remainder of the matching experiments a modified version of the procedure was used, the details of which were given in section 2.5.2. The revised procedure was used to obtain an extensive set of conspicuity matches from which an empirical model of conspicuity was derived. Measurements of natural pupil diameter were made alongside the measurements of conspicuity to allow calculation of retinal illuminance. Descriptions of the procedures used to obtain pupil diameters were given in section 2.1.2.

For all experiments the test target was defined by its photopic contrast (C_p), scotopic contrast (C_s) and chromatic difference (CD) to the background. For the

pilot study CD was defined according to the CIE 2° colorimetric observer and V(λ) was used to compute photopic luminance, see section 2.5.1 Eq. 2-8 - Eq. 2-11. For subsequent investigations CD was defined according to the CIE 10° colorimetric observer and $\bar{y}_{10}(\lambda)$ was used to compute 10° luminance (L_{10}), see section 2.5.2, Eq. 2-12 and Eq. 2-13. The reference/match target was defined by achromatic luminance contrast, i.e. the match target had the same spectral power distribution as the background. The luminance contrast of an achromatic stimulus is independent of the spectral luminous efficiency function; hence an achromatic stimulus has equal values of photopic and scotopic contrast. The conspicuity of an achromatic reference stimulus can, therefore, be defined unambiguously in terms of contrast.

The matching achromatic-contrast scale was restricted to a single polarity: that of positive achromatic luminance contrast. It is also possible to measure the conspicuity of a target defined by colour and luminance contrast using a negative achromatic contrast reference scale, but initial investigations indicated that the conspicuity of a negative contrast target differed from the conspicuity of a positive contrast target. Measures of conspicuity obtained using a positive and a negative contrast reference scale cannot, therefore, be expected to yield identical results. For the purpose of the current study, it was not necessary to obtain matches for both negative and positive contrast reference scales.

5.2.1 Subjects

Two female observers HA and HW (age 22 and 26) carried out the pilot matching experiments. Five observers participated in the remainder of the matching experiments. Observer A was male and observers B, C, D and E were female. The mean age was 28.6, range 20-42. These five observers are also referred to as observers 1-5 in some of the figures, where 1 is equivalent to A and so on. JO, a 27 year old male, acted as an additional subject for the measurements of pupil size. All subjects were normal trichromats according to the Ishihara plates and the computerised colour vision test described in section 2.3.1, and had good chromatic discrimination according to the FM 100-hue test. All subjects also had a high

contrast visual acuity of 0.0 log minimum angle of resolution (logMAR) or better and low contrast acuity of 0.2 logMAR or better, measured using the Bailie-Lovie high and low contrast acuity test chart. None of the subjects had central visual field defects (30° field), or signs of any other ocular abnormality.

5.2.2 Methods for the pilot study

In the pilot study the test target had zero photopic contrast ($C_p = 0$) and zero scotopic contrast ($C_s = 0$), but a non-zero chromatic difference to the background (CD). Under these conditions with a three primary system such as a CRT monitor, the target chromaticity is restricted to a range of values that lie on a single line in chromaticity space (S by P line), which passes through the background chromaticity (see section 2.1.4). Chromatic difference values may be measured from the background chromaticity in either of two directions of chromaticity space described by this line. With the CRT monitor used, the two directions corresponded to reddish stimuli and greenish stimuli (see Figure 5-1); these two directions will be referred to as the red condition and the green condition.

Nominal filter density	Mean optical density at 45° incidence	Background luminance (cd m^{-2})	Dark adaptation time (min)	CD (min-max)	
				red cond.	green cond.
NONE	0	45	5	0.01 - 0.06	0.01 - 0.09
NONE	0	20	5	0.01 - 0.15	0.01 - 0.09
NONE	0	10	5	0.01 - 0.15	0.01 - 0.09
1.0	1.17	0.68	10	0.02 - 0.16	0.02 - 0.09
2.0	2.25	0.056	18	0.05 - 0.16	0.06 - 0.09

Table 5-1. Stimulus values used in the pilot conspicuity matching experiments. Test targets had zero photopic and zero scotopic contrast. For the lowest two light levels, neutral density filters were used to lower the luminance of the display. A range of suprathreshold CD values was investigated for both possible colour conditions (red and green), in steps of 0.01 CD.

The two observers HA and HW, obtained measurements over five light levels in the low photopic and mesopic range (45 - 0.056 cd m^{-2}). For the lowest two light levels neutral density filters were used to lower the background luminance, as described in section 2.1.1.

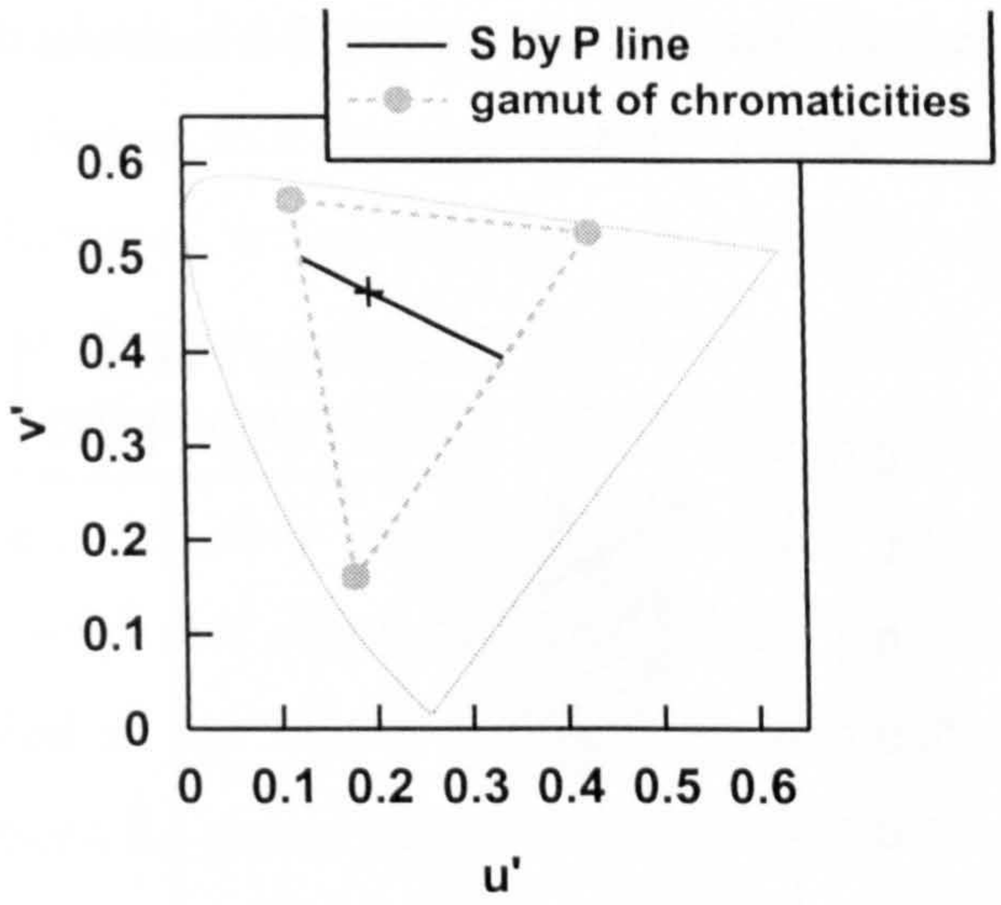

Figure 5-1. S by P line in CIE 1976 (u′, v′)-chromaticity space denoting the range of chromaticities available for a stimulus with zero photopic and zero scotopic contrast on a typical CRT monitor. Filled circles indicate the chromaticities of the red, green and blue phosphors.

At each light level, matches were made for suprathreshold CD values for both the red and green conditions, in steps of 0.01 CD up to the maximum CD that could be reproduced on the display. The maximum achievable CD value for both the red and green conditions was restricted by the limits of the phosphors of the display, and varied with light level. Matches were made monocularly with the right eye for both subjects. The two subjects adapted to the luminance of the background prior to beginning measurements. Dark adaptation times were calculated using the method described in section 2.4.1. The stimulus conditions investigated are shown in Table 5-1.

5.2.3 Methods for collection of a conspicuity matching data set

A revised version of the matching procedure was used to obtain an extensive set of conspicuity matches; see section 2.5.2 for details of the revised procedure. Matches were obtained for a large range of test target combinations of C_p, C_s and CD, at six discrete light levels spanning a three and a half log unit range of luminance. The test target parameters were chosen to cover a wide range of contrast combinations spread over a large region of colour space. The background light levels will be referred to as level 1 to level 6, where level 1 has the highest value of L_{10} and level 6

the lowest value of L_{10}. Again, neutral density filters were used to lower the background luminance, as described in section 2.1.1, while the luminance of the display remained approximately constant.

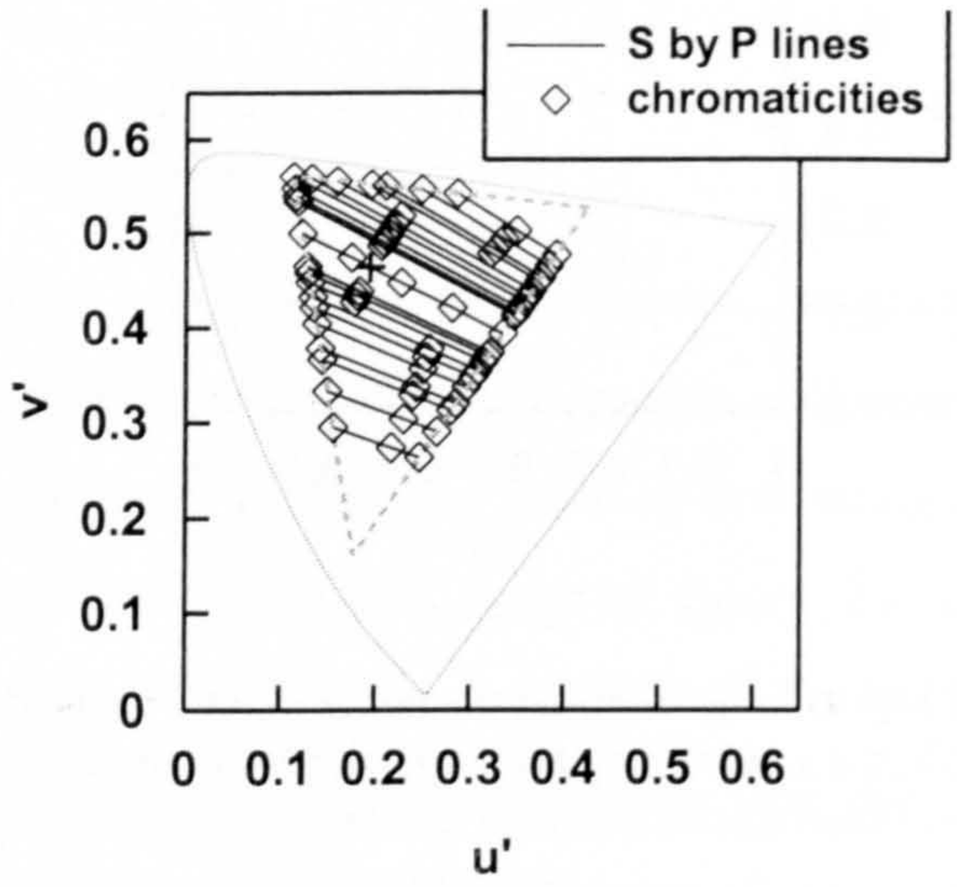

Figure 5-2. S by P lines in CIE 1976 (u′, v′)-chromaticity space denoting the range of chromaticities available for stimuli with the combinations of photopic and scotopic contrast used in the conspicuity matching experiments. Symbols indicate the chromaticities investigated.

Due to the finding from preliminary measurements of differences in the conspicuity of positive and negative contrast stimuli, conditions with combinations of both positive and negative values of C_p and C_s were included in the experimental design. Results of the pilot study also advocated inclusion of conditions with zero C_p and C_s. Contrast thresholds were measured, for an achromatic target similar to that used in the matching procedure, at each of the six light levels. Contrast thresholds increased with reduction in luminance. At the lowest light level, a contrast of 0.2 was approximately double the measured threshold and thus considered sufficiently above threshold to be included in the range of conditions for the matching experiments. Initially, five values of photopic contrast and scotopic contrast were incorporated into the experimental design, creating 25 contrast pairs. For each ratio of scotopic to photopic contrast the target chromaticity was restricted to a range of values lying on a single line in chromaticity space (S by P line), see section 2.1.4. For each contrast pair three CD values were chosen, distributed along each S by P line to incorporate different colour directions and different CD values. The chosen stimulus chromaticities are shown in Figure 5-2. These combinations of C_p, C_s and

CD resulted in a total of 75 test target specifications for each light level. To increase the sampling of zero contrast conditions, an additional two zero contrast conditions were included in the design, to make a total of 77 specifications for each light level. During a trial run, however, it was found that not all the combinations produced targets that were sufficiently suprathreshold to perform the matching task, particularly at the lower light levels. Target combinations were subjectively eliminated on the basis that they were so poorly visible that it was not possible to carry out the task. After this elimination procedure, an additional magnitude of contrast was included at the lowest two light levels to increase the number of experimental conditions for these background luminances. A total of 473 conditions were included in the final experimental design, the luminance contrast values incorporated are shown in Table 5-2.

Light levels 1, 2, 3, 4		Light levels 5, 6	
C_p (actual values)	C_s (nominal values)	C_p (actual values)	C_s (nominal values)
		0.5	0.5
0.4	0.4	0.4	0.4
0.2	0.2	0.2	0.2
0	0	0	0
-0.2	-0.2	-0.2	-0.2
-0.4	-0.4	-0.4	-0.4
		-0.5	-0.5

Table 5-2. The values of photopic and scotopic contrast incorporated into the experimental design used to collect a data set of conspicuity matches. The scotopic contrast values are only nominal because errors present in the algorithm used to reproduce each C_p, C_s, CD triplet were reflected in the scotopic contrast value, see section 2.1.4. An additional magnitude of contrast was included for the lowest two light levels to increase the number of viable conditions.

The five observers A-E carried out six matches for all 473 conditions over the six light levels, using a randomised order of presentation. Observers adapted to the luminance of the background prior to beginning measurements, with appropriate dark adaptation times calculated using the method described in section 2.4.1. Measurements were carried out using one of two experimental systems: system-1 and system-2, as described in chapter 2. The background luminances used for system-1 and system-2, calculated using the neutral density filter transmittances particular to each system, are shown in Table 5-3 along with the respective dark adaptation times. Table 5-3 also shows the number of conditions included in the

experimental design at each light level. All matches were performed binocularly to simulate viewing in the real world. Measurements of the right eye pupil diameter were made during each run of the experiment, using the methods described in section 2.1.2. This allowed calculation of the retinal illuminance or Troland Value (E) according to Eq. 5-1, for every pair of match contrast values obtained in a single experimental run, for each subject.

$$E = \pi\left(\frac{d}{2}\right)^2 L_b \qquad \text{Eq. 5-1}$$

where E: retinal illuminance in trolands, d: pupil diameter in mm, L_b: background luminance in cd m^{-2}. All observers were trained with the matching procedure for several hours in order to stabilise their criterion for judging differences in conspicuity, prior to collection of matches for the conspicuity matching data set.

			System-1		System-2		
light level	num. cond	nominal filter density	mean optical density at 45° incidence	bkgd luminance L_{10}	mean optical density at 45° incidence	bkgd luminance L_{10}	dark adapt. time (min)
1	77	NONE	0	10	0	10	5
2	76	0.8	0.95	1.1	0.98	1.0	10
3	73	1.5	1.64	0.23	1.71	0.19	15
4	63	2.0	2.34	0.046	2.40	0.040	20
5	105	2.5	2.93	0.012	3.02	0.010	25
6	79	3.0	3.42	0.0038	3.78	0.0017	30

Table 5-3. Filter densities, background luminances and dark adaptation times for system-1 and system-2 at each of the six light levels investigated. Also shown, are the numbers of conditions included in the experimental design at each light level.

Outlier results were found for individual observers and repeat measurements made once the complete set of 473 matches had been obtained. Outliers were determined on the basis of having a coefficient of variation (c.var) beyond the normal range, i.e. $c.var > \bar{X} + 2S$, where $\bar{X}$ and S are the mean and standard deviation of the c.var values computed per background light level. The coefficient of variation for each target condition was calculated from the six measured match contrast values (C_m), according to Eq. 5-2.

$$\text{coefficient of variation} = \frac{\sqrt{\frac{\sum(x-\bar{x})^2}{n-1}}}{\frac{\sum x}{n}} \qquad \textbf{Eq. 5-2}$$

where n: number of samples, i.e. 6; x: each C_m value; $\bar{x}$: mean of each 6 C_m values. It was appropriate to calculate outliers in this way because the coefficient of variation corrected for the increase in standard deviation of the matches with increasing contrast (see section 2.5.2), which is a consequence of Weber-Fechner behaviour, and the c.var values for each light level were approximately normally distributed. For each outlier condition, two additional C_m values were measured in order to improve the estimate of the mean match contrast.

Subject D obtained matches for a sample of test target conditions using both experimental systems. Six matches were made on each of three days for seven conditions at light level 1 and seven at light level 4. Results obtained using the two systems were compared by performing a two-way analysis of variance (ANOVA) on the resulting C_m values, for factors "system" and "test target condition".

To examine differences in the perceived conspicuity of positive and negative achromatic contrast stimuli, each observer performed a series of matches for targets of achromatic contrast. Twenty four matches were acquired over three days for a test target with $C_p = 0.4$, $C_s = 0.4$, $CD = 0$ and for a test target with $C_p = -0.4$, $C_s = -0.4$, $CD = 0$, in both cases the match target was of positive achromatic contrast. Measurements were performed for two light levels: light level 1 and light level 4.

5.2.4 Analysis of the conspicuity matching data set

Firstly, the variability of the matching procedure was assessed. The within-subject variability was calculated from the standard error of the mean of the six C_m values obtained for each test target condition, expressed as a percentage of the mean C_m. The between-subject variability was calculated from the standard deviation of the five mean C_m values for each observer, expressed as a percentage of the mean across the five observers. Both the within-subject and between-subject variability was expressed as a percentage of the mean value to account for the increase in spread of

the matches with increasing C_m. The within-subject variability was compared to the precision of each of the five observer's judgements. Measurement precision was assessed from the spread of results for matching a positive achromatic test target with a positive achromatic reference as this was assumed to be the most precise judgement. Precision was calculated as the standard error of a sample of six matches made for a test target with $C_p = C_s = 0.4$, CD = 0, expressed as a percentage of the mean C_m.

The design of the conspicuity matching experiment incorporated a single dependent variable (C_m) and four explanatory variables (C_p, C_s, CD and E). The dependent variable (or response variable) was taken as the mean of the six match contrast values obtained for each experimental condition by each observer (mean C_m). An Analysis of variance (ANOVA) was carried out to investigate the effects of the explanatory variables and their interactions on the response variable. The response variable (mean C_m) had a positively skewed distribution and so was transformed to obtain a normal distribution and obtain approximate interval scaling. The transformation applied was the natural logarithmic function, one of the Box-Cox family of transformations (Box and Cox 1964). Retinal illuminance (E) also had a positively skewed distribution due to the choice of logarithmically scaled light levels; hence, E was transformed using the logarithmic function to the base 10. An analysis of variance assumes that the explanatory variables are approximately independent, to verify this a correlation matrix was calculated for the explanatory variables. The correlation coefficient between two variables is given by Eq. 5-3,

$$r = \frac{\sum (x_i - \bar{x})(y_i - \bar{y})}{\sqrt{\left(\sum (x_i - \bar{x})^2\right)\left(\sum (y_i - \bar{y})^2\right)}} \qquad \text{Eq. 5-3}$$

where r: correlation coefficient, and (x_1, y_1), (x_2, y_2), $\ldots(x_n, y_n)$ are n paired observations of the two variables X and Y.

Separate ANOVAs were implemented to investigate different subsets of the data. The initial ANOVA was performed on the complete data set of 2365 mean C_m values (473 conditions for each of the five observers). A second ANOVA was carried out to investigate the effects of both the magnitude and sign of the

luminance contrast terms (C_p and C_s). Further ANOVAs were performed to assess the dependence of match contrast on the explanatory variables with change in light level. The level of significance for all analyses was taken as $\alpha = 0.05$.

An empirical model was derived from the conspicuity matching data set, in which the conspicuity of a stimulus defined by colour and luminance contrast was related to the conspicuity of an achromatic stimulus. Model parameters were based on the explanatory variables C_p, C_s, CD and $\log_{10}E$, and their interactions. A multiple regression procedure based on the principle of minimising the squared error was implemented to obtain fits to the raw data.

5.3 Results

5.3.1 Results of the pilot study

The results of the conspicuity matches made for test targets with zero photopic and scotopic contrast, but a non-zero chromatic difference, are shown in Figure 5-4 for observers HA and HW. For the three highest light levels, 45-10 cd m^{-2}, a CD of 0.01 was sufficiently above threshold to perform the matching task; below these light levels, the lowest CD for which a match could be measured, rose to 0.02 at 0.68 cd m^{-2} and 0.05 at 0.056 cd m^{-2}. This rise reflects the large increase in chromatic thresholds with reduction in light level, reported by Walkey et al (2001) and described in chapter 4. It can be seen from Figure 5-3 and Figure 5-4 that the achromatic contrast required to match, in terms of conspicuity, a target defined solely by colour difference, rises approximately linearly with increasing CD. This relationship was similar for the two observers and roughly independent of light level for the majority of light levels investigated.

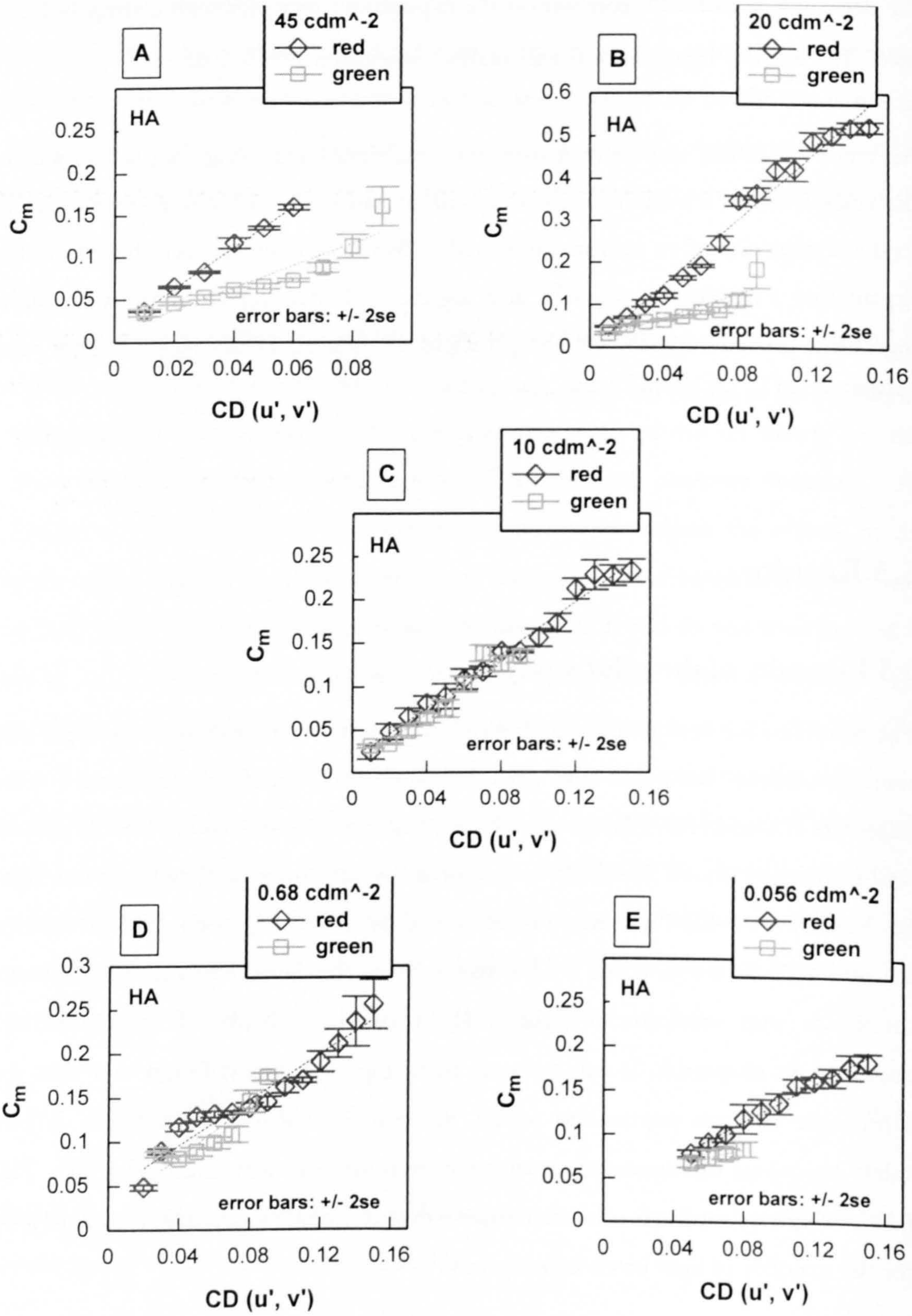

Figure 5-3 (A)-(E). Conspicuity matches for targets with zero photopic and scotopic contrast obtained by subject HA over five light levels (A)-(E). Equivalent achromatic match contrast is plotted against stimulus chromatic difference for the two directions in chromaticity space. Dashed lines indicate linear fits to the data. Note that there is a different scale on the ordinate for 20 cd m^{-2} data (B).

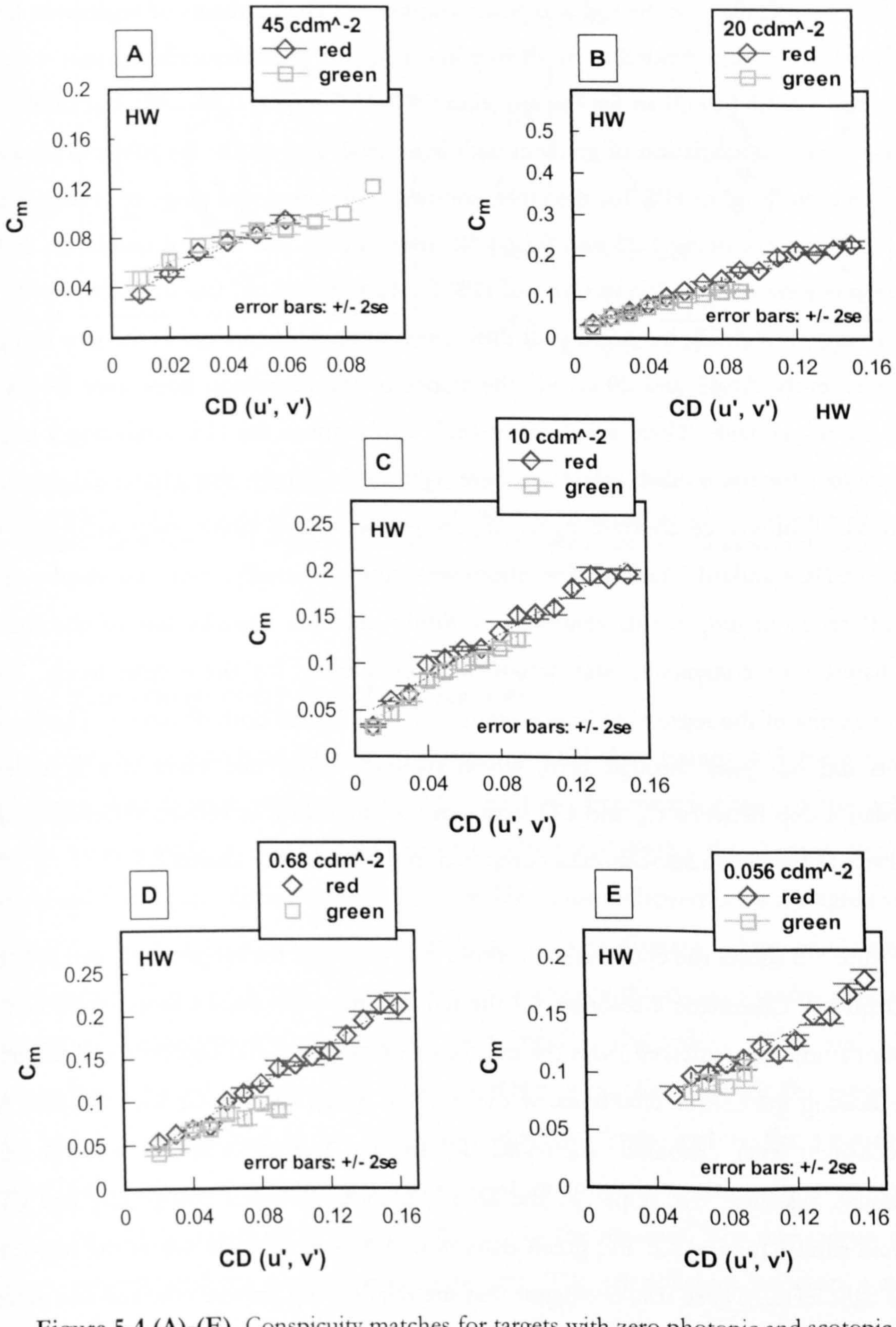

Figure 5-4 (A)-(E). Conspicuity matches for targets with zero photopic and scotopic contrast obtained by subject HW over five light levels (A)-(E). Equivalent achromatic match contrast is plotted against stimulus chromatic difference for the two directions in chromaticity space. Dashed lines indicate linear fits to the data.

For subject HW, the relationship between CD and matching achromatic contrast (C_m) was similar for the red and green conditions. The gradients of regression lines fitted to the data tended to be slightly lower for the green condition (mean = 0.85, range = 0.49-1.08) than for the red (mean = 1.15, range = 0.83-1.44), but there was no systematic variation of gradient with light level. The results for subject HA were similar to those of HW for the green condition: the mean and range of gradients for the linear fits being 1.25 and 0.52-1.52, respectively. For the red condition, HA's results were comparable to those of HW for 10-0.056 cd m^{-2} (mean gradient = 1.30, range = 1.07-1.52), but somewhat different relationships resulted at the two highest light levels. At 45 and 20 cd m^{-2} the slopes of the regression lines were 2.46 and 3.86, respectively. There are three possible explanations for HA producing a larger gradient for the reddish targets at these light levels. Firstly, that HA could detect a residual luminance contrast signal (the targets were only isoluminant according to the CIE standard observer for photopic vision). Secondly, that HA displayed a difference in judgements criterion, or thirdly that the contribution of chromatic channels to conspicuity was weighted more heavily for these light levels. The intercepts of the regression lines were roughly similar for both observers. The linear fits did not pass through zero, which suggests either that there is a nonlinear relationship between C_m and CD very close to threshold, or reflects different noise levels in the chromatic channels compared to the luminance channel.

Figure 5-5 shows the chromatic threshold data obtained for subjects HA and HW in chapter 4. Chromatic thresholds for the red and green conditions investigated in the pilot study were inferred from the intercepts of the threshold contours and the line indicating the colour directions of the red and green stimuli, for each subject. At each light level, chromatic thresholds for the red and green stimuli were grossly similar. Likewise, the slopes of the linear functions between conspicuity and CD were similar for the red and green conditions for both subjects across the majority of light levels. These results suggest that the relationship between the red and green stimuli at threshold was preserved in the suprathreshold measurements of conspicuity.

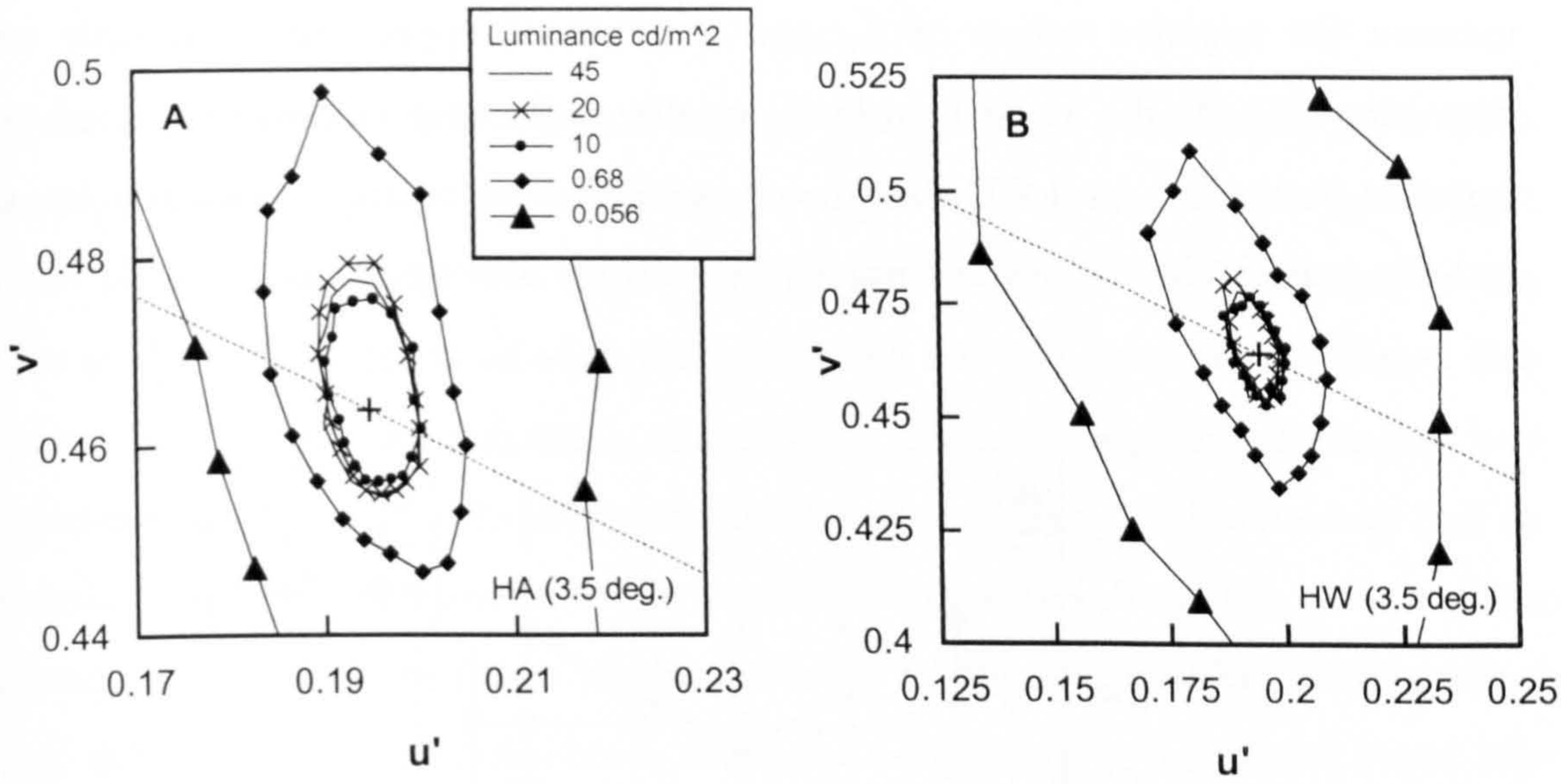

Figure 5-5 (A)-(B). Chromatic thresholds for subjects HA (A) and HW (B) at 3.5° eccentricity for a number of light levels in the mesopic range, obtained in chapter 4. The dashed line indicates the colour directions of the red and green stimuli used in the pilot study.

5.3.2 The conspicuity matching data set

The conspicuity matching data set consisted of 2365 data points: 473 from each observer. The average results obtained by the five observers for two of the light levels investigated, are shown in Figure 5-6. The plots display the average results obtained for several different test target combinations collapsed onto a single axis: either C_p, C_s or CD. For each light level up to seven discrete values of C_p were investigated. The plot with C_p as the abscissa represents the average match contrast across all conditions with each given value of C_p. The values of C_s and CD investigated, varied from one test target condition to another. Hence, the range of C_s and CD values had to be coded into discrete levels with a flat frequency distribution, and match contrast averaged over all conditions with each given level of C_s or CD, to create plots with C_s and CD as the abscissa. For this reason the plots are intended for qualitative analysis only. The relationships between match contrast and these three test target parameters, changed considerably over the 3 log units fall in background luminance. For the higher light level, match contrast increased linearly with increasing magnitude of C_p, with a marginally higher slope for negative contrast. Match contrast varied little with C_s, although there was some

increase for negative values of C_s, and it increased approximately linearly with increasing CD. At the lower light level, an almost flat response was obtained with variation in both C_p and CD, but match contrast increased approximately linearly with the magnitude of C_s, with a much steeper slope for negative contrasts.

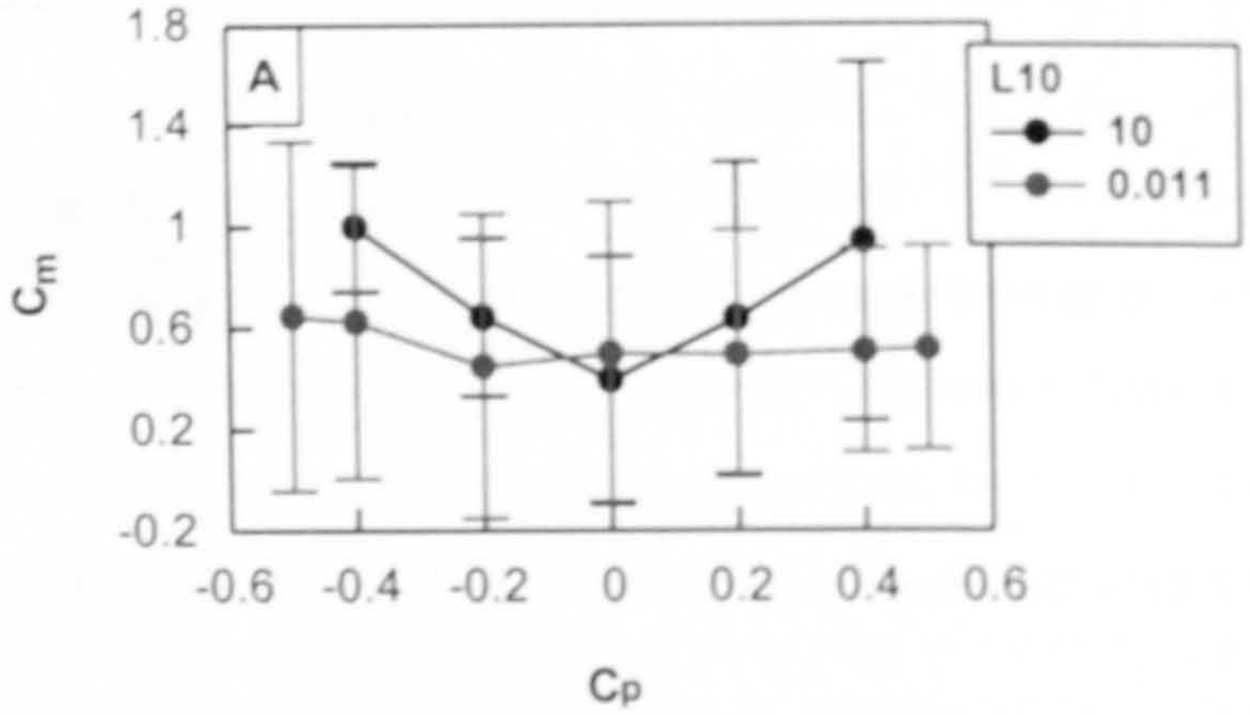

Figure 5-6 (A)-(C). Average conspicuity matches for the five observers at a low photopic ($L_{10} = 10$) and a low mesopic ($L_{10} = 0.011$) light level. Data points represent the mean match contrast (C_m) over a number of test target conditions collapsed onto a single axis: either C_p (A), C_s (B) or CD (C). Error bars indicate ± 2 standard deviations from the mean.

Figure 5-7 shows the individual observer's responses to test targets with zero photopic contrast and approximately zero scotopic contrast for the two highest light levels investigated. These test target conditions were similar to those used in the pilot study, and incorporated stimuli for both the red and the green condition (see section 5.2.2). The variation in C_m with CD at both background luminances was approximately linear for all subjects, with little or no effect of stimulus hue (red or green). Linear fits were made to the combined responses from the two possible colour directions. Comparison of the gradients of these regression lines revealed large differences between observers: the range of gradient at light level 1 was 1.6-5.5, and at light level 2 was 1.2-3.4.

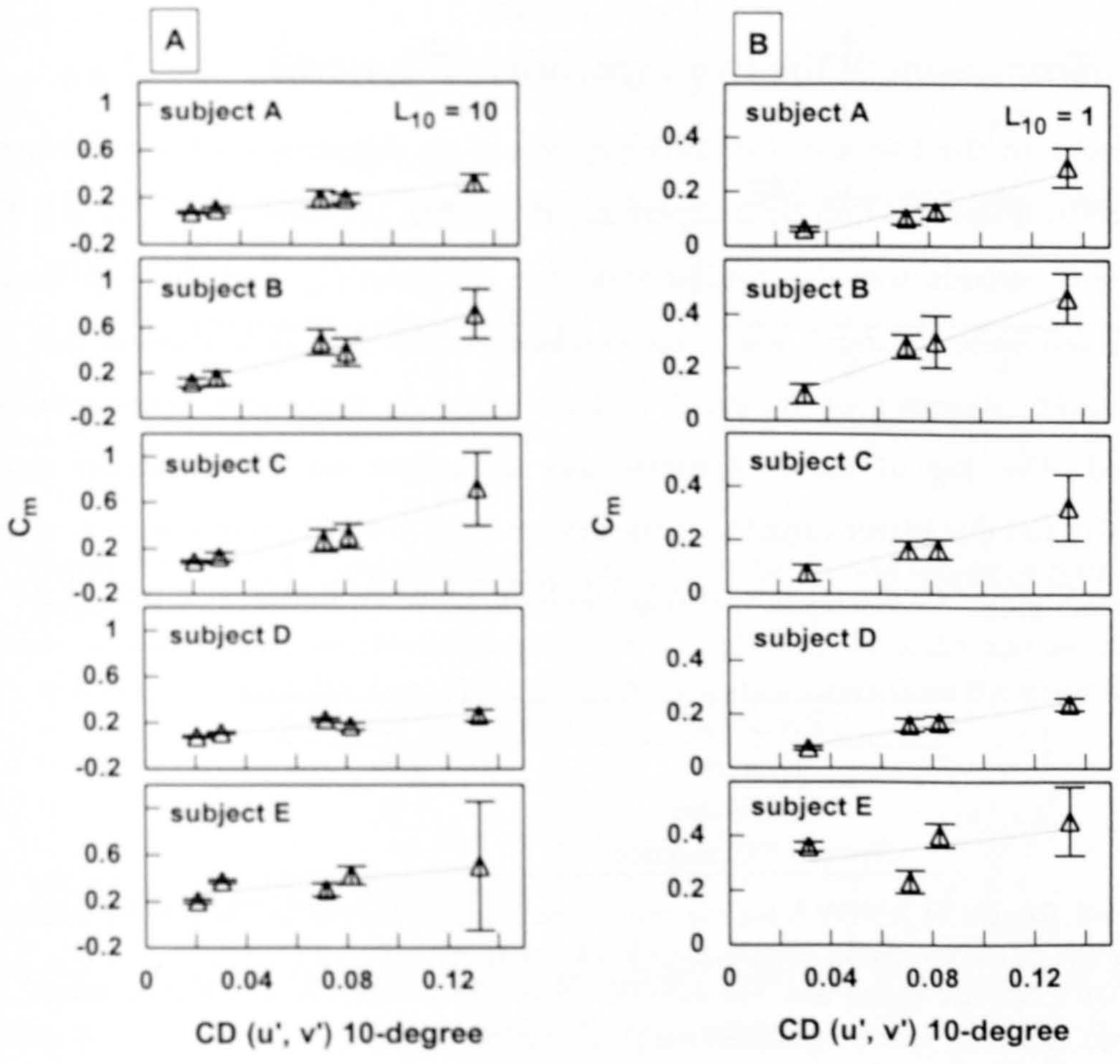

Figure 5-7 (A)-(B). Conspicuity matches for targets with zero photopic contrast and approximately zero scotopic contrast obtained by all five subjects. Achromatic match contrast vs. stimulus chromatic difference is shown for a low photopic (L_{10} = 10) light level (A) and a high mesopic (L_{10} = 1) light level (B). Dashed lines indicate linear fits to the data. Error bars indicate ± 2 standard errors from the mean of 6 matches.

The stimuli investigated, were designed to be isoluminant for both the CIE 10° observer and the CIE standard observer for scotopic vision (d-isoluminant), but may not have been d-isoluminant for the participating observers, as the spectral luminous efficiency curves of normal trichromats are known to vary (Gibson and Tyndall 1923). One possible explanation for the differences in gradient then, is that the observers were able, to different extents, to detect luminance contrast signals in addition to colour signals. An alternative explanation for the differences in gradient is that the observers could detect little or no luminance contrast, but weighted the chromatic content of the stimuli differently. This in turn could either be due to differences in criterion, or possibly individual differences in the contribution of colour channels to the perception of conspicuity.

5.3.3 Comparison of the two experimental systems

The results of the two-way ANOVA performed on the sample of measurements acquired by observer D on both experimental systems, are shown in Table 5-4. The dependent variable was the natural logarithm of mean C_m, and the two factors investigated were "system" and "test condition". The ANOVA showed that the system used (system-1 or system-2) had no effect on the match contrast values obtained. The log of match contrast was dependent on the condition tested ($p<0.001$) and this effect varied with the system used ($p<0.01$), but there was no net effect attributable to the system. The full ANOVA table is shown in appendix A.

FACTOR	SIGNIFICANCE
System	NS
Condition	***
System * Condition	**

Table 5-4. Results of ANOVA for the system comparison, for two levels of the system and 14 levels of the condition. Significance levels are given as ***: $p<0.001$, **: $p<0.01$, *: $p<0.05$, NS: not significant. The ANOVA shows that there was no effect on match contrast due to the system used.

5.3.4 Achromatic matches

A comparison of matches obtained for test targets with positive achromatic contrast and negative achromatic contrast can be seen in Figure 5-8. All five observers

judged the negative achromatic test target to be more conspicuous than the positive achromatic test target. The increase in conspicuity for the negative achromatic target, however, differed greatly with observer: mean C_m for the negative contrast target was judged to be 1.02 to 2.72 times greater than the positive contrast target across the two light levels, although a similar trend can be seen for each observer across the two light levels. These differences in the observer's responses suggest either differences in judgement criterion, or differences in visual processing of luminance increments and decrements between individuals.

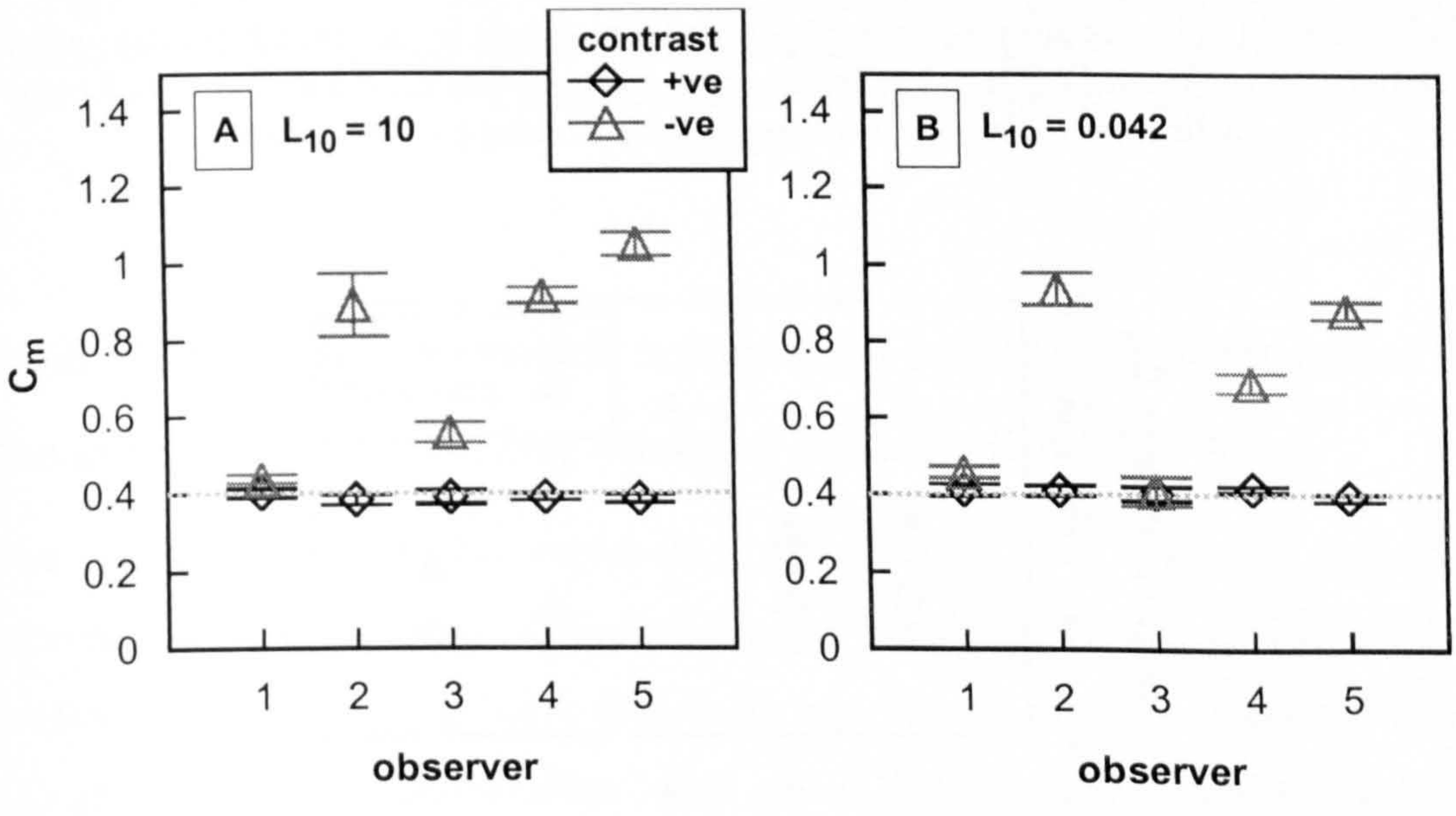

Figure 5-8 (A)-(B). Comparison of conspicuity matches for test targets of positive or negative achromatic contrast, for all five subjects. The magnitude of contrast was 0.4. Matches were obtained at a low photopic (L_{10} = 10) light level (A) and a mid-mesopic (L_{10} = 0.042) light level (B). Error bars indicate ± 2 standard errors from the mean of six matches.

5.3.5 Measurement variability

The within-subject variability and measurement precision was calculated for each observer, see section 5.2.4. The within-subject variability varied with test condition, light level and observer. The mean within-subject variability for any one data point is shown in Figure 5-9 for each observer. The mean within-subject variability was 10%, but variability could be large for individual data points for some subjects; for example, two of the subjects showed a maximum variability of 41% for a single

condition. Measurement precision calculated for light levels 1 and 4 is shown in Table 5-5, and the mean value for each observer is plotted in Figure 5-9. Measurement precision also varied with observer, from 4.1%-8.9%. The mean within-subject variability for each observer was 1.5 to 1.8 times their measurement precision, indicating that in general, the conspicuity matches were fairly precise.

Precision (se as % of mean)	observer 1	observer 2	observer 3	observer 4	observer 5
light level 1	5.2	6.0	8.1	4.3	4.9
light level 4	7.5	6.0	8.9	4.1	4.7

Table 5-5. Match precision for each observer for two light levels. Match precision was calculated as the standard error of the mean of six matches made for a test target of positive achromatic contrast, expressed as a percentage of the mean.

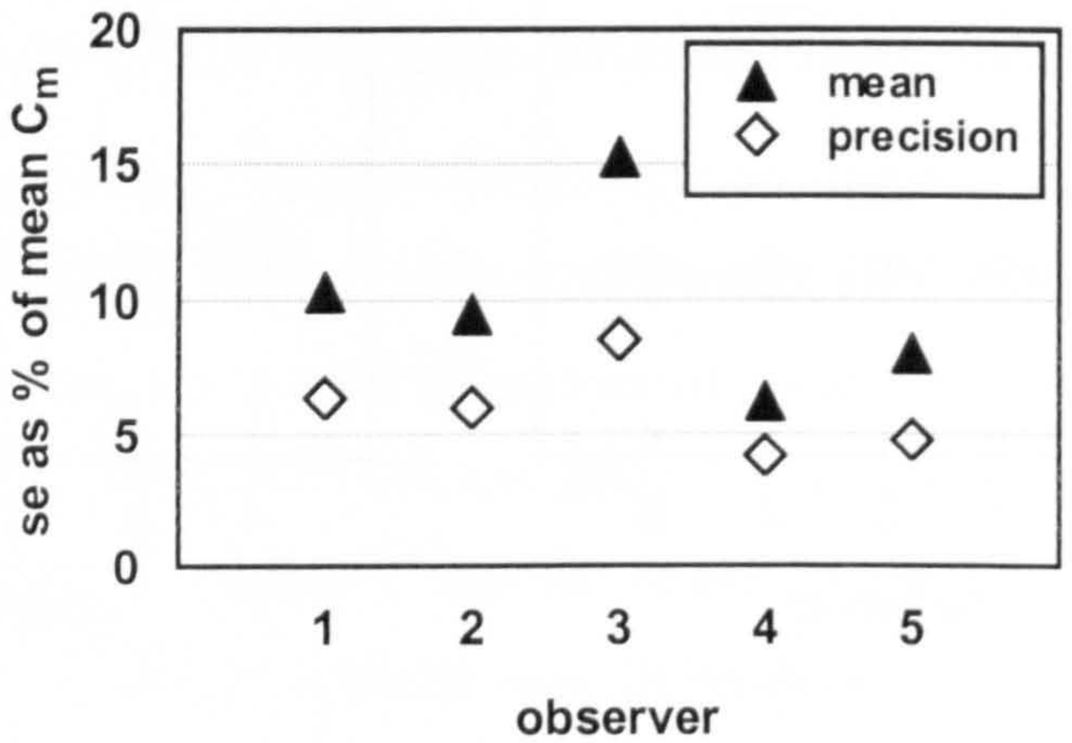

Figure 5-9. Within-subject variability and measurement precision for each observer. Within-subject variability was calculated for all 473 test conditions, here the mean values are plotted. Definitions of within-subject variability and measurement precision are given in the text (see section 5.2.4).

The between-subject variability was calculated for each light level across all test conditions. The mean variability for each light level is shown in Figure 5-10. Between-subject variability was large for some conditions (up to 85%) and tended to be high on average, but decreased with reduction in light level from 46% to 22%. It should be noted that estimates of within-subject and between-subject variability may not be representative of population variability because of the small sample size of only five subjects.

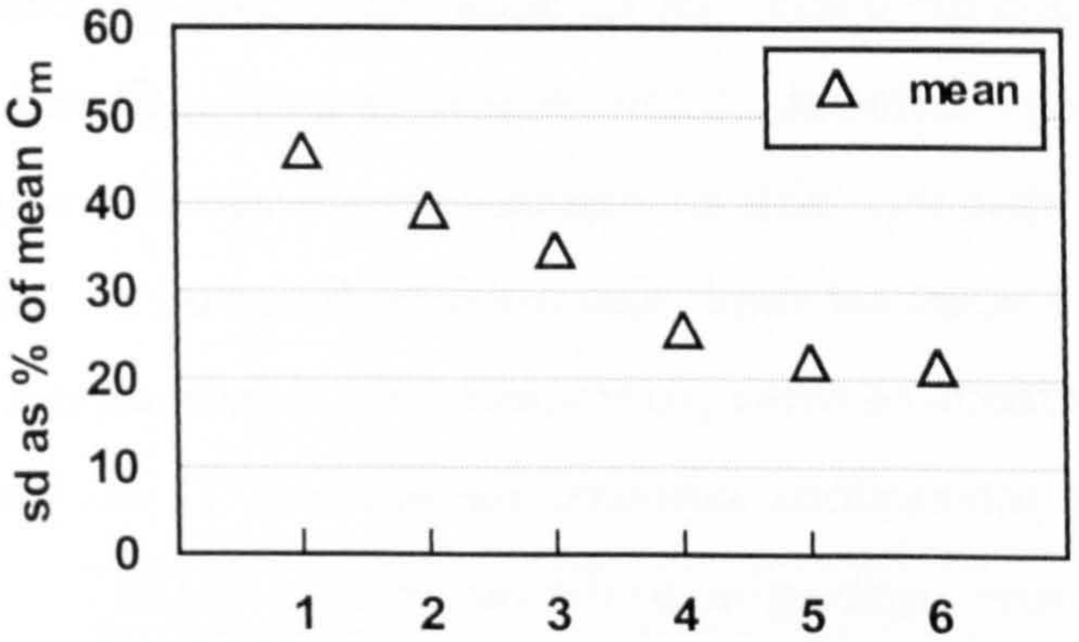

Figure 5-10. Between-subject variability as a function of light level. Between-subject variability was calculated for all test conditions within each light level, here the mean values are plotted. The definition of between-subject variability is given in the text (see section 5.2.4).

5.3.6 Dependence of match contrast on test target parameters in the conspicuity matching data set (results of ANOVA)

The independence of the explanatory variables C_p, C_s, CD and $\log_{10}E$ was investigated by computing a correlation matrix, which is shown in Table 5-6. The correlation coefficients indicate that there was almost no correlation between C_p, CD and $\log_{10}E$, but that there was some correlation between C_p and C_s, and C_s and CD. The correlations involved, however, were small and, therefore, were unlikely to affect markedly the analyses of variance.

	C_p	C_s	CD
C_s	0.267		
CD	-0.007	-0.375	
$\log_{10}E$	-0.053	0.099	-0.094

Table 5-6. The correlation matrix for the explanatory variables C_p, C_s, CD and $\log_{10}E$.

The results of the initial ANOVA, performed on the complete set of 2365 matches, is shown in Table 5-7, and the full ANOVA table is given in appendix A. The factors entered into the analysis were C_p, C_s, CD and $\log_{10}E$, plus all two-way and three-way interactions. Effects of the factor "observer" were also considered. The analysis revealed that C_p, C_s, CD and $\log_{10}E$ had significant effects ($p<0.001$) on the response ($\log_e C_m$). All two-way interactions between the factors were also found to

be highly significant ($p<0.001$, bar C_s x CD: $p<0.01$). Only one of the three-way interactions was significant: the interaction between C_p, C_s and CD ($p<0.001$). The analysis indicated that the value of match contrast was dependent on the photopic contrast, scotopic contrast and chromatic difference of the test plus retinal illuminance. The effects of these parameters were, however, not simply additive due to the significant interactions between parameters. There was also a significant effect on the response attributable to the observer ($p<0.001$).

factor	significance
C_p	***
C_s	***
CD	***
$\log_{10}E$	***
observer	***
Cp x C_s	***
Cp x CD	***
C_p x $\log_{10}E$	***
C_s x CD	**
C_s x $\log_{10}E$	***
CD x $\log_{10}E$	***
C_p x C_s x CD	***
C_p x C_s x $\log_{10}E$	NS
C_p x CD x $\log_{10}E$	NS
C_s x CD x $\log_{10}E$	NS

Table 5-7. Results of ANOVA performed on the complete data set for all main effects, two-way interactions and three-way interactions between the explanatory variables. The dependent variable was $\log_e$(mean C_m). Significance levels are labelled as ***: $p<0.001$, **: $p<0.01$, *: $p<0.05$, NS: not significant.

Results of the second ANOVA, designed to investigate effects of the magnitude and sign of the luminance contrast terms (C_p and C_s), are shown in Table 5-8, with the full table shown in appendix A. The magnitude and sign of the luminance contrast terms were defined according to Eq. 5-4 and Eq. 5-5, respectively.

$$|C| = \begin{cases} C & \text{if } C \geq 0 \\ -C & \text{if } C < 0 \end{cases} \qquad \textbf{Eq. 5-4}$$

$$\text{sign } C = \begin{cases} 1 & \text{if } C > 0 \\ 0 & \text{if } C = 0 \\ -1 & \text{if } C < 0 \end{cases} \qquad \textbf{Eq. 5-5}$$

where C may be photopic or scotopic contrast (C_p or C_s). The results indicated that there were significant effects due to the magnitude and sign of both photopic and scotopic contrast ($p<0.001$). For both sign C_p and sign C_s the response variable was higher for the level "-1", indicating that negative contrast stimuli were judged to be more conspicuous.

factor	significance
CD	***
$\log_{10}E$	***
observer	***
$\|C_p\|$	***
$\|C_s\|$	***
sign C_p	***
sign C_s	***
CD x $\log_{10}E$	***
CD x $\|C_p\|$	*
CD x $\|C_s\|$	***
CD x sign C_p	***
CD x sign C_s	NS
$\log_{10}E$ x $\|C_p\|$	***
$\log_{10}E$ x $\|C_s\|$	***
$\log_{10}E$ x sign C_p	***
$\log_{10}E$ x sign C_s	***
$\|C_p\|$ x $\|C_s\|$	NS
$\|C_p\|$ x sign C_p	***
$\|C_p\|$ x sign C_s	**
$\|C_s\|$ x sign C_p	***
$\|C_s\|$ x sign C_s	*
sign C_p x sign C_s	***

Table 5-8. Results of the ANOVA designed to investigate the effect of both the magnitude and sign of the luminance contrast terms, performed on the complete data set. The dependent variable was $\log_e$(mean C_m), and the factors were $|C_p|$, $|C_s|$, sign C_p, sign C_s, CD and $\log_{10}E$, plus all two-way interactions. Significance levels are labelled as ***: $p<0.001$, **: $p<0.01$, *: $p<0.05$, NS: not significant.

An analysis of variance was also performed for each individual light level to investigate the dependence of match contrast on the explanatory variables, with change in background luminance. The results of these ANOVAs are shown in Table 5-9, with full tables shown in appendix A. Photopic contrast retained a significant effect until the lowest light level tested. Scotopic contrast had a significant effect at all but the highest light level. Chromatic difference was highly significant over the three highest light levels and exhibited minimal or no

significance over the lowest three light levels. No effect was found for log retinal illuminance at any individual light level. For all light levels the effect of photopic contrast varied with the level of scotopic contrast. The effect of photopic contrast also varied with the level of chromatic difference for five of the six background luminances. Effects of scotopic contrast varied with the level of CD at the lowest two light levels only. Some variations in the effect of C_p, C_s and CD were apparent for different levels of log retinal illuminance, but these variations did not follow trends with background luminance.

factor	light level 1	light level 2	light level 3	light level 4	light level 5	light level 6
C_p	***	***	***	***	***	NS
C_s	NS	*	***	***	***	***
CD	***	***	***	NS	*	*
$\log_{10}E$	NS	NS	NS	NS	NS	NS
observer	***	***	***	***	***	***
C_p x C_s	**	***	***	***	***	***
C_p x CD	***	***	**	NS	***	**
C_p x $\log_{10}E$	**	***	NS	NS	NS	NS
C_s x CD	NS	NS	NS	NS	***	***
C_s x $\log_{10}E$	NS	NS	**	NS	**	***
CD x $\log_{10}E$	***	**	NS	NS	NS	*

Table 5-9. Results of the ANOVAs performed for each individual light level, for all main effects and two-way interactions between the explanatory variables. The dependent variable was $\log_e$(mean C_m). Significance levels are labelled as ***: $p<0.001$, **: $p<0.01$, *: $p<0.05$, NS: not significant.

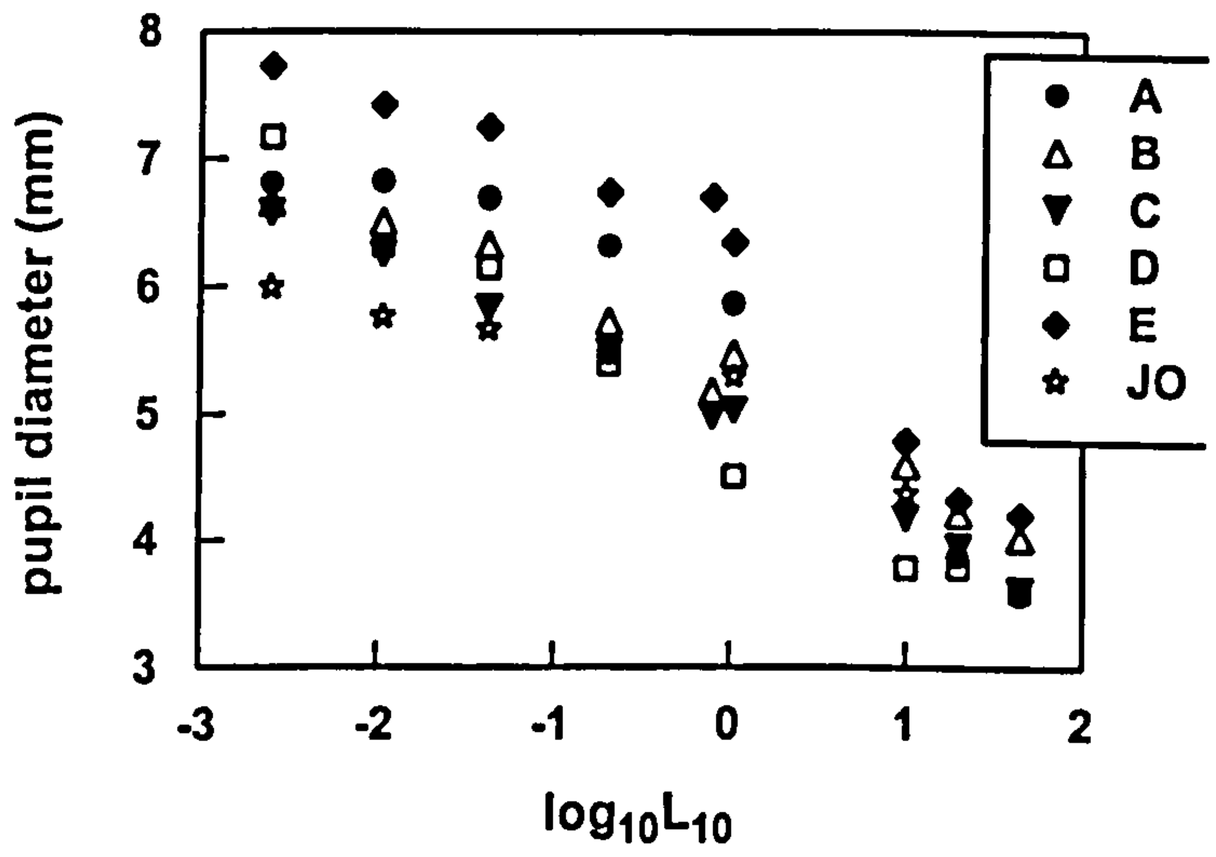

Figure 5-11. Mean pupil diameter as a function of log luminance for six subjects.

5.3.7 Pupil measurements

The measurements of pupil diameter made during collection of each data point in the conspicuity matching data set, have been averaged for each subject to provide an empirical function of pupil size versus background luminance. The function aims to predict steady state pupil diameter throughout the mesopic range, for a uniform, neutral background field of approximately 25° in diameter. Pupil diameters measured at each of the background luminances used in the matching experiments plus three additional light levels, are shown in Figure 5-11 for the five observers A-E and a sixth subject, JO. The L_{10} values of the additional light levels are shown in Table 5-10. The values of pupil diameter plotted for each subject represent the mean value of a large number of measurements (typically over 200) carried out over a number of days.

light level	average background luminance ($L_{b,10}$)
a1	45
a2	20
a3	0.79

Table 5-10. The background luminance (L_{10}) for the three additional light levels at which pupil measurements were made (a1-a3).

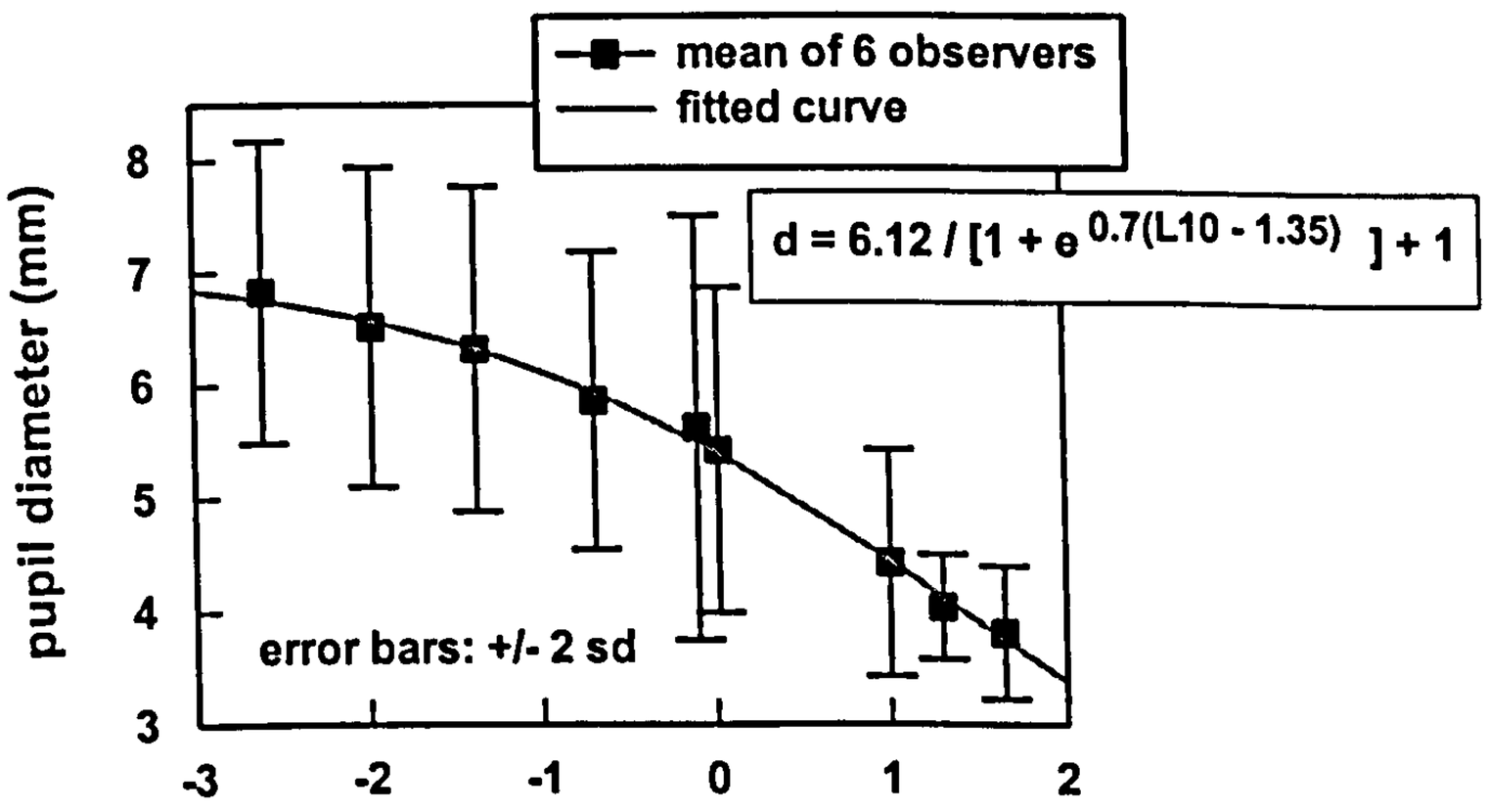

Figure 5-12. Mean pupil diameter as a function of log luminance. Closed symbols represent the mean results of six subjects. The solid line represents a curve of the form given in Eq. 5-6 fitted to the data.

A function of the form given in Eq 5-6 was fit to the mean data for the six observers, with the restraint that the minimum pupil size could not be less than 1 mm and the maximum size could not be greater than 9 mm.

$$d = \frac{D - d_0}{1 + e^{k[\log_{10}(L_b) - a]}} + d_0 \qquad \textbf{Eq. 5-6}$$

where d: pupil diameter, D: maximum pupil diameter, d_0: minimum pupil diameter L_b: background luminance, a and k: adjustable parameters. Figure 5-12 shows the mean data and the fitted function, where L_b was calculated for the 10° observer, resulting in D = 7.12, d_0 = 1, k = 0.7 and a = 1.35.

5.3.8 Development of an empirical model from the conspicuity matching data set

Predictor variables based on the variables C_p, C_s, CD and $\log_{10}E$ and their interactions were entered into a multiple regression procedure to develop a parametric model relating the conspicuity of an achromatic target to a target defined by colour and luminance contrast. Candidate predictor variables reflected the need to separate contrast polarity and to represent important two-way interactions between the experimental variables. The fitting procedure was repeated several times, and the choice and form of predictor variables refined with each iteration on the basis of increasing the multiple coefficient of determination, R^2.

The best fit to the complete data set of 2365 matches, explained 67% of the variance (R^2 = 0.67). It was thought that much of the relatively large proportion of unexplained variance was likely to be due to the large between-subject variability of the data. The finding that the effect of CD on match contrast diminished with fall in light level, see section 5.3.6, plus the observed decrease of between-subject variability with reduction in light level, see section 5.3.5, suggested that differences between the observer's responses might be primarily attributable to differences in response to stimulus CD. To investigate this further, a fit was obtained in which the predictor CD was subdivided into five variables: CD_i, i = 1,...5, which were nonzero for one observer's responses only, see Eq. 5-7.

$$CD_i = \begin{cases} CD, \text{ if } C_m = C_{m,i} \\ 0, \text{ otherwise} \end{cases} \qquad \textbf{Eq. 5-7}$$

where C_m: match contrast (response variable), $C_{m,i}$: match contrast for observer i. Separate regression coefficients were then calculated for each CD parameter. Partitioning the CD parameter in this way greatly improved the fit: the new model yielding an R^2 equal to 0.83. Thus, a substantial portion of the unexplained variance for the fit to the complete data set could be attributed to subject differences in response to stimulus CD.

In order to obtain a single conspicuity-matching model from which an achromatic contrast could be predicted for different photopic contrast/scotopic contrast/chromatic difference combinations, differences in response to CD were overcome by averaging. The five observer's matches were averaged across all conditions, and a new fit acquired. This again improved the percentage of variance explained by the model ($R^2 = 0.89$), but did not alter the parameters in the model, or greatly alter their coefficients, indicating that none of the significant features of the data were lost through averaging. The form of the model is given in Eq. 5-8; and the full model is given in appendix B.

$$C_m = e^{\{k + f(\text{main effects}) + f(\text{interactions})\}} \qquad \textbf{Eq. 5-8}$$

where C_m: match contrast (achromatic), k: constant, f(main effects): function of the main predictor variables, f(interactions): function of pairwise multiples of the predictor variables. Figure 5-13 shows the achromatic contrasts predicted by the model vs. the mean measured values for each test target specification, for all six light levels.

Considering that in many situations values of retinal illuminance are not available, a second version of the model was developed with retinal illuminance replaced by background luminance. To distinguish the form of the model that included retinal illuminance from the form that included background luminance, they will be referred to as version-a and version-b, respectively. Version-b was also of the form given in Eq. 5-8, and is given in full in appendix B. It was found that replacing retinal illuminance with background luminance, not only did not degrade the fit ($R^2 = 0.89$), but also did not alter the form of the terms in the model, or greatly alter the

parameter coefficients. This is not unexpected considering that the retinal illuminance was not found to have a significant effect on match contrast within a single light level, see section 5.3.6. It should be noted, however, that one interaction term for the variable retinal illuminance, found to be significant in version-a, was not significant when replaced with background luminance in version-b.

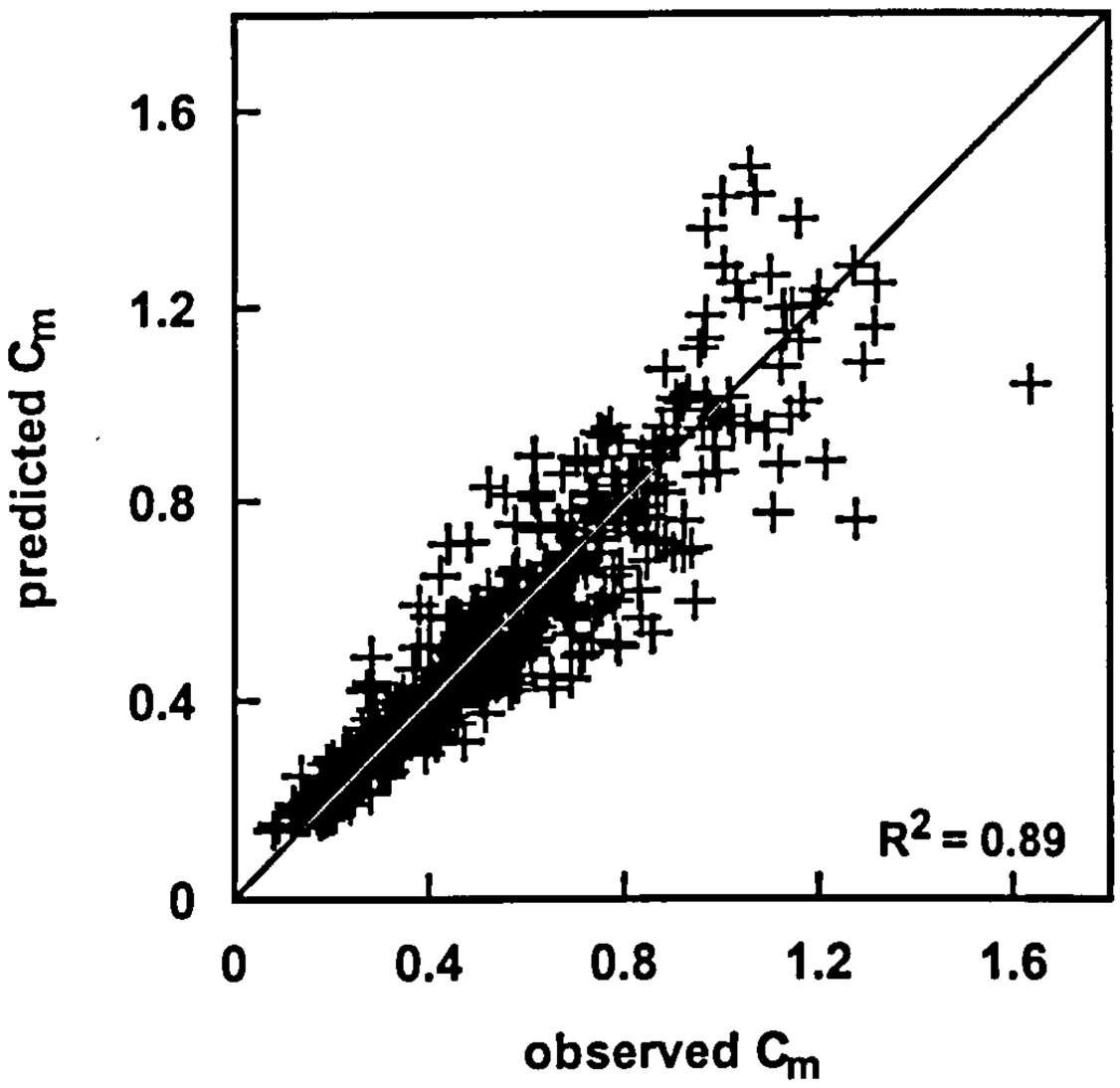

Figure 5-13. Predictions of match contrast (C_m) for version-a of the conspicuity matching model, plotted against the measured values for all 473 test conditions by each of the five observers. The solid line indicates a relationship of unity.

The two forms of the model described above (version-a and version-b) consisted of 19 and 18 significant terms, respectively. To obtain a simpler model, both versions were reduced to a set of 10 terms, these will be referred to as version-a_r and version-b_r. In the regression analysis, a t-test was performed for each regression coefficient to determine whether the coefficient was significantly different from zero. Predictor variables were excluded in a step-wise fashion on the basis of having a regression coefficient with the smallest absolute t-value. Main effect variables were retained regardless of the t-values of their regression coefficients, until all interaction terms for the particular variable had been excluded. This procedure resulted in retention of interaction terms with retinal illuminance/background luminance only. Both reduced models explained 84% of the variance of the data set ($R^2 = 0.84$), hence, the fit was not greatly compromised by reducing the number of model terms. Full

descriptions of version-a_r and version-b_r of the model are given in appendix B. Figure 5-14 shows the achromatic contrasts predicted by the reduced model-a_r vs. the mean measured values for each test target specification, for all six light levels.

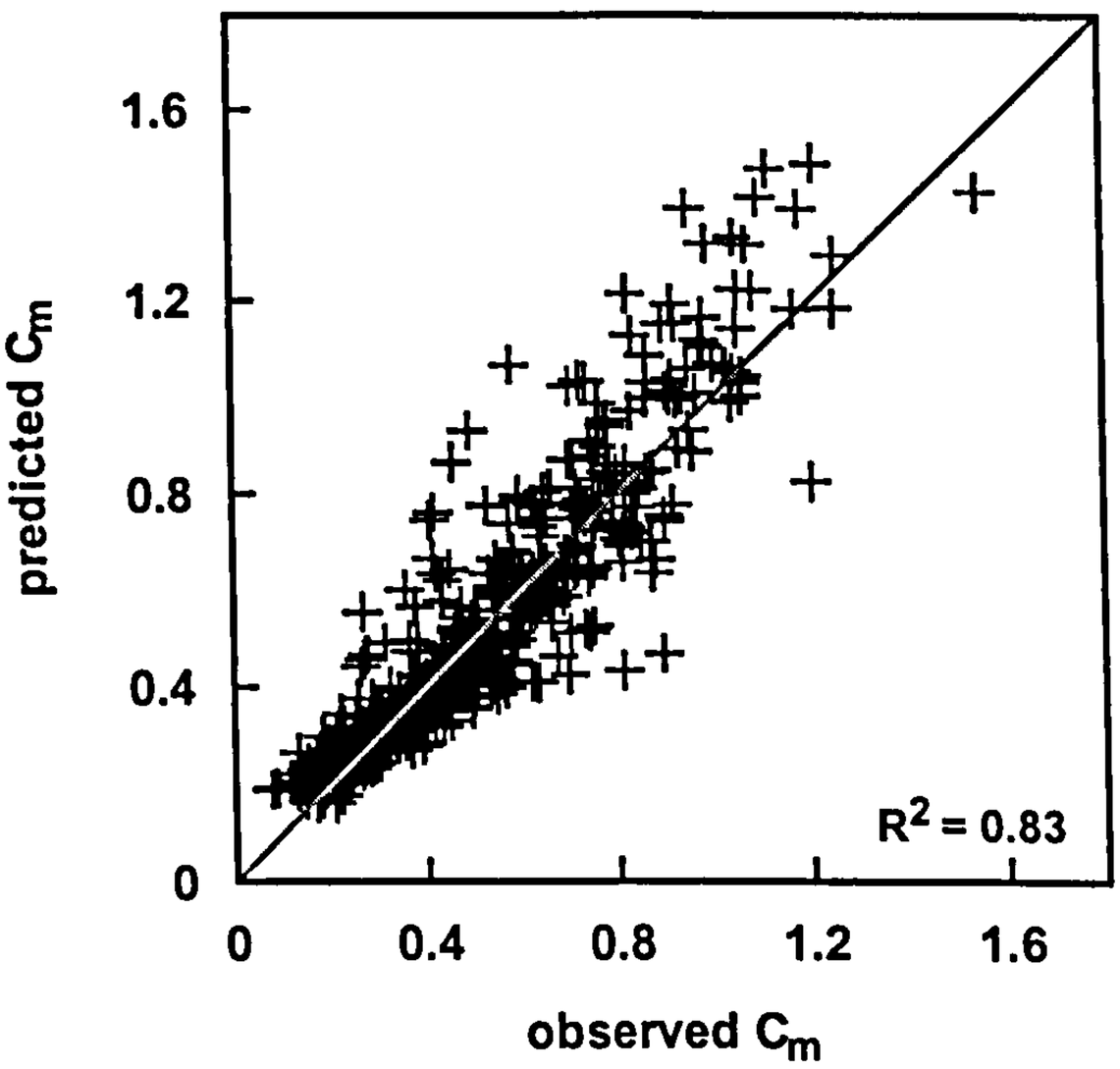

Figure 5-14. Predictions of match contrast (C_m) for version-a_r (reduced version) of the conspicuity matching model, plotted against the measured values for all 473 test conditions by each of the five observers. The solid line indicates a relationship of unity.

5.3.9 Model prediction errors as a function of light level

Prediction errors were calculated for two versions of the model and errors compared at each of the six light levels investigated. Prediction errors were taken as the root mean squared (rms) error, for the total number of pairs of measured and predicted match contrast values at each background luminance, calculated according to Eq. 5-9,

$$E_{rms} = \sqrt{\frac{1}{n}\sum_{i=1}^{n}\left(x_{meas,i} - x_{pred,i}\right)^2} \qquad \text{Eq. 5-9}$$

where E_{rms}: root mean squared error, x_{meas}: measured C_m values, x_{pred}: predicted C_m values, n: number of C_m pairs. The measured match contrast values were taken as the mean of the responses of the five observers. The predictions of match contrast were obtained firstly from version-a, and secondly from version-a_r (the full and reduced versions of the model containing retinal illuminance as a predictor variable,

respectively). Figure 5-15 shows the rms errors for version-a and version-a_r of the model, plotted against log background luminance. The rms error in predicting match contrast for the full version of the model varied with light level, but exhibited no trend with background luminance; the largest error occurring for the highest background luminance (light level 1), and the smallest for light level 2. For the reduced version of the model a similar pattern of errors was seen, with the largest error occurring for light level 1, but in this case the lowest error occurred for light level 5. Comparison of prediction errors for the two versions of the model at each light level, revealed an interesting finding: errors for the reduced version of the model were higher than those of the full version across light levels 2-5, but, remarkably, were lower at the highest and lowest light level. This suggests that although inclusion of all significant terms in the model improved the fit across all light levels, the reduced model performed better at the extremes of illuminance level investigated.

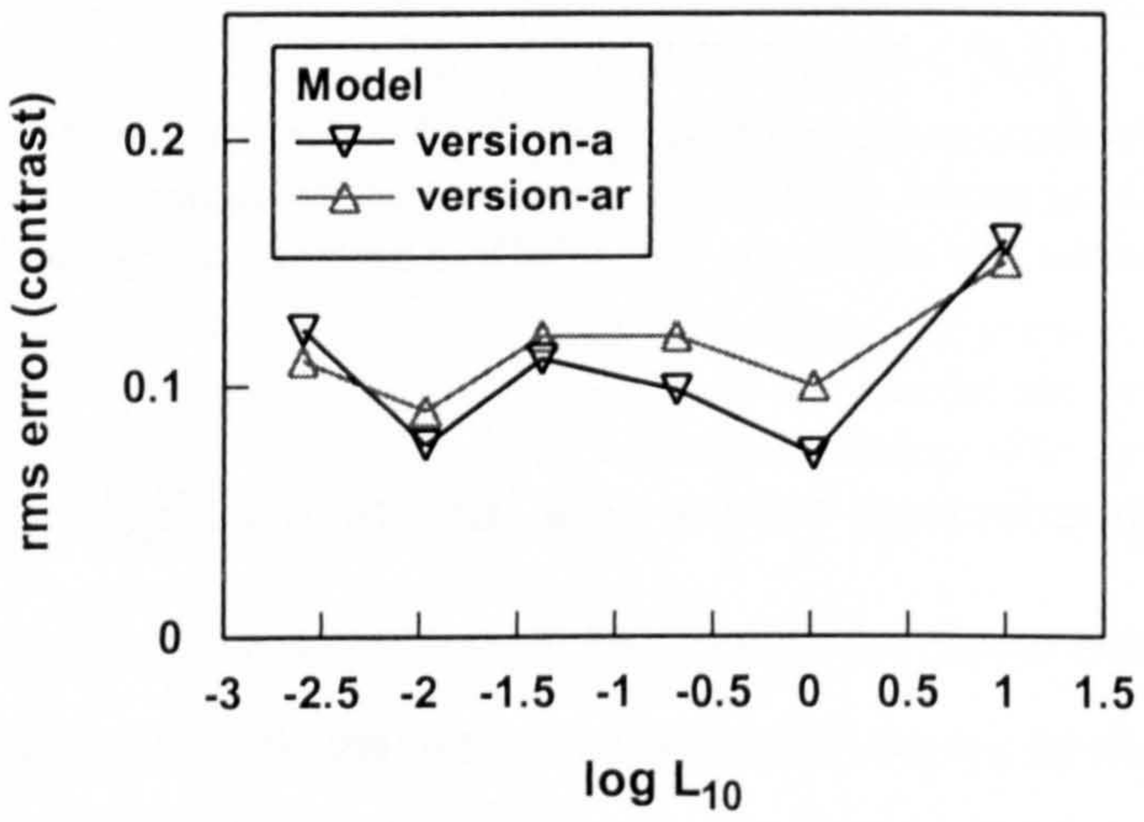

Figure 5-15. Errors in predicting measured match contrast computed for two versions of the conspicuity matching model, as a function of log background luminance. Errors are plotted for version-a and version-a_r: the full and reduced versions of the model with retinal illuminance as a variable. Prediction errors were calculated according to Eq. 5-9.

5.3.10 Comparison of conspicuity with photopic contrast, scotopic contrast and mesopic brightness contrast

To assess how the measure of conspicuity developed in this study relates to measures of luminance contrast in the mesopic range, predictions from a selection

of models proposed as systems of mesopic photometry were compared to the set of acquired conspicuity matches. Several mesopic vision models have been proposed as systems of mesopic photometry. The models considered in the current study, were six systems designed to predict heterochromatic brightness matches for fields of 10° in diameter, which corresponds to the region of the visual field investigated in this study. The systems will be referred to collectively as the 10° systems and individually as the following: Palmer 1st (Palmer 1968), Palmer 2nd (CIE 1989), Sagawa-Takeichi (Sagawa and Takeichi 1987; Sagawa and Takeichi 1992), Nakano-Ikeda (Nakano et al. 1988; CIE 2001), Kokoschka-Bodmann (CIE 1989), and Trezona (CIE 1989; Trezona 1991). For these systems, the perceived brightness of a test stimulus is defined in terms of the luminance of an equally bright reference stimulus. The CIE defined the term "equivalent luminance" to describe luminance equated to a 540 THz (~555 nm) reference stimulus, but the use of different reference stimuli led to the additional definition of "system equivalent luminance" (L_{seq}) to describe the luminance of a test stimulus matched in brightness with a reference other than a 540 THz stimulus. The six 10° systems listed above will predict L_{seq} for a test stimulus, given certain photometric and colorimetric input data. The input requirements and a description of each model is given in appendix C. To compare predictions of these six 10° systems to the measure of conspicuity developed herein, L_{seq} was computed from each system, for both the test and match target and the background of the stimulus, and a "system equivalent contrast" (C_{seq}) calculated for each test and match target, see Eq. 5-10.

$$C_{seq} = \frac{L_{seq,\,target} - L_{seq,\,bkgd}}{L_{seq,\,bkgd}} \qquad \textbf{Eq. 5-10}$$

where $L_{seq,\ target}$: system equivalent luminance for the target, $L_{seq,\ bkgd}$: system equivalent luminance for the background. Values of C_{seq} could then be compared to those of conspicuity determined from the matching procedure. For each of the six 10° systems, L_{seq} was kindly computed for each paired data point in the conspicuity matching data set by Dr. Ken Sagawa.

The conspicuity matching data set consisted of pairs of test and match targets that were judged to be equally conspicuous, i.e. have the same measure of conspicuity. To assess how this measure relates to measures of mesopic luminance contrast, C_{seq}

values were predicted for test-match pairs in the data set, for each of the six 10° systems, according to Eq. 5-10. Of the combinations of test target parameters comprising the conspicuity matching data set, some appeared darker than the background, because the C_p and C_s values could be negative as well as positive. The match target, on the other hand, was always defined by positive achromatic contrast and, therefore, always appeared lighter than the background. Hence, the conspicuity matching data set contained many test-match pairs that differed in contrast polarity. Due to the lack of equivalence between the conspicuity of stimuli with negative and positive contrast found in this study, it was not possible to compare values of $|C_{seq}|$ for test-match pairs that differed in contrast polarity. For all test-match pairs the match target was defined by positive achromatic contrast, so all test targets with negative effective contrast had to be eliminated from the analysis. It is not possible to determine theoretically which test target combinations of $\pm C_p$, $\pm C_s$ and CD had a positive effective contrast, but it is possible to assume that all test targets with positive C_p and C_s values will appear lighter than the background. Therefore, C_{seq} values were only obtained for the subset of test-match conditions for which the test target specification consisted of $C_p \geq 0$ and $C_s \geq 0$. An advantage of the conspicuity model is that it can be used to compare stimuli of either contrast polarity, because it predicts a positive achromatic contrast for any test stimulus specification.

Using the subset of test-match conditions with positive contrast polarity, differences in C_{seq} for the test target and C_{seq} for the match target were calculated at each light level, for each 10° system. The prediction error for each light level was taken as the root mean squared (rms) error, computed according to Eq. 5-11.

$$E_{rms} = \sqrt{\frac{1}{n}\sum_{i}^{n}\left(C_{seq,\,test,\,i} - C_{seq,\,match,\,i}\right)^2} \qquad \textbf{Eq. 5-11}$$

where E_{rms}: root mean squared error, n: number of test-match pairs per light level, $C_{seq,\ test}$: system equivalent contrast for the test target, $C_{seq,\ match}$: system equivalent contrast for the match target. In this way, E_{rms} reflects the extent to which two stimuli matched in terms of conspicuity, also match in terms of the measure of mesopic luminance contrast obtained from one of the 10° systems. The root mean squared error was also calculated for differences between the test and match contrast, computed using either the $\bar{y}_{10}(\lambda)$ function or the $V'(\lambda)$ function, i.e.

differences between test and match target luminance contrast obtained from either L_{10} or L′. Lastly, prediction errors were calculated for the conspicuity model. Version-b of the model was used to predict values of conspicuity for both the test and match targets, and these values were treated as $C_{seq,\ test}$ and $C_{seq,\ match}$ in the calculation of E_{rms} according to Eq. 5-11.

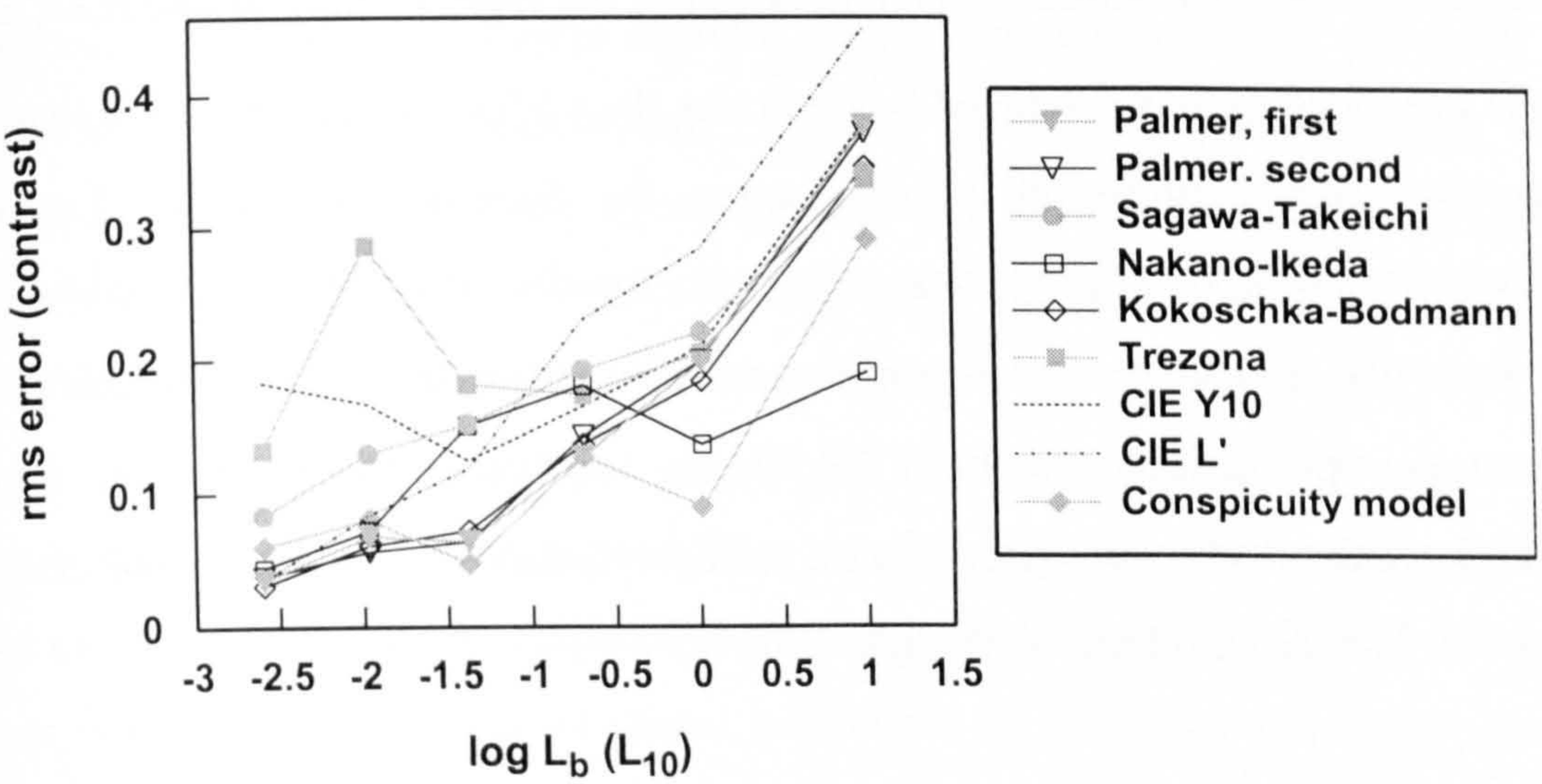

Figure 5-16. A comparison of the ability of nine different models to predict matches in conspicuity throughout the mesopic range. Prediction errors were computed for six proposed systems of mesopic photometry, the conspicuity matching model (version-b), the $\bar{y}_{10}(\lambda)$ function and the V′(λ) function. Prediction errors were calculated according to Eq. 5-11.

Figure 5-16 shows the prediction errors (E_{rms}) for the data set of pairs of stimuli matched for conspicuity, computed for each of the six 10° systems, the conspicuity model, the $\bar{y}_{10}(\lambda)$ function and the V′(λ) function. The errors are plotted as a function of log background luminance. Of the 10° systems, prediction error curves for Palmer 1st, Palmer 2nd and the Kokoschka-Bodmann systems were very similar at all light levels. These curves approximately followed the error curve for the $\bar{y}_{10}(\lambda)$ function at the highest two light levels (light levels 1-2) and the error curve for the V′(λ) function at the lowest two light levels (light levels 5-6). All three systems produced smaller prediction errors than those for either $\bar{y}_{10}(\lambda)$ or V′(λ) at the five highest light levels, and at the lowest light level, Palmer 2nd and Kokoschka-Bodmann were the only systems to perform better than both $\bar{y}_{10}(\lambda)$

and $V'(\lambda)$. Error curves for the remaining three models followed the two Palmer curves and the Kokoschka-Bodmann curve either at the higher or lower luminances and produced different prediction errors at other light levels. The Sagawa-Takeichi and Trezona models produced significantly larger errors at the lower four light levels, whereas the Nakano-Ikeda model produced larger errors for light levels 3-4, but markedly smaller errors for light levels 1-2. The Nakano-Ikeda system performed better than either $\bar{y}_{10}(\lambda)$ or $V'(\lambda)$ at the highest three luminances, and also at light level 5, but produced larger errors than $V'(\lambda)$ at the lowest luminance. In general, compared to the other systems, the Sagawa-Takeichi and Trezona systems were not good at predicting conspicuity matches at any light level. Although five of the 10° systems produced smaller prediction errors that $V'(\lambda)$ at light level 5, differences in prediction errors for $V'(\lambda)$, Palmer 1st, Palmer 2nd, the Nakano-Ikeda and Kokoschka-Bodmann systems were relatively small. This was also the case at the lowest background luminance (light level 6).

Figure 5-16 also shows that prediction errors for the conspicuity model were smaller than those based on either $\bar{y}_{10}(\lambda)$ or $V'(\lambda)$ for light levels 1-5, but larger than the errors for $V'(\lambda)$ at the lowest light level. The conspicuity model performed better than all six 10° systems for a large part of the mesopic range: light levels 2-4, although a marked difference in prediction error was only seen at light level 2. The conspicuity model produced larger errors than the Palmer 1st, Palmer 2nd and the Kokoschka-Bodmann systems at light level 5, but only by a relatively small factor, but much larger errors than the Nakano-Ikeda system at the low photopic light level (light level 1).

These results suggest that conspicuity can successfully be computed using the $V'(\lambda)$ function below a photopic L_{10} luminance of about 0.01, but that at higher light levels an alternative function to either $V'(\lambda)$ or $\bar{y}_{10}(\lambda)$ should be used. Over the mid to high mesopic range the conspicuity model exhibited some advantage over the six 10° systems of mesopic photometry investigated. At the low photopic level, the Nakano-Ikeda system was the best candidate for predicting conspicuity.

5.4 Discussion

The results of this chapter have shown that it is possible to measure the conspicuity of a target defined by colour and luminance contrast in terms of an achromatic luminance contrast reference scale, by equating its perceived conspicuity with a similar target defined by achromatic luminance contrast. For the matching procedure employed to measure stimulus conspicuity, measurement variability was, in general, close to the measurement precision. Under the definition given above, conspicuity depended strongly upon sign-dependent photopic contrast (C_p), sign-dependent scotopic contrast (C_p), chromatic difference (CD) and retinal illuminance (E)/background luminance (L_b) of the stimulus, plus interactions between these four parameters. An empirical model of this relationship was successfully developed, which produced a good fit to the data. Analysis performed on the data set of conspicuity matches acquired in this study, and the model derived from these matches, revealed features of visual processing in the mesopic range that are discussed below.

5.4.1 Luminance contrast and conspicuity

The results for test targets of achromatic contrast and the high statistical significance found for the effects of the sign as well as the magnitude of photopic and scotopic contrast in the data set, suggest that negative luminance contrast is more effective than positive luminance contrast in the mesopic range. Higher suprathreshold discrimination thresholds have been found for luminance increments compared to decrements under photopic conditions (Vingrys and Mahon 1998), and the perceived contrast of negative contrast gratings was found to be greater than that of positive contrast gratings, when investigated under photopic conditions (Barbur and Forsyth 1990). In the mesopic range shorter search times have been reported for negative compared to positive contrast stimuli (Barbur et al. 1998a), and Blackwell (1946) reported 20% lower detection thresholds for negative compared to positive contrast stimuli at low adaptation levels. Results of the present study also showed a large variation in the magnitude of this luminance contrast asymmetry between observers, but the reason for this variability is unclear. The

differences between observers were similar over the two light levels investigated, and may have been due to differences in criterion, or could be explained as between-observer differences in the gain control of the mechanisms that signal luminance increments and luminance decrements.

The relative contribution of stimulus photopic contrast and scotopic contrast to conspicuity was found to vary with light level as expected. Analysis of the conspicuity matching data set revealed that C_p had a highly significant effect on match contrast (C_m) at all but the lowest light level investigated, whereas C_s was found to have a significant effect on C_m at all but the highest light level. These results indicate that over the majority of the mesopic range, conspicuity depends strongly on both C_p and C_s. These findings are similar to those of Barbur et al. (1998a), who reported that the main determinant of visual search in the high mesopic range was photopic contrast and in the low mesopic range was scotopic contrast. Examination of the relationship between C_m and C_p across all test conditions at a high background luminance (light level 1), revealed an approximately bilinear function (see Figure 5-6). Likewise, an approximately bilinear relationship was seen between C_m and C_s (see Figure 5-6) across all test conditions at a low background luminance (light level 5).

5.4.2 Colour and conspicuity

Analysis of the conspicuity matching data set confirmed that the contribution of colour to conspicuity, measured in terms of chromatic difference (CD), diminished with reduction in light level. Chromatic difference was found to be a highly significant determinant of achromatic match contrast (C_m) at the low photopic and high mesopic light levels investigated (light levels 1-3), but less significant, or not significant at the mid to low mesopic levels (light levels 4-6). Results obtained at the higher light levels revealed an approximately linear relationship of conspicuity with CD, not only for the conditions with zero luminance contrast (Figures 1-3, 1-4 and 1-7), but across all conditions investigated (Figure 5-6). Considering the relationship observed between conspicuity and photopic contrast at the highest light level investigated, this suggests that conspicuity is predominantly dependent on a

combination of photopic contrast and chromatic difference in the high mesopic range. The statistical analysis indicated that the contribution of CD to conspicuity was, in general, dependent on the value of photopic contrast (C_p) across all light levels, and dependent on the value of scotopic contrast (C_s) at the lower light levels. The fitting procedure, however, showed that a good fit could be obtained to the data (model version-a_r and version-b_r) even when these interactions were ignored.

The metric CD was chosen to represent an approximate measure of chromatic saturation. CD was defined as the distance in a chromaticity space derived from colour matches carried out under photopic conditions. Although colour matches carried out under mesopic conditions differ from those at photopic levels, the only standard spaces in which colour stimuli may be specified relate to the photopic range. If a chromaticity space were to be derived from mesopic colour matches, it is expected that a mesopic CD metric would also have a diminishing contribution to conspicuity with reduction in light level. The reason that CD become less effective in the mesopic range is that when the cones move towards the lower end of their operating range the signal to noise ratio falls. A larger colour signal i.e. a larger CD is required, therefore, to obtain a stimulus of equivalent perceived chromatic saturation. In order to obtain a colour metric whose contribution to conspicuity would not diminish with reduction in light level, one would have to scale CD in relation to the operating characteristics of the cones. It is not possible merely to scale the CD metric in relation to the increase in chromatic threshold observed with reduction in stimulus luminance (see the results of chapter 4). One reason being that the extension of threshold to suprathreshold behaviour cannot be generalised across all colour directions. As far as the conspicuity model is concerned, it is sufficient to include the parameter CD, unmodified, and reduce its weighting with the fall in background luminance.

Analysis of the data also revealed a number of findings indicative of inter-observer differences in the weighting of the contribution of colour to conspicuity. Firstly, inter-subject differences were observed in the slope of the C_m vs. CD relationship for zero contrast conditions. Secondly, between-subject variability decreased with light level as stimulus colour became less effective. Thirdly, the fit of the model to

the data was much improved when the predictor variable CD was subdivided into five variables, relating to the responses of each observer. The following discussion compares inter-observer differences in response to colour in the case of conspicuity matching, to reports in the literature of inter-observer differences in response to colour in relation to brightness matching. The measure of conspicuity adopted in this study, as stated in the introduction, is essentially a measure of effective contrast. Du Buf (1992) observed that brightness matching relationships differed from, but were closely related to effective contrast matching relationships for achromatic stimuli, and modelled effective contrast with some success as a function of brightness difference at target edges. This evidence for a close relationship between brightness and effective contrast or conspicuity provides justification for extending known effects of brightness matching to the conspicuity matching data.

It is well known that under photopic conditions the perception of brightness does not correspond to luminance, i.e. that heterochromatic brightness matches differ from flicker photometric matches (from which $V(\lambda)$ was derived) (Wagner and Boynton 1972; Comerford and Kaiser 1975). The basis for this difference is thought to be that flicker photometry reflects processing of the achromatic magnocellular pathway, and that heterochromatic brightness matching also involves the parvocellular pathway (Ingling and Martinez-Uriegas 1983). Heterochromatic brightness matches must, therefore, include contributions from the postulated achromatic mechanism and two colour opponent mechanisms. The difference between heterochromatic brightness matches and flicker photometric matches is often expressed as a brightness to luminance ratio (B/L). Studies have reported large inter-observer variations in the photopic B/L ratio (Burns et al. 1982; Yaguchi et al. 1993; Ayama and Ikeda 1998). Yaguchi et al. (1993) suggested that the origins of individual differences in B/L ratio, are inter-observer differences in the contribution of chromatic mechanisms to brightness. Nakano et al (1988) successfully modelled individual differences in photopic heterochromatic brightness matches by varying the contribution of opponent colour mechanisms. Individual differences are also found in the upper mesopic range, between the perceived lightness of coloured objects when matched with a grey scale (Ikeda et al. 1989; Ikeda and Ashizawa 1991). Similar to findings of the present study, these differences

diminish with light level, i.e. inter-observer differences diminish as chromatic sensitivity is reduced. This combined evidence from photopic and mesopic brightness matching investigations, suggests that inter-observer differences in the weighting of CD to conspicuity observed at mesopic levels in this study, could be a consequence of individual differences in the contribution of chromatic mechanisms to conspicuity.

5.4.3 The conspicuity model

For the two versions of the conspicuity model that include all significant predictor variables (version-a and version-b), achromatic match contrast is a nonlinear function of C_p, C_s and CD, with luminance contrast terms weighted by sign, and includes contributions weighted by retinal illuminance (version-a) or luminance (version-b). For the reduced designs of the model, which consist of 10 parameters (version-a_r and version-b_r), achromatic match contrast is a linear function of $|C_p|$, positive C_s, negative C_s and CD, with contributions weighted by retinal illuminance (version-a_r) or luminance (version-b_r).

Results from the pilot study and measurements performed during collection of the conspicuity matching data set showed that the conspicuity of coloured stimuli with zero photopic and scotopic luminance contrast, was found to increase linearly with chromatic difference from the background. For these conditions it was only possible to investigate two directions of chromaticity space using a CRT display, for which stimuli appeared either red or green. In general, equal achromatic contrast was required to match a given CD of either hue. This finding of a linear response, which is independent of hue, supports the use of CD as a variable in the conspicuity model. Reports that search time for stimuli with equal luminance contrast measured under photopic conditions, is dependent on stimulus hue (Barbur and Forsyth 1990; Nagy and Sanchez 1990; D'Zmura 1991) suggest, however, that equal-luminance chromatic stimuli in other areas of chromaticity space would not exhibit the same relationship between conspicuity and CD. The implications are, that by averaging out the contribution of colour contrast to conspicuity across all directions of chromaticity space, the model may fail to sufficiently explain the variability in

response to colour. This may account for a proportion of the 11 % of unexplained variance in the model..

5.4.4 Photopic contrast, scotopic contrast and mesopic brightness contrast as predictors of conspicuity

The comparison of conspicuity with predictions of mesopic luminance contrast obtained from proposed systems of mesopic photometry, revealed some interesting similarities and differences between these two measures. The six proposed systems of mesopic photometry were all based on heterochromatic brightness matching, but the ability of each system to predict the data set of acquired conspicuity matches differed, with differences depending on light level.

At the highest two light levels investigated (L_{10} = 10 and L_{10} = 1), five of the systems (Palmer 1st, Palmer 2nd, Sagawa-Takeichi, Kokoschka-Bodmann and Trezona) produced large prediction errors, which suggests that none of these systems adequately accounts for the chromatic contribution to conspicuity. Furthermore, prediction errors for the five systems at these two light levels were similar to those computed for the $\bar{y}_{10}(\lambda)$ function. Although the $\bar{y}_{10}(\lambda)$ function was derived from colour matches and with flicker measurements carried out at only three wavelengths, it is generally accepted that it is representative of a spectral luminous efficiency function measured for a 10° field (Wyszecki and Stiles 1982), and as such is likely to reflect predominantly magnocellular processing. Heterochromatic brightness matching on the other hand, as mentioned above, includes a chromatic contribution. It is surprising then, that the five of the mesopic systems do not perform significantly better that the $\bar{y}_{10}(\lambda)$ function at the highest light levels. It must be considered, however, that the Palmer 1st system and the Palmer 2nd system, are functions of L_{10} and L', only and do not consider the chromatic contribution to brightness, therefore they would not be expected to perform better than $\bar{y}_{10}(\lambda)$ at light levels for which the scotopic contribution is minimal (low photopic/high mesopic).

The Nakano-Ikeda system outperformed all other systems including the conspicuity model at the low photopic light level (L_{10} = 10). This system converts photopic luminance to a photopic brightness using chromatic input, and combines it with a scotopic factor. The relatively low error obtained at L_{10}=10 is evidence that the computation of photopic brightness for this system, produces a superior prediction of conspicuity in the low photopic range. The relatively poor performance of the conspicuity model at this light level may be attributed to the inadequacy of the variable CD to represent the contribution of colour to conspicuity for different stimulus hues. The Nakano-Ikeda system also outperformed the remaining five mesopic systems at light level 2 (L_{10} = 1), but produced a larger prediction error that the conspicuity model for this background luminance. It is suggested that the dependence of conspicuity on stimulus hue is markedly reduced at this light level, leading to an improved fit for the conspicuity model.

Over the mid-mesopic range (light levels 3-4, L_{10} = 0.2-0.04), the conspicuity model produced the smallest prediction errors, but was closely followed by three of the mesopic systems. Two of these systems were the Palmer 1st and Palmer 2nd systems, which contain no chromatic component. This suggests that consideration of the contribution of colour to conspicuity is unnecessary in the mid-mesopic range, because it can be adequately predicted from a suitable combination of $\bar{y}_{10}(\lambda)$ and $V'(\lambda)$.

At the lowest two light levels (L_{10} = 0.01-0.002), the majority of the mesopic systems did not predict conspicuity matches significantly better than the $V'(\lambda)$ function. Some systems produced much larger prediction errors than $V'(\lambda)$, including the conspicuity model at the lowest light level. These findings indicate that conspicuity can be adequately predicted using $V'(\lambda)$, below a luminance of L_{10} = 0.01.

The measure of conspicuity investigated in this study appears to be related to a measure of mesopic luminance based on a suitable combination of $\bar{y}_{10}(\lambda)$ and $V'(\lambda)$, over the mid to low mesopic range. In the high mesopic range, the chromatic

contribution to conspicuity becomes more important, and conspicuity bears a good relationship to mesopic luminance based on brightness matches, but only if the chromatic contribution to brightness is successfully modelled.

6 Conspicuity and visual search performance in the mesopic range

6.1 Introduction

Visual search describes the process whereby a subject locates and identifies a target stimulus presented amongst a scene of distracter stimuli. Stimulus conspicuity has been proposed as an essential determinant of visual search performance (Verghese and Nakayama 1994; Itti and Koch 2000; Palmer et al. 2000). Engel (1977) showed that visual search time is strongly related to a measure of stimulus conspicuity based on the maximum eccentricity at which a briefly presented target object can be detected with a given probability (conspicuity area). Engel restricted his investigations to achromatic stimuli under conditions that fall in the high mesopic range. A strong correlation was also found between visual search time and the conspicuity distance measure (related to Engel's definition of conspicuity) used by Kooi and Toet (1999). They investigated complex greyscale images in dim lighting conditions. Barbur and Forsyth (1990) showed at photopic levels that stimuli defined by both colour and luminance contrast and those defined purely by colour (isoluminant stimuli), matched for conspicuity with similar stimuli defined by achromatic luminance contrast, had highly correlated search times. These studies suggest that conspicuity is closely related to visual search performance, but the investigations focused either on achromatic stimuli or coloured stimuli under photopic viewing conditions. In many real life situations, visual search is performed under mesopic conditions in a coloured scene. One of the aims of this study, therefore, was to investigate the relationship between an appropriate measure of conspicuity and visual search performance for targets defined by a combination of colour and luminance contrast, throughout the mesopic range.

A recent study of visual search performance in the mesopic range (Hurden et al. 1997; Barbur et al. 1998a; Hurden et al. 1999) reported that visual search times were strongly related to the level of illumination, the photopic contrast, scotopic contrast and colour difference of the stimulus to the background. They showed, however, that low photopic/mesopic search performance could be successfully modelled as a function of background luminance and luminance contrast of the target, only, ignoring any effects of colour. Other investigations have stressed the relevance of stimulus colour in determining visual search performance. Nothdurft (1993), and Turatto and Galfano (Turatto and Galfano 2000) reported that among other stimulus features, colour can facilitate visual search by attracting attention, whether colour is task-relevant or task-irrelevant. During active visual search, Motter and Belky (1998) hypothesised that as a guide for saccades, colour is more effective than orientation. D'Zmura (1991) found that pop-out of chromatic targets during search was not restricted to colour directions associated with the cardinal colour mechanisms, suggesting that chromatic detection mechanisms also exist for intermediate hues. Monnier and Nagy (2001) also provided evidence in support of individual detection mechanisms for intermediate hues. Carter and Carter (1981) showed that visual search performance for chromatic stimuli was strongly related to both CIELAB and CIELUV colour difference. Barbur and Forsyth (1990) also investigated the relationship between CIELUV colour difference and search performance, but found it correlated less well with search performance than their measure of conspicuity. These studies focussed on visual search under photopic conditions. It is evident that colour plays an important role in photopic visual search, but the model produced by Hurden et al. (Hurden et al. 1997; Barbur et al. 1998a; Hurden et al. 1999) indicates that colour may have minimal effect under mesopic conditions.

The measure of conspicuity developed in chapter 5 relates the conspicuity of a target defined by colour and luminance contrast to that of a similar target defined by achromatic contrast. In chapter 5, measurements of conspicuity were obtained throughout the mesopic range from which an empirical model was derived. According to this model, conspicuity is strongly dependent on the level of illumination, and stimulus photopic contrast (C_p), scotopic contrast (C_s) and colour

difference to the background (CD), plus interactions between these parameters. The significance of colour difference in determining stimulus conspicuity, was found to diminish with the reduction in light level, but remained a significant variable in the model throughout the mesopic range. The secondary aim of the current study, therefore, was to assess whether colour difference remains an important parameter in mesopic visual search.

Visual search performance is often dependent on the number of stimuli presented to the subject; a phenomenon known as the set-size effect. Set-size effects are in turn dependent on the discriminability or conspicuity of the target, along with other stimulus features (Bergen and Julesz 1983; Palmer 1994; Verghese and Nakayama 1994). For example, search for a highly conspicuous target will show little dependence on set-size, whereas search performance for a less conspicuous target will deteriorate with an increase in the number of distracters. Search performance may also be affected by the heterogeneity of distracters. Again, these effects depend on the discriminability or conspicuity of the target (Duncan and Humphreys 1989; Duncan 1989). If a target is sufficiently conspicuous, search performance will be independent of distracter variability, whereas for a target that is similar to the distracters, search will be degraded by increases in distracter heterogeneity.

The relationship between conspicuity and visual search performance in the mesopic range was investigated using the measure of conspicuity developed in chapter 5. As conspicuity was obtained in reference to an achromatic contrast scale, search performance for targets with a combination of colour and luminance contrast was compared to performance for achromatic targets. Visual search was characterised for targets defined by achromatic luminance contrast and measured for a selection of targets defined by colour and luminance contrast (CD, C_p and C_s) at different light levels in the mesopic range. Search performance for the colour/luminance targets were then compared with search times for the achromatic targets predicted by the model to be equally conspicuous as the colour/luminance stimuli.

6.2 Subjects and methods

The visual search procedure used in this investigation was described in section 2.6. Search performance was measured using an orientation task, with targets based on Landolt rings. An intermediate difference between orientation of the target and distracter rings was employed, to ensure that search performance was dependent on target colour and luminance contrast rather than orientation pop-out. Distracter number was kept constant for all experiments to maintain constant set-size effects. Although the task (orientation discrimination) was not related to the dimension in which the distracters varied, i.e. colour and luminance contrast, possible effects of across dimension distracter heterogeneity were minimised by presenting every achromatic and colour/luminance target specification as a distracter in the search stimulus for each light level and restricting the variability of additional distracters.

Search time was measured for achromatic targets as a function of achromatic luminance contrast at four light levels spanning the low photopic and mesopic range. Search times were also measured for targets with different combinations of colour and luminance contrast at these light levels. These data were then used to examine changes in achromatic visual search with reduction in light level, to investigate the relationship between conspicuity and visual search performance under mesopic conditions, and assess the role of colour in mesopic visual search.

6.2.1 Subjects

Four observers participated in the experiments. Observer D, who also took part in the conspicuity matching experiments in chapter 5, and observers F, G and H. All observers were female with mean age 25.3, range 22-30. All observers were normal trichromats according to the Ishihara plates, and had a high contrast visual acuity of 0.0 log minimum angle of resolution (logMAR) or better and low contrast acuity of 0.2 logMAR or better.

6.2.2 Methods

Visual search times were measured for four of the six light levels used in the conspicuity matching experiments (light levels 1, 2, 4 and 5). Table 6-1, shows the background luminances for these light levels. The measurement of search time for targets defined by achromatic contrast and those defined by a combination of colour and luminance contrast at each light level were obtained simultaneously. At each light level, 12 target specifications were investigated. Six of the target specifications consisted of positive achromatic contrast. The other six specifications were a subset of the conditions used in the conspicuity matching experiments, and consisted of combinations of the parameters C_p, C_s and CD. All 12 specifications were present in every stimulus, one as the target and the remainder as distracters. The target specification varied randomly between the 12 conditions. Nineteen distracters were present in every stimulus. Of the remaining eight distracters, four were randomly given values of positive or negative achromatic contrast within a fixed range, and four were randomly given values of C_p, C_s and CD from the set of all possible combinations that could be reproduced on the stimulus display.

Light level	Nominal filter density	Mean optical density at 45° incidence	Background luminance L_{10}	Dark adaptation time (min)
1	NONE	0	10	5
2	0.8	0.95	1.1	10
4	2.0	2.34	0.046	20
5	2.5	2.93	0.012	25

Table 6-1. Filter densities, background luminances and dark adaptation times, for system-1, at each of the four light levels investigated in the visual search experiments. Dark adaptation times were identical to those used in Chapter 5.

The six target specifications consisting of achromatic contrast were selected on the basis of preliminary measurements, to give approximately linearly increasing search times. The preliminary measurements revealed changes in visual search performance for achromatic contrast targets as stimulus luminance was reduced. For this reason, different sets of target conditions were used at each light level. The values of achromatic contrast investigated at each light level are given in Table 6-2. The six target specifications with chromatic content defined in terms of C_p, C_s and CD (colour/luminance targets) were chosen to have ranked match contrast values as

predicted from the empirical model developed in chapter 5, which relates achromatic contrast to C_p, C_s and CD in terms of conspicuity. For the same reason that different sets of achromatic target conditions were used at each light level, different sets of colour/luminance targets were investigated at each background luminance. The six colour/luminance target specifications for each light level are given in Table 6-3, and the achromatic contrast values predicted for these conditions according to the conspicuity model (C_m), are shown in Table 6-4.

Light level	Target no.	C_{ach}	Light level	Target no.	C_{ach}
1	1	0.04	2	1	0.05
	2	0.06		2	0.06
	3	0.085		3	0.08
	4	0.12		4	0.12
	5	0.18		5	0.20
	6	0.75		6	0.75
Light level	Target no.	C_{ach}	Light level	Target no.	C_{ach}
4	1	0.15	5	1	0.25
	2	0.21		2	0.30
	3	0.29		3	0.36
	4	0.40		4	0.44
	5	0.59		5	0.58
	6	2.00		6	1.60

Table 6-2. Values of positive achromatic contrast for six of the 12 targets in the visual search experiments, given for each of the four light levels investigated.

All four observers (D, F-H) performed search time experiments for the four light levels in the low photopic/mesopic range. The stimuli were viewed binocularly to duplicate the viewing conditions used in the conspicuity matching experiments. Observers were adapted to the luminance of the background prior to beginning measurements. The calculation of dark adaptation times is described in section 2.4.1. The percentage that each test target stimulus went undetected during a single presentation (time-out rate), and the percentage that each target was incorrectly identified (response error rate) were monitored throughout to assess target detectability and observer response accuracy.

Light level	Target no.	C_p	C_s	CD	Light level	Target no.	C_p	C_s	CD
1	7	0	0.020	0.019	2	7	0	-0.036	0.033
	8	0	-0.035	0.032		8	0	0.155	0.032
	9	0	0.155	0.032		9	0	0.069	0.070
	10	0	0.208	0.058		10	0	-0.099	0.085
	11	0	-0.098	0.084		11	0	-0.282	0.088
	12	-0.2	-0.487	0.147		12	-0.4	-0.306	0.094
Light level	Target no.	C_p	C_s	CD	Light level	Target no.	C_p	C_s	CD
4	7	0.0	-0.103	0.088	5	7	0.4	0.155	0.141
	8	0.2	0.144	0.098		8	0.2	-0.283	0.102
	9	-0.4	0.138	0.170		9	-0.5	-0.177	0.148
	10	0.2	0.419	0.057		10	0.2	0.487	0.057
	11	0	-0.415	0.122		11	0.5	0.600	0.068
	12	-0.2	-0.492	0.152		12	0.0	-0.497	0.140

Table 6-3. Values of C_p, C_s and CD for the six colour/luminance combination targets investigated in the visual search experiments, given for each of the four light levels.

Light level	Target no.	C_m	Light level	Target no.	C_m
1	7	0.15	2	7	0.14
	8	0.17		8	0.17
	9	0.19		9	0.19
	10	0.24		10	0.23
	11	0.28		11	0.30
	12	0.74		12	0.74
Light level	Target no.	C_m	Light level	Target no.	C_m
4	7	0.17	5	7	0.28
	8	0.24		8	0.33
	9	0.30		9	0.38
	10	0.40		10	0.47
	11	0.55		11	0.62
	12	0.90		12	1.29

Table 6-4. Values of positive achromatic contrast predicted by the conspicuity model for the colour/luminance combinations shown in Table 6-3.

6.3 Results

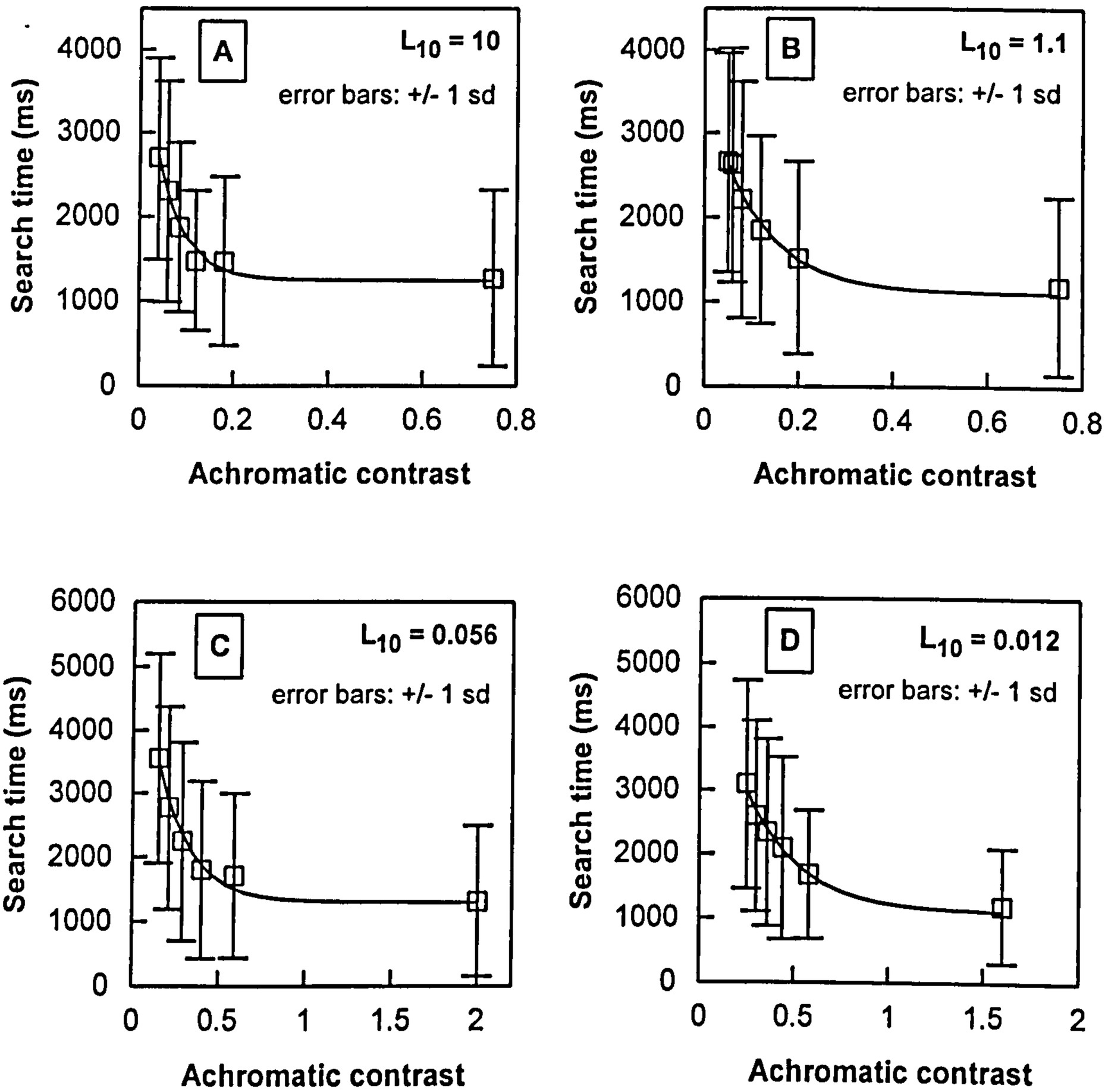

Figure 6-1 (A)-(D). Visual search times for achromatic contrast targets, over four light levels. Symbols represent the mean search time for four observers averaged over a circular field 22° in diameter. Solid lines indicate curves fit to the data at each light level, according to Eq. 6-1. Note that (A) and (B) have a different scale on the abscissa to (C) and (D).

6.3.1 Achromatic visual search

Figure 6-1 shows plots of search time vs. contrast for the achromatic targets, over the four light levels investigated. The data points represent the mean results for the four observers, where 48 search times were recorded per target for each observer,

with the target presented randomly within the central 22° diameter field. The standard deviation from the mean search time, indicated by the error bars in Figure 6-1, was large because the results were averaged over the whole 22° field. The number of incorrect responses recorded for each observer was ≤ 3 per target condition, but on average was 0.15 incorrect responses per target condition; therefore, correct detection was assumed. No target was missed for five consecutive presentations, but the time-out rate recorded for subject H was high for the low contrast conditions, suggesting that this subject had higher contrast detection thresholds than the other three observers.

The curves shown in Figure 6-1, are fitted functions of the form shown in Eq. 6-1.

$$ST = T + (t_0 - T)e^{-kC} \qquad \textbf{Eq. 6-1}$$

where ST: search time, T: minimum search time, t_0: limiting search time, k: decay constant, C: contrast. The parameters for the fitted curves are shown in Table 6-5. The results revealed that the relationship between search time and achromatic contrast changes with light level. It can be seen from Figure 6-1 that the minimum contrast for which search times could be measured, increased as background luminance was lowered. The other noticeable feature of these data was that the curves in Figure 6-1 became less steep with the fall in background luminance. Hence, there was a reduction in the rate of decay of the search time vs. contrast relationship as the light level was decreased. This can be seen from the decrease in value of the decay constant of the fitted curves with fall in light level, shown in Table 6-5. When in the asymptotic region the minimum search time T, showed little variation with light level, and is, therefore, likely to reflect the minimum time for visual processing plus a motor response.

Light level	T	t_0	k
1	1250	4250	17.79
2	1100	3500	9.02
4	1300	6250	5.40
5	1100	5750	3.59

Table 6-5. Parameters for the fitted curves shown in Figure 1-1, which are of the form shown in Eq. 6-1.

6.3.2 Visual search performance for targets with colour and luminance contrast, and the conspicuity model

Search times recorded for targets defined by a combination of colour and luminance contrast are shown in Figure 6-2. The data points again show the mean results for the four observers, where 48 search times were recorded per target for each observer, with the target presented randomly within a 22° diameter field. The conspicuity model developed in chapter 5 was used to predict the conspicuity of each test target consisting of a combination of C_p, C_s and CD, with respect to a reference scale of achromatic contrast. Search time for each colour/luminance target was plotted against the predicted achromatic contrast value, as shown in Figure 6-2. The number of incorrect responses recorded for each observer was 0.2 per target condition on average (≤ 2 for each target condition), indicating that correct detection could be assumed. No target was missed for five consecutive presentations, but the time-out rate recorded for subject H was again high for some target specifications, suggesting that these targets were closer to threshold for this observer.

At the lower two light levels, the mean search times for the colour/luminance targets closely followed the achromatic search time curve, but at the higher two light levels, several data points for the colour/luminance targets did not fall close to the achromatic curve. The mean search time data for light level 1, appeared to follow a similar curve to that of the achromatic data, but shifted along the abscissa towards higher contrast and along the ordinate in the direction of reduced search time. The results for light level 2 exhibited a relationship that was qualitatively similar to the achromatic curve, but shifted along the abscissa in the direction of higher contrast.

A quantitative analysis of differences in search performance for the colour/luminance targets and achromatic contrast predicted by the model was also carried out. Inspection of the data in Figure 6-2 showed that the search performance curves for the colour/luminance targets and the achromatic targets were similar in shape, suggesting that a close relationship existed between the two curves. The similarity of the relationship at each light level was quantified by calculating the correlation coefficient between measured and predicted search times

according to Eq 5-3. The correlation coefficients shown in Table 6-6, indicated that a good relationship existed between search times for the colour/luminance targets and search times for achromatic targets of equivalent conspicuity, at all four light levels.

	light level 1	light level 2	light level 4	light level 5
correlation	0.95	0.81	0.97	0.85

Table 6-6. The correlation between measured search times for the colour/luminance targets and search times for achromatic targets of equal conspicuity, at each light level.

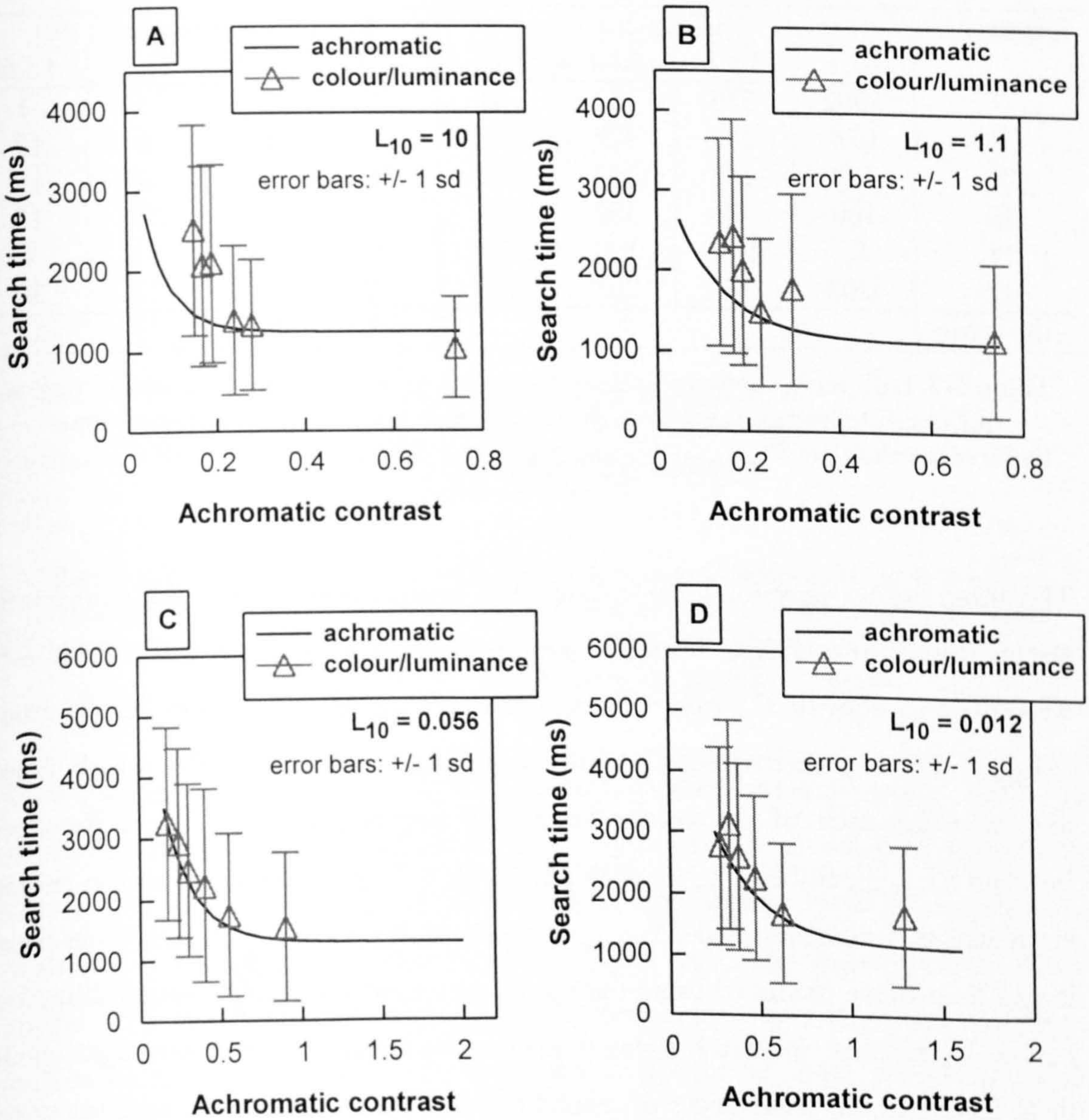

Figure 6-2 (A)-(D). Visual search times for targets defined by colour and luminance contrast, plotted against achromatic contrast predicted by the conspicuity matching model. Results are shown for the four light levels investigated (A)-(D). Symbols represent the mean search time for four observers averaged over a circular field 22° in diameter. Solid lines

indicate curves fit to the achromatic visual search data obtained at each light level, shown in Fig 6-1. Note that (A) and (B) have a different scale on the abscissa to (C) and (D).

The finding of a strong relationship between search performance for colour/luminance targets and achromatic targets of equal conspicuity, led to an assessment of the ability of the measure of conspicuity to directly predict search times for the colour/luminance targets given the search time curves for the achromatic targets.

Target no.	Differences				Percentage differences (%)			
	LL1	LL2	LL4	LL5	LL1	LL2	LL4	LL5
7	1062	575	-22	-31	42	24	-1	-1
8	676	810	277	602	33	33	9	19
9	749	468	208	307	36	23	8	12
10	100	82	359	286	7	6	16	13
11	63	509	190	71	5	29	11	4
12	-203	54	207	494	-19	5	13	30
rms error					28	23	11	16

Table 6-7. Differences between measured search times for the colour/luminance targets and search times calculated from the model predictions of match contrast, in ms. Difference values are $ST_{measured}$ - ST_{model}, percentage difference values are 100.($ST_{measured}$ - ST_{model})/$ST_{measured}$.

The fitted curves describing the relationship between search time and achromatic target contrast at each light level (the parameters for which are shown in Table 6-5, were used to convert C_m values for the colour/luminance targets to search times (ST_{model}). These predicted search times were then compared to the search times measured for each of the colour/luminance targets ($ST_{measured}$). The differences between $ST_{measured}$ and ST_{model} are shown in Table 6-7, the differences are also shown expressed as a percentage of $ST_{measured}$. In general, the measured search times were longer than those predicted using the conspicuity model and achromatic calibration curves. Differences in search times tended to be larger for the higher light levels (light level 1-2), but differences of several hundred milliseconds were seen for some conditions across all four light levels. The percentage differences also tended to be larger for the higher light levels. To assess the overall error in predicting search times for the colour/luminance conditions using the conspicuity model and the achromatic search curves (combined model), the root mean squared (rms) error was calculated for the percentage differences, according to Eq. 6-2.

$$E_{rms} = 100.\sqrt{\frac{1}{6}\sum_{i=1}^{6}\left(\frac{x_{meas,i} - x_{pred,i}}{x_{meas,i}}\right)^2} \qquad \text{Eq. 6-2}$$

where E_{rms}: root mean squared error, x_{meas}: $ST_{measured}$, and x_{pred}: ST_{model}. Root mean squared errors are shown in Table 6-7. The rms error was largest for light level 1 and lowest for light level 4, and rms errors for the highest two light levels were larger than those calculated for the lowest two light levels.

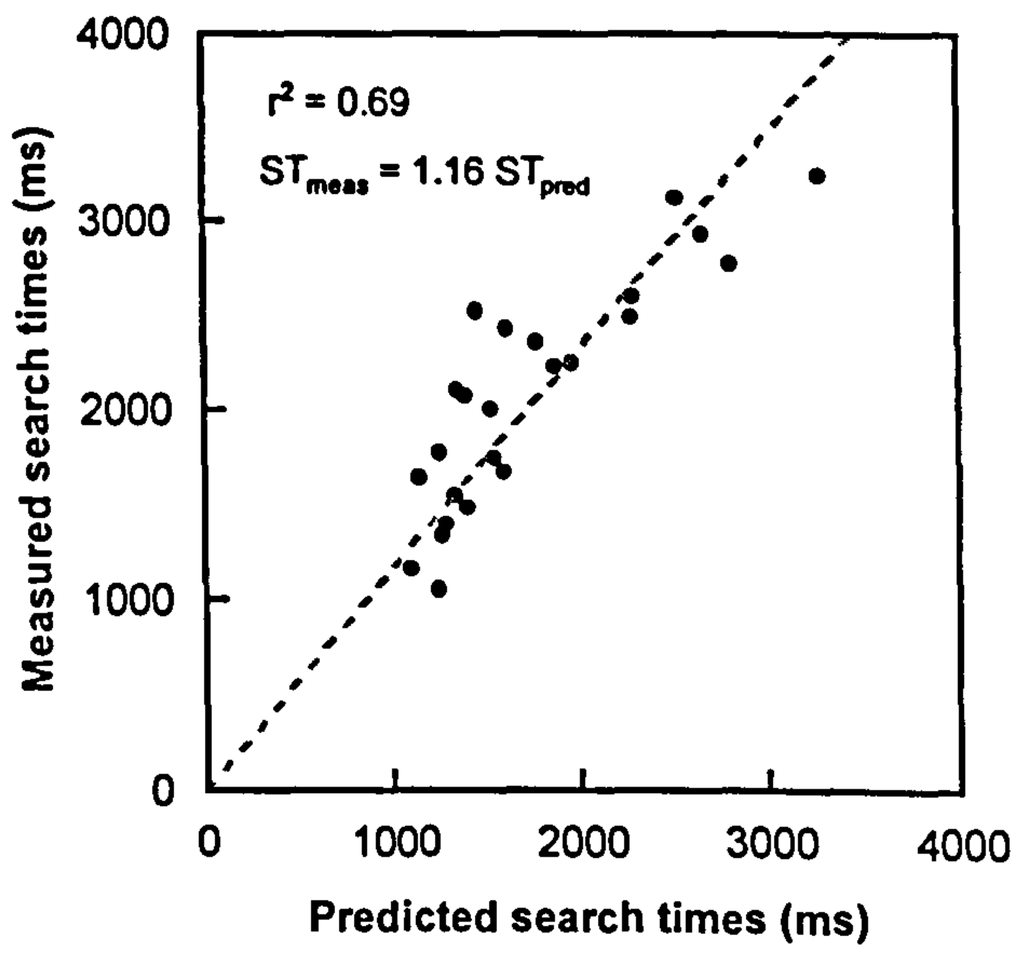

Figure 6-3. Search times measured for the targets with a combination of colour and luminance contrast, plotted against search times predicted using the combined model. Symbols represent points for all targets investigated over four light levels. The dotted line represents the best fit to the data, passing through the origin.

Investigation of the differences in milliseconds between measured search times and those predicted using the combined model (conspicuity model plus achromatic search performance curves), revealed small to large discrepancies in search time, with larger percentage differences occurring at the higher two light levels compared to the lower levels. These results suggest that the measure of conspicuity developed in chapter 5, could be used to directly predict a measure of visual performance such as search time for targets defined by colour and luminance contrast using an intermediate task-specific achromatic calibration, but with some errors. The relationship between measured search times for the colour/luminance targets and those predicted using the combined model across all conditions investigated over all four light levels is illustrated in Figure 6-3. A proportional relationship was obtained

between measured search times and the search times predicted using the combined model, the equation for which is given below.

$$ST_{measured} = 1.16\, ST_{model} \qquad \textbf{Eq. 6-3}$$

This relationship produced a coefficient of determination of 0.69, and represented an improvement over the direct relationship. The proportionality constant is greater than 1, which results from the model underestimating search time compared to the measured values.

Target no.	Differences				Percentage differences (%)			
	LL1	LL2	LL4	LL5	LL1	LL2	LL4	LL5
7	-0.065	-0.063	-0.02	0.004	-74	-83	-13	1
8	-0.054	-0.052	-0.026	0.045	-46	-44	-12	12
9	-0.028	-0.033	-0.072	0.034	-17	-21	-32	8
10	0.026	-0.053	-0.052	0.010	10	-30	-15	2
11	-0.023	-0.082	-0.088	-0.005	-9	-37	-19	-1
12	0.068	-0.094	-0.237	-0.338	8	-15	-36	-36
rms error					37	44	23	16

Table 6-8. Assessment of the conspicuity model to accurately predict conspicuity at each of the four light levels used in the visual search experiments. Difference values for each colour/luminance target are: measured C_m - predicted C_m, percentage difference values are 100.(measured C_m – predicted C_m)/measured C_m.

The finding of larger differences between search times for targets defined by colour and luminance contrast and achromatic targets with equal conspicuity at the low photopic/high mesopic light levels compared to the mid to low mesopic light levels, may depend on the ability of the model to accurately predict conspicuity at high and low luminances, respectively. To investigate the accuracy of the conspicuity model's predictions for the colour/luminance targets used in the visual search experiments, the average response of the five observers, on whose matches the model was based, were compared to the model's predictions of matching contrast. The differences in match contrast values (C_m) are shown in Table 6-8, along with differences shown expressed as a percentage of the mean measured match contrast. For light levels 1, 2 and 4, the values of match contrast predicted by the model tended to be higher than the average match contrasts measured by the five observers for each of the colour/luminance targets (target numbers 7-12). For light level 5, the model tended to underestimate match contrast compared to the average measured value for each target condition. The root mean squared errors for the predicted C_m values

compared to the measured C_m values were calculated according to Eq. 6-2, with x_{meas}: measured C_m values, x_{pred}: predicted C_m values, and are shown in Table 6-8. The root mean squared errors were indeed larger for light levels 1 and 2 than for light levels 4 and 5. These results indicate that the ability of the model to predict conspicuity was better for the lower background luminances than for the high light levels. As an extension to this avenue of investigation, the achromatic search time curves were used to convert the original observers mean conspicuity matches to equivalent search times ($ST_{orig\ obs}$), to ascertain whether an improvement in the prediction of search times could be obtained using the original measured values of match contrast.

Target no.	Differences				Percentage differences (%)			
	LL1	LL2	LL4	LL5	LL1	LL2	LL4	LL5
7	633	51	-238	-17	25	2	-7	-1
8	440	491	81	826	21	20	3	26
9	682	334	-264	459	32	17	-11	18
10	118	-113	132	310	8	-8	6	14
11	53	337	36	72	4	19	2	4
12	-203	49	105	386	-19	4	7	24
rms error					21	14	7	17

Table 6-9. Differences between measured search times and search times calculated from the measured match contrasts. Difference values are $ST_{measured} - ST_{orig.\ obs}$, percentage difference values are $100.(ST_{measured} - ST_{orig.\ obs})/ST_{measured}$.

Differences and percentage differences between search times measured for the colour/luminance targets and those predicted from the original observers conspicuity matches are shown in Table 6-9 The rms error was again calculated according to Eq. 6-2, with in this case x_{pred}: $ST_{orig\ obs}$, and these values are also shown in Table 6-9. For light levels 1, 2 and 4, the rms errors were smaller for $ST_{orig.\ obs}$ than for ST_{model}, indicating that search times calculated from the measured match contrasts agreed more closely with the measured search times. For light level 5, ST_{model} agreed more closely with the measured search times, although the difference was marginal. However, the percentage errors between measured search times and converted search times could still be large, whether they were calculated from C_m values predicted by the conspicuity model or from C_m values measured by the observers in chapter 5, with the measured search times again tending to be longer than equivalent search times computed from the measure of conspicuity.

These results, taken together, indicate that the larger prediction errors for the combined model (conspicuity model, plus achromatic calibration curves) seen at the higher light levels compared to the lower light levels, may not entirely be the result of a poorer fit of the conspicuity model for the conditions investigated at these higher luminances. Another factor to consider is the consequence of the more rapid change of search time with achromatic contrast at the higher light levels. For a steeper curve, any errors in the prediction of conspicuity (matching achromatic contrast, C_m) will introduce a greater error in the predictions of search time. This would explain the larger errors obtained at these background luminances. Further inspection of search times computed from the original conspicuity measurements suggests that there are systematic differences between visual search performance computed for colour/luminance targets from the conspicuity metric used, and the search times measured for those targets. The origins of such differences are discussed in section 6.4.2.

6.3.3 Photopic contrast, scotopic contrast and chromatic difference as predictors of visual search performance

In the same way that search times for the colour/luminance targets were predicted from C_m values produced by the conspicuity model in section 6.3.2, search times were also predicted from values of C_p and C_s for each target specification. Values of C_p or C_s were converted to search times using the achromatic calibration curves. This was possible because achromatic contrast is independent of the spectral luminous efficiency function, and so C_p, C_s and achromatic contrast all have the same value. The achromatic calibration curves were obtained for positive achromatic contrast targets only, therefore, negative values of C_p and C_s had to be converted to positive values to enable a comparison. Although a conversion was not attempted in similar circumstances in chapter 5 section 5.3.10, the small number of conditions investigated meant that it was not possible to consider only those conditions with $C_p>0$ and $C_s>0$; hence the conversion was considered to be a interesting exercise in this case.

Target no.	Differences				Percentage differences (%)			
	LL1	LL2	LL4	LL5	LL1	LL2	LL4	LL5
7	-1730	-1146	-2996	564	-69	-33	-48	26
8	-2179	-1072	-50	-244	-105	-31	-2	-7
9	-2149	-1500	1086	1313	-102	-43	-77	102
10	-2858	-2017	-751	-1122	-205	-58	-25	-33
11	-2916	-1731	-4507	-199	-219	-49	-72	-11
12	-208	53	-463	-4110	-20	5	-23	-71
rms error					139	40	49	54

Table 6-10. Differences between measured search times for the colour/luminance targets and search times calculated from target photopic contrast. Difference values are $ST_{measured} - ST_{photopic}$, percentage difference values are $100.(ST_{measured} - ST_{photopic})/ST_{measured}$.

Target no.	Differences				Percentage differences (%)			
	LL1	LL2	LL4	LL5	LL1	LL2	LL4	LL5
7	-839	-79	128	-1000	-33	-3	4	-27
8	-147	736	-642	1279	-7	44	-18	69
9	661	-387	-1162	18	31	-16	-32	1
10	68	-98	416	336	5	-6	23	18
11	-46	645	356	35	-3	57	26	2
12	-203	40	203	412	-19	4	15	34
rms error					21	30	21	34

Table 6-11. Differences between measured search times for the colour/luminance targets and search times calculated from target scotopic contrast. Difference values are $ST_{measured} - ST_{scotopic}$, percentage difference values are $100.(ST_{measured} - ST_{scotopic})/ST_{measured}$.

The results of chapter 5 highlighted differences between the conspicuity of positive and negative contrast targets; in order to take account of these differences, negative values of C_p and C_s were scaled by a factor of 1.8 and the absolute value taken. The factor 1.8 was determined from the mean ratio of conspicuity for negative achromatic contrast conditions compared to positive achromatic contrast conditions, measured in chapter 5 over the whole data set. Differences were then calculated between search times measured for the colour/luminance targets ($ST_{measured}$) and those predicted from either C_p ($ST_{photopic}$) or C_s ($ST_{scotopic}$). The calculated differences and percentage differences are shown in Table 6-10 and Table 6-11 for photopic contrast predictions and scotopic contrast predictions, respectively. These differences are also illustrated in Figure 6-4 and Figure 6-5, where search times for the colour/luminance targets have been plotted against either target C_p (Figure 6-4) or C_s (Figure 6-5). The figures also show the fitted

achromatic search curves for comparison. The root mean squared error was also calculated in each case to assess the overall error in predicting search times for the colour/luminance targets using either target C_p or C_s. These errors were calculated according to Eq. 6-2, with x_{meas}: $ST_{measured}$, and x_{pred}: $ST_{photopic}$ or $ST_{scotopic}$, and are shown in Table 6-10 and Table 6-11, respectively.

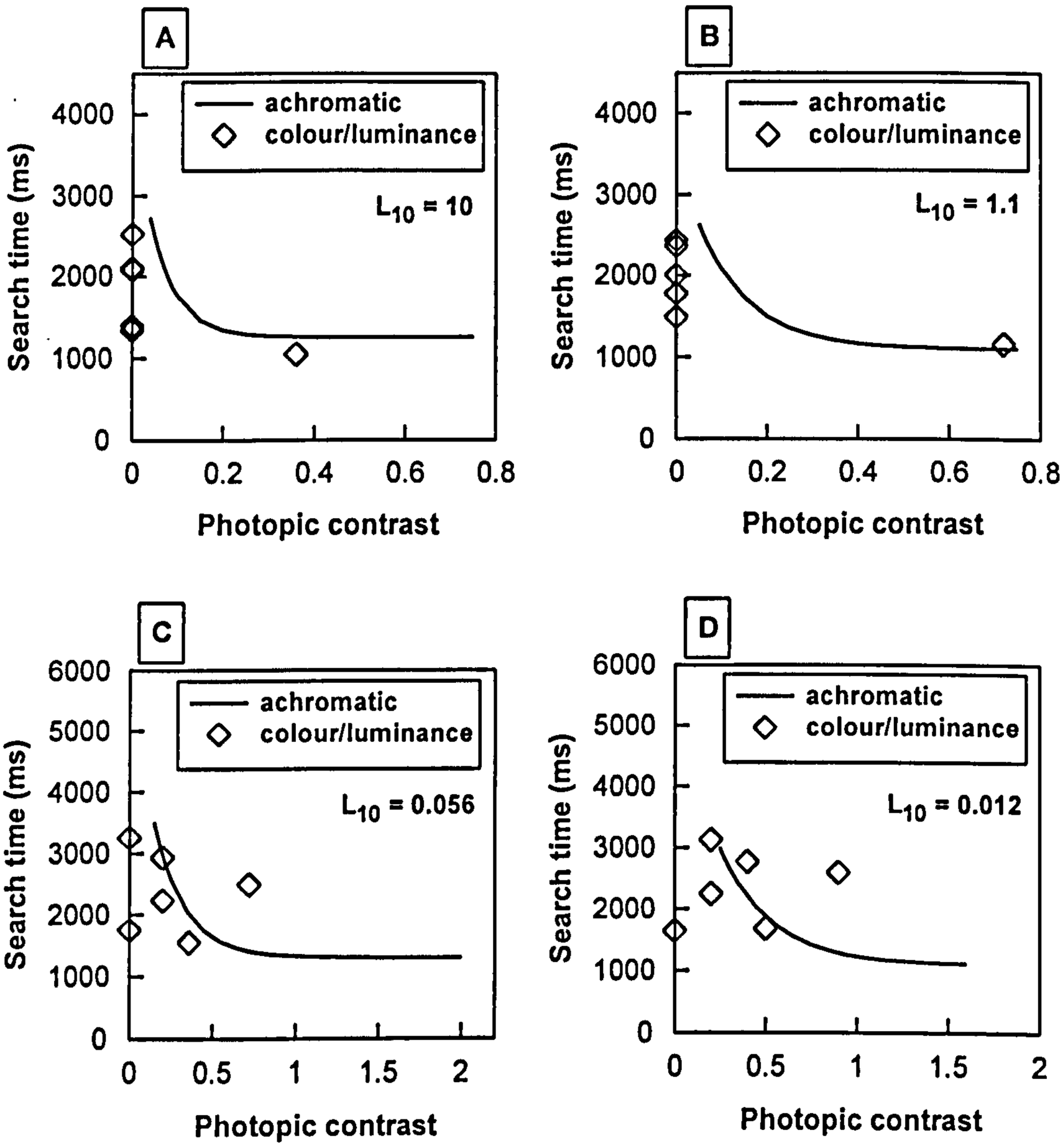

Figure 6-4 (A)-(D). Visual search times for targets defined by colour and luminance contrast, plotted against target photopic contrast. Results are shown for the four light levels investigated (A)-(D). Targets with different values of photopic contrast were investigated at each light level. Many of the targets at the higher two light levels were isoluminant, see section 6.2.2 for a description of how the targets were chosen. Symbols represent the mean search time for four observers averaged over a circular field 22° in diameter. Solid lines indicate curves fit to the achromatic visual search data obtained at each light level, also shown in Figure 6-1.

The evidence presented in both Table 6-10 and Figure 6-4 suggests that for the colour/luminance target specifications investigated, photopic contrast was not a

good predictor of visual search performance. The differences between $ST_{measured}$ and $ST_{photopic}$ were very large in almost all cases, leading to high rms errors for predicting search time across all four light levels. The results of chapter 5 indicated that photopic contrast is a less significant factor in determining conspicuity at low mesopic light levels, therefore, C_p would be expected to be a poor predictor of task-specific visual performance at such background luminances.

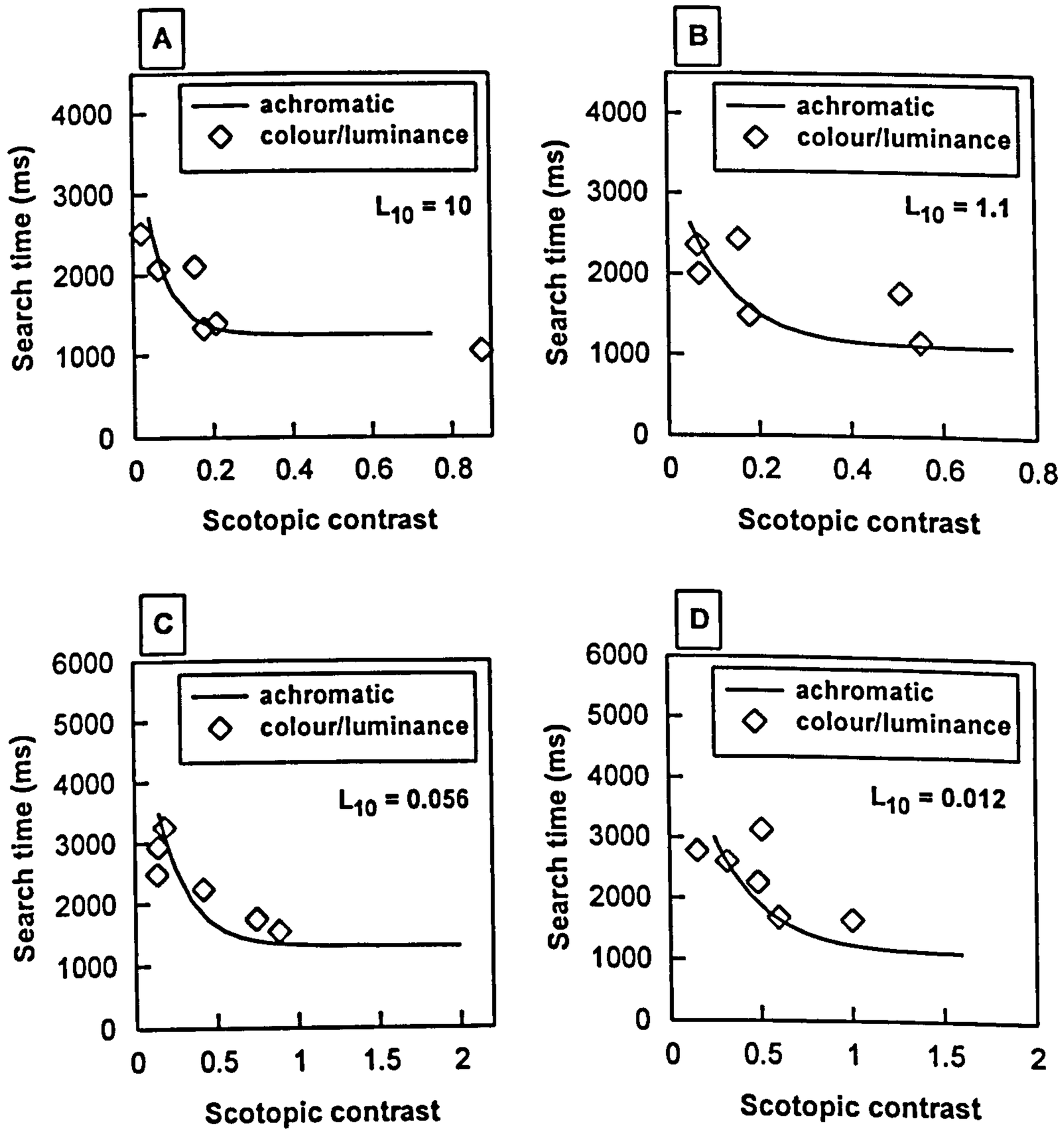

Figure 6-5 (A)-(D). Visual search times for targets defined by colour and luminance contrast, plotted against target scotopic contrast. Results are shown for the four light levels investigated (A)-(D). Targets with different values of scotopic contrast were investigated at each light level, see section 6.2.2 for a description of how the targets were chosen. Symbols represent the mean search time for four observers averaged over a circular field 22° in diameter. Solid lines indicate curves fit to the achromatic visual search data obtained at each light level, also shown in Figure 6-1.

At the low photopic and high mesopic light level investigated C_p was almost always zero, therefore, some other parameter had to be responsible for the observed changes in search performance. Note that this indicates a situation in the photopic range where C_p cannot account for visual search performance. Nonzero photopic contrast values might be expected to produce predictions of search times that correlate better with search performance at these light levels. There is some evidence for this from the results for the two conditions with nonzero C_p values (target number 12 for light levels 1-2), for which differences between measured and predicted search times were relatively small.

The results shown in Table 6-11 and Figure 6-5 suggest that for the colour/luminance target specifications investigated, scotopic contrast was a moderately good predictor of visual search performance. The differences between measured and predicted search times were relatively low in some cases, but could be of the order of several hundred milliseconds to a second in others. Percentage differences and rms errors were of a similar order of magnitude across all light levels. The findings of chapter 5 indicated that scotopic contrast was the main determinant of conspicuity in the low mesopic range. It is feasible to expect scotopic contrast to also be the main determinant of visual search performance at low light levels. For the high mesopic range, the results of chapter 5 indicated that scotopic contrast was not a significant factor in determining conspicuity. It is reasonable, therefore, to assume that this might extend to visual search performance, but is at odds with the finding of similar percentage differences and rms errors across all light levels when C_s was used as a predictor. However, the results of chapter 5 also showed that there was reasonable correlation between scotopic contrast and the chromatic difference of the target (see section 5.3.6), therefore, the dependence of search time on CD value must also be considered before conclusions can be drawn about the role of scotopic contrast the current visual search measurements.

Figure 6-6 shows search time measured for the colour/luminance targets plotted against target CD. At the lower two light levels, search time did not show a strong relationship with CD. This ties in with the findings of chapter 5, which indicated

that CD was a less significant factor in determining conspicuity at low mesopic light levels. This suggests that scotopic contrast was in fact the main determinant of search performance measured in the mid to low mesopic range. Predictions of search times from values of scotopic contrast, however, were not as good as those made using values of conspicuity. This implies stimulus photopic contrast and chromatic difference may also contribute to search performance at these light levels.

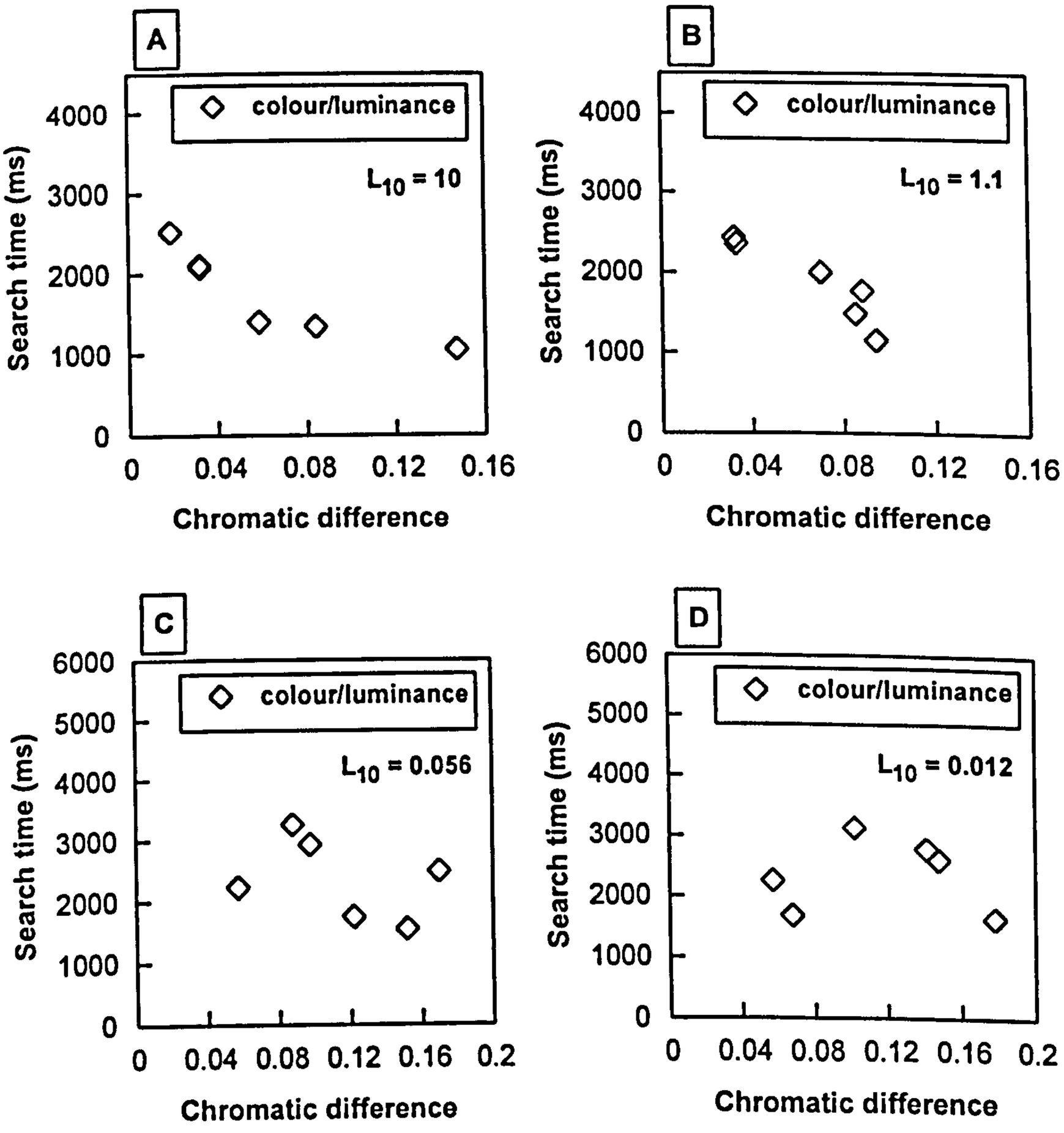

Figure 6-6 (A)-(D). Visual search times for targets defined by colour and luminance contrast, plotted against target chromatic difference. Results are shown for the four light levels investigated (A)-(D). Symbols represent the mean search time for four observers averaged over a circular field 22° in diameter.

At the higher two light levels search time exhibited a good relationship with CD. At the low photopic level (L_{10} = 10), this relationship was qualitatively similar to the relationship of search time with achromatic contrast. It is likely that for this

background luminance where photopic contrast was mostly zero, CD was the sole determinant of search performance, and that the apparently good prediction of performance from C_s, may be an artefact arising from the correlation between CD and C_s. It is also possible, however, that C_s is a more important factor in visual search than the conspicuity model predicts. Visual search involves large areas of the peripheral retina where there is a high density of rod receptors compared to cones. The target employed was quite large, which may also favour the spatial summation properties of rods. At the high mesopic level (L_{10} = 1.1), the relationship between search time and CD appears to be approximately linear, rather than the nonlinear decay function characteristic of achromatic search, and seen for CD at the highest light level. It is likely, therefore, that at this light level where photopic contrast was mostly zero, search performance is determined from a combination of CD, nonzero C_p and C_s, although C_s may only be an important factor for minimal values of C_p. These results emphasise the importance of colour in determining mesopic visual search performance, particularly in the high mesopic range and when luminance contrast is low.

6.4 Discussion

The results of this study have shown that it is possible to measure visual search performance throughout the mesopic range using an identical contrast acuity-based orientation task with detection based on target conspicuity, despite changes in visual acuity (Patel 1966; Van Nes and Bouman 1967). Search times recorded for achromatic targets revealed changes in the characteristics of search performance with reduction in light level. Search times measured for targets with a combination of colour and luminance contrast, showed that the relationships between visual search and colour, photopic luminance contrast and scotopic luminance contrast are altered as the level of illumination is decreased. The measure of stimulus conspicuity developed in chapter 5 was shown to be a reasonably good predictor of mesopic search performance for targets defined by both colour and luminance contrast.

6.4.1 Changes in visual search performance with light level

The results of search time measurements for both targets defined by achromatic contrast and targets defined by a combination of colour and luminance contrast, revealed changes in visual search performance with light level. For the achromatic conditions, the minimum contrast for which search time could be measured increased with reduction in light level. This reflects the increase of contrast threshold with reduction in light level (Blackwell 1946). The investigation of achromatic visual search also revealed that the rate of decay of the search time function decreases with reduction in background luminance. This shows that not only do the search time curves shift towards higher values of contrast as contrast thresholds increase, but the curves become less steep with reduction in background luminance. This finding implies that in addition to the increase in contrast threshold, the relationship between visual search performance and luminance contrast varies nonlinearly with background luminance, meaning that equal steps in contrast do not produce equal changes in visual search performance at different light levels in the mesopic range.

The analysis of search time measurements for the targets defined by a combination of photopic contrast (C_p), scotopic contrast (C_s) and chromatic difference to the background (CD), showed that the effect of each of these parameters on visual search performance changes with light level. In the mid to low mesopic range, C_p was found to be a poor predictor of search performance, and search times did not appear to be related to CD. Scotopic contrast, on the other hand, was found to be a reasonable predictor of search time at such light levels, and is likely to be the predominant factor in determining search performance. The improved predictions obtained from the measure of stimulus conspicuity suggest that C_p and CD also contribute to visual performance in the mid to low mesopic range.

Results for the low photopic and high mesopic light level investigated, illustrate the importance of CD in determining search time, especially when luminance contrast is low. At these light levels C_p was mostly zero and found to be a poor predictor of search time. The appearance of stimulus C_s as a reasonable predictor of search time was unexpected. One possible explanation for this finding is that it reflects the

remaining correlation between CD and C_s for stimuli generated on the experimental system used. An alternative explanation is that C_s is an important factor in determining visual search performance even at high mesopic light levels. The visual search task involved searching for a sizeable target over a large peripheral field. Such conditions are likely to favour rods, and may result in the observed dependence of search performance on scotopic contrast. Further investigation is required to assess the dependence of search performance on scotopic contrast in the low photopic/ high mesopic range. Conditions with a nonzero C_p value provided some evidence that C_p is an important determinant of search performance in the low photopic/high mesopic range. In general, the results for these two light levels indicated that the effects of CD and possibly C_s must considered along with C_p, especially in cases where C_p is low.

The results for all four light levels are in agreement with the findings of a previous study of visual search performance in the mesopic range (Hurden et al. 1997; Barbur et al. 1998a; Hurden et al. 1999). The authors showed that the main determinant of search time in the mesopic range is photopic contrast at low photopic/high mesopic light levels and scotopic contrast at mid to low mesopic levels. Their study did not, however, include a systematic investigation into the effects of colour on visual search.

6.4.2 Conspicuity as a predictor of visual search performance

The measure of conspicuity used in this study, relates the conspicuity of a target defined by a combination of colour and luminance contrast to that of a similar achromatic target. The measurement of visual search performance curves for achromatic targets made it possible to predict search times for targets defined by colour and luminance contrast of known conspicuity. Conspicuity was predicted directly by the model described in chapter 5, based on CIE defined stimulus parameters. The results showed that this measure of conspicuity can be applied to produce a good predictor of visual search performance for targets defined by a combination of colour and luminance contrast in the mesopic range. The proportional relationship developed between measured search times for targets

defined by colour and luminance contrast, and those predicted from the combined model (conspicuity model plus achromatic search calibration), over all four light levels investigated, produced a coefficient of determination of 0.69.

As defined in this study, conspicuity is a measure of the combined effectiveness of photopic contrast, scotopic contrast and colour. In the mesopic range where there is currently no internationally accepted mesopic luminous efficiency function, there is a need for a metric that will produce better predictions of task-specific visual performance than either stimulus photopic contrast or scotopic contrast. The evidence of this study indicates that, in relation to visual search, conspicuity provides an improved measure of stimulus effectiveness in the mesopic range than either photopic or scotopic contrast.

Despite the good relationship found between predictions of search time made using the combined model and measured search times for the colour/luminance targets, predicted search times were found, in general, to be shorter than measured values. This was also the case when the original measurements of conspicuity were converted to search times and compared to the measured values. Three possible explanations are suggested for this finding. The first and second possibilities consider that some factor in the conspicuity matching task, which has the effect of increasing the value of resulting match contrast, is less effective in the visual search task. This could arise firstly, from the fact that the visual search task involves more peripheral retinal areas than used in the conspicuity matching task on which the model was based (i.e. 7° eccentricity). This might lead to a different dependence on photopic contrast, scotopic contrast and colour difference in each task, related to differences in eccentricity. Secondly, differences may exist in the relative weighting of photopic contrast, scotopic contrast and colour difference in judgements of conspicuity compared to measurements of search time, irrespective of differences in eccentricity. The third possibility considers that there was a bias towards achromatic targets in the visual search procedure, resulting in shorter search times for achromatic targets. These possibilities are discussed below.

If the conspicuity matching task had been carried out an eccentricity greater than 7°, it is likely that the contribution of C_s to achromatic match contrast would have been greater and the contributions of C_p and CD would have been less. This is because of the different spatial distributions of rods and cones in the retina (see section 1.1.2 h). The results of chapter 5 showed that weakening the chromatic signal leads to a reduction in the value of achromatic match contrast. This means that the chromatic contribution at 7° would result in a higher value of match contrast than expected at a larger eccentricity. This would explain the finding of shorter search times predicted from the conspicuity model, than those measured for the search time task, which involves larger eccentricities.

The second explanation considers that, irrespective of eccentricity, the chromatic signal may be less effective in the search time task compared to the conspicuity matching procedure. Hurden et al. (Hurden et al. 1997; Barbur et al. 1998a; Hurden et al. 1999) provided evidence that visual search in the mesopic range could be adequately modelled as a function of luminance contrast alone (combinations of photopic and scotopic contrast), without consideration of the effects of colour. Both Lit et al. (1971) and Pollack (1968) reported that reaction time measurements for stimuli with combined colour and luminance at photopic levels of illumination, depend only on luminance contrast, showing no variation with wavelength. Furthermore, reaction times for isoluminant chromatic stimuli are significantly longer than those for luminance increments (Barbur et al. 1998c). During visual search, fixation duration is typically 150-350 ms (Hooge and Erkelens 1998; Andrews and Coppola 1999; Nasanen et al. 2001). It may be the case that during the relatively short fixations that observers make whilst performing visual search (150-350 ms), the chromatic signal is weighted differently in relation to the luminance contrast signal, than during the 500 ms presentation used in the conspicuity matching experiments.

The third possibility stated above, considers the presence of bias in the visual search procedure that resulted in shorter search times for the achromatic targets. Such a bias may be a consequence of the effects of distracter heterogeneity and the visual mechanisms used to detect the target. Nagy and Winterbottom (2000) reported that

for white targets differing in luminance from the distracters, variability in distracter chromaticity had little effect on search performance, whereas for coloured targets differing in luminance from the distracters, search performance was poorer when distracter colour was varied. They suggested that detection of white targets was mediated by the luminance mechanism only, but mechanisms tuned to both chromaticity and luminance were required to search for the coloured targets. In the present case, the target had a unique orientation, but detection of the achromatic targets may have been mediated by the achromatic mechanism alone, and detection of the colour/luminance targets mediated by a combination of chromatic and achromatic mechanisms. Variability in the chromaticity of the distracters may then have resulted in degraded performance for the colour/luminance targets.

For all three possibilities considered above, one might expect to see larger differences between measured search times and those predicted from measures of conspicuity at the higher light levels where the contribution of colour to conspicuity is more significant (see chapter 5). This wasn't the case, however, for search times predicted from the original measurements of conspicuity, where comparable percentage differences were seen across all light levels. It seems that a further explanation may be needed to account for the observed differences. Engel (1977) reported that for measurements of conspicuity area and visual search performance, estimates of conspicuity area assuming random fixations during the search procedure, were 30% smaller than the original conspicuity area measurements obtained using constant fixation. This finding of poorer search performance than predicted on the basis of the conspicuity measurements is similar to the present results. It cannot be a consequence of colour, because Engel used only achromatic stimuli. It is possible that temporal differences between fixations during visual search and the longer presentation times used for the conspicuity measurements are responsible for the differences in performance even for purely achromatic search. At present the reason for the systematic differences between predicted and measured search times is unclear and requires further investigation.

The results of this study have shown that the measure of conspicuity developed in chapter 5 can be applied to provide a good predictor of visual search performance

in the mesopic range, and produce improved predictions than either photopic contrast or scotopic contrast. If such a measure of conspicuity was shown to be an important factor in different visual performance tasks, along with other task specific factors, it may be possible to predict performance for a range of visual tasks from the same measure of conspicuity. An advantage of the measure of conspicuity employed in the current work is that performance need only be ascertained for achromatic targets of a single polarity (positive achromatic contrast) at any given light level, to enable prediction of performance for targets defined by both colour and luminance contrast. Thus, for a given visual task the exercise of determining performance for a wide range of target conditions would be reduced to a single polarity of the achromatic domain.

7 General discussion and concluding remarks

The investigations undertaken in this body of work encompassed aspects of chromatic processing at threshold levels, both in the photopic and mesopic range, and suprathreshold behaviour of the visual system under mesopic conditions in relation to stimulus conspicuity and visual search. The results have revealed a number of interesting findings pertaining to the processing of visual mechanisms and visual performance in the mesopic range.

Chromatic sensitivity was investigated using dynamic luminance contrast noise techniques that isolate the use of colour signals. The independent processing of luminance signals and chromatic signals has previously been demonstrated at photopic levels (Barbur et al. 1992), and was shown here to also be applicable to mesopic conditions.

At photopic levels of illumination, chromatic sensitivity measured at the fovea using a colour defined pattern, was shown to depend on the spatial content of the stimulus, in both normal trichromats and dichromats. These results were in agreement with the dependence of chromatic sensitivity on grating frequency reported by Mullen (1985). Similar measurements in subjects with optic neuropathy revealed an exaggerated loss of sensitivity with increasing spatial frequency compared to normals. This was thought to reflect a reduced ability in such subjects to sum chromatic signals over receptive fields, due to neuronal damage. Additional measurements of chromatic sensitivity obtained in these subjects, supported previous findings of differential thresholds for detection of a colour defined pattern and detection of pure colour changes in a pattern defined by luminance contrast, in a subject with optic neuritis (Barbur et al. 1997). Small, but significant differences in thresholds for the two stimulus paradigms were also observed in normals. These results are likely to reflect the dependence of chromatic sensitivity on the spatial characteristics of the stimulus; illustrated in the results for detection of a colour

defined pattern. An alternative possibility, however, discussed in chapter 3, section 3.4.2, is that differences exist between the processing of form based on chromatic signals and the detection of colour independent of structure, early in the visual pathway (Lakowski 1966; Watanabe et al. 1998). The scope of the present study did not make it possible to discriminate between these two hypotheses; hence, further investigation is needed to address this question.

Measurements of chromatic sensitivity in the mesopic range for a uniform stimulus, showed that sensitivity was markedly reduced with decreasing retinal illuminance both at the fovea, consistent with the results of Brown (1951), and in the near periphery. It was suggested that this loss of sensitivity might be attributed to a reduction in the quantal catch of the cone receptors. Loss of sensitivity was nonuniform, with a greater degradation occurring along the axis of S-cone modulation. Below about 10 cd m^{-2} three of the four subjects tested also exhibited asymmetrical thresholds along the S-cone axis, consistent with either a reduced sensitivity for S-cone decrements and/ or an improved sensitivity for S-cone increments. Threshold measurements carried out under conditions that reflect predominantly cone processing were compared to thresholds obtained under conditions where both rods and cone contribute to the response. These results revealed that neither the observed elongation of the threshold contour along the S-cone axis, nor the asymmetry of S-cone thresholds, could be attributed to rod intrusion in chromatic processing at threshold. The greater loss of chromatic sensitivity seen along the S-cone axis and the finding of asymmetrical thresholds for S-cone increments and decrements are, therefore, likely to be a consequence of the response characteristics of the S-cones, which only exhibit Weber behaviour at relatively high levels of excitation (Boynton and Kambe 1980; Yeh et al. 1993).

Both the study of chromatic sensitivity under photopic conditions and the measurements of chromatic thresholds in the mesopic range highlighted differences in the performance of the two postreceptoral chromatic mechanisms. Chromatic threshold measurements under photopic conditions for a colour defined pattern consisting of vertical bars, showed greater threshold changes in the blue-yellow direction compared to the red-green direction as the spatial frequency of the bars

was decreased. These results coupled with the preferential loss of sensitivity observed for the S-cone mediated blue-yellow postreceptoral mechanism compared to the red-green mechanism observed under mesopic conditions, illustrate that the blue-yellow mechanism is not as robust as the red-green mechanism with respect to changes in the spatial characteristics of a stimulus, or the level of retinal illuminance.

The investigation of chromatic sensitivity under mesopic conditions showed that there was no effect of rod intrusion on chromatic thresholds at either 3.5° or 7° eccentricity. These results do not support reports of rod mediated impairment of wavelength discrimination and chromatic discrimination in the near periphery (Stabell and Stabell 1977; Nagy and Doyal 1993; Knight et al. 1998; Knight et al. 2001). It is not clear whether differences in methodology can account for these seemingly contradictory findings, for example in this study chromatic discrimination thresholds were measured from a neutral stimulus as opposed to measuring discrimination between suprathreshold chromatic stimuli. The major difference between the present study and previous investigations, however, relates to the methods used to eliminate detection of luminance contrast signals. It is not sufficient to set a brightness match "by eye", which was the method employed by the Stabells (1977). The effectiveness of eliminating luminance contrast signals by setting isoluminance using flicker photometry in the mesopic range, (the method used by both Nagy and Doyal (1993) and Knight et al. (2001)) was also called into question in the discussion section of chapter 4. It is suggested that using these methods, residual luminance contrast signals may have been present, and that the results of studies based on such methodology may not represent the behaviour of isolated colour mechanisms. The conclusions drawn by Knight et al. in relation to the FM 100-hue test relies on the computations of cone and rod excitations performed for each cap, from which specific axes of photoreceptor modulation were defined. These computations have not been replicated here and, therefore, cannot be commented on. In the present investigation, where dynamic luminance contrast noise was employed to mask detection of luminance contrast signals it is more likely that the measured thresholds represent the processing of colour mechanisms alone. Results obtained under experimental conditions of the present

study demonstrated that the processing of chromatic signals is independent of dynamic luminance contrast noise even when rod contrast signals are involved.

Chromatic threshold contours obtained in the near periphery, as part of the study of mesopic chromatic sensitivity, exhibited a tilt in orientation with increasing eccentricity. These changes in orientation could not be attributed to rod intrusion for the reasons discussed above, and neither could they be attributed to changes in pre-receptoral filtering, because little or no changes were expected under some of the conditions tested. It was suggested, therefore, in chapter 4, section 4.4.1. that this result may reflect changes in sensitivity of multiple colour mechanisms, and that the representation of post-receptoral chromatic processing by two cardinal directions may not be a sufficient description of threshold behaviour under the conditions investigated.

An investigation of suprathreshold visual performance under mesopic conditions was carried out by obtaining a measure of stimulus conspicuity, and relating this measure to performance in a visual search procedure. The conspicuity of a target defined by colour and luminance contrast was defined in terms of the luminance contrast of a similar achromatic target that matched the perceived conspicuity of the coloured target. According to the model developed in this study, conspicuity in the mesopic range is dependent on stimulus photopic contrast, scotopic contrast and chromatic difference to the immediate background, the level of illumination, and a number of interactions between these parameters. Inspection of the data set of conspicuity measurements and the empirical conspicuity model, indicated that in the low mesopic range conspicuity is determined predominantly by scotopic contrast, and at low photopic/ high mesopic light levels conspicuity is determined predominantly from a combination of photopic contrast and the chromatic difference between the stimulus and the immediate background.

An analysis of variance performed on the data set of conspicuity measurements revealed that the magnitude and sign of both photopic and scotopic luminance contrast had significant effects on stimulus conspicuity. This finding is in agreement with other evidence of an asymmetry relating to luminance polarity (Barbur and

Forsyth 1990; Hurden et al. 1997; Vingrys and Mahon 1998). The asymmetry for scotopic luminance contrast was more pronounced than that for photopic contrast.

Measurement of the conspicuity of chromatic stimuli with minimal luminance contrast revealed a linear relationship between conspicuity and chromatic difference to the background measured in a uniform chromaticity space. A similar relationship was observed for both the red and green stimuli investigated, and chromatic thresholds for these specific colour directions inferred from measured threshold contours were very similar. These results indicated that relative behaviour in these two colour directions was maintained in the transition from threshold to suprathreshold measurements and that suprathreshold function measured in terms of conspicuity was similar for the two hues. Suprathreshold behaviour, however, is generally also dependent on stimulus hue (Ueno et al. 1985; Barbur and Forsyth 1990; Nagy and Sanchez 1990; D'Zmura 1991), and suprathreshold behaviour cannot usually be predicted from threshold measurements. In the case of chromatic processing, the relationship between threshold and suprathreshold measurements is known to vary with colour direction (Nagy and Sanchez 1990; Vingrys and Mahon 1998).

For the measurements of target conspicuity, sizeable inter-observer variations were obtained in response to negative luminance contrast due to the difficulty of matching two targets with opposite contrast polarity (the match target was always defined by positive contrast). The largest between-observer variations, however, were seen in response to colour. Inter-observer variability in response to colour has previously been reported for measurements of perceived brightness (Burns et al. 1982; Nakano et al. 1988; Yaguchi et al. 1993; Ayama and Ikeda 1998). Nakano (1988) modelled successfully, individual differences in perceived brightness as variations in contributions of the chromatic postreceptoral mechanisms. Although psychophysical measures of red-green colour vision at low temporal frequencies show little variation between observers with different ratios of L- to M- cones (Brainard et al. 2000; Kremers et al. 2000; Knau et al. 2001), it is evident that the relative contribution of the red-green and blue-yellow mechanisms to the perception of suprathreshold colour stimuli exhibits considerable variation.

Visual search times recorded for achromatic targets in the mesopic range using an orientation task, revealed differences in the nonlinear variation of search performance with contrast as illumination is reduced. With reduction in light level, curves describing the search time vs. achromatic luminance contrast relationship were shifted along the abscissa towards higher contrast, reflecting the increase in contrast detection thresholds (Blackwell 1946). The rate of decay of these curves also markedly decreased with reduction in light level, indicating that a fixed change in luminance contrast is worth less in terms of its effectiveness for visual search, as ambient illumination is decreased.

Visual search performance was also measured for targets with a combination of colour and luminance contrast, and compared to values of stimulus conspicuity (equivalent achromatic contrast) predicted from the empirical model, which were converted to search times using the search performance curves measured for achromatic targets. This comparison showed that the measure of conspicuity investigated in this study could be used to predict successfully, search performance throughout the mesopic range. The lack of an international standard for spectral luminous efficiency in the mesopic range, means that there is a real need for a measure of stimulus effectiveness under mesopic conditions that will correlate better with task-specific visual performance than either photopic contrast or scotopic contrast. A comparison of photopic contrast, scotopic contrast, and conspicuity as predictors of mesopic visual search performance, revealed that for the targets with a combination of colour and luminance contrast investigated, conspicuity produces better estimates of search time than either photopic or scotopic contrast. The predominant factor determining search performance at mid to low mesopic light levels was found to be scotopic contrast. This paralleled the finding that conspicuity was mainly determined from scotopic contrast in the mid to low mesopic range. At the highest two light levels examined, the coloured targets had minimal photopic luminance contrast and were defined predominantly by their chromatic difference to the background. Results for these targets emphasised the importance of colour in determining visual search performance, particularly when luminance contrast is low, a factor not acknowledged in a recent model of visual

search in the mesopic range (Barbur et al. 1998; Hurden et al. 1999), but in agreement with photopic studies of colour and visual search (Carter and Carter 1981; Barbur and Forsyth 1990; Nagy and Sanchez 1990; D'Zmura 1991). Surprisingly, visual search times for coloured targets investigated at the low photopic/ high mesopic light levels, also appeared to depend on the value of scotopic contrast. It was suggested that this result might be a consequence of the correlation between stimulus scotopic contrast and chromatic difference in this study, but, interestingly, may reflect the importance of scotopic contrast in determining visual performance for a task that involves large areas of the peripheral visual field.

The data set consisting of pairs of stimuli matched for conspicuity (one stimulus defined by a combination of colour and luminance contrast and the other by achromatic contrast) acquired throughout the mesopic range as part of this study, was used to assess how well photopic contrast, scotopic contrast and measures of mesopic luminance contrast, predict conspicuity matches. The measures of mesopic luminance contrast were obtained from six proposed systems of mesopic photometry (CIE 1989; CIE 2001; Palmer 1968; Sagawa and Takeichi 1987; Sagawa and Takeichi 1992; Nakano et al. 1988; CIE 2001; Trezona 1991), and the results compared to predictions of the conspicuity model derived from the conspicuity matching data set. The results showed that above the lowest light level investigated (L_{10} = 0.0025), both photopic contrast and scotopic contrast were poorer predictors of conspicuity matches than the empirical model of conspicuity, but scotopic contrast predicted closer matches at the lowest light level. This was similar to the finding that conspicuity produced improved estimates of visual search performance than either photopic or scotopic contrast. The comparison of conspicuity match prediction errors for the empirical model and the measures of mesopic luminance contrast, suggested that over much of the mesopic range, conspicuity could be adequately predicted from a suitable combination of photopic and scotopic contrast. For low photopic/high mesopic light levels, however, successful prediction of conspicuity matches also requires modelling of the chromatic contribution to conspicuity. In the conspicuity model the metric for specifying suprathreshold colour differences was based on distances in the CIE 1976 uniform

colour space. The finding that one of the measures of mesopic brightness contrast outperformed the empirical conspicuity model at the highest light level investigated, suggests that modelling of the contribution of colour to conspicuity using this colour difference metric in the high mesopic range, may not be appropriate when suprathreshold colours are involved.

7.1 Conclusions

Chromatic sensitivity in normals is dependent on many stimulus factors, including size, spatial distribution, eccentricity of presentation and level of illumination. These factors appear to reflect variations in the performance of cone receptors (with greater changes observed for the S-cone system at high spatial frequencies and low light levels) coupled with changes in the relative cone contributions to the chromatic postreceptoral mechanisms. Under the mesopic conditions investigated in this study, no changes in chromatic sensitivity could be attributed to the effects of rod intrusion. This result suggests that at chromatic threshold, rod signals and chromatic signals are processed separately in the mesopic range, as it has been demonstrated in the photopic range (Barbur et al. 1992). Threshold differences for detection of a colour defined pattern and detection of pure colour changes in a pattern defined by luminance contrast, are likely to reflect the spatial summation characteristics of chromatic mechanisms, but may suggest differential processing of colour inherently associated with and independent of spatial structure. These results have implications for the comparison of results from different types of colour vision test, e.g., pseudoisochromatic plates vs. tests employing uniform colour stimuli, particularly in subjects with retinal/ optic nerve pathology.

Stimulus conspicuity, the suprathreshold measure of stimulus effectiveness developed in this study, is higher for negative than positive luminance contrast stimuli. There are also individual variations in response to both suprathreshold luminance contrast signals and chromatic signals, which are likely to reflect differences in individual gain control of the achromatic and chromatic postreceptoral mechanisms. Conspicuity in the mesopic range is dependent on

stimulus photopic contrast, scotopic contrast, chromatic difference to the background and level of illumination. Photopic contrast and chromatic difference account largely for measured conspicuity at low photopic/high mesopic levels, and scotopic contrast becomes the dominant factor in the low mesopic range.

The characteristics of visual search are altered with changes in the level of illumination. Reduction of illumination produces a decrease in the decay rate of the nonlinear relationship between search performance and luminance contrast. At low photopic/high mesopic light levels, colour is an important determinant of search performance, particularly when luminance contrast is low, whereas luminance contrast is the predominant determinant of performance in the mid to low mesopic range. However, a novel finding that has emerged from this study is that for the stimulus conditions employed in the visual search task, scotopic contrast appeared to contribute to visual performance, even in the low photopic range. The empirical model of stimulus conspicuity developed in this study can be used to predict successfully visual search performance in the mesopic range, and represents a better predictor of visual performance than either photopic or scotopic contrast.

The conspicuity model provides a useful alternative means of assessing the effectiveness of visual stimuli, which has been shown to be valid for a visual search task. This model may have applications in the design of lighting in situations where a desired level of performance for a defined visual task can be set, for example in nighttime driving.

Appendices

Appendix A. Statistical tables

ANOVA table for the change in minor semi-axis length with stimulus size, of an ellipse fitted to the mean chromatic thresholds of six normal trichromats for the pattern test employed in chapter 3.

Source	Sum of Squares	df	Mean Square	F	Sig.
Between groups	22.704	2	11.352	11.117	0.000
Within groups	33.699	33	1.021		
Total	56.404	35			

Table A1.

Results of the ANOVA for the change in major semi-axis length with stimulus size, of an ellipse fitted to the mean chromatic thresholds of three normal trichromats for the colour test employed in chapter 3.

Source	Sum of Squares	df	Mean Square	F	Sig.
Between groups	3.328	2	3.164	2.244	0.140
Within groups	21.149	15	1.410		
Total	27.478	17			

Table A2.

ANOVA table for the change in minor semi-axis length with stimulus size, of an ellipse fitted to the mean chromatic thresholds of three normal trichromats for the colour test employed in chapter 3.

Source	Sum of Squares	df	Mean Square	F	Sig.
Between groups	3.545	2	1.773	4.540	0.029
Within groups	5.857	15	0.390		
Total	9.402	17			

Table A3.

Table for the ANOVA carried out to compare results obtained using experimental system-1 and system-2, on which the matching procedure was run in chapter 5. The analysis took into account differences in the results due to the 14 test target conditions investigated (condition) and the experimental system used (system).

Source	Sum of Squares	df	Mean Square	F	Sig.
Corrected Model	102.758	27	3.806	127.808	0.000
Intercept	505.845	1	505.845	16987.206	0.000
Condition	101.647	13	7.819	262.575	0.000
System	7.196E-03	1	7.196E-03	0.242	0.623
Condition * System	1.104	13	8.496E-02	2.853	0.001
Error	14.174	476	2.978E-02		
Total	622.778	504			
Corrected Total	116.933	503			

R Squared = .879 (Adjusted R Squared = .872)

Condition	14 levels
System	2 levels

Table A4.

ANOVA table investigating the effect of test target photopic contrast (C_p), scotopic contrast (C_s), chromatic difference (CD), log retinal illuminance ($L_{10}E$), and all two-way interactions, plus the effect due to the observer (Obs) on achromatic match contrast measured in chapter 5, over all six light levels examined.

Source	Sum of Squares	df	Mean Square	F	Sig.
Corrected Model	749.422	382	1.962	30.876	0.000
Intercept	265.936	1	265.936	4185.393	0.000
C_p	13.884	6	2.314	36.417	0.000
C_s	23.850	6	3.975	62.559	0.000
CD	7.281	3	2.429	38.195	0.000
$L_{10}E$	32.652	5	6.530	102.779	0.000
Obs	91.270	4	22.817	359.108	0.000
$C_p * C_s$	9.311	32	0.291	4.579	0.000
$C_p * CD$	5.001	17	0.294	4.629	0.000
$C_p * L_{10}E$	4.373	22	0.199	3.128	0.000
$C_S * CD$	2.431	16	0.152	2.391	0.001
$C_S * L_{10}E$	14.420	28	0.515	8.105	0.000
$CD * L_{10}E$	2.883	15	0.192	3.025	0.000
$C_P * C_S * CD$	2.464	14	0.176	2.770	0.000
$C_P * C_S * L_{10}E$	2.338	82	6.509E-02	1.024	0.420
$C_p * CD * L_{10}E$	1.520	49	3.103E-02	0.488	0.999
$C_s * CD * L_{10}E$	1.575	42	3.751E-02	0.590	0.983
Error	125.935	1982	6.354E-02		
Total	2436.847	2365			
Corrected Total	875.357	2364			

R Squared = .856 (Adjusted R Squared = .828)

C_p	7 levels
C_s	7 levels (raw values coded into discrete levels with a flat frequency distribution)
CD	4 levels (raw values coded into discrete levels with a flat frequency distribution)
$log_{10}E$	6 levels (raw values coded into discrete levels with the distribution of $log_{10}L_b$)
Obs	5 levels

Table A5.

Results of the ANOVA carried out to investigate the effect of test target parameters on achromatic match contrast measured in chapter 5, taking into account both the magnitude and sign of the luminance contrast terms ($|C_p|$, sign C_p, $|C_s|$ and sign

C_s), over all six light levels examined. Main effects of $|C_p|$, sign C_p, $|C_s|$, sign C_s, CD and $L_{10}E$, and all two-way interactions were entered into the analysis.

Source	Sum of Squares	df	Mean Square	F	Sig.
Corrected Model	715.455	155	6.221	87.503	0.000
Intercept	448.493	1	448.493	6308.024	0.000
CD	14.253	3	4.751	66.825	0.000
$L_{10}E$	53.218	5	10.644	149.702	0.000
Obs	95.217	4	23.804	334.806	0.000
$\|C_p\|$	22.168	2	11.084	155.895	0.000
$\|C_s\|$	28.825	3	9.608	135.140	0.000
sign C_p	2.578	1	2.578	36.257	0.000
sign C_s	1.564	1	1.564	21.998	0.000
CD * $L_{10}E$	18.849	15	1.257	17.674	0.000
CD * $\|C_p\|$	1.142	6	0.190	2.676	0.014
CD * $\|C_s\|$	4.636	9	0.515	7.245	0.000
CD * sign C_p	2.327	3	0.776	10.912	0.000
CD * sign C_s	0.501	3	0.167	2.351	0.071
$L_{10}E$ * $\|C_p\|$	3.958	6	0.660	9.278	0.000
$L_{10}E$ * $\|C_s\|$	17.638	14	1.260	17.720	0.000
$L_{10}E$ * sign C_p	2.785	5	0.557	7.833	0.000
$L_{10}E$ * sign C_s	9.889	5	1.978	27.817	0.000
$\|C_p\|$ * $\|C_s\|$	0.282	6	1.704E-02	0.662	0.681
$\|C_p\|$ * sign C_p	1.118	2	0.559	7.859	0.000
$\|C_p\|$ * sign C_s	1.059	2	0.529	7.446	0.001
$\|C_s\|$ * sign C_p	1.966	3	0.655	9.219	0.000
$\|C_s\|$ * sign C_s	0.795	3	0.265	3.726	0.011
sign C_p * sign C_s	1.821	1	1.821	25.614	0.000
Error	159.901	2249	7.110E-02		
Total	2436.847	2365			
Corrected Total	875.357	2364			

R Squared = .817 (Adjusted R Squared = .808)

CD	4 levels (raw values coded into discrete levels with a flat frequency distribution)
$\log_{10}E$	6 levels (raw values coded into discrete levels with the distribution of $\log_{10}L_b$)
Obs	5 levels
$\|C_p\|$	4 levels
$\|C_s\|$	4 levels (raw values coded into discrete levels with a flat frequency distribution)
sign C_p	3 levels
sign C_s	2 levels (no zero C_s values)

Table A6.

The results of ANOVAs performed for each individual light level to investigate the effects of test target parameters (main effects and two-way interactions) on achromatic match contrast as measured in chapter 5.

Light level 1 (highest).

Source	Sum of Squares	df	Mean Square	F	Sig.
Corrected Model	157.441	90	1.749	27.584	0.000
Intercept	35.272	1	35.272	556.188	0.000
C_p	24.218	4	6.055	95.470	0.000
C_s	0.111	4	2.775E-02	0.438	0.781
CD	13.867	3	4.622	72.888	0.000
$L_{10}E$	6.495E-02	3	2.165E-02	0.341	0.795
Obs	27.991	4	6.998	110.345	0.000
$C_p * C_s$	2.448	15	0.163	2.573	0.001
$C_p * CD$	4.327	12	0.361	5.686	0.000
$C_p * L_{10}E$	2.216	12	0.185	2.912	0.001
$C_S * CD$	0.578	11	5.2595E-02	0.829	0.611
$C_S * L_{10}E$	0.639	12	5.328E-02	0.840	0.609
$CD * L_{10}E$	2.899	9	0.322	5.079	0.000
Error	18.645	294	6.342E-02		
Total	297.707	385			
Corrected Total	176.086	384			

R Squared = .894 (Adjusted R Squared = .862)

C_p	5 levels
C_s	5 levels (raw values coded into discrete levels with a flat frequency distribution)
CD	4 levels (raw values coded into discrete levels with a flat frequency distribution)
$log_{10}E$	4 levels (raw values coded into discrete levels with a flat frequency distribution)
Obs	5 levels

Table A7.

Light level 2.

Source	Sum of Squares	df	Mean Square	F	Sig.
Corrected Model	120.193	90	1.335	28.019	0.000
Intercept	88.675	1	88.675	1860.43	0.000
C_p	27.030	4	6.757	141.774	0.000
C_s	0.473	4	0.118	2.481	0.044
CD	7.440	3	2.480	52.033	0.000
$L_{10}E$	0.143	3	4.751E-02	0.997	0.395
Obs	16.386	4	4.097	85.948	0.000
$C_p * C_s$	2.400	15	0.160	3.357	0.000
$C_p * CD$	3.806	12	0.317	60654	0.000
$C_p * L_{10}E$	2.370	12	0.198	4.144	0.000
$C_S * CD$	0.342	11	3.109E-02	0.652	0.783
$C_S * L_{10}E$	0.540	12	4.499E-02	0.944	0.503
$CD * L_{10}E$	1.328	9	0.148	3.095	0.001
Error	13.775	289	4.766E-02		
Total	421.228	380			
Corrected Total	133.968	379			

R Squared = .897 (Adjusted R Squared = .865)

C_p	5 levels
C_s	5 levels (raw values coded into discrete levels with a flat frequency distribution)
CD	4 levels (raw values coded into discrete levels with a flat frequency distribution)
$log_{10}E$	4 levels (raw values coded into discrete levels with a flat frequency distribution)
Obs	5 levels

Table A8.

Light level 3.

Source	Sum of Squares	df	Mean Square	F	Sig.
Corrected Model	76.526	90	0.850	17.290	0.000
Intercept	90.787	1	90.787	1846.127	0.000
C_p	11.957	4	2.989	60.784	0.000
C_s	1.428	4	0.357	7.261	0.000
CD	2.291	3	0.764	15.529	0.000
$L_{10}E$	0.131	3	4.382E-02	0.891	0.446
Obs	22.152	4	5.529	122.613	0.000
$C_p * C_s$	2.963	15	0.198	4.017	0.000
C_p * CD	1.708	12	0.142	2.895	0.001
$C_p * L_{10}E$	0.925	12	7.709E-02	1.568	0.101
C_S * CD	0.831	11	7.555E-02	1.536	0.118
$C_S * L_{10}E$	1.474	12	0.123	2.498	0.004
CD * $L_{10}E$	0.640	9	7.109E-02	1.446	0.168
Error	13.474	274	4.918E-02		
Total	447.898	365			
Corrected Total	90.000	364			

R Squared = .850 (Adjusted R Squared = .801)

C_p	5 levels
C_s	5 levels (raw values coded into discrete levels with a flat frequency distribution)
CD	4 levels (raw values coded into discrete levels with a flat frequency distribution)
$log_{10}E$	4 levels (raw values coded into discrete levels with a flat frequency distribution)
Obs	5 levels

Table A9.

Light level 4.

Source	Sum of Squares	df	Mean Square	F	Sig.
Corrected Model	55.736	87	0.641	15.636	0.000
Intercept	79.173	1	79.273	1934.819	0.000
C_p	2.532	4	0.633	15.450	0.000
C_s	5.184	4	1.296	31.633	0.000
CD	274	3	9.146E-02	2.232	0.085
$L_{10}E$	0.154	3	5.14E-02	1.255	0.291
Obs	8.432	4	2.108	51.451	0.000
$C_p * C_s$	4.288	14	0.306	7.475	0.000
$C_p * CD$	0.760	10	7.602E-02	1.855	0.053
$C_p * L_{10}E$	0.579	12	4.821E-02	1.177	0.301
$C_S * CD$	0.662	9	7.360E-02	1.796	0.070
$C_S * L_{10}E$	0.854	12	7.115E-02	1.737	0.060
$CD * L_{10}E$	0.335	9	3.719E-02	0.908	0.519
Error	9.301	227	4.097E-02		
Total	472.713	315			
Corrected Total	35.036	314			

R Squared = .857 (Adjusted R Squared = .802)

C_p	5 levels
C_s	5 levels (raw values coded into discrete levels with a flat frequency distribution)
CD	4 levels (raw values coded into discrete levels with a flat frequency distribution)
$log_{10}E$	4 levels (raw values coded into discrete levels with a flat frequency distribution)
Obs	5 levels

Table A10.

Light level 5.

Source	Sum of Squares	df	Mean Square	F	Sig.
Corrected Model	181.018	131	1.382	27.923	0.000
Intercept	27.327	1	27.327	552.209	0.000
C_p	2.005	6	0.334	6.753	0.000
C_s	8.882	6	1.480	29.912	0.000
CD	0.461	3	0.154	3.106	0.027
$L_{10}E$	0.236	3	7.878E-02	1.592	0.191
Obs	6.883	4	1.721	34.771	0.000
$C_p * C_s$	4.734	31	0.153	3.086	0.000
$C_p * CD$	2.927	16	0.183	3.696	0.000
$C_p * L_{10}E$	0.677	18	3.761E-02	0.760	0.747
$C_S * CD$	2.226	14	0.159	3.213	0.000
$C_S * L_{10}E$	2.063	18	0.115	2.316	0.002
$CD * L_{10}E$	0.233	9	2.585E-02	0.522	0.858
Error	19.448	393	4.949E-02		
Total	544.102	252			
Corrected Total	200.466	524			

R Squared = .903 (Adjusted R Squared = .871)

C_p	7 levels
C_s	7 levels (raw values coded into discrete levels with a flat frequency distribution)
CD	4 levels (raw values coded into discrete levels with a flat frequency distribution)
$log_{10}E$	4 levels (raw values coded into discrete levels with a flat frequency distribution)
Obs	5 levels

Table A11.

Light level 6 (lowest).

Source	Sum of Squares	df	Mean Square	F	Sig.
Corrected Model	109.472	111	0.986	29.840	0.000
Intercept	23.908	1	23.908	723.359	0.000
C_p	0.242	6	4.037E-02	1.221	0.295
C_s	11.916	5	2.383	72.160	0.000
CD	0.339	3	0.113	3.414	0.018
$L_{10}E$	0.134	3	4.476E-02	1.354	0.257
Obs	5.973	4	1.493	45.177	0.000
$C_p * C_s$	1.782	21	8.485E-02	2.567	0.000
$C_p * CD$	1.009	13	7.765E-02	2.349	0.005
$C_p * L_{10}E$	0.885	18	4.919E-02	1.488	0.093
$C_S * CD$	2.070	9	0.230	6.959	0.000
$C_S * L_{10}E$	1.434	15	9.561E-02	2.893	0.000
$CD * L_{10}E$	0.704	9	7.821E-02	2.366	0.014
Error	9.353	283	3.305E-02		
Total	253.199	395			
Corrected Total	118.826	394			

R Squared = .921 (Adjusted R Squared = .890)

C_p	7 levels
C_s	6 levels (raw values coded into discrete levels with a flat frequency distribution)
CD	4 levels (raw values coded into discrete levels with a flat frequency distribution)
$log_{10}E$	4 levels (raw values coded into discrete levels with a flat frequency distribution)
Obs	5 levels

Table A12.

Appendix B: Versions of the conspicuity model

The following equations describe the relationship in terms of conspicuity, between achromatic match contrast (C_m) and the predictor variables: photopic contrast, scotopic contrast, chromatic difference and either retinal illuminance or background luminance, determined empirically in chapter 5. Four versions of the model were developed. Two versions included all terms that were statistically significant in the fit; one included retinal illuminance as a predictor variable (version-a) and the other included background luminance as a parameter (version-b). Two reduced versions of the model were also developed, which consisted of a total of 10 terms, again one included the parameter retinal illuminance (version-a_r) and the other included background luminance (version-b_r). The form of all four versions was

$$C_m = \exp\{k + f(\text{main effects}) + f(\text{interactions})\} \qquad \textbf{Eq. B-1}$$

where C_m: achromatic match contrast, k: constant, f(main effects): function of the main predictor variables, f(interactions): function of pairwise multiples of the predictor variables. The following terms appear in two or all four versions of the conspicuity model.

$\lvert C_p \rvert$	absolute value of photopic contrast	
sC_p	sign of photopic contrast	$sC_p = \begin{cases} 1 \text{ if } C_p > 0 \\ 0 \text{ if } C_p = 0 \\ -1 \text{ if } C_p < 0 \end{cases}$
C_{s+}	positive scotopic contrast	$C_{s+} = \begin{cases} C_s \text{ if } C_s > 0 \\ 0, \text{ otherwise} \end{cases}$
C_{s-}	negative scotopic contrast	$C_{s-} = \begin{cases} C_s \text{ if } C_s < 0 \\ 0, \text{ otherwise} \end{cases}$
logE	base-10 logarithm of retinal illuminance, where retinal illuminance is measured in milli-trolands.	
$\log L_b$	base-10 logarithm of the background luminance, where luminance is measured in milli-cdm^{-2}.	

Table B1.

Version-a

constant	=	k_1			
f(main effects)	=	$k_2.\|C_p\|$	$+k_3.sC_p$	$+k_4.C_{s+}$	$+k_5.C_{s-}$
		$+k_6.CD$	$+k_7.logE$		
f(interactions)	=	$k_8.\|C_p\|.C_{s+}$	$+k_9.\|C_p\|.C_{s-}$	$+k_{10}.\|C_p\|.CD$	$+k_{11}.\|C_p\|.logE$
		$+k_{12}.sC_p.C_{s+}$	$+k_{13}.sC_p.C_{s-}$	$+k_{14}.sC_p.CD$	$+ k_{15}.sC_p.logE$
		$+k_{16}.C_{s+}.CD$	$+k_{17}.C_{s+}.log_{10}E$		
		$+k_{18}.C_{s-}.log_{10}E$			
		$+ k_{19}.CD.logE$			

Table B2.

Coeff	Value	Description
k_1	-3.2084	base factor
k_2	1.1069	sign independent photopic contrast term
k_3	-0.17486	sign of photopic contrast term
k_4	5.8407	positive scotopic contrast term
k_5	-7.8774	negative scotopic contrast term
k_6	-1.9330	chromatic difference term
k_7	0.21472	retinal illuminance term
k_8	-3.3979	sign independent photopic x positive scotopic contrast interaction
k_9	2.9447	sign independent photopic x negative scotopic contrast interaction
k_{10}	-7.239	sign independent photopic contrast x chromatic difference interaction
k_{11}	0.48815	retinal illuminance dependent, sign independent photopic contrast term
k_{12}	0.4812	photopic contrast-sign dependent positive scotopic contrast term
k_{13}	0.27911	photopic contrast-sign dependent negative scotopic contrast term
k_{14}	1.9718	photopic contrast-sign dependent chromatic difference term
k_{15}	-0.02205	photopic contrast-sign dependent retinal illuminance term term
k_{16}	-6.280	positive scotopic contrast x chromatic difference interaction
k_{17}	-0.92429	positive scotopic contrast x retinal illuminance interaction
k_{18}	1.47915	retinal illuminance dependent negative scotopic contrast term
k_{19}	2.1775	retinal illuminance dependent chromatic difference term

Table B3.

Version-b

constant	=	k_1'			
f(main effects)	=	$k_2'.\|C_p\|$	$+k_3'.sC_p$	$+k_4'.C_{s+}$	$+k_5'.C_{s-}$
		$+k_6'.CD$	$+k_7'.\log L_b$		
f(interactions)	=	$k_8'.\|C_p\|.C_{s+}$	$+k_9'.\|C_p\|.C_{s-}$	$+k_{10}'.\|C_p\|.CD$	$+k_{11}'.\|C_p\|.\log L_b$
		$+k_{12}'.sC_p.C_{s+}$	$+k_{13}'.sC_p.C_{s-}$	$+k_{14}'.sC_p.CD$	
		$+k_{15}'.C_{s+}.CD$	$+k_{16}'.C_{s+}.\log L_b$		
		$+k_{17}'.C_{s-}.\log L_b$			
		$+k_{18}'.CD.\log L_b$			

Table B4.

Coeff	Value	Description
k_1'	-2.8601	base factor
k_2'	1.9276	sign independent photopic contrast term
k_3'	-0.27990	sign of photopic contrast term
k_4'	4.3897	positive scotopic contrast term
k_5'	-5.3736	negative scotopic contrast term
k_6'	1.832	chromatic difference term
k_7'	0.19427	background luminance term
k_8'	-3.4293	sign independent photopic x positive scotopic contrast interaction
k_9'	2.9834	sign independent photopic x negative scotopic contrast interaction
k_{10}'	-7.202	sign independent photopic contrast x chromatic difference interaction
k_{11}'	0.43425	luminance dependent, sign independent photopic contrast term
k_{12}'	0.5525	photopic contrast-sign dependent positive scotopic contrast term
k_{13}'	0.22653	photopic contrast-sign dependent negative scotopic contrast term
k_{14}'	2.0687	photopic contrast-sign dependent chromatic difference term
k_{15}'	-6.968	positive scotopic contrast x chromatic difference interaction
k_{16}'	-0.85106	positive scotopic contrast x background luminance interaction
k_{17}'	1.30554	luminance dependent negative scotopic contrast term
k_{18}'	1.9127	luminance dependent chromatic difference term

Table B5.

Version-a_r

constant	=	k_{1r}			
f(main effects)	=	$k_{2r}.\|C_p\|$	$+k_{3r}.C_{s+}$	$+k_{4r}.C_{s-}$	$+k_{5r}.CD$
		$+k_{6r}.logE$			
f(interactions)	=	$k_{7r}.\|C_p\|.logE$	$+k_{8r}.C_{s+}.logE$	$+k_{9r}.C_{s-}.logE$	$+k_{10r}.CD.logE$

Table B6.

Coeff	Value	Description
k_{1r}	-2.1758	base factor
k_{2r}	-1.1452	sign independent photopic contrast term
k_{3r}	4.3315	positive scotopic contrast term
k_{4r}	-7.3079	negative scotopic contrast term
k_{5r}	-7.7927	chromatic difference term
k_{6r}	0.07793	retinal illuminance term
k_{7r}	0.69076	retinal illuminance dependent, sign independent photopic contrast term
k_{8r}	-0.88485	retinal illuminance dependent positive scotopic contrast term
k_{9r}	1.42916	retinal illuminance dependent negative scotopic contrast term
k_{10r}	2.7880	retinal illuminance dependent chromatic difference term

Table B7.

Version-b_r

constant	=	k_{1r}'			
f(main effects)	=	$k_{2r}'.\lvert C_p \rvert$	$+k_{3r}'.C_{s+}$	$+k_{4r}'.C_{s-}$	$+k_{5r}'.CD$
		$+k_{6r}'.\log L_b$			
f(interactions)	=	$k_{7r}'.\lvert C_p \rvert.\log L_b$	$+k_{8r}'.C_{s+}.\log L_b$	$+k_{9r}'.C_{s-}.\log L_b$	$+k_{10r}'.CD.\log L_b$

Table B8.

Coeff	Value	Description
k_{1r}'	-2.02544	base factor
k_{2r}'	0.0014	sign independent photopic contrast term
k_{3r}'	2.8101	positive scotopic contrast term
k_{4r}'	-4.8870	negative scotopic contrast term
k_{5r}'	-3.2028	chromatic difference term
k_{6r}'	0.06257	background luminance term
k_{7r}'	0.61745	luminance dependent, sign independent photopic contrast term
k_{8r}'	-0.77321	luminance dependent positive scotopic contrast term
k_{9r}'	1.25783	luminance dependent negative scotopic contrast term
k_{10r}'	2.5077	luminance dependent chromatic difference term

Table B9.

Appendix C. 10° systems of mesopic photometry

The six 10° systems of mesopic photometry used in the investigations in chapter 5 are described below. The various input parameters are defined as follows

E_λ	Spectral radiance	
L	CIE 1924 photopic luminance	$683\int E_\lambda V(\lambda)\,d\lambda$
L_{10}	CIE 1964 photopic luminance	$683\int E_\lambda \bar{y}_{10}(\lambda)\,d\lambda$
L′	CIE 1951 scotopic luminance	$1700\int E_\lambda V'(\lambda)\,d\lambda$
X_{10}	CIE 1964 X-tristimulus value	$683\int E_\lambda \bar{x}_{10}(\lambda)\,d\lambda$
Y_{10}	CIE 1964 Y-tristimulus value	$683\int E_\lambda \bar{y}_{10}(\lambda)\,d\lambda$
Z_{10}	CIE 1964 Z-tristimulus value	$683\int E_\lambda \bar{z}_{10}(\lambda)\,d\lambda$
x	CIE 1931 x-chromaticity coordinate	$\frac{X}{X+Y+Z}$, $X=683\int E_\lambda \bar{x}(\lambda)\,d\lambda$
		$Y=683\int E_\lambda \bar{y}(\lambda)\,d\lambda$
		$Z=683\int E_\lambda \bar{z}(\lambda)\,d\lambda$
y	CIE 1931 y-chromaticity coordinate	$\frac{Y}{X+Y+Z}$
x_{10}	CIE 1964 x-chromaticity coordinate	$\frac{X_{10}}{X_{10}+Y_{10}+Z_{10}}$
y_{10}	CIE 1964 y-chromaticity coordinate	$\frac{Y_{10}}{X_{10}+Y_{10}+Z_{10}}$

Table C1.

Palmer 1st

The Palmer 1st system is a linear combination of L_{10} and L′.

Input parameters L_{10} and L′

Calculation of L_{seq}

$$a = \frac{M}{L_{10} + M}, \text{ where } M = 0.04$$

$$L_{seq} = aL' + (1-a)L_{10}$$

Palmer 2nd

The Palmer 2nd system consists of a nonlinear combination of L_{10} and L′.

Input parameters L_{10} and L′

Calculation of L_{seq}

$$L_{seq} = (ML')^{1/2} + L_{10} + \frac{M}{2} - \left\{M\left[(ML')^{1/2} + L_{10} + \frac{M}{4}\right]\right\}^{1/2}$$

where M=0.06

Sagawa-Takechi

The Sagawa-Takeichi system is based on a weighted mean of L′ and a photopic component caluclated from L and the CIE 1931 (x, y)-chromatcity coordinates.

Input parameters x, y, L and L′

Calculation of L_{seq}

$$c = 0.256 - 0.184y - 2.527xy + 4.656x^3y + 4.657xy^4$$

$$c' = 2(c + 0.047)$$

$$L_{seq,p} = L.10^{c'}$$

$$L_{seq,s} = 1.84L'$$

$$L_{seq} = (L_{seq,s})^{a} + (L_{seq,p})^{1-a}$$

On a graph of a vs. L_{seq} (given in the table below) draw a straight line through the points ($L_{seq,\,p}$, 0) an ($L_{seq,\,s}$, 1) and from the intersection read off the value of a.

L_{seq} (log cdm^{-2})	Adaptation coefficient a
-3.18	1.00
-2.68	0.87
-2.17	0.71
-1.71	0.54
-1.30	0.38
-0.83	0.26
-0.31	0.13
0.28	0.05
0.84	0.00

Table C2.

Nakano-Ikeda

In the Nakano-Ikeda system L_{seq} is computed from the combination of a scotopic component and a photopic component that takes into account the chromaticity of the stimulus; these components are weighted in relation to proportions of 10° photopic luminance and scotopic luminance.

Input parameters L_{10} and L', x_{10} and y_{10}

Calculation of L_{seq}

$$L_p = \frac{621.1}{683} L_{10}$$

$$L_s = \frac{689.7}{1700} L'$$

$$\begin{pmatrix} \xi \\ \eta \\ \zeta \end{pmatrix} = \begin{pmatrix} 0.38355 & 0.73268 & -0.08977 \\ -0.24931 & 1.20294 & 0.03116 \\ -0.00063 & 0.00163 & 0.93097 \end{pmatrix} \begin{pmatrix} \frac{x_{10}}{y_{10}} \\ 1 \\ \frac{1-x_{10}-y_{10}}{y_{10}} \end{pmatrix}$$

$$\alpha = 0.374 \frac{\xi}{\xi+\eta+\zeta} + 0.002(\eta-\zeta)\xi$$

$$\beta = 0.374 \frac{\eta}{\xi+\eta+\zeta} + 0.002(\zeta-\xi)\eta$$

$$\gamma = 0.374 \frac{\zeta}{\xi+\eta+\zeta} + 0.002(\xi-\eta)\zeta$$

$$F_{L-M} = (1.015+\alpha)\ln(\xi+1) + (-0.389+\beta)\ln(\eta+1) + (0.000+\gamma)\ln(\zeta+1)$$

$$F_{M-L} = (-0.537+\alpha)\ln(\xi+1)+(1.341+\beta)\ln(\eta+1) \\ (-0.178+\gamma)\ln(\zeta+1)$$

$$F = \max(F_{L-M}, F_{M-L})$$

$$s = \frac{L_s}{L_p}$$

$$p = \exp(F)-1$$

$$c = \left[\frac{0.026}{L_p+0.026}\right]\log s + \left[\frac{L_p}{L_p+0.032}\right]\log p$$

$$L_{seq} = L_p.10^c$$

Kokoschka-Bodmann

The Kokoschka-Bodmann model is based on a linear weighted sum of four variables: scotopic luminance and the CIE 1964 tristimulus values X_{10}, Y_{10}, and Z_{10}. The weighting is dependent on L_{seq}, rmaking computation of L_{seq} an interative procedure.

Input parameters X_{10}, Y_{10}, Z_{10} and L'

Calculation of L_{seq} Calculate a number of L_{est} values using the F coefficients in the table below for tabulated L_{seq} values close to Y_{10}. Interpolate between values in the rows of the table to obtain $L_{est} = L_{seq}$.

$$L_{est} = F_x X_{10} + F_y Y_{10} + F_z Z_{10} + F_s L'$$

$$c_{10} = 0.256 - 0.184y_{10} - 2.527x_{10}y_{10} + 4.656x_{10}^{3}y_{10} \\ + 4.657x_{10}y_{10}^{4}$$

$$c^* = c_{10} + 0.067$$

$$f_0 = 10^{c^*}$$

$$f = 1+(f_0-1)(0.6+0.2\log L_{10})$$

$$L_{seq} = L_{est}.f$$

L_{seq} (cdm^{-2})	F_x	F_y	F_z	F_s
0.00000204	0	0	0	1
0.00000323	-0.0019	0.00649	0.000354	0.996
0.00000512	-0.00685	0.0237	0.00136	0.985
0.00000813	-0.0138	0.0483	0.00295	0.969
0.0000129	-0.0216	0.0769	0.00504	0.95
0.0000204	-0.0292	0.106	0.00754	0.93
0.0000326	-0.0356	0.133	0.0104	0.911
0.0000522	-0.041	0.158	0.0132	0.892
0.0000835	-0.0453	0.18	0.0159	0.875
0.000134	-0.0488	0.201	0.0181	0.858
0.000214	-0.0516	0.221	0.0195	0.842
0.000314	-0.0543	0.241	0.02	0.825
0.000557	-0.0591	0.269	0.0201	0.803
0.000899	-0.0687	0.313	0.0206	0.772
0.00145	-0.0858	0.38	0.0219	0.726
0.00234	-0.113	0.479	0.0249	0.661
0.00386	-0.151	0.614	0.0299	0.573
0.00639	-0.194	0.77	0.036	0.471
0.0106	-0.234	0.927	0.0422	0.364
0.0175	-0.264	1.07	0.0473	0.263
0.0288	-0.276	1.17	0.0501	0.175
0.0495	-0.265	1.22	0.05	0.11
0.0854	-0.236	1.23	0.0472	0.0653
0.147	-0.195	1.21	0.0426	0.0364
0.254	-0.151	1.17	0.0368	0.0194
0.437	-0.111	1.13	0.0307	0.01
0.78	-0.0806	1.09	0.0248	0.00458
1.4	-0.0592	1.07	0.0194	0.00173
2.52	-0.0445	1.05	0.0145	0.000711
4.53	-0.0343	1.04	0.0103	0.0003
8.13	-0.0262	1.03	0.00679	0
14.5	-0.0185	1.02	0.0041	0
47	-0.00552	1.01	0.000906	0
84.3	-0.00149	1	0	0
151	0	1	0	0
258	0	1	0	0
444	0	1	0	0
762	0	1	0	0
999	0	1	0	0

Table C3.

Trezona

The Trezona model is also based on four variables, which are derived from $V'(\lambda)$, the CIE 1964 colour matching functions $\bar{x}_{10}(\lambda), \bar{y}_{10}(\lambda)$, and $\bar{z}_{10}(\lambda)$, and the spectral radiometric data for the stimulus.

Input parameters E_λ

Calculation of L_{seq}

$$X_t = \frac{\int E_\lambda \bar{x}_{10}(\lambda)\,d\lambda}{\int E_\lambda\,d\lambda}$$

$$Y_t = \frac{\int E_\lambda \bar{y}_{10}(\lambda)\,d\lambda}{\int E_\lambda\,d\lambda}$$

$$Z_t = \frac{\int E_\lambda \bar{z}_{10}(\lambda)\,d\lambda}{\int E_\lambda\,d\lambda}$$

$$V'_t = \frac{\int E_\lambda V'(\lambda)\,d\lambda}{\int E_\lambda\,d\lambda}$$

$$S' = -1.2834 + 0.1242\frac{X_t}{Y_t} + 0.1207\frac{Z_t}{Y_t} - 1.3919\frac{V'_t}{Y_t} - 0.1507\frac{X_t^2}{Y_t^2} - 0.0190\frac{X_t Z_t}{Y_t^2} + 0.0156\frac{Z_t^2}{Y_t^2} - 0.1166\frac{Z_t V'_t}{Y_t^2} + 0.3301\frac{V'^2_t}{Y_t^2} + 0.1493\frac{V'_t X_t}{Y_t^2}$$

$$S = S' - \log Y_t$$

$$P' = +0.4423 - 0.7054\frac{X_t}{Y_t} - 0.1100\frac{Z_t}{Y_t} - 0.1099\frac{V'_t}{Y_t} + 0.2020\frac{X_t^2}{Y_t^2} + 0.0341\frac{X_t Z_t}{Y_t^2} - 0.0188\frac{Z_t^2}{Y_t^2} + 0.0017\frac{Z_t V'_t}{Y_t^2} + 0.0519\frac{V'^2_t}{Y_t^2} + 0.3458\frac{V'_t X_t}{Y_t^2}$$

$$P = P' - \log Y_t$$

$$a = \log V'_t + 1.1278$$

$$b' = 0.325 - 0.184 y_{10} - 2.527 x_{10} y_{10} + 4.656 x_{10}^3 y_{10} + 4.657 x_{10} y_{10}^4$$

$$b = b' + \log Y_t$$

$$d = \frac{(S+P)}{2}$$

$$m = 2\tanh^{-1}\left[\frac{1-\left(\frac{0.1}{a-b}\right)}{P-S}\right]$$

Convert log Y_{10} (log cdm^{-2}) into photopic retinal illuminance N_p (log photpic trolands) using the table below and interpolating between values.

$$N = N_p + 0.1656 - \log Y_t$$

$$M = N + \frac{a+b}{2-\left(\frac{a-b}{2}\right)\tanh\left[m(N-d)\right]}$$

$$R = M - 0.4148 + 0.3172\left[\tanh 1.845(M+0.489)\right] - 0.1660$$

Luminance (log cdm^{-2})	Retinal illuminance (log Td)
-8	-6.30
-7	-5.30
-6	-4.30
-5	-3.31
-4	-2.32
-3	-1.35
-2	-0.42
-1	0.47
0	1.29
1	2.07
2	2.85
3	3.69
4	4.59
5	5.54
6	6.52

Table C4.

References and bibliography

ABRAMOV, I., GORDON, J., and CHAN, H. (1991). Color appearance in the peripheral retina: effects of stimulus size.
Journal of the Optical Society of America, A, 8(2): 404-414.

AGUILAR, M. and STILES, W.S. (1954). Saturation of the rod mechanism of the retina at high levels of illumination.
Optica Acta, 1: 59-65.

ALEXANDER, K.R. and FISHMAN, G.A. (1984). Rod-cone interaction in flicker perimetry.
British Journal of Ophthalmology, 68: 303-309.

ALEXANDER, K.R. and FISHMAN, G.A. (1986). Rod influence on cone flicker detection: variation with retinal eccentricity.
Vision Research, 26(6): 827-834.

ALPERN, M., LEE, G.B., MAASEIDVAAG, F. et al. (1971). Colour vision in blue-cone monochromacy.
Journal of Physiology, 212: 211-233.

ALVAREZ, S.L. and KING-SMITH, P.E. (1984). Dichotomy of psychophysical responses in retrobulbar neuritis.
Ophthalmic and Physiological Optics, 4(1): 101-105.

ANDREWS, T.J. and COPPOLA, D.M. (1999). Idiosyncratic characteristics of saccadic eye movements when viewing different visual environments.
Vision Research, 39(17): 2947-2953.

ARDEN, G.B. and HOGG, C.R. (1985). Rod-cone interactions and analysis of retinal disease.
British Journal of Ophthalmology, 69: 404-415.

AYAMA, M. and IKEDA, M. (1998). Brightness-to-luminance ratio of colored light in the entire chromaticity diagram.
Color Research and Application, 23(5): 274-287.

BAKER, H.D. and RUSHTON, W.A.H. (1965). The red-sensitive pigment in normal cones.
Journal of Physiology, 176: 56.

BARBUR, J.L., BIRCH, J., and HARLOW, J.A. (1992). Threshold and suprathreshold responses to chromatic stimuli using psychophysical and pupillometric methods.
In: Noninvasive assessment of the visual system. Technical digest. Vol1. Washington, D.C.: Optical Society of America; p51-54.

BARBUR, J.L. and FORSYTH, P.M. (1990). The effective contrast of coloured targets and its relation to visual search.
In: Proceedings of the first international conference on visual search. Ed: Brogan, D. London: Taylor and Francis Ltd; p319-328.

BARBUR, J.L., FORSYTH, P.M., and WOODING, D.S. (1991). Colour, effective contrast and search performance.
In: Ocularmotor control and cognitive processes. Ed: Schmid, R. and Zambarbieri, D. North Holland: Elsevier Science.

BARBUR, J.L., HARLOW, A.J., SAHRAIE, A. et al. (1994a). Responses to chromatic stimuli in the absence of V1: pupillometric and psychophysical studies.
In: Vision Science and its Application. Technical Digest. Vol 2. Washington DC: Optical Society of America; p312-315.

BARBUR, J.L., HARLOW, A.J., SMITH, P. et al. (1998a). Visual performance in the mesopic range.
In: Non-invasive Assessment of the Visual System. Technical Digest Series. Vol 1. Washington DC: Optical Society of America; p140-143.

BARBUR, J.L., HOLLIDAY, I.E., and RUDDOCK, K.H. (1986). The spatial and temporal organisation of motion perception units in human vision.
Acta Psychologica, 48: 35-47.

BARBUR, J.L., SAHRAIE, A., SIMMONS, A. et al. (1998b). Residual processing of chromatic signals in the absence of a geniculostriate projection.
Vision Research, 38(21): 3347-3353.

BARBUR, J.L., THOMSON, W.D., and FORSYTH, P.M. (1987). A new system for the simultaneous measurement of pupil size and two-dimensional eye movements.
Clinical Vision Sciences, 2(2): 131-142.

BARBUR, J.L., WOLF, J., and LENNIE, P. (1998c). Visual processing levels revealed by response latencies to changes in different visual attributes.
Proceedings of the Royal Society of London, Series B, 265(1412): 2321-2325.

BARBUR, J.L., COLE, V.A., and PLANT, G.T. (1997). Chromatic discrimination in subjects with both congenital and acquired colour vision deficiencies.
In: Colour Vision Deficiencies XIII, Documenta Ophthalmologica Proceedings Series. Ed: Cavonius, C.R. Dordrecht: Kluwer; p211-223.

BARBUR, J.L., HARLOW, J.A., and PLANT, G.T. (1994b). Insights into the different exploits of colour in the visual cortex.
Proceedings of the Royal Society of London, Series B, 258: 327-334.

BARLOW, H.B. (1958). Temporal and spatial summation in human vision at different background intensities.
Journal of Physiology, 141: 337-350.

BARLOW, H.B. (1964). Dark adaptation: a new hypothesis.
Vision Research, *4*: 47-58.

BARLOW, H.B. (1972). Dark and light adaptation.
In: Handbook of sensory physiology VII/4: Visual psychophysics. Ed: Jameson, D. and Hurvich, L.M. Berlin: Springer-Verlag; p1-28.

BAUMGARDT, E. (1972). Threshold quantal problems.
In: Handbook of sensory physiology VII/4: Visual psychophysics. Ed: Jameson, D. and Hurvich, L.M. Berlin: Springer-Verlag; p29-55.

BAYLOR, D.A. (1987). Photoreceptor signals and vision. Proctor lecture.
Investigative Ophthalmology and Visual Science, *28*(1): 34-49.

BERGEN, J.R. and *JULESZ, B. (1983)*. Rapid discrimination of visual patterns.
IEEE Transactions on Systems, Man, and Cybernetics, *SMC-13*(5): 857-863.

BLACKWELL, H.R. (1946). Contrast thresholds of the human eye.
Journal of the Optical Society of America, *36*(11): 624-643.

BLAKEMORE, C.B. and RUSHTON, W.A.H. (1965a). Dark adaptation and increment threshold in a rod monochromat.
Journal of Physiology, *181*: 612-628.

BLAKEMORE, C.B. and RUSHTON, W.A.H. (1965b). The rod increment threshold during dark adaptation in normal and rod monochromat.
Journal of Physiology, *181*: 629-640.

BLOOMFIELD, S.A. and DACHEUX, R.F. (2001). Rod Vision: Pathways and processing in the mammalian retina.
Progress in Retinal and Eye Research, *20*(3): 351-384.

BOWMAN, K.J. and COLE, B.L. (1980). A recommendation for the illumination of the Farnsworth-Munsell 100-hue test.
American Journal of Optometry and Physiological Optics, *57*: 839-843.

BOX, G.E.P. and COX, D.R. (1964). An analysis of transformations.
Journal of the Royal Statistical Society, Series B, *26*: 211-243.

BOYNTON, R.M. (1979). Human color vision. (Optical Society of America).

BOYNTON, R.M. and BARON, W.S. (1975). Sinusoidal flicker characteristics of primate cones in response to heterochromatic stimuli.
Journal of the Optical Society of America, *65*: 1091-1100.

BOYNTON, R.M. and KAMBE, N. (1980). Chromatic difference steps of moderate size measured along theoretically critical axes.
Colour Research and Application, *5*(1): 13-23.

BRAINARD, D.H., ROORDA, A., YAMAUCHI, Y. et al. (2000). Functional consequences of the relative numbers of L and M cones.
Journal of the Optical Society of America, A, 17(3): 607-614.

BRAINARD, D.H. (1996). Cone contrast and opponent modulation color spaces.
In: Human color vision. 2nd ed. Ed: Kaiser, P.K. and Boynton, R.M.
Washington DC: Optical Society of America; p563-579 (Appendix, part IV).

BROWN, W.R.J. (1951). The influence of luminance level on visual sensitivity to color differences.
Journal of the Optical Society of America, 41(10): 684-688.

BROWN, W.R.J. (1957). Color discrimination of twelve observers.
Journal of the Optical Society of America, 47: 137-143.

BROWN, W.R.J. and MACADAM, D.L. (1949). Visual sensitivities to combined chromaticity and luminance differences.
Journal of the Optial Society of America, 39(10): 808-834.

BUCK, S.L. (1985a). Cone-rod interaction over time and space.
Vision Research, 25(7): 907-916.

BUCK, S.L. (1985b). Determinants of the spatial properties of cone-rod interaction.
Vision Research, 25(9): 1277-1284.

BUCK, S.L. and MAKOUS, W. (1981). Rod-cone interaction on large and small backgrounds.
Vision Research, 21: 1181-1187.

BUCK, S.L. (1997). Influence of rod signals on hue perception: Evidence from successive scotopic contrast.
Vision Research, 37(10): 1295-1301.

BUCK, S.L., KNIGHT, R., FOWLER, G.A. et al. (1998). Rod influence on hue-scaling functions.
Vision Research, 38: 3259-3263.

BUNT, A.H. and MINKLER, D.S. (1977). Foveal sparing: new anatomical evidence for bilateral representation of the central retina.
Archives of Ophthalmology, 95: 1445.

BURNS, S.A., SMITH, V.C., POKORNY, J. et al. (1982). Brightness of equal-luminance lights.
Journal of the Optical Society of America, 72(9): 1225-1231.

CALKINS, D.J. (1999). Synaptic organisation of cone pathways in the primate retina.
In: Colour vision: From genes to perception. Ed: Gegenfurtner, K.R. and Sharpe, L.T. Cambridge: Cambridge University Press; p163-179.

CARTER, E.C. and CARTER, R.C. (1981). Color and conspicuousness.
Journal of the Optical Society of America, 71(6): 723-729.

CASAGRANDE, V.A. (1994). A third parallel visual pathway to primate area V1.
Trends in Neurosciences, 17(7): 305-310.

CIE (1978). Light as a true visual quantity: Principles of measurement.
Paris: Central Bureau of the CIE.

CIE (1989). Mesopic photometry: History, special problems and practical solutions.
Publication no. CIE 81.
Vienna: CIE Central Bureau. ISBN 390073416X.

CIE (2001). Testing of supplementary systems of photometry. Publication no. CIE 141.
Vienna: CIE Central Bureau. ISBN 3 901 906 05 3.

COBLENTZ, W.W. and EMERSON, W.B. (1918). Relative sensibility of the average eye to light of different colors and some practical applications of radiation problems.
U.S.Bureau of Standards Bulletin, 14: 167.

COLE, B.L. and JENKINS, S.E. (1984). The effect of variability of background elements on the conspicuity of objects.
Vision Research, 24(3): 261-270.

COLETTA, N.J. and ADAMS, A.J. (1984). Rod-cone interaction in flicker detection.
Vision Research, 24(10): 1333-1340.

COLETTA, N.J. and ADAMS, A.J. (1986). Spatial extent of rod-cone and cone-cone interactions for flicker detection.
Vision Research, 26(6): 917-925.

COMERFORD, J.P. and KAISER, P.K. (1975). Luminous-efficiency functions determined by heterochromatic brightness matching.
Journal of the Optical Society of America, 65: 466-468.

CONNER, J.D. (1982). The temporal properties of rod vision.
Journal of Physiology, 332: 139-155.

CONNER, J.D. and MACLEOD, D.I.A. (1977). Rod photoreceptors detect rapid flicker.
Science, 195: 698-699.

CORNSWEET, T.N. (1962). The staircase method in psychophysics.
American Journal of Psychology, 75: 485-491.

CRAWFORD, B.H. (1937). The change of visual sensitivity with time.
Proceedings of the Royal Society of London, Series B, 123: 69-89.

CRAWFORD, B.H. (1947). Visual adaptation in relation to brief conditioning stimuli.
Proceedings of the Royal Society of London, Series B, 134: 283-302.

CRAWFORD, B.H. (1949). The scotopic visibility function.
Proceedings of the Physical Society, B62: 321.

CURCIO, C.A. and ALLEN, K.A. (1990). Topography of ganglion cells in human retina.
Journal of Comparative Neurology, 300: 5-25.

CURCIO, C.A., ALLEN, K.A., SLOAN, K.R. et al. (1991). Distribution and morphology of human cone photoreceptors stained with blue anti-blue opsin.
Journal of Comparative Neurology, 312: 610-624.

CURCIO, C.A., SLOAN, K.R., and KALINA, R.E. (1990). Human photoreceptor topography.
Journal of Comparative Neurology, 292: 497-523.

D'ZMURA, M. (1991). Color in visual search.
Vision Research, 31(6): 951-966.

D'ZMURA, M. and LENNIE, P. (1986). Shared pathways for rod and cone vision.
Vision Research, 26: 1273-1280.

DACEY, D.M. (1996). Circuitry for color coding in the primate retina.
Proceedings of the National Academy of Sciences (U.S.A.), 93: 582-588.

DACEY, D.M. and LEE, B.B. (1994a). Physiology of identified ganglion cell types in an *in vitro* preparation of macaque retina.
Investigative Ophthalmology and Visual Science, 35: 2001.

DACEY, D.M. and LEE, B.B. (1994b). The 'blue-on' opponent pathway in primate retina originates from a distinct bistratified ganglion cell type.
Nature, 367: 731-735.

DACEY, D.M. and LEE, B.B. (1999). The functional architecture of cone signal pathways in the primate retina.
In: Colour vision: From genes to perception. Ed: Gegenfurtner, K.R. and Sharpe, L.T. Cambridge: Cambridge University Press; p181-202.

DACEY, D.M., LEE, B.B., STAFFORD, D.K. et al. (1996). Horizontal cells of the primate retina: Cone specificity without spectral opponency.
Science, 271: 656-659.

DARTNALL, H.J.A. (1953). The interpretation of spectral sensitivity curves.
British Medical Bulletin, 9: 24-30.

DARTNALL, H.J.A., BOWMAKER, J.K., and MOLLON, J.D. (1983). Microspectrophotometry of human photoreceptors.

In: Colour vision: Physiology and psychophysics. Ed: Mollon, J.D. and Sharpe, L.T. London: Academic Press; p69-80.

DAW, N.W., JENSEN, R.J., and BRUNKEN, W.J. (1990). Rod pathways in mammalian retina.
Trends in Neurosciences, 13(3): 110-114.

DEMARCO, P.J., SMITH, V.C., and POKORNY, J. (1994). Effect of sawtooth polarity on chromatic and luminance detection.
Visual Neuroscience, 11: 491-499.

DERRINGTON, A.M., KRAUSKOPF, J., and LENNIE, P. (1984). Chromatic mechanisms in lateral geniculate nucleus of macaque.
Journal of Physiology, 357:241-65.: 241-265.

DEVALOIS, R.L. and DEVALOIS, K.K. (1993). A multi-stage color model.
Vision Research, 33: 1053-1065.

DEVALOIS, R.L. and DEVALOIS, K.K. (1975). Neural coding of color.
In: Handbook of perception, volume 5: seeing. 1st ed. Ed: Carterette, E.C. and Friedman, M.P. London: Academic Press Inc; p117-166.

DEYOE, E.A. and VAN ESSEN, D.C. (1985). Segregation of efferent connections and receptive field properties in visual area V2 of the macaque.
Nature, 317: 58.

DOWLING, J.E. and BOYCOTT, B.B. (1966). Organisation of the primate retina: Electron microscopy.
Proceedings of the Royal Society of London, Series B, 166B: 80-111.

DU BUF, J.M. (1992). Brightness versus apparent contrast. 1: Incremental and decremental disks with varying diameter.
Spatial Vision, 6(3): 159-182.

DUNCAN, J. (1989). Boundary conditions on parallel processing in human vision.
Perception, 18 : 457-469.

DUNCAN, J. and HUMPHREYS, G.W. (1989). Visual search and stimulus similarity.
Psychological Review, 96(3): 433-458.

ENGEL, F.L. (1971). Visual conspicuity, directed attention and retinal locus.
Vision Research, 11(6): 563-576.

ENGEL, F.L. (1974). Visual conspicuity and selective background interference in eccentric vision.
Vision Research, 14(7): 459-471.

ENGEL, F.L. (1977). Visual conspicuity, visual search and fixation tendencies of the eye.
Vision Research, 17(1): 95-108.

FITZGIBBON, A., PILU, M., and FISHER, R.B. (1999). Direct Least Square Fitting of Ellipses.
IEEE Transactions on Pattern Analysis and Machine Intelligence, 21(5): 476-480.

FRUMKES, T.E., NAARENDORP, F., and GOLDBERG, S.H. (1986). The influence of cone adaptation upon rod mediated flicker.
Vision Research, 26(8): 1167-1176.

FRUMKES, T.E. and TEMME, L.A. (1977). Rod-cone interaction in human scotopic vision-II. Cones influence rod increment thresholds.
Vision Research, 17: 673-679.

FUKUDA, Y., SAWAI, H., and WATANABE, M. (1989). Nasotemporal overlap of crossed and uncrossed retinal ganglion projections in the Japanese monkey (Macaca fuscata).
Journal of Neuroscience, 9: 2353-2373.

GEGENFURTNER, K.R. and SHARPE, L.T. (1999). Color vision: from genes to perception. (Cambridge: Cambridge University Press).

GIBSON, K.S. and TYNDALL, E.P.T. (1923). Visibility of radiant energy.
Bulletin Bureau of Standards, 19: 131.

GOLDBERG, S.H., FRUMKES, T.E., and NYGAARD, R.W. (1983). Inhibitory influence of unstimulated rods in the human retina: Evidence provided by examining cone flicker.
Science, 221: 180-182.

GUILD, J. (1931). The colorimetric properties of the spectrum.
Philosophical Transactions of the Royal Society (London), A, 230: 149-187.

HAMMOND, B.R.J., WOOTEN, B.R., and SNODDERLY, D.M. (1997). Individual variations in the spatial profile of human macular pigment.
Journal of the Optical Society of America, A, 14(6): 1187-1196.

HART JR., W.M. (1992). Adler's physiology of the eye: clinical application. 9 Ed. (St. Louis, Missouri: Mosby Year Book).

HARTMAN, L.W. (1918). Visibility of radiation in the blue end of the spectrum.
Astrophysics Journal, 47: 83-95.

HARWERTH, R.S. and LEVI, D.M. (1978). Reaction time as a measure of suprathreshold grating detection.
Vision Research, 18: 1579-1586.

HE, Y., REA, M., BIERMAN, A. et al. (1997). Evaluating light source efficacy under mesopic conditions using reaction times.
Journal of the Illuminating Engineering Society, Winter: 125-138.

HE, Y., BIERMAN, A., and REA, M.S. (1998). A system of mesopic photometry.
Lighting Research and Technology, 30(4): 175-181.

HECHT, S., HAIG, C., and CHASE, A.M. (1937). The influence of light-adaptation on subsequent dark-adaptation of the eye.
Journal of General Physiology, *20*: 831.

HECHT, S., HAIG, C., and WALD, G. (1935). Dark adaptation of retinal fields of different size and location.
Journal of General Physiology, *19*: 321.

HECHT, S., SHLAER, S., and PIRENNE, M.H. (1942). Energy, quanta, and vision.
Journal of General Physiology, *25*: 819-840.

HECHT, S. and VERRIJP, C.D. (1933). Intermittent stimulation by light. IV. A theoretical interpretation of the quantatative data of flicker.
Journal of General Physiology, *17*: 266-286.

HELMHOLTZ, H.V. (1924). Physiological optics (Ed. Southall, J.P.C.). (Rochester, NY: Optical Society of America).

HENDRY, S.H. and YOSHIOKA, T. (1994). A neurochemically distinct third channel in the macaque dorsal lateral geniculate nucleus.
Science, *264*(5158): 575-577.

HESS, R.F. (1990). Rod mediated vision: role of post-receptoral filters.
In: Night vision: basic, clinical, and applied aspects. Ed: Hess, R.F., Sharpe, L.T., and Nordby, K. Cambridge: Cambridge University Press; p3-48.

HESS, R.F., MULLEN, K.T., and ZRENNER, E. (1989). Human photopic vision with only short wavelength cones: post-receptoral properties.
Journal of Physiology, *417*: 151-172.

HESS, R.F. and NORDBY, K. (1986). Spatial and temporal limits of vision in the achromat.
Journal of Physiology, *371*(365): 385.

HESS, R.F., NORDBY, K., and POINTER, J.S. (1987). Regional variation of contrast sensitivity across the retina of the achromat: sensitivity of human rod vision.
Journal of Physiology, *388*: 101-119.

HILZ, R. and CAVONIUS, C.R. (1970). Wavelength discrimination measured with square-wave gratings.
Journal of the Optical Society of America, *60*(2): 273-277.

HOOGE, I.T. and ERKELENS, C.J. (1998). Adjustment of fixation duration in visual search.
Vision Research, *38*(9): 1295-1302.

HUBEL, D.H. and WIESEL, T.N. (1965). Receptive fields and functional architecture in two non striate areas (18 and 19) of the cat.
Journal of Neurophysiology, *28*: 229-289.

HUBEL, D.H. and WIESEL, T.N. (1961). Integrative action in the cat's lateral geniculate body.
Journal of Physiology, 155: 385.

HUBEL, D.H. and WIESEL, T.N. (1962). Receptive fields, binocular interaction and functional architecture in the cat's visual cortex.
Journal of Physiology, 160: 106-154.

HUBEL, D.H. and WIESEL, T.N. (1968). Receptive fields and functional architecture of the monkey striate cortex.
Journal of Physiology, 195: 215-243.

HUBEL, D.H. and WIESEL, T.N. (1974). Sequence regularity and geometry of orientaiton columns in the monkey striate cortex.
Journal of Comparative Neurology, 158: 267.

HUNT, R.W.G. (1987). Measuring colour. (Chichester: Ellis Horwood).

HURDEN, A., SMITH, P., EVANS, G. et al. (1997). A model for visual performance at mesopic light levels: Final report and recommendations.
Published by Scientific Generics.

HURDEN, A., SMITH, P., EVANS, G. et al. (1999). Visual performance at mesopic light levels: an empirical model.
Lighting Research and Technology, 31(3): 127-131.

HYDE, E.P., FORSYTHE, W.E., and CADY, F.E. (1918). The visibility of radiation.
Astrophysics Journal, 35: 237.

IKEDA, M. and ASHIZAWA, S. (1991). Equivalent lightness of colored objects of equal Munsell chroma and of equal Munsell value at various illuminances.
Color Research and Application, 16(2): 72-80.

IKEDA, M., HUANG, C.C., and ASHIZAWA, S. (1989). Equivalent lightness of colored objects at illuminances from the scotopic to the photopic.
Color Research and Application, 14(4): 198-206.

IKEDA, M. and SHIMOZONO, H. (1981). Mesopic luminous-efficiency functions.
Journal of the Optical Society of America, 71(3): 280-284.

INGLING, C.R. and MARTINEZ-URIEGAS, E. (1983). The relationship between spectral sensitivity and spatial sensitivity for the primate r-g X-channel.
Vision Research, 23(12): 1495-1500.

ITTI, L. and KOCH, C. (2000). A saliency-based search mechanism for overt and covert shifts of visual attention.
Vision Research, 40(10-12): 1489-1506.

IVES, H.E. (1912). Studies in the photometry of lights of different colours. I. Spectral luminosity curves obtained by the equality of brightness photometer and flicker photometer under similar conditions.
Philosophical Magazine Series, 6(24): 149-188.

JENKINS, S.E. and COLE, B.L. (1982). The effect of the density of background elements on the conspicuity of objects.
Vision Research, 22(10): 1241-1252.

JONES, E.G. and HENDRY, S.H. (1989). Differential calcium binding protein immunoreactivity distinguishes classes of relay neurons in monkey thalamic nuclei.
European Journal of Neuroscience.

JUDD, D.B. (1951). Report of U.S. Secretariat Committee on Colorimetry and Artificial Daylight.
In: Proceedings of the Twelfth Session of the CIE, Stockholm. Paris: Bureau Central de la CIE; p11.

KAAS, J.H., HUERTA, M.F., and HARTING, J.K. (1978). Patterns of retinal terminations and laminar organization of the lateral geniculate nucleus of primates.
J.Comp.Neurol., 182(3): 517-553.

KAISER, P.K. and BOYNTON, R.M. (1996). Human color vision. 2nd Ed. (Washington, DC: Optical Society of America).

KINNEY, J.A.S. (1958). Comparison of scotopic, mesopic, and photopic spectral sensitivity curves.
Journal of the Optical Society of America, 48(3): 185-190.

KNAU, H., JAGLE, H., and SHARPE, L.T. (2001). L/M cone ratios as a function of retinal eccentricity.
Color Research and Application, Supplement, 26: S128-S132.

KNIGHT, R., BUCK, S.L., FOWLER, G.A. et al. (1998). Rods affect S-cone discrimination on the Farnswoth-Munsell 100-hue test.
Vision Research, 38: 3477-3481.

KNIGHT, R., BUCK, S.L., and PEREVERZEVA, M. (2001). Stimulus size affects rod influence on tritan chromatic discrimination.
Color Research and Application, Supplement, 26: S65-S68.

KNOBLAUCH, K., SAUNDERS, F., KUSUDA, M. et al. (1987). Age and illuminance effects in the Farnsworth-Munsell 100-hue test.
Applied Optics, 26(8): 1441-1448.

KOLB, H., MARIANI, A., and GALLEGO, A. (1980). A second type of horizontal cell in the monkey retina.
Journal of Comparative Neurology, 189: 31-44.

KOOI, F.L. and TOET, A. (1999). Conspicuity: An Efficient Alternative for Search Time.
In: Vision in Vehicles VII. Elsevier Science Ltd; p451-462.

KOUYAMA, N. and MARSHAK, D.W. (1992). Bipolar cells specific for blue cones in the macaque retina.
Journal of Neuroscience, 12: 1233-1252.

KRAFT, T.W., NEITZ, J., and NEITZ, M. (1998). Spectra of human L cones.
Vision Research, 38: 3663-3670.

KRAUSKOPF, J., WILLIAMS, D.R., and HEELEY, D.W. (1982). Cardinal directions of color space.
Vision Research, 22: 1123-1131.

KREMERS, J., SCHOLL, H.P., KNAU, H. et al. (2000). L/M cone ratios in human trichromats assessed by psychophysics, electroretinography, and retinal densitometry.
Journal of the Optical Society of America, A, 17(3): 517-526.

LAKOWSKI, R. (1966). A critical evaluation of colour vision tests.
British Journal of Physiological Optics, 23: 186-209.

LATCH, M. and LENNIE, P. (1977). Rod-cone interaction in light adaptation.
Journal of Physiology, 269: 517-534.

LEE, B.B., MARTIN, P.R., and VALBERG, A. (1989). Sensitivity of macaque retinal ganglion cells to chromatic and luminance flicker.
Journal of Physiology, 414: 223-243.

LEE, B.B., POKORNY, J., SMITH, V.C. et al. (1990). Luminance and chromatic modulation sensitivity of macaque ganglion cells and human observers.
Journal of the Optical Society of America, A, 7: 2223-2236.

LEE, B.B., SMITH, V.C., POKORNY, J. et al. (1997). Rod inputs to macaque ganglion cells.
Vision Research, 37(20): 2813-2828.

LEE, B.B. (1996). Receptive field structure in the primate retina.
Vision Research, 36(5): 631-344.

LEGGE, G.E., RUBIN, G.S., and LUEBKER, A. (1987). Psychophysics of reading - V. The role of contrast in normal vision.
Vision Research, 27(7): 1165-1177.

LEVENE (1960).
In: Contributions to probability and statistics, essays in honour of Harold Hotelling. Ed: Olkin, I. Stanford University Press; p278-292.

LIT, A., YOUNG, R.H., and SHAFFER, M. (1971). Simple time reaction as a function of luminance for various wavelengths.
Perception and Psychophysics, *10*(6): 397-399.

LIVINGSTONE, M.S. and HUBEL, D.H. (1984). Anatomy and physiology of a color system in the primate visual cortex.
Journal of Neuroscience, *4*: 309-356.

LIVINGSTONE, M.S. and HUBEL, D.H. (1987). Connections between layer 4B of area 17 and the thick cytochrome oxidase sripes of area 18 in the squirrel monkey.
Journal of Neuroscience, *7*: 3371-3377.

LUDVIGH, E. (1941). Effect of reduced contrast on visual acuity as measured with Snellen test letters.
Archives of Ophthalmology, *25*: 469-474.

MACADAM, D.L. (1942). Visual sensitivities to color differences in daylight.
Journal of the Optical Society of America, *32*: 247-274.

MACLEOD, D.I.A. (1972). Rods cancel cones in flicker.
Nature, *235*: 173-174.

MACLEOD, D.I.A. and BOYNTON, R.M. (1979). Chromaticity diagram showing cone excitation by stimuli of equal luminance.
Journal of the Optical Society of America, *69*(8): 1183-1186.

MAKOUS, W. (1998). Optics.
In: Vision research: a practical guide to laboratory methods. Ed: Carpenter, R.H.S. and Robson, J.G. Oxford: Oxford University Press; p1-49.

MAKOUS, W. and BOOTHE, R. (1974). Cones block signals from rods.
Vision Research, *14*: 285-294.

MAKOUS, W. and PEEPLES, D. (1979). Rod-cone interaction: Reconciliation with Flamant and Stiles.
Vision Research, *19*: 695-698.

MARRIOTT, F.H.C. (1963). The foveal absolute visual threshold for short flashes and small fields.
Journal of Physiology , *169*: 416-423.

MARTIN, P.R., WHITE, A.J.R., GOODCHILD, A.K. et al. (1997). Evidence that blue-on cells are part of the third geniculocortical pathway in primates.
European Journal of Neuroscience, *9*(7): 1536-1541.

MCCANN, J.J. and BENTON, J.L. (1969). Interaction of the long-wave cones and the rods to produce color sensations.
Journal of the Optical Society of America, *59*(1): 103-107.

MCCREE, K.J. (1960). Small-field tritanopia and the effects of voluntary fixation.
Optica Acta, 7: 317-323.

MCKEE, S.P., MCCANN, J.J., and BENTON, J.L. (1977). Color vision from rod and long-wave cone interactions: Conditions in which rods contribute to multicolored images.
Vision Research, 17: 175-185.

MOLLON, J.D. and POLDEN, P.G. (1977). Saturation of a retinal cone mechanism.
Nature, 20;265(591): 243-246.

MOLLON, J.D., ASTELL, S., and CAVONIUS, C.R. (1992). A reduction in stimulus duration can improve wavelength discriminations mediated by short-wave cones.
Vision Research, 32(4): 745-755.

MONNIER, P. and NAGY, A.L. (2001). Uncertainty, attentional capacity and chromatic mechanisms in visual search.
Vision Research, 41(3): 313-328.

MORELAND, J.D. and CRUZ, A. (1959). Colour perception with the peripheral retina.
Optica Acta, 6: 117-151.

MOTTER, B.C. and BELKY, E.J. (1998). The guidance of eye movements during active visual search.
Vision Research, 38: 1805-1815.

MULLEN, K.T. (1985). The contrast sensitivity of human colour vision to red-green and blue-yellow chromatic gratings.
Journal of Physiology, 359: 381-400.

MULLEN, K.T., CROPPER, S.J., and LOSADA, M.A. (1997). Absence of linear subthreshold summation between red-green and luminance mechanisms over a wide range of spatio-temporal conditions.
Vision Research, 37(9): 1157-1165.

MULLEN, K.T. and PLANT, G.T. (1986). Colour and luminance vision in human optic neuritis.
Brain, 109(1): 1-13.

NAGY, A.L. and DOYAL, J.D. (1993). Red-green color discrimination as a function of a stimulus field size in peripheral vision.
Journal of the Optical Society of America, A, 10(6): 1147-1156.

NAGY, A.L. and SANCHEZ, R.R. (1990). Critical color differences determined with a visual search task.
Journal of the Optical Society of America, A, 7(7): 1209-1217.

NAGY, A.L. and WINTERBOTTOM, M. (2000). The achromatic mechanism and mechanisms tuned to chromaticity and luminance in visual search.
Journal of the Optical Society of America, A, 17(3): 369-379.

NAKANO, Y., IKEDA, M., and KAISER, P.K. (1988). Contributions of the opponent mechanisms to brightness and nonlinear models.
Vision Research, 28(7): 799-810.

NAKANO, Y. (1996). Color vision mathematics: A tutorial.
In: Human color vision. 2 ed. Ed: Kaiser, P.K. and Boynton, R.M. Washington DC: Optical Society of America; p545-562 (Appendix, part III).

NASANEN, R., OJANPAA, H., and KOJO, I. (2001). Effect of stimulus contrast on performance and eye movements in visual search.
Vision Research, 41(14): 1817-1824.

NOORLANDER, C., KOENDERINK, J.J., DEN, O.R. et al. (1983). Sensitivity to spatiotemporal colour contrast in the peripheral visual field.
Vision Research, 23(1): 1-11.

NORDBY, K., STABELL, B., and STABELL, U. (1984). Dark adaptation of the human rod system.
Vision Research, 24: 897-905.

NOTHDURFT, H.C. (1993). Saliency effects across dimensions in visual search.
Vision Research, 33(5-6): 839-844.

OSTERBERG, G.A. (1935). Topography of the layer of rods and cones in the human retina.
Acta Ophthalmologica, 13: 1-97.

OYSTER, C.W. (1999). The human eye: structure and function. (Sunderland, Massachusetts: Sinauer Associates Inc.).

PALMER, D.A. (1968). Standard observer for large field photometry at any level.
Journal of the Optical Society of America, 58: 1296-1299.

PALMER, J. (1994). Set-size effects in visual search: the effect of attention is independent of the stimulus for simple tasks.
Vision Research, 34(13): 1703-1721.

PALMER, J., VERGHESE, P., and PAVEL, M. (2000). The psychophysics of visual search.
Vision Research, 40(10-12): 1227-1268.

PARRY, N.R.A. (2001). Contrast dependence of reaction times to chromatic gratings.
Color Research and Application, 26: S161-S164.

PATEL, A.S. (1966). Spatial resolution by the human visual system. The effect of mean retinal illuminance.
Journal of the Optical Society of America, 56(5): 689-694.

PERRY, V.H., OEHLER, R., and COWEY, A. (1984). Retinal ganglion cells that project to the dorsal lateral geniculate nucleus in the macaque monkey.
Neuroscience, 12: 1110-1123.

PIRENNE, M.H., MARRIOTT, F.H.C., and O'DOHERTY, E.F. (1957). Individual differences in night-vision efficiency.
Med.Res.Council Sp.Rep.Ser., No.294.

PITT, F.H.G. (1935). Characteristics of dichromatic vision.Committee on the Physiology of Vision, Report No. 14.
London: His Majesty's Stationery Office.

POKORNY, J., SMITH, V.C., and LUTZE, M. (1987). Aging of the human lens.
Applied Optics, 26: 1437-1440.

POKORNY, J., SMITH, V.C., and SWARTLEY, R. (1970). Threshold measurements of spectral sensitivity in a blue monocone monochromat.
Investigative Ophthalmology and Visual Science, 9(10): 807-813.

POKORNY, J. and SMITH, V.C. (1997). How much light reaches the retina?
In: Colour vision deficiencies. Ed: Cavonius, C.R. Dordrecht: Kluwer; p491-511.

POLDEN, P.G. and MOLLON, J.D. (1980). Reversed effect of adapting stimuli on visual sensitivity.
Proceedings of the Royal Society of London, Series B, 210: 235-272.

POLLACK, J.D. (1968). Reaction time to different wavelengths at various luminances.
Perception and Psychophysics, 3(1A): 17-24.

POLYAK, S.L. (1941). The retina. (Chicago: University of Chicago Press).

REGAN, B.C., REFFIN, J.P., and MOLLON, J.D. (1994). Luminance noise and the rapid determination of discrimination ellipses in colour deficiency.
Vision Research, 34(10): 1279-1299.

REID, R.C. and SHAPLEY, R.M. (1992). Spatial structure of cone inputs to receptive fields in primate lateral geniculate nucleus.
Nature, 356: 716-718.

REITNER, A., SHARPE, L.T., and ZRENNER, E. (1991). Is colour vision possible with only rods and blue-sensitive cones?
Nature, 352: 798-800.

RODIECK, R.W. (1973). The vertebrate retina. (San Francisco: Freeman).

RODIECK, R.W. (1991). Which cells code for color?
In: From pigments to perception. Advances in understanding visual processes. Ed: Valberg, A. and Lee, B.B. New York: Plenum Press; p83-93.

ROORDA, A. and WILLIAMS, D.R. (1999). The arrangement of the three cone classes in the living human eye.
Nature, *397*(6719): 520-522.

RUDDOCK, K.H. (1963). Evidence for macular pigmentation from colour matching data.
Vision Research, *3*: 417-429.

RUSHTON, W.A.H. (1961). Rhodopsin measurement and dark-adaptation in a subject deficient in cone vision.
Journal of Physiology, *156*: 193-205.

RUSHTON, W.A.H. (1963). A cone pigment in the protanope.
Journal of Physiology, *168*: 345-359.

RUSHTON, W.A.H. and BAKER, H.D. (1964). Red/green sensitivity in normal vision.
Vision Research, *4*: 75-85.

SAGAWA, K. and TAKEICHI, K. (1986). Spectral luminous efficiency functions in the mesopic range.
Journal of the Optical Society of America, A, *3*(1): 71-75.

SAGAWA, K. and TAKEICHI, K. (1987). Mesopic spectral luminous efficiency functions: Final experimental report.
J.Light Vis.Env., *11*: 22-29.

SAGAWA, K. and TAKEICHI, K. (1992). System of mesopic photometry for evaluating lights in terms of comparative brightness relationships.
Journal of the Optical Society of America, A, *9*(8): 1240-1246.

SCHILLER, P.H. and MALPELI, J.G. (1978). Functional specificity of lateral geniculate nucleus laminae of the rhesus monkey.
Journal of Neurophysiology, *41*: 788.

SCHWARTZ, S.H. (1994). Visual perception: a clinical orientation. (Stamford: Appleton and Lange).

SHAPIRO, A.G. (2002). Cone-specific mediation of rod sensitivity in trichromatic observers.
Investigative Ophthalmology and Visual Science, *43*(3): 898-905.

SHAPIRO, A.G., POKORNY, J., and SMITH, V.C. (1994). Rod contribution to large-field colour matching.
Color Research and Application, *19*(4): 236-245.

SHARPE, L.T., FACH, C., NORDBY, K. et al. (1989). The increment threshold of the rod visual system and Weber's law.
Science, *244*: 354-356.

SHARPE, L.T. and NORDBY, K. (1990). Total colour blindness: an introduction. In: Night vision: basic, clinical and applied aspects. Ed: Hess, R.F., Sharpe, L.T., and Nordby, K. Cambridge: Cambridge University Press; p253-289.

SHARPE, L.T. and STOCKMAN, A. (1999). Rod pathways: the importance of seeing nothing.
Current Trends in Neurosciences, *22*(11): 497-504.

SHARPE, L.T., STOCKMAN, A., JAGLE, H. et al. (1998). Red, green, and red-green hybrid pigments in the human retina: correlations between deduced protein sequences and psychophysically-measured spectral sensitivities.
Journal of Neuroscience, *18*: 10053-10069.

SHARPE, L.T., STOCKMAN, A., JAGLE, H. et al. (1999). Opsin genes, cone photopigments, colour vision, and colour blindness.
In: Colour vision: From genes to perception. Ed: Gegenfurtner, K.R. and Sharpe, L.T. Cambridge: Canbridge University Press; p3-51.

SHARPE, L.T., VAN, N.D., and NORDBY, K. (1988). Pigment regeneration, visual adaptation and spectral sensitivity in the achromat.
Clinical Vision Sciences, *3*: 9-17.

SHEVELL, S.K. (1977). Saturation in human cones.
Vision Research, *17*(427): 434.

SHINOMORI, K., SPILLMANN, L., and WERNER, J.S. (1999). S-cone signals to temporal OFF-channels: asymmetrical connections to postreceptoral chromatic mechanisms.
Vision Research, *39*(1): 39-49.

SHIPP, S. and ZEKI, S. (1985). Segregation of pathways leading from area V2 to areas V4 and V5 of macaque monkey visual cortex.
Nature, *315*: 322.

SHIPP, S. and ZEKI, S. (1989a). Modular connections between areas V2 and V4 of macaque monkey visual cortex.
European Journal of Neuroscience, *1*: 494-506.

SHIPP, S. and ZEKI, S. (1989b). The organisation of connections between areas V5 and V2 in macaque monkey visual cortex.
European Journal of Neuroscience, *1*: 333-354.

SMITH, V.C. and POKORNY, J. (1975). Spectral sensitivity of the foveal cone photopigments between 400 and 500 nm.
Vision Research, *15*(2): 161-171.

SMITH, V.C. and POKORNY, J. (1995). Chromatic-discrimination axes, CRT phosphor spectra, and individual variation in color vision.
Journal of the Optical Society of America, A, 12(1): 27-35.

SMITH, V.C., VAN EVERDINGEN, J., and POKORNY, J. (1991). Sensitivity of arrangement tests as evaluated in normals at reduced levels of illumination.
In: Colour Vision Deficiencies X, Documenta Ophthalmologica Proceedings Series. Ed: Drum, B., Moreland, J.D., and Serra, A. Dordrecht: Kluwer; p177-185.

SPERANSKAYA, N.I. (1959). Determination of spectrum color co-ordinates for twenty-seven normal observers.
Optics and Spectroscopy, 7: 424-428.

STABELL, B. and STABELL, U. (1976a). Rod and cone contributions to peripheral colour vision.
Vision Research, 16: 1099-1104.

STABELL, B. and STABELL, U. (1996). Peripheral colour vision: Effects of rod intrusion at different eccentricities.
Vision Research, 36(21): 3407-3414.

STABELL, U. and STABELL, B. (1976b). Absence of rod activity from peripheral vision.
Vision Research, 16: 1433-1437.

STABELL, U. and STABELL, B. (1977). Wavelength discrimination of peripheral cones and its change with rod intrusion.
Vision Research, 17: 423-426.

STABELL, U. and STABELL, B. (1994). Mechanisms of chromatic rod vision in scotopic illumination.
Vision Research, 34(8): 1019-1027.

STILES, W.S. (1939). The directional sensitivity of the retina and the spectral sensitivities of the rods and cones.
Proceedings of the Royal Society of London, Series B, B127: 64.

STILES, W.S. and BURCH, J.M. (1955). Interim report to the Commission Internationale de l'Eclairage, Zurich, 1955, on the National Physical Laboratory's investigation of colour-matching (1955).
Optica Acta, 2: 168-181.

STILES, W.S. and BURCH, J.M. (1959). NPL colour-matching investigation: Final report (1958).
Optica Acta, 6: 1-26.

STILES, W.S. and CRAWFORD, B.H. (1933). The luminous efficiency of rays entering the pupil at different points.
Proceedings of the Royal Society of London, Series B, 112: 428-450.

STILES, W.S. (1959). Color vision: The approach through increment threshold sensitivity.
Proceedings of the National Academy of Sciences (U.S.A.), 45: 100-114.

STOCKMAN, A., MACLEOD, D.I.A., and JOHNSON, N.E. (1993). Spectral sensitivities of the human cones.
Journal of the Optical Society of America, A, 10: 2471-2490.

STOCKMAN, A. and SHARPE, L.T. (2000). The spectral sensitivities of the middle- and long-wavelength-sensitive cones derived from measurements in observers of known genotype.
Vision Research, 40: 1711-1737.

STOCKMAN, A., SHARPE, L.T., and FACH, C.C. (1999). The spectral sensitivity of the human short-wavelength sensitive cones derived from thresholds and color matches.
Vision Research, 39: 2901-2927.

TEMME, L.A. and FRUMKES, T.E. (1977). Rod-cone interaction in human scotopic vision-III. Rods influence cone increment thresholds.
Vision Research, 17: 681-685.

TREZONA, P.W. (1991). A system of mesopic photometry.
Color Research and Application, 16(3): 202-216.

TREZONA, P.W. (1970). Rod participation in the 'blue' mechanism and its effect on colour matching.
Vision Research, 10: 317-332.

TURATTO, M. and GALFANO, G. (2000). Color, form and luminance capture attention in visual search.
Vision Research, 40(13): 1639-1643.

UENO, T., POKORNY, J., and SMITH, V.C. (1985). Reaction times to chromatic stimuli.
Vision Research, 25(11): 1623-1627.

VAN DER BERG, T.J.T.P. and SPEKREIJSE, H. (1977). Interaction between rod and cone signals studied with temporal sine wave stimulation.
Journal of the Optical Society of America, 67: 1210-1217.

VAN LOO, J.A. and ENOCH, J.M. (1975). The scotopic Stiles-Crawford effect.
Vision Research, 15: 1005-1009.

VAN NES, F.L. and BOUMAN, M.A. (1967). Spatial modulation transfer in the human eye.
Journal of the Optical Society of America, 57: 401-406.

VAN NORREN, D. and VOS, J.J. (1974). Spectral transmission of the human ocular media.
Vision Research, 14: 1237-1244.

VERGHESE, P. and NAKAYAMA, K. (1994). Stimulus discriminability in visual search.
Vision Research, 34(18): 2453-2467.

VERRIEST, G. (1963). Further studies on acquired deficiency of color discrimination.
Journal of the Optical Society of America, 53(1): 185-195.

VIENOT, F. and CHIRON, A. (1992). Brightness matching and flicker photometric data obtained over the full mesopic range.
Vision Research, 32(3): 533-540.

VINGRYS, A.J. and MAHON, L.E. (1998). Colour and luminance detection and discrimination asymmetries and interactions.
Vision Research, 38(8): 1085-1095.

VON KRIES, J. (1970). Influence of adaptation on the effcts produced by luminous stimuli.
In: Sources of color science. Ed: MacAdam, D.L. Cambridge, MA.: The MIT Press.

VOS, J.J. (1972). Literature review of human macular pigment absorption in the visible and its consequences for the cone photoreceptor primaries.
Soesterberg, The Netherlands: TNO Report, Institute for Perception.

VOS, J.J. (1978). Colorimetric and photometric properties of a 2°fundamental observer.
Color Research and Application, 3: 125-128.

VOS, J.J., ESTEVEZ, O., and WALRAVEN, P.L. (1990). Improved color fundamentals offer a new view on photometric additivity.
Vision Research, 30: 936-943.

VOS, J.J. and WALRAVEN, P.L. (1971). On the derivation of the foveal receptor primaries.
Vision Research, 11: 799-818.

WAGNER, G. and BOYNTON, R.M. (1972). Comparison of four methods of heterochromatic photometry.
Journal of the Optical Society of America, 62: 1508-1515.

WALD, G. (1945a). Human vision and the spectrum.
Science, 101: 653-658.

WALD, G. (1945b). The spectral sensitivity of the human eye; a spectral adaptometer.
Journal of the Optical Society of America, 35: 187.

WALD, G. and BROWN, P.K. (1965). Human color vision and color blindness.
Cold Spring Harbor Symp Quant Biol, 30: 345.

WALKEY, H.C., BARBUR, J.L., HARLOW, J.A. et al. (2001). Measurements of chromatic sensitivity in the mesopic range.
Color Research and Application, Supplement, 26: S36-S42.

WALLS, G.L. (1953). The lateral geniculate nucleus and visual histophysiology. (Berkeley and Los Angeles: University of California Press).

WASSLE, H. (1999). Parallel pathways from the outer to the inner retina in primates.
In: Colour vision: From genes to perception. Ed: Gegenfurtner, K.R. and Sharpe, L.T. Cambridge: Cambridge University Press; p145-162.

WASSLE, H. and BOYCOTT, B.B. (1991). Functional architecture of the mammalian retina.
Physiological Reviews, 71(2): 447-480.

WASSLE, H., GRUNERT, U., MARTIN, P.R. et al. (1994). Immunocytochemical characterisation and spatial distribution of midget bipolar cells in the macaque monkey retina.
Vision Research, 34: 561-579.

WATANABE, A., POKORNY, J., and SMITH, V.C. (1998). Red-green chromatic discrimination with variegated and homogeneous stimuli.
Vision Research, 38(21): 3271-3274.

WEALE, R.A. (1953). Spectral sensitivity and wavelength discrimination of the peripheral retina.
Journal of Physiology, 119: 170-190.

WEBSTER, M.A. and MOLLON, J.D. (1991). Changes in colour appearance following post-receptoral adaptation.
Nature, 349: 235-238.

WERNER, J.S., DONNELLY, S.K., and KLIEGL, R. (1987). Ageing and human macular pigment density.
Vision Research, 27(2): 257-268.

WIESEL, T. and HUBEL, D.H. (1966). Spatial and chromatic interactions in the lateral geniculate body of the rhesus monkey.
Journal of Neurophysiology, 29: 1115-1156.

WRIGHT, W.D. and PITT, F.H.G. (1934). Hue discrimination in normal colour vision.
Proceedings of the Physical Society, 46: 459.

WRIGHT, W.D. (1928). A re-determination of the trichromatic coefficients of the spectral colours.
Transactions of the Optical Society, 30: 141-164.

WRIGHT, W.D. (1941). The sensitivity of the eye to small colour differences.
Proceedings of the Physiological Society of London, 53: 93-112.

WRIGHT, W.D. (1946). Researches in normal and defective colour vision. (London: Henry Kimpton).

WRIGHT, W.D. (1952). The characterisitics of tritanopia. *Journal of the Optical Society of America*, *42*: 509-521.

WYSZECKI, G.W. and STILES, W.S. (1967). Color Science - Concepts and Methods, Quantitative Data and Formulae. 1 Ed. (New York: John Wiley & Sons).

WYSZECKI, G.W. and STILES, W.S. (1982). Color Science - Concepts and Methods, Quantitative Data and Formulae. 2 Ed. (New York: John Wiley & Sons).

WYSZECKI, G. and FIELDER, G.H. (1971). New color-matching ellipses. *Journal of the Optial Society of America*, *61*(9): 1135-1152.

YAGUCHI, H. and IKEDA, M. (1983). Subadditivity and superadditivity in heterochromatic brightness matching. *Vision Res.* , *23*(12): 1711-1718.

YAGUCHI, H. and IKEDA, M. (1984). Mesopic luminous-efficiency functions for various adapting levels. *Journal of the Optical Society of America, A, 1*(1): 120-123.

YAGUCHI, H., KAWADA, A., SATOSHI, S. et al. (1993). Individual differences of the contribution of chromatic channels to brightness. *Journal of the Optical Society of America, A, 10*(6): 1373-1379.

YEH, T., POKORNY, J., and SMITH, V.C. (1993). S-cone discrimination sensitivity and performance on arrangement tests. In: Colour Vision Deficiencies XI, Documenta Ophthalmologica Proceedings Series. Ed: Drum, B. Dordrecht: Kluwer; p293-302.

ZEKI, S. (1973). Colour coding in the rhesus monkey prestriate cortex. *Brain Research*, *53*: 422.

ZEKI, S. (1974). Functional organisation of a visual area in the posterior bank of of the superior sulcus of the rhesus monkey. *Journal of Physiology*, *236*: 549.

ZEKI, S. (1978). The third visual complex of rhesus monkey prestriate cortex. *Journal of Physiology*, *277*: 245-272.

ZEKI, S. (1993). A vision of the brain. (Oxford: Blackwell Scientific Publications).